OAK RIDGE NATIONAL LABORATORY LIBRARIES
3 4456 0570480 5
CENTRAL RESEARCH LIBRARY

ORNL-4936

cy. 1

MECHANICAL PROPERTIES TEST DATA FOR STRUCTURAL MATERIALS QUARTERLY PROGRESS REPORT FOR PERIOD ENDING OCTOBER 31, 1973

[redacted]

OAK RIDGE NATIONAL LABORATORY
CENTRAL RESEARCH LIBRARY
DOCUMENT COLLECTION
LIBRARY LOAN COPY
DO NOT TRANSFER TO ANOTHER PERSON
If you wish someone else to see this document, send in name with document and the library will arrange a loan.
UCN-7969
(3 3-67)

OAK RIDGE NATIONAL LABORATORY
OPERATED BY UNION CARBIDE CORPORATION • FOR THE U.S. ATOMIC ENERGY COMMISSION

Printed in the United States of America. Available from
the U.S. Atomic Energy Commission, Technical Information Center
P.O. Box 62, Oak Ridge, Tennessee 37830
Price: Printed Copy $7.60 , Microfiche $1.45

This report was prepared as an account of work sponsored by the United States Government. Neither the United States nor the United States Atomic Energy Commission, nor any of their employees, nor any of their contractors, subcontractors, or their employees, makes any warranty, express or implied, or assumes any legal liability or responsibility for the accuracy, completeness or usefulness of any information, apparatus, product or process disclosed, or represents that its use would not infringe privately owned rights.

ORNL-4936
UC-79b, -h, -k
(Liquid Metal Fast
Breeder Reactors)

Contract No. W-7405-eng-26

METALS AND CERAMICS DIVISION

MECHANICAL PROPERTIES TEST DATA FOR STRUCTURAL MATERIALS QUARTERLY PROGRESS REPORT FOR PERIOD ENDING OCTOBER 31, 1973

Aerojet Nuclear Company

Argonne National Laboratory

Hanford Engineering Development Laboratory

Naval Research Laboratory

Oak Ridge National Laboratory

Westinghouse Advanced Reactors Division

Compiled by M. R. Hill

JANUARY 1974

OAK RIDGE NATIONAL LABORATORY
Oak Ridge, Tennessee 37830
operated by
UNION CARBIDE CORPORATION
for the
U.S. ATOMIC ENERGY COMMISSION

FOREWORD

This is the first in a series of progress reports, the purpose of which is to record and distribute on a quarterly basis the collected results of all structural materials mechanical properties test programs sponsored by the Reactor Research and Development Division of the USAEC.

To be useful as resource documents, the reports in this series must be published and distributed in a timely manner to those in the reactor design and materials technology community who have a need of mechanical property test data for nuclear reactor and power plant applications. Contributions to this first report were due at ORNL on December 15, 1973. The second quarterly report will be for the period ending January 31, 1974, and contributions are due at ORNL by February 15, 1974.

W. R. Martin
Metals and Ceramics Division
Oak Ridge National Laboratory

CONTENTS

SUMMARY vii

1. AEROJET NUCLEAR COMPANY 1

1.1 INTRODUCTION 1

1.2 FATIGUE AND CREEP-FATIGUE BEHAVIOR OF SMA TYPE 304/308 STAINLESS STEEL WELDMENTS 2

1.2.1 Irradiation Effects on Low-Cycle Fatigue of Type 308 Weld Metal 2

1.2.2 Tensile Hold-Time Effects (Creep-Fatigue) of SMA Type 304/308 Stainless Steel Weldments 2

1.3 INCONEL 718 CODE CASE 5

1.3.1 Strain Fatigue Tests with Hold Times 5

1.3.2 Strain Rate Effects on Low-Cycle Fatigue 8

1.3.3 Impact Tests for Materials Characterization on 1900°F (1038°C) Solution Annealed Material 8

1.3.4 Tensile and Impact Tests on Weldments 10

2. ARGONNE NATIONAL LABORATORY 15

2.1 INTRODUCTION 15

2.2 FRACTURE AND FATIGUE STUDIES ON STAINLESS STEELS 16

2.2.1 Low-Cycle Creep-Fatigue Behavior of Type 304 Stainless Steel 16

2.2.2 Analysis of ANL High-Temperature Fatigue Data for AISI Type 304 Stainless Steel Using Common Phenomenological Methods 24

2.3 SODIUM EFFECTS ON LMFBR MATERIALS 30

2.3.1 Effect of Reduced Carbon and Nitrogen Content on the Creep Rupture Strength of Type 316 Stainless Steel 30

3. HANFORD ENGINEERING DEVELOPMENT LABORATORY (no report)

4. NAVAL RESEARCH LABORATORY 37

4.1 INTRODUCTION 37

4.2 FATIGUE CRACK GROWTH IN TYPE 304 STAINLESS STEEL 37

4.2.1 Background 37

4.2.2 Materials and Test Procedures 37

4.2.3 Results 38

4.3 J-INTEGRAL CHARACTERIZATION OF STAINLESS STEEL 46
4.3.1 Background 46
4.3.2 Preliminary Investigations 46
4.3.2.1 Materials and Specimen Types 46
4.3.2.2 Results 46
4.3.3 Conclusions 47
4.4 NOTCH DUCTILITY OF AUSTENITIC STAINLESS STEEL WELDMENTS . . 51
4.4.1 Background 51
4.4.2 Materials 51
4.4.3 Specimen Location and Preparation 55
4.4.4 Results 55
4.4.4.1 As-Fabricated Notch Ductility 55
4.4.4.2 Notch Ductility With Thermal Conditioning . 61
4.4.5 Summary of Observations 61
4.5 NOTCH DUCTILITY AND STRENGTH PROPERTIES OF ADVANCED NiCrMo STEEL PLATES, FORGINGS AND WELDMENTS 62
4.5.1 Background 62
4.5.2 Materials 62
4.5.3 Notch Ductility of Plates and Forgings 62
4.5.4 Notch Ductility of Weld Metal 69
4.5.5 Summary of Observations 70
4.6 REFERENCES 77
5. OAK RIDGE NATIONAL LABORATORY 79
5.1 INTRODUCTION 79
5.2 MECHANICAL PROPERTIES AND BEHAVIOR FOR STRUCTURAL MATERIALS 81
5.2.1 Base-Line Mechanical Property Testing of Reference Heat of Type 304 Stainless Steel 81
5.2.1.1 Creep Properties of the 2-in. Plate of Reference Heat 81
5.2.1.2 Strain Rate Effect on the Tensile Properties of 2-in. Plate 88
5.2.1.3 Variation of Properties of Reference Heat with Product Form (Plate, Bar, and Pipe). 94
5.2.1.3.1 Room-Temperature Properties . . . 96
5.2.1.3.2 Elevated-Temperature Properties . 101

5.2.2 Heat-to-Heat Variation Study of Type 304 Stainless Steel 107

5.2.2.1 Tensile and Short-Term Creep Tests 107

5.2.2.2 Long-Term Creep Tests 111

5.2.2.3 Statistical Analysis of Type 304 Stainless Steel Creep-Rupture Data 111

5.2.3 Exploratory Studies on Type 304 Stainless Steel in Support of Structural Design Methods 117

5.2.3.1 Tensile Testing of Reference Heat 9T2796 1-in. Plate 117

5.2.3.2 Creep Testing of 5/8-in.-diam Bar and 1-in. Plate of Type 304 Stainless Steel (Heat 9T2796) 123

5.2.3.3 Relaxation Testing of 1-in. Plate — Reference Heat 125

5.2.3.4 Creep-Plasticity Interaction of 1-in. Plate — Reference Heat 127

5.2.4 Variation in the Mechanical Properties of Type 316 Stainless Steel 129

5.3 MECHANICAL AND METALLURGICAL BEHAVIOR OF WELDMENTS FOR LMFBR 133

5.3.1 Welding Development and Mechanical Testing of the Weldments for Stainless Steel Components 133

5.3.1.1 Creep and Tensile Properties of SMA Type 316 CRE Stainless Steel Weld Metal . . 133

5.3.2 High-Temperature Structural Design Data for Austenitic Stainless Steel Weldments 138

5.3.2.1 Characterization of FFTF Vessel Test Welds: SMA Type 308 (CRE) Stainless Steel Welds 138

5.3.2.2 Tensile Properties of As-Welded SMA Type 308 (CRE) Stainless Steel FFTF Vessel Test Welds 142

5.3.2.3 Tensile Properties of Aged SMA Type 308 CRE Stainless Steel FFTF Vessel Test Welds . 145

5.4 MECHANICAL PROPERTIES OF STEAM GENERATOR MATERIAL 152

5.4.1 The Effect of Carbon on the Mechanical Properties of 2 1/4 Cr-1 Mo Steel 152

5.4.2 Mechanical Properties of Overlaid Stainless Steel Forgings 154

5.4.3 Mechanical Properties of 9 Cr-1 Mo Steel 158
5.4.3.1 Elevated-Temperature Tensile Properties . . 158
5.4.3.2 Creep and Stress Rupture 160
5.4.3.3 Stress Intensity Limits 166
5.4.3.4 Conclusions 168
5.5 HIGH-TEMPERATURE DESIGN 168
5.5.1 Characterization of Product Form 168
5.5.2 Exploratory Testing to Identify Behavioral Features 174
5.5.2.1 Stress-Strain Testing 174
5.5.2.2 Creep Testing 176
5.5.2.3 Relaxation Testing 178
5.5.2.4 Creep-Plasticity Testing 178
5.5.3 Investigations of Creep Failure Under Uniaxial and Multiaxial Conditions 180
5.6 REFERENCES 184
6. WESTINGHOUSE ADVANCED REACTORS DIVISION 187
6.1 INTRODUCTION 187
6.2 BASIC SPECIMEN TESTING 187
6.2.1 Uniaxially Loaded Specimen Models with Uniform Gage Section (304 SS, Heat 9T796) 187
6.2.1.1 Type A 187
6.2.1.2 Type B 187
6.2.1.3 Type G 191
6.2.1.4 Current Results 191
6.2.2 Specimens with Welds 192
6.3 TUBULAR SPECIMEN TESTING 194
6.3.1 Uniaxial Creep Testing 194
6.3.2 Multiaxial Creep Testing 195
INDEX 203

SUMMARY

1. AEROJET NUCLEAR COMPANY

Results of strain controlled fatigue tests of Type 308 weld metal at 1100°F (593°C) are presented. The effects of irradiation to fluences of 0.5 to 1.0 × 10^{22} n/cm^2 (E>0.1 MeV) are shown. Also the effects of tensile hold times on irradiated and unirradiated weld metal is presented. Irradiation does reduce the cyclic life of fatigue tests with and without hold times at the higher strain ranges but trends show that at lower strain ranges (<0.5%) the irradiated weld metal becomes superior to both unirradiated weld and base metal.

Creep-fatigue interaction was investigated on Alloy Inconel 718 by incorporating either tensile or compressive hold times during fatigue tests and also by varying the strain rate at 1000°F (538°C) and 1200°F (649°C). Reductions in cyclic life was observed with both tensile and compressive hold times at 1200°F (649°C), compressive being the most damaging. Hold times had only a slight effect of 1000°F (530°C), but lower strain rates resulted in shorter fatigue lives at both temperatures.

Tensile and impact test results on Inconel 718 base material and weldments has been presented. The impact energy absorbed varied with the heat of base material, but was considerably less for the weldments which were heat treated at the 1750°F (954°C) solution heat treatment. The tensile ductility of the weldments heat treated at 1900°F (1038°C) solution anneal was greater than the 1750°F (954°C) solution anneal, as also was the yield and ultimate strength.

2. ARGONNE NATIONAL LABORATORY

Most of the creep-fatigue data for Types 304 and 316 stainless steel generated during the past three years at ANL are from relatively simple tests. These results may be used as the base-line data for comparison with the results of more complex tests outlined in the ANL program for fracture and fatigue studies on stainless steels. The present report summarizes the influences of several variables on the fatigue life of Type 304 stainless steel, including (a) strain range ($\Delta\varepsilon_t$ from 0.4 to 4%), (b) strain rate ($\dot{\varepsilon}$ from 4 x 10^{-3} to 4 x 10^{-6} sec^{-1}), (c) tension hold time (t_H from 1 to 60 min), and (d) mean strains between -0.5 and +1.5%.

The variation of fatigue life with strain range at 1100°F and a strain rate of 4 x 10^{-3} sec^{-1} is shown in Fig. 2.1 for Type 304 stainless steel. These data were obtained for material solution annealed and aged for 1000 hr at 1100 or 1200°F before testing. Below a strain range of ∿2%, the shapes of the curves are similar to those observed at 806, 1050, and 1202°F.

It is observed that (a) at lower strain ranges (<1%) the annealed and aged material appears to have somewhat longer fatigue life than the annealed material, (b) a decrease in strain rate from 4 x 10^{-4} to 4 x 10^{-6}

sec^{-1} reduces the fatigue life by more than a factor of six, and (c) the effect of mean strain on fatigue life is found to be small for the range of strains considered.

Extensive low-cycle fatigue data generated on Type 304 stainless steel at 1100°F in air have been analyzed using frequency-modified fatigue-life equations, and the transition fatigue lives have been determined. For zero and tension hold times $\leq$1 hr, the predicted and actual lives are in agreement within a factor of 1.5, but the prediction becomes less accurate when the data obtained with compression and symmetrical hold times are also included in the analysis. The low-cycle fatigue properties are found to be strongly dependent on the frequency of loading at temperatures >900°F.

ANL is also conducting studies to evaluate the effect of sodium on the mechanical properties of reactor materials. The current emphasis is on Types 304 and 316 stainless steel, and the results of creep-rupture tests on a special low-carbon, low-nitrogen heat of Type 316 stainless steel are presented. As expected, the time to failure at a given stress level is greatly reduced.

3. HANFORD ENGINEERING DEVELOPMENT LABORATORY

(No Report)

4. NAVAL RESEARCH LABORATORY

The research program of the NRL, Metallurgy Division, Reactor Materials Branch, includes the study of the behavior of structural materials useful in reactor construction. This report is developed in support of the USAEC objective of compiling structural materials properties data for use in national reactor development programs. The NRL program is sponsored by the Office of Naval Research, the U.S. Atomic Energy Commission, and the U.S. Army Engineer Power Group. The unirradiated materials properties data developed in the course of research in the areas of high temperature materials, radiation damage, and fracture mechanics are contributed.

The fatigue crack growth characteristics of annealed and 25% cold-worked Type 304 stainless steel were investigated at 77, 800, and 1100°F (25, 427, and 593°C) as a function of the stress intensity factor range. The crack growth rates were markedly lower in the cold-worked material when compared to the annealed material at high ΔK values. With increasing temperature, the crack growth rates were found to increase. The improved fatigue crack growth resistance due to cold work was retained to 1100°F (593°C). The effect of test environment was also investigated.

The J Integral is being investigated as a means to define the toughness of structural alloys in the elastic-plastic regime. Preliminary results are presented for specimens cut from Type 304 stainless steel and Type 308 weld metal and tested in a three-point bend. Results

indicate differences in the value of J depending upon whether the computation is made on the basis of maximum load or on the basis of crack initiation. Ongoing research is addressed to questions of specimen geometry dependence and the effect of slow stable crack extension.

The dynamic tear and Charpy-V notch ductility of austenitic stainless steel plates and weld deposits representing different filler compositions and welding processes have been explored. Significant differences in notch ductility were found between plates (high) and weld deposits (low); however, energy absorption values appeared relatively independent of test temperature for the range 75 to 900°F (24 to 482°C). Reduction in dynamic tear and Charpy-V energy absorption values with 1000-hr thermal conditioning at 700 to 900°F (371 to 482°C) were also observed.

A recent NRL study has explored the radiation performance characteristics of several thick section Ni-Cr-Mo steel plates, forgings, and weldments in anticipation of advanced reactor application. One phase of the investigation involved the development of preirradiation notch ductility and tensile properties to serve as base lines for radiation effects assessments and comparisons. In general, very good notch ductility was observed for the several ASTM Type A543 plates and A508 forgings examined. A trend toward higher brittle/ductile transition temperatures by submerged arc and electroslag weld deposits was noted, to evidence a need for improved filler metals for A543 and A508 materials.

5. OAK RIDGE NATIONAL LABORATORY

Creep data collection for the Design Methods Program is continuing. The data currently are being analyzed. Some of the creep curves have been fitted to an eight-constant polynomial equation. Using our high-precision averaging extensometers the standard error for these equations was 20 to 44 μin./in., in comparison with 200 to 500 μin./in. in tests conducted with nonaveraging extensometers.

The collection of data on the effect of strain rate on the tensile properties of 2-in. plate of the type 304 stainless steel reference heat has been completed. The effect of strain rate within the range of 0.0004 to 0.4/min was small for yield stress but significant at the higher temperatures for the ultimate tensile stress. Correlations for the data were prepared. Tensile data for the 1-in. plate have been fitted to the Holloman and Ludwik equations. Tensile data from heat 8043813 were fitted to the Ludwik, Ludwigson, and Voce equations.

Studies of variation of properties of the type 304 stainless steel reference heat with product form have been completed except for the long-term tests. Heat-to-heat variation studies of type 304 stainless steel are continuing. Three heats representing strongest, average, and weakest were selected for long-term testing. A statistical analysis of creep-rupture data has been initiated. Using a data base of 407 points on

type 304 stainless steel, equations representing the behavior have been formulated. Correlation of relaxation data with creep data was examined. Our studies show that instantaneous creep rates calculated from relaxation data are in poor agreement with instantaneous creep rates calculated from constant-load creep data at comparable stresses.

Investigation of deformation behavior of the 1-in. plate of type 304 stainless steel reference heat under conditions of interspersed strain cycling and creep are under way. From our tests to date, we conclude that creep strain can have either a hardening or softening influence, and the sign of the flow stress change depends upon the prior history.

The tensile properties of type 316 stainless steel weld metal with controlled residual elements were used to compute "allowable stresses" using ASME Code rules for base metal. They were always greater than the allowable stresses for base metal. In creep tests at 649°C (1200°F) the total fracture strains exceeded 12% for times to 5930 hr, and the smallest measured reduction in area was about 55%. The rupture time behavior was compared with type 316 stainless steel metal by use of the Larson-Miller parameter and Blackburn's analysis. The fracture surfaces of the specimens were covered with dimples indicative of a relatively ductile fracture.

The type 308 stainless welds made in type 304 stainless steel base metal to simulate the FFTF vessel longitudinal seam and girth welds are characterized.

The tensile properties of CRE type 308 stainless steel welds made from several batches of electrodes and two heats of base metal are reported. Tensile properties of control welds made with conventional electrodes are reported for comparison. Preliminary evaluations do not indicate any statistically significant differences between any of these welds.

A program to investigate the effects of thermal aging on the type 308 CRE stainless steel weld metal is in progress. The greatest effect of aging occurred at 482°C (900°F) where large changes in ultimate and fracture strengths and in uniform and total elongations were observed. Creep tests on aged specimens indicate that the greatest effect of aging is to reduce rupture time at 482°C (900°F).

The yield strengths of 0.09 and 0.12% C 2 1/4 Cr-1 Mo steels differ about 30% in tests at either room temperature or 510°C (950°F) of samples cooled at either 55 or 110°C/hr (100 or 200°F/hr) from 899 to 704°C (1650 to 1300°F). Further, there is a 50% increase in tensile strength for a given carbon content as a consequence of increasing the cooling rate during the anneal cycle from 20 to 55°C/hr (35 to 100°F/hr). The ultimate tensile strength is higher at 510°C (950°F) than at room temperature. This suggests a sensitivity to strain aging. We have now completed our studies of microstructure, room-temperature hardness, tensile properties, and creep-rupture properties for 2 1/4 Cr-1 Mo steel with 0.009, 0.030, 0.120, and 0.135% C. The results are summarized.

Room-temperature tensile tests on specimens taken from the intermediate heat exchanger overlayed tubesheet forging indicated that the type 304 stainless steel just below the overlay-forging fusion line is considerably stronger than the material at a distance from the fusion line and slightly stronger than the type 308 stainless steel filler metal of the overlay. We completed tensile tests on three specimen orientations (axial, tangential, and radial) at 0.04/min at 25, 427, 482, 538, 593, and 649°C (77–1200°F). Axial specimens were also tensile tested at 0.004 and 0.0004/min at 482, 593, and 649°C (900, 1100, and 1200°F).

We have developed recommended minimum values of 0.2% offset yield strength and ultimate tensile strength for 9 Cr-1 Mo steel based on data from 24 heats of material. We have defined lower central tolerance limits on previously treated creep- and stress-rupture data, using a Larson-Miller parameter analysis. Tensile and creep minima have been used to select stress intensity limits pertinent to an ASTM Code Case. We have constructed average isochronous stress-strain curves by using a Larson-Miller analysis of 47 creep curves.

Uniaxial material behavior tests are being continued to characterize the mechanical, metallurgical, and chemical properties of each product form of the type 304 stainless steel reference heat (9T2796); 1.0-in.-thick plate was added to those forms that are being examined on a priority basis. Room-temperature stress-strain curves to 2% strain show that differences observed for as-received material (yield stress range from 26,500 to 34,400 psi) were greatly reduced by reanneal (yield stress range of 26,000 to 27,700 psi). Stress rupture data, which were obtained using reannealed specimens from seven product forms, do not indicate large differences in rupture life associated with product form or with specimen location and orientation relative to the stock material. The minimum creep rates for these seven product forms differed by only small amounts.

Special stress-strain tests were performed on specimens from the reference heat (9T2796) to allow careful exploration of inelastic behavior at relatively low strains. It was again shown that deviations from linearity begin at low stresses and develop gradually at stresses below 10,000 psi. The nonlinearity causing mechanisms at low stresses remains to be studied and identified.

Studies on the influences of thermo-mechanical variables on creep rupture of the type 304 reference heat material have been de-emphasized. Reannealing at temperatures in the range from 1010 to 1121°C (1850 to 2050°F) did not produce discernible changes. In addition, cooling rate was found to be unimportant, except in the case of a very slow rate.

Effects of cyclic deformation on subsequent creep behavior at 593°C (1100°F) is being examined. Results obtained suggest that small amounts of cold work have very little influence on subsequent creep response. In the case of cyclic creep loading, the creep rates were lower than indicated by monotonic-loading test results. The cumulative creep curve

for one cycled tubular specimen paralleled that for a second monotonically-loaded tubular specimen, but both curves were below that for a monotonically-loaded rod specimen.

Results from a multiply loaded relaxation specimen show that relaxation hardening is a gradual process. Each reloading to the original stress produced a relaxation curve that was slightly above the previous curve. In another study, it was shown that the hardening influences of creep strains are about the same as in the case of plastic strains. Although this is in agreement with other observations, additional testing is needed to clearly establish this suggested equivalency.

A machine to be used in performing creep-plasticity interaction studies was made operational and preliminary experiments were initiated. In addition, a new 50,000-lb electro-hydraulic testing machine was commissioned during this quarter.

Uniaxial-constant and step-load tests are being continued by Babcock & Wilcox. The five constant load tests that were in progress during the last reporting period remain in test, with no failures having occurred. The total test times range to 9000 hr. Similarly, the six step-load tests under way during the last period are still in progress; each specimen has undergone two load changes.

New tests were initiated on three specimens in the so-called "interrupted" constant-load series. The objective for this series is to obtain information on material degradation as a function of creep exposure through destructive examinations.

Investigations are under way to identify sources for differences between results from creep and from rupture machines. A test now in progress indicates that differences between strains determined from measurements over the load train and those from measurements over the specimen gage length do not account for the overall discrepancies. The influences of specimen bending remain to be determined.

The first tubular rupture specimen was loaded in simple tension. Creep testing was delayed due to a minor failure in the loading system.

6. WESTINGHOUSE ADVANCED REACTORS DIVISION

Creep testing of the reference ORNL Type 304 stainless steel heat (9T2796) was continued with a variety of test specimen design and conditions. Tests of two plane stress rectangular specimens and two plate specimens were completed, and an alternate damage rule has been proposed. A test matrix for specimens including welds has been pepared. Multiaxial testing of tubular specimens was initiated with two of these tests in progress and a third being set up.

1. AEROJET NUCLEAR COMPANY

W. C. Francis

1.1 INTRODUCTION

Aerojet Nuclear Company is conducting mechanical properties investigations under two programs sponsored by the AEC Division of Reactor Research and Development. Program 06031, Fatigue Tests on Cladding and Structural Materials, involves experimental fatigue tests on stainless steel Types 304 and 316 as well as Type 304 weldments. These tests are intended to determine the influence of irradiation, cold work, heat treatment, heat-to-heat property variations, and temperature on fatigue behavior. Irradiations have been conducted in EBR-II to fluences of 0.01 to 3.0×10^{22} n/cm^2 (E>0.1 MeV) at temperatures of 850 to 1100°F (454-593°C). Irradiated, thermal control, as-received, and annealed specimens are being tested at temperatures of 900 to 1300°F (482-705°C). Recent investigations of the creep-fatigue interaction, relaxation, irradiation effects and cumulative damage behavior of Type 304[1,2,3,4], Type 316[4,5,6] and Type 304/308 weldments[2,7] have been previously reported. Current work involves irradiation and hold time effects of Type 308 weld metal and interim results are reported in Section 1.2.

Program 06084, Inconel Alloy 718 Code Case Project has as its objective the planning and testing activities deemed necessary to provide data and information on base metal and welded metal properties to satisfy requirements for Code Case approval from the ASME Boiler and Pressure Vessel Committee. The service temperature ranges: ambient to 800°F (427°C) and 800 to 1200°F (427-649°C), are covered in two separate phases of the experimental work, and a separate code case application will be submitted for each temperature range. Data from the literature are used wherever they appear sufficient. Otherwise, experimental programs were initiated to acquire the necessary data. Both base material and weldments are to be covered by the applications.

For Phase I (800°F [427°C] maximum service temperature), the mechanical property tests, apart from material characterization, are related to strain fatigue behavior of the base matal, and weldability and weld qualification studies.

Phase II tests include strain fatigue, strain rate effects, and creep/fatigue interaction, both tensile and compressive, all on base metal. Creep-rupture studies were initiated for weldment material.

1.2 FATIGUE AND CREEP-FATIGUE BEHAVIOR OF SMA TYPE 304/308 STAINLESS STEEL WELDMENTS - G. E. Korth and M. D. Harper

1.2.1 Irradiation Effects on Low Cycle Fatigue of Type 308 Weld Metal

Specimens cut from SMA weldments with controlled residual elements were prepared from 2 3/8" thick FFTF residual plates and irradiated in EBR-II at 1076-1130°F (580-610°C) to fluences of $0.5\text{-}1.0\times10^{22}$ n/cm^2 (E>0.1 MeV). The specimens were cycled in strain controlled fully reversed tests at 1100°F (593°C) at a strain rate of $4\times10^{-3}s^{-1}$ with a closed loop electrohydraulic system. Testing was conducted in air using induction heating to obtain the elevated temperature. The specimens had a cylindrical gage section of 0.250 inch diameter and 0.400 inch long. An axial extensometer with a 0.375 inch gage length was used on all weld metal specimens. Further testing details can be found elsewhere[3]. Fig. 1.1 illustrates the irradiation effects of the weld metal fatigue behavior when compared to unirradiated base and weld metal previously reported[3]. At the higher total strain ranges of 2% and 1% the irradiated specimens exhibited cyclic lives of just about one-half that of the unirradiated weld metal; but at a total strain range of 0.5% the irradiated material has cyclic lives of equal to or superior to the unirradiated material, and a cross over appears eminent. The relative positions of the irradiated data on Fig. 1.1 of the various orientations has remained essentially the same, i.e. specimens orientated parallel to the weld seam still have better fatigue resistance than transverse specimens and specimens with the fusion line in the gage section have the shortest fatigue lives.

1.2.2 Tensile Hold Time Effects (Creep-Fatigue) of SMA Type 304/308 Stainless Steel Weldments

To Investigate creep-fatigue interaction of the weld metal, tests are currently being conducted with a hold period at the maximum tensile

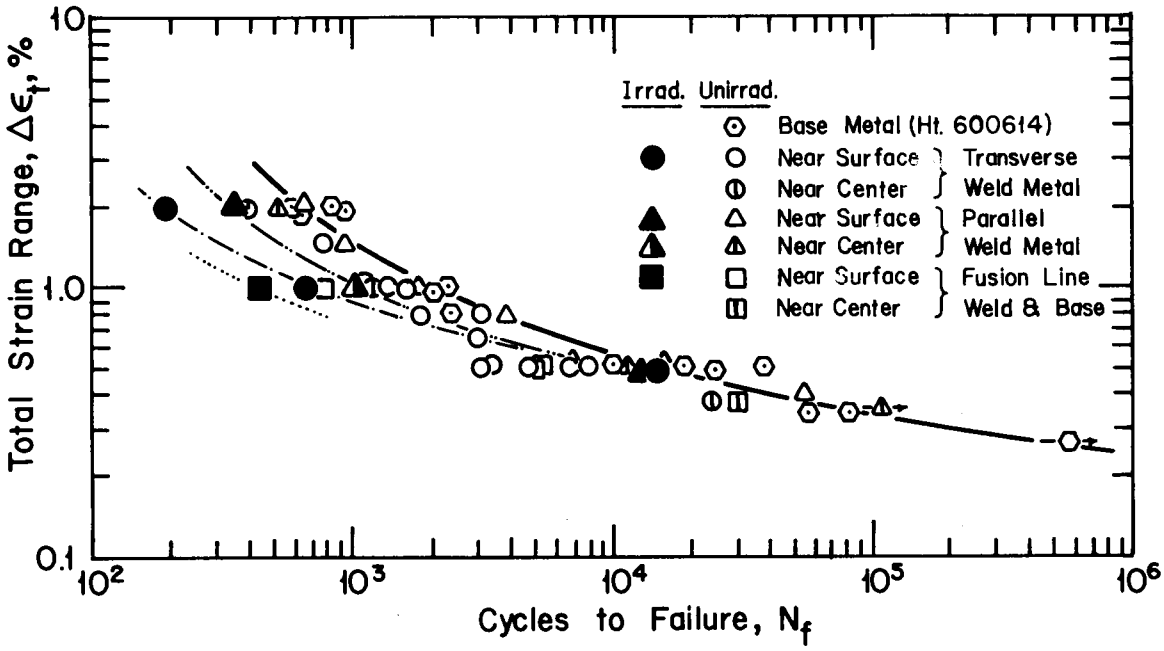

Fig. 1.1. Effects of Irradiation on the Strain Fatigue Behavior of Type 308 Stainless Steel Weld Metal at 1100°F (593°C) at a Strain rate of $4x10^{-3}s^{-1}$ Fluences are 0.5 to $1.0x10^{22}n/cm^2$ (E>0.1 MeV).

strain of each cycle. Since the strain is being held constant, stress relaxation occurs during the hold period as some of the elastic strain is converted to plastic strain. Fig. 1.2 is a time to fail, t_f, vs cycles to fail, N_f, plot of current hold time irradiated and unirradiated weldment tests conducted at a total strain range of 1% at 1100°F (593°C). The irradiation history of the irradiated specimens is the same as given in the previous section (1.2.1). Tests were conducted with hold times of 0.01, 0.1 and 0.5 hours and compared to cyclic lives of tests without hold periods. Fatigue resistance of the weld metal without hold times is inferior to the base at 1% strain range (see also Fig. 1.1), but

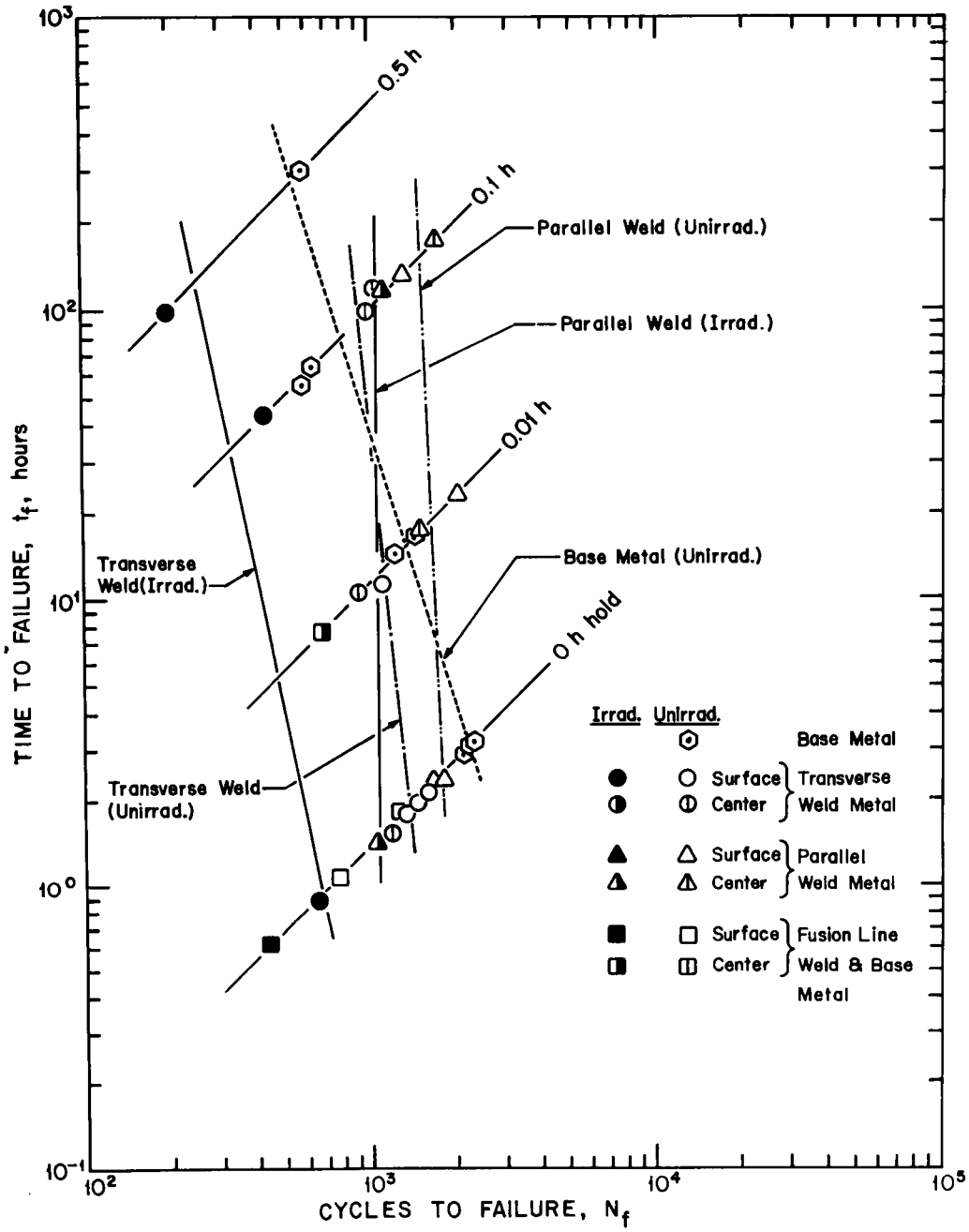

Fig. 1.2. Time to Fail vs Cycles to Fail Plot for Irradiated and Unirradiated Type 308 Weld Metal Tested at 1100°F (593°C) at a Total Strain Range of 1.0%. Fluence Levels of 0.5 to $1.0 \times 10^{22} n/cm^2$ (E>0.1 MeV).

unirradiated weld metal becomes superior as hold times increase beyond 0.01 hour. As hold periods are added to each cycle, a certain amount of creep damage occurs and the number of cycles to fail decreases for the base metal as the hold period increases. However, reductions in cyclic life is much less for the weld metal with increasing hold times except for the irradiated transverse weld material. In fact, tests conducted to date indicate that hold times have little effect on the parallel orientation, even in the irradiated condition. Specimens taken from the center of the weldment tend to have longer lives than those taken from near the surface indicating that center weld material has better creep resistance. Investigations at ORNL[8] on this same weld material have also shown that the weld material from center sections has better creep properties, but they do not show the weld metal as having any better creep properties than base metal.

Neutron irradiation has a more marked effect on specimens cut from the transverse orientation than the parallel direction. Although confirming electron metallography is not yet available, it is believed that the interpass weld boundaries and long columnar grains, both of which are perpendicular to the loading axis, collect neutron produced helium bubbles and thereby accelerate failure mechanisms. Helium bubbles collecting on boundaries of parallel specimens would have a much lower probability of being located on a boundary perpendicular to the loading axis.

1.3 INCONEL 718 CODE CASE - D. D. Keiser, H. L. Brown, G. E. Korth and J. M. Beeston

1.3.1 Strain Fatigue Tests with Hold Times

Low cycle fatigue specimens and tensile specimens were fabricated from three different heats of Inconel 718 and were tested in two conditions reflecting solution annealing at either 1750°F (954°C) or 1900°F (1038°C) and subsequently duplex aged at 1325/1150°F (718/621°C) and 1400/1200°F (760/649°C) respectively. Test details and results of the low cycle fatigue and tensile tests have been reported previously[9].

To investigate creep-fatigue interactions of Inconel 718 at 1000°F (538°C) and 1200°F (649°C) either tensile or compressive hold times were incorporated into each cycle. All specimens had received the 1750°F (954°C) solution anneal and corresponding duplex age and were tested in air at a total strain range of 2.0%. The dynamic portion of the cycle was at a strain rate of $4 \times 10^{-3} s^{-1}$. Results are shown in Figs. 1.3 & 1.4 by time to fail vs cycles to fail plots, At 1000°F (538°C) test temperature tensile hold had little effect on the cyclic life and reductions in cycles to fail was not significant. However, with compressive hold times, some reduction in cyclic life were seen.

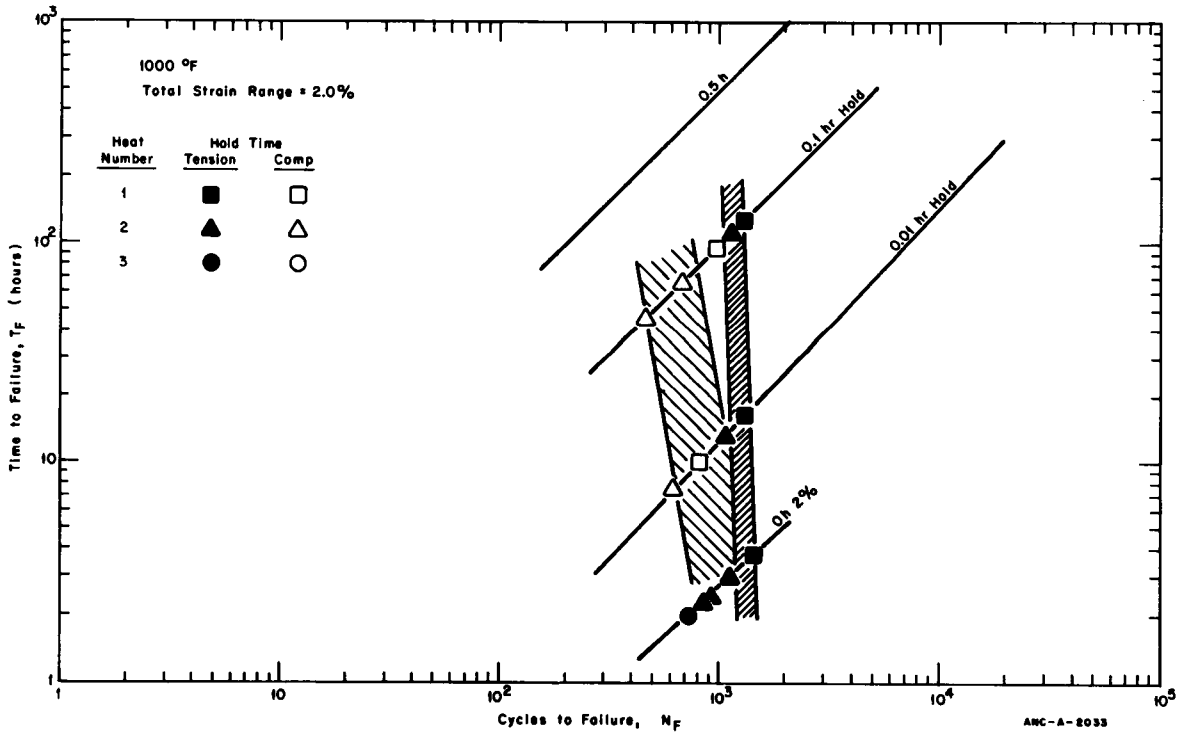

Fig. 1.3. Time to Fail vs Cycles to Fail Plot for Inconel 718 Tested at 1000°F (538°C) with Various Tensile or Compressive Hold Periods.

At 1200°F (649°C) more significant reductions in cycles to fail were noted with the compressive hold periods remaining more damaging than tensile hold times. One test conducted at 1% total strain range at 1200°F (649°C), Fig. 1.4, indicated no effect of hold time on cyclic life. There was a consistant heat to heat trend with Heat No. 1 consistently having a longer life at both temperatures. Heat No. 2 always exhibited the higher stress, however, for identical conditions in the hold time tests as well as other cyclic and tensile tests[9].

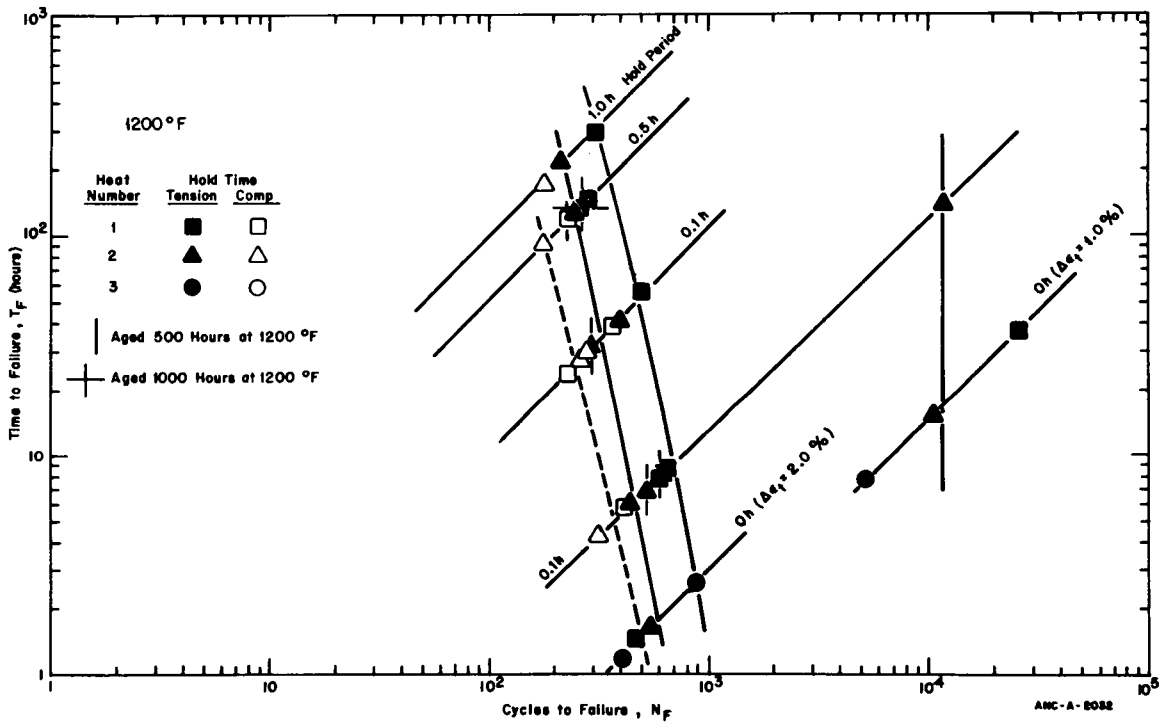

Fig. 1.4. Time to Fail vs Cycles to Fail Plot for Inconel 718 Tested at 1200°F (649°C) with Various Tensile or Compressive Hold Periods.

To investigate relatively short time stability a few specimens were aged subsequent to their normal heat treatment for either 500 or 1000 hours and then tested. No significant degradation of properties was noted (see Fig. 1.4).

Compressive hold times on Type 304 and 316 stainless steels have been shown[4,6] to be almost negligible, but for Inconel 718 the compressive hold period is the most damaging. These results are not unique and have been observed on other high strength materials such as cast Rene 80[10].

1.3.2 Strain Rate Effects on Low Cycle Fatigue

A number of fatigue tests were conducted at 1000°F (538°C) and 1200°F (649°C) by Mar-Test, Inc., Cincinnati, Ohio in support of the Inconel 718 Code Case at various strain rates. Results are illustrated in Fig. 1.5. This investigation does show that Inconel 718 is strain rate sensitive at both test temperatures.

1.3.3 Impact Tests for Materials Characterization on 1900°F (1038°C) Solution Annealed Material

Impact tests at room temperature and 650°F (343°C) were conducted on Charpy-Notch specimens. The specimens from three heats of material had been given the 1900°F (1038°C) solution anneal and 1400/1200 duplex aging heat treatment. The impact tests were conducted according to ASTM E23 "Standard Methods for Notched Bar Impact Tests of Metallic Material." The machine had been proof-tested using standard specimens as required. The proof tests corresponded to the nominal values of the standardized specimens within 1.0 ft-lb or 5.0 per cent whichever was greater. For the tests at 650°F (343°C) the specimens were held at 655°F (346°C) for one hour as determined from a dummy specimen, and tested within five seconds after removal from the furnace. The proof-test indicated the temperature did not drop more than five degrees in the five seconds.

The results are given in Table 1.1.

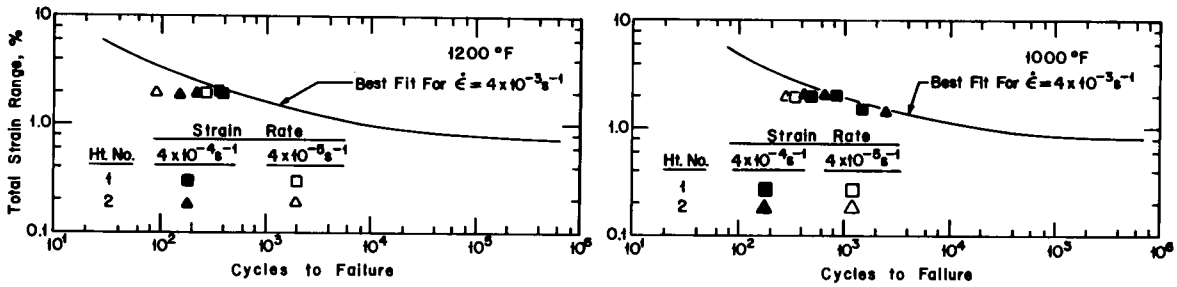

Fig. 1.5. Strain Rate Effects on the Low Cycle Fatigue Behavior of Inconel 718 with the 1750°F (954°C) Solution Anneal Plus Duplex Age.

Table 1.1. Characterization Impact Tests

Spec No.	Proj Heat No.	Temp. °F	Energy Absorbed ft-lbs	Spec. No.	Proj Heat No.	Temp. °F	Energy Absorbed ft-lbs
1122	1	RT	29.8	11131	1	650	34.5
1128	1	RT	26.2	11143	1	650	33.0
2122	2	RT	22.0	21131	2	650	29.2
2118	2	RT	23.5	21143	2	650	32.3
31140	3	RT	41.2	31154	3	650	53.0
31147	3	RT	47.0	31161	3	650	55.5

1.3.4 Tensile and Impact Tests on Weldments

Tensile and impact tests were made on specimens made from weldments prepared by the GTAW process. These tests were conducted at room temperature since this is the temperature at which qualification tests are performed. The impact tests were performed on two heats of material, HT17F8EY and HT22F2EY, and with two heat treatments on each heat. The heat treatments were a 1750°F (954°C) solution anneal with a 1325/1150°F (718/621°C) duplex age (labeled A) or a direct age at 1325/1150°F (718/621°C) (labeled C). The tensile tests additionally included a heat treatment on these two material heats of a 1925°F (1051°C) solution anneal with a 1400/1200°F (760/649°C) duplex age (labeled B).

The results of the impact tests are given in Table 1.2, and the results of the tensile tests in Table 1.3.

Table 1.2 - Impact Tests on Weldments
(Room Temperature)

Spec No.	Heat Treatment	Proj. Heat No.	Energy Absorbed ft-lbs	Spec. No.	Heat Treatment	Proj. Heat No.	Energy Absorbed ft-lbs
4-1-10	A	4	6.9	4-7-5	C	4	6.0
4-2-10	A	4	6.2	4-8-5	C	4	5.2
				4-9-5	C	4	5.4
4-4-10	A	4	8.2	4-7-10	C	4	6.0
4-5-10	A	4	7.7	4-8-10	C	4	5.5
5-1-10	A	5	9.0	5-7-5	C	5	5.0
5-2-10	A	5	7.6	5-8-5	C	5	7.0
5-3-10	A	5	8.0	5-9-5	C	5	5.7
5-4-10	A	5	7.3	5-10-5	C	5	4.5
5-5-10	A	5	8.7				

Table 1.3. Tensile Test Results for Weldments
(Room Temperature)

Spec. No.	Heat No.	Post Weld Heat Treatment	Specimen Center Dia.	Area in^2	Yield Strain 0.2% Offset ksi	U.T.S. ksi	Elong in 1" %	Reduction in Area %
4-5-8	4	A	.3535	.098145	153.9	183.7	6.0	8.6
5-1-8	5	A	.3465	.094297	152.7	182.8	5.0	10.4
5-3-8	5	A	.3520	.097314	153.1	185.5	12.7	10.5
5-4-8	5	A	.3330	.087092	151.6	161.1	2.7	5.3
5-5-8	5	A	.3525	.97591	151.7	185.0	7.3	10.8
4-2-4	4	B	.3530	.097868	168.6	194.7	20.7	39.8
4-3-4	4	B	.3520	.097314	167.5	196.8	20.7	40.3
4-4-4	4	B	.3510	.096762	171.0	196.6	20.0	40.8
5-1-4	5	B	.3530	.097868	171.7	198.2	21.3	39.3
5-2-4	5	B	.3510	.096762	171.0	198.4	13.3	19.0
5-3-4	5	B	.3520	.097314	171.6	199.4	21.3	19.9
5-4-4	5	B	.3405	.091059	170.2	198.0	20.7	40.6
5-5-4	5	B	.3525	.097591	172.2	198.8	20.0	36.0
4-8-4	4	C	.3525	.097591	170.1	200.3	11.3	17.6
5-7-8	5	C	.3515	.097038	173.1	198.9	7.3	16.0
5-7-4	5	C	.3520	.097314	174.7	200.4	8.7	14.8
5-10-4	5	C	.3610	.096762	166.4	192.2	16.0	44.1

REFERENCES

1. C. R. Brinkman, G. E. Korth, and R. R. Hobbins, *Nucl. Technol.* 16:297-307 (1972).

2. C. R. Brinkman, G. E. Korth, *J. Nucl. Mats.* 48:293-306 (1973).

3. C. R. Brinkman and G. E. Korth, *Heat-to-Heat Variations in the Fatigue and Creep-Fatigue Behavior of AISI Type 304 Stainless Steel, and the Fatigue Behavior of Type 308 Stainless Steel Weld Material,* Aerojet Nuclear Co., ANCR-1097, 1973.

4. C. R. Brinkman, G. E. Korth, and J. M. Beeston, *Comparisons of the Fatigue and Creep-Fatigue Properties of Unirradiated and Irradiated Type 304 and 316 Stainless Steel at 593°C (1100°F)*, Aerojet Nuclear Co., ANCR-1078, 1972.

5. C. R. Brinkman, G. E. Korth, and J. M. Beeston, *ASTM STP-529* (1973).

6. C. R. Brinkman and G. E. Korth, "Low Cycle Fatigue and Hold Time Comparisons of Irradiated and Unirradiated Type 316 Stainless Steel," Accepted Nov. 1973 for publication in *Met. Trans.*

7. C. R. Brinkman, G. E. Korth, and J. M. Beeston, *Comparison of the Strain-Controlled Low Cycle Fatigue Behavior of Stainless Type 304/308 Weld and Base Material*, International Conference on Creep and Fatigue in Elevated Temperature Applications, ASTM, ASME, Instn Mech Engrs, Philadelphia, Pa., Sept. 23-27, 1973 and Sheffield UK April, 1974.

8. R. T. King, J. O. Stiegler, and G. M. Goodwin, *Creep Properties of Type 308 Stainless Steel Pressure Vessel Weld with Controlled Residual Elements*, International Conference on Creep and Fatigue in Elevated Temperature Applications, ASTM, ASME, Instn Mech Engrs, Philadelphia, Pa. Sept 23-27, 1973 and Sheffield UK, April 1974.

9. C. R. Brinkman and G. E. Korth, *Strain Fatigue and Tensile Behavior of Inconel 718 from Room Temperature to 650°C*, Aerojet Nuclear Co. ANCR-1125, 1973.

10. D. C. Lord and L. F. Coffin, *Met. Trans.* 4:1647-1654 (1973).

2. ARGONNE NATIONAL LABORATORY

R. W. Weeks

2.1 INTRODUCTION

Argonne National Laboratory (ANL) is conducting an extensive program to obtain low-cycle, high-temperature, creep-fatigue data on materials of interest for Liquid Metal Fast Breeder Reactor (LMFBR) component design. The program[1] is currently providing low-cycle, high-temperature, creep-fatigue data on Types 304 and 316 austenitic stainless steel, and, in the near future, fatigue and crack-propagation data on stainless steel weldments will be obtained. The work is in immediate and direct support of fast-reactor component-design efforts. In addition, the ANL program is attempting to obtain a better understanding of creep-fatigue damage accumulation under LMFBR operating conditions (including sodium effects), so that greater design confidence levels can eventually be achieved with fewer required tests and less cost.

The information generated in the ANL fracture and fatigue studies is communicated to the LMFBR community in several ways. ANL participates in the Creep-Fatigue Task Force of the ASME Boiler and Pressure Vessel Code Committee Subgroup on Elevated Temperature Design, which is working on Code Case 1331 for high-temperature nuclear-component design. ANL data are communicated regularly through ANL Monthly Reactor Development Program Progress Reports.[2] Also, several papers have been published covering the effects of temperature and heat treatment and a comparison of Types 304 and 316 stainless steel fatigue properties;[3] the separation and analysis of the fatigue-fracture process as crack initiation and crack propagation;[4] the relative merits of various cumulative damage theories;[5] a summary of what is known about the effects of irradiation and sodium on creep-fatigue life;[6] bilinear representations of cyclic stress-strain behavior;[7] and a report of true-stress, true-strain tensile testing results.[8]

ANL is also conducting a program to evaluate the effects of sodium on the mechanical properties of LMFBR materials. The program is concentrating initially on Types 304 and 316 stainless steel, although tests on

ferritic steels are also planned. In general, the sodium acts as a mass-transfer agent in depleting nonmetallic elements (C and N) from the hotter parts of the reactor system and depositing them in the cooler portions of the system. The program entails testing of special heats of materials to simulate sodium effects, testing of specimens after long-term exposure to sodium, and postexposure testing of specimens exposed to either or both sodium and irradiation in a controlled manner. Early stress-rupture results on a special low-carbon, low-nitrogen heat of Type 316 stainless steel are presented.

2.2 FRACTURE AND FATIGUE STUDIES ON STAINLESS STEELS -- D. R. Diercks, C. F. Cheng, and P. S. Maiya

2.2.1 Low-cycle Creep-fatigue Behavior of Type 304 Stainless Steel

Most of the creep-fatigue data for Types 304 and 316 stainless steel generated during the past three years at ANL are from relatively simple tests. These results may be used as base-line data for comparison with the results of more complex tests presently under way as a part of the ANL program for fracture and fatigue studies on stainless steels.[1] The present report summarizes the influences of several variables on the fatigue life of Type 304 stainless steel, including (a) strain range ($\Delta\varepsilon_t$ from 0.4 to 4%), (b) strain rate ($\dot{\varepsilon}$ from 4×10^{-3} to 4×10^{-6} sec^{-1}), (c) tension hold time (t_H from 1 to 60 min), and (d) mean strains between -0.5 and +1.5%. Some data for Type 316 stainless steel are also reported.

The variation of fatigue life with strain range at 1100°F and a strain rate of 4×10^{-3} sec^{-1} is shown in Fig. 2.1 for Type 304 stainless steel. These data were obtained for material solution annealed and aged for 1000 hr at 1100 or 1200°F before testing. (The heat treatments are described in detail in Ref. 3.) Below a strain range of ∿2%, the shapes of the curves are similar to those observed at 806, 1050, and 1202°F.[3] However, the higher strain-range data show a rather unexpected tendency toward a less negative slope with increasing strain range for both the total and plastic strain-range curves. Preliminary examination of the specimens indicates that buckling in compression may have played a part

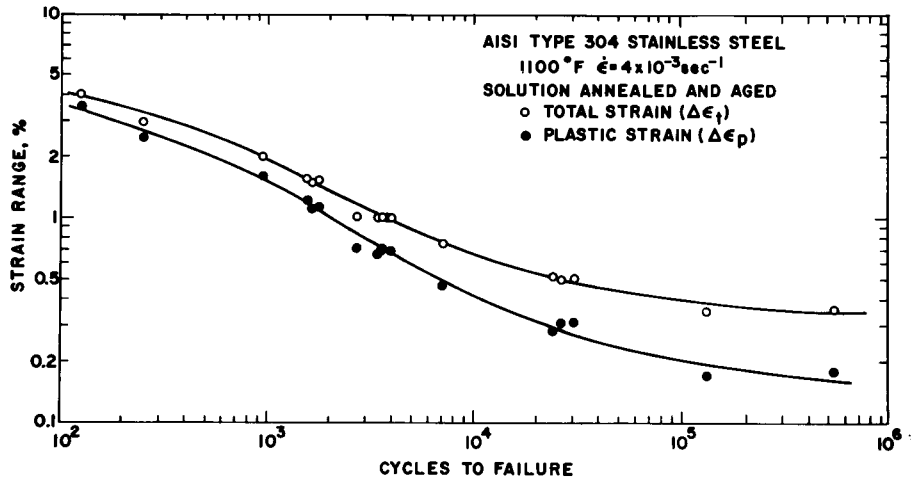

Fig. 2.1. Total and Plastic Strain Ranges vs Cycles to Failure for Solution-annealed and Aged AISI Type 304 Stainless Steel at 1100°F. Neg. No. MSD-59177.

in the failure of these higher strain specimens, thus leading to unexpectedly low values of fatigue life. A similar effect has been observed in Type 304 stainless steel tubing.[9]

Figure 2.2 shows the effect of prior heat treatment on fatigue life at 1100°F. Data for the solution-annealed material are plotted and fit by the solid curves, and the fit to the data of the solution-annealed and aged specimens in Fig. 2.1 is reproduced as dashed curves. It may be seen that, for strain ranges less than ∿2%, the aged material has a slightly longer fatigue life. The greatest difference appears to exist at lower strain ranges; the cyclic life of the aged material at a total strain range of 0.5% exceeds that of the annealed material by a factor of <1.5. Overall, the difference in fatigue life appears to be detectable, but not significant for most purposes.

At 1200°F, the effect of prior heat treatment on the fatigue life of Type 304 stainless steel is even smaller than at 1100°F, as seen in Fig. 2.3. Four pretest heat treatments are represented, and one curve can fit all points reasonably well. In general, it has been observed that with increasing test temperature the effects of prior heat treatment become less pronounced. This is apparently due to the fact that the

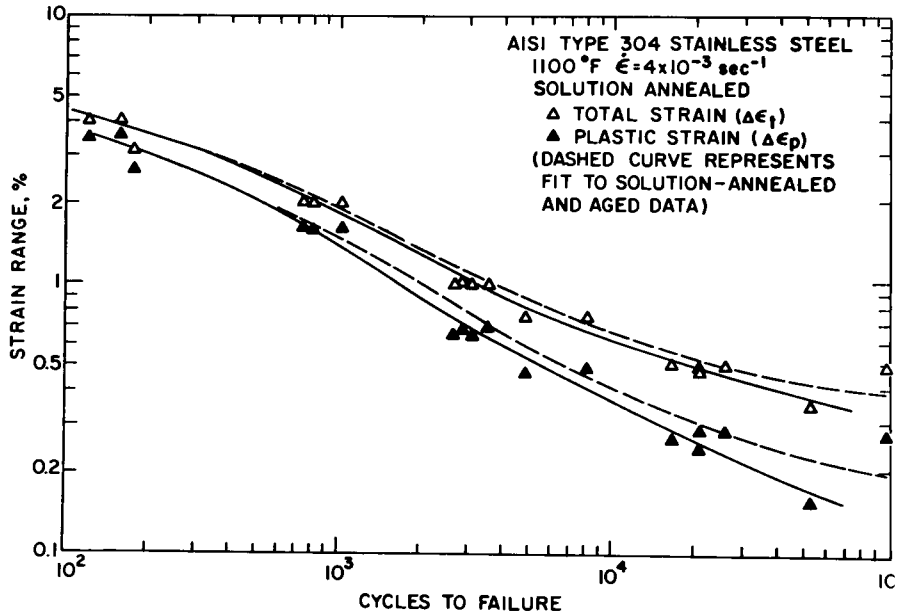

Fig. 2.2. Total and Plastic Strain Ranges vs Cycles to Failure for Solution-annealed AISI Type 304 Stainless Steel at 1100°F. The curves of Fig. 2.1 are shown for comparison. Neg. No. MSD-59182.

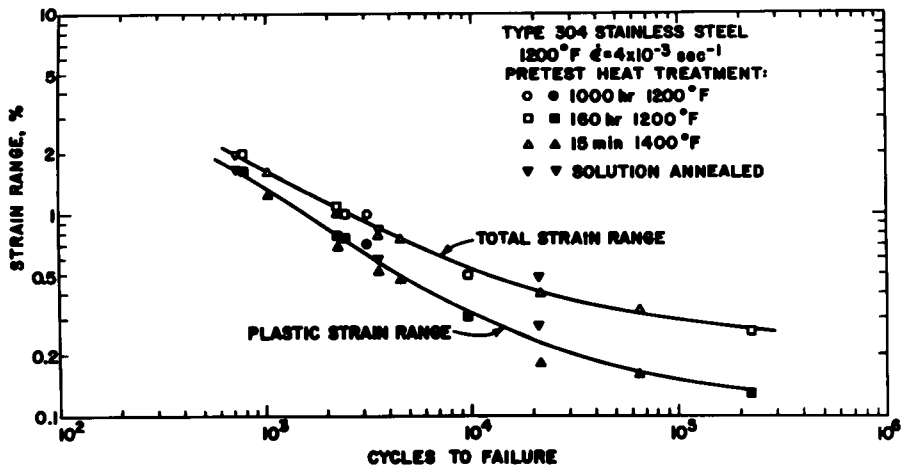

Fig. 2.3. Total and Plastic Strain Ranges vs Cycles to Failure for Type 304 Stainless Steel at 1200°F. Four heat treatments are represented. Neg. No. MSD-59266.

higher test temperatures permit carbide precipitation to occur at a more rapid rate, and, during the course of the test, carbide precipitation in the initially solution-annealed specimen essentially "catches up" with the precipitation in the aged specimen. The time required to catch up can be relatively short, since the kinetics of precipitation are greatly increased by cyclic deformation.[3]

Figure 2.4 shows the effect of strain rate on the fatigue life of Type 304 stainless steel at 1100°F. The cyclic life at a given strain range decreases with a decrease in strain rate simply because the specimen spends more time in tension at the lower strain rates; thus, the opportunity for creep to occur increases. For a total strain range of 1%, a decrease in strain rate from 4×10^{-3} to 4×10^{-6} sec^{-1} decreases the fatigue life by more than a factor of six.

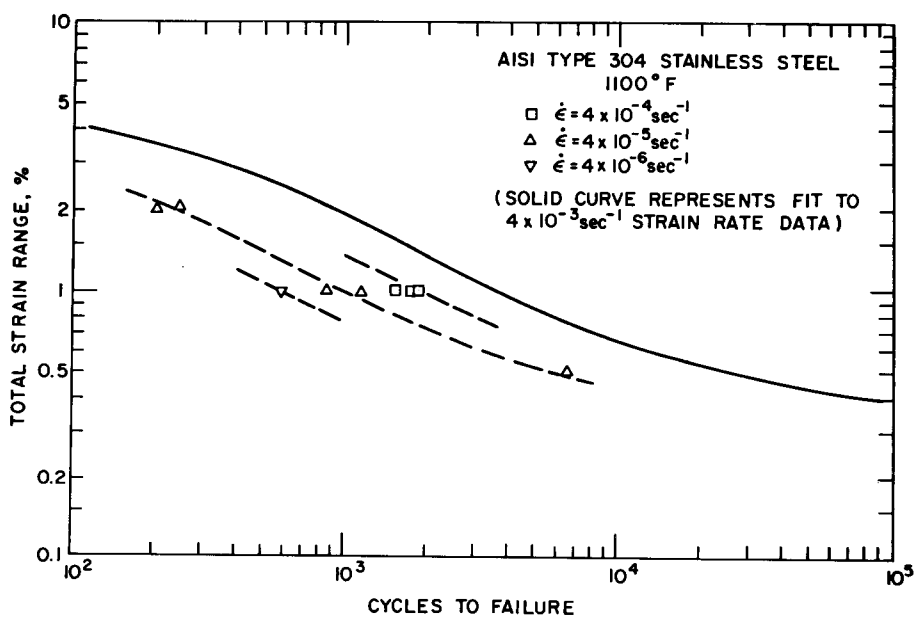

Fig. 2.4. Effect of Strain Rate on the Fatigue Life of AISI Type 304 Stainless Steel at 1100°F. Neg. No. MSD-59181.

The introduction of a tension hold time also decreases the cyclic life at 1100°F, as seen in Fig. 2.5. For a total strain range of 1%, the number of cycles to failure is decreased by about a factor of two for a 1-min tension hold time, a factor of four for a 10-min hold time, and a factor of 10 for a 60-min hold time. It is interesting to note that, for the 60-min hold-time data, points for strain rates of 4×10^{-3} and 4×10^{-5} sec^{-1} essentially coincide. This would be expected, since the difference in time spent in tension per cycle between the two tests is small relative to the 60-min tension hold time per cycle. Figure 2.6 reveals a similar effect of tension hold time on the fatigue life of Type 304 stainless steel at 1200°F.

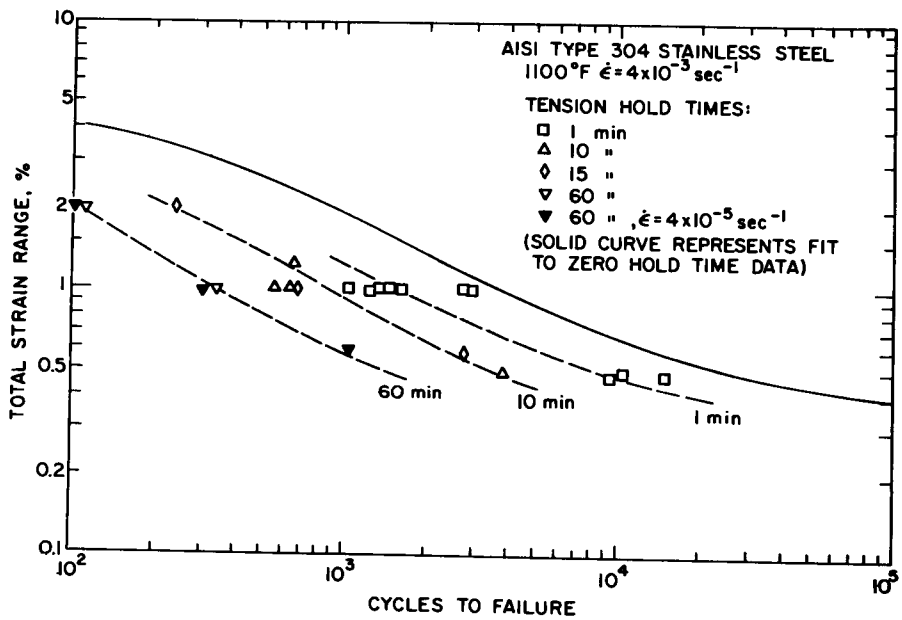

Fig. 2.5. Effect of Tension Hold Time on the Fatigue Life of AISI Type 304 Stainless Steel at 1100°F. Neg. No. MSD-59180.

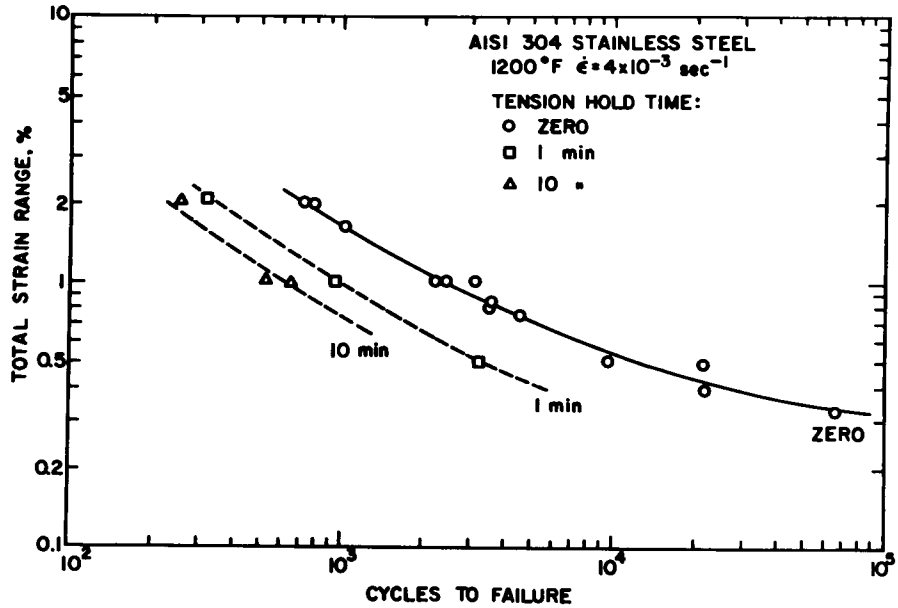

Fig. 2.6. Effect of Tension Hold Time on the Fatigue Life of AISI Type 304 Stainless Steel at 1200°F. Neg. No. MSD-59267.

Fatigue tests have also been conducted on Type 304 stainless steel employing hold time in compression and symmetrical (equal tension and compression) hold times. A detailed discussion of the results will not be given here, but it is found that holding for a given length of time in both tension and compression is less damaging than holding in tension only, i.e., the compressive portion of the cycle tends to "heal" the damage. Holding in compression only is much less damaging than holding in tension only. In addition, the fracture mode varies with loading pattern. Intergranular fracture is associated with tension hold times and transgranular fracture with zero, compressive, and symmetrical hold times.[1,4]

The effect of mean strain on fatigue life at 1100°F has also been studied for Type 304 stainless steel, and the results are shown in Fig. 2.7. Except for one point corresponding to a mean strain of -0.5%, the data are for tensile mean strains. The data for the annealed and for

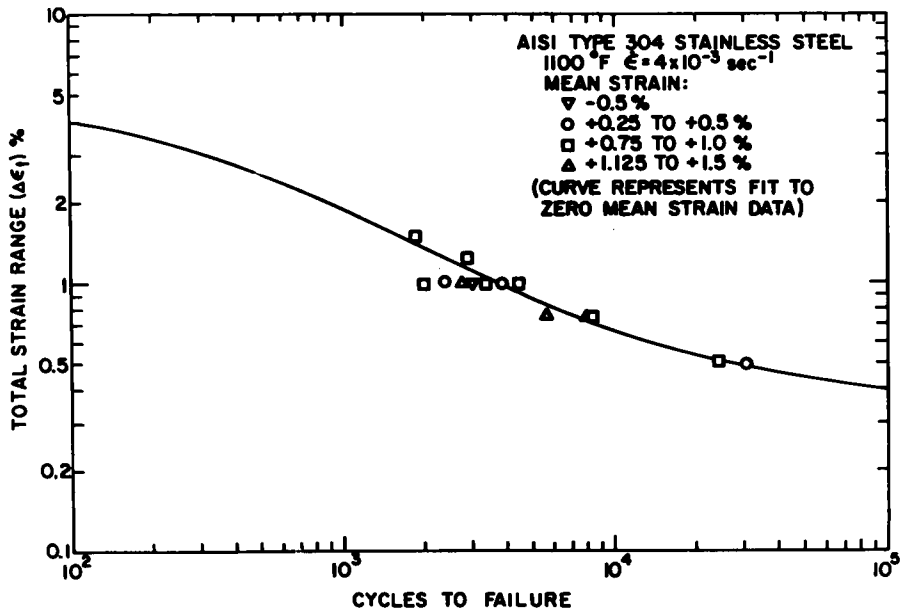

Fig. 2.7. Effect of Mean Strain on the Fatigue Life of AISI Type 304 Stainless Steel at 1100°F. Neg. No. MSD-59178.

the aged specimens are shown and are not differentiated in the figure. The data show a fair amount of scatter, but no clear trend is evident for fatigue life to decrease with an increase in tensile mean strain. Thus, the effect of mean strain for the range of strains considered is found to be small.

Fig. 2.8 summarizes zero hold-time fatigue data at four temperatures for Type 304 stainless steel (pretest heat treatments are not differentiated). The expected decrease in fatigue life as the temperature increases is evident.

A limited number of low-cycle fatigue tests have also been conducted on Type 316 stainless steel. It was found that Type 316 stainless steel exhibited the same trends toward decreasing fatigue life with increasing temperature and increasing tension hold time as had been noted for Type 304, and no data will be presented here. However, it is interesting to compare the fatigue lives of the two stainless steels under similar conditions. Figure 2.9 makes this comparison[3] for solution-annealed materials

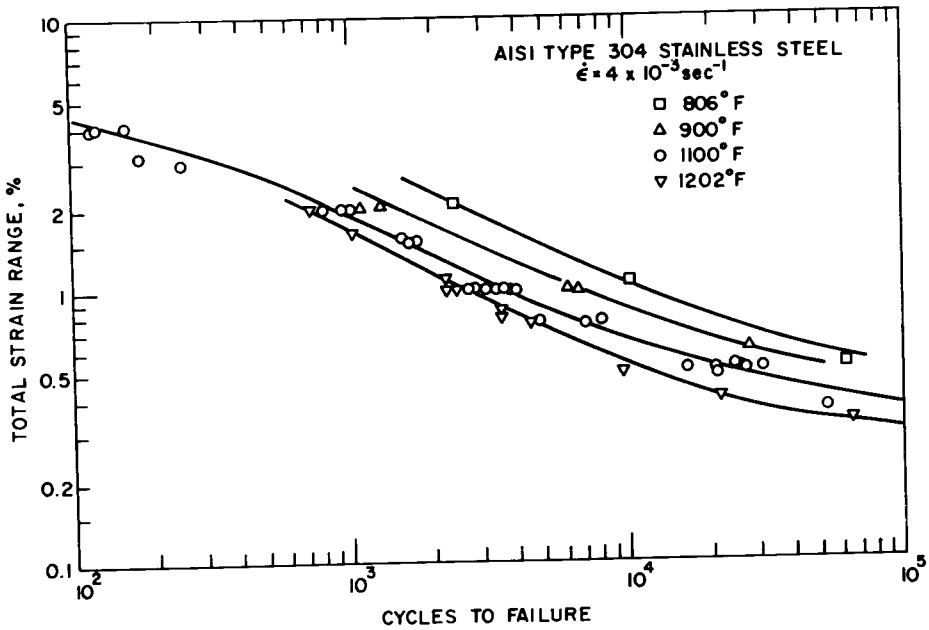

Fig. 2.8. Total Strain Range vs Cycles to Failure for AISI Type 304 Stainless Steel between 806 and 1202°F. Neg. No. MSD-59179.

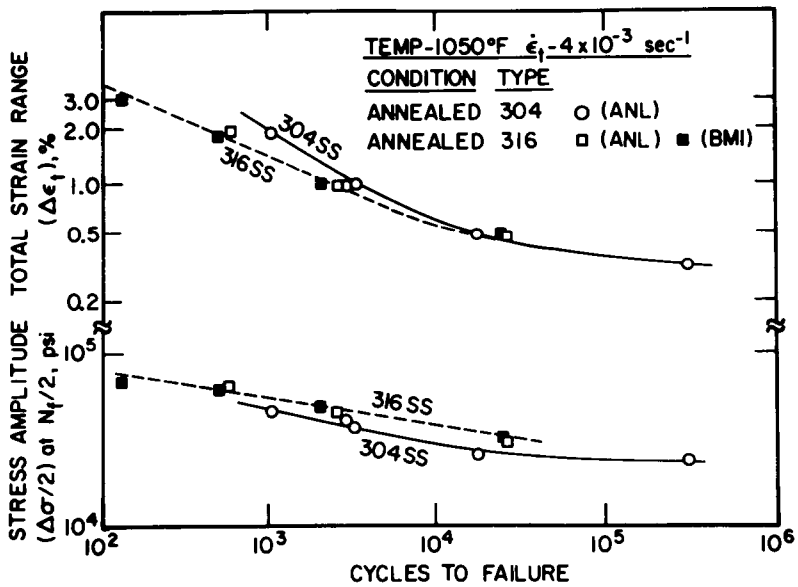

Fig. 2.9. Comparison between the Fatigue Lives of Types 304 and 316 Stainless Steel at 1050°F. Neg. No. ANL-306-2339.

tested at 1050°F and a strain rate of 4×10^{-3} sec^{-1}. Some data points generated at Battelle-Columbus (BMI) for Type 316 stainless steel are included. It can be seen that, when compared on the basis of total strain range, Type 304 stainless steel appears to be superior, but, when compared on the basis of stress amplitude, Type 316 has the longer fatigue life. This behavior may be explained by the fact that Type 316 stainless steel has a higher yield strength than Type 304 and also shows somewhat more strain hardening, based on a comparison of tensile strain-hardening exponents. Thus, a higher stress is necessary to attain the same strain for Type 316 stainless steel.

2.2.2 Analysis of ANL High-temperature Fatigue Data for AISI Type 304 Stainless Steel Using Common Phenomenological Methods

Coffin[10] has suggested that, for elevated-temperature fatigue data, the elastic strain range $\Delta\varepsilon_e$, the plastic strain range $\Delta\varepsilon_p$, the number of cycles to failure N_f, and the cyclic frequency ν may be related by an equation of the form

$$\Delta\varepsilon_t = \Delta\varepsilon_e + \Delta\varepsilon_p = \frac{A'}{E} N_f^{-\beta'} \nu^{k'} + C_2 (N_f \nu^{k-1})^{-\beta}, \qquad (1)$$

where $\Delta\varepsilon_t$ is the total strain range, and E is the elastic modulus. The coefficients A', β, β', k, k', and C_2 are constants that depend upon the material and test temperature. [The frequency (ν) in this equation is defined as $\nu \equiv [t_H + (1/\nu')]^{-1}$, where t_H is the tension hold time, and ν' is the ramp frequency ($\dot{\varepsilon}_r = 2\nu' \Delta\varepsilon_t$).] The low-cycle fatigue data generated on Type 304 stainless steel at 1100°F in air with and without hold times have been used to determine the various high-temperature coefficients by a nonlinear regression analysis, and the capabilities of Coffin's approach to prediction of life have been examined. The frequency effects at elevated temperature have been determined by comparing the test results obtained at 1100°F with the results obtained at 900°F. The six coefficients determined by using ANL test results obtained for different heat treatments and hold-time conditions are listed in Table 2.1.

Table 2.1. Coefficients for Frequency-modified Fatigue-life Equations for AISI Type 304 Stainless Steel. Constant obtained from zero hold-time data only, unless otherwise indicated.

Temperature, °F	Initial Heat Treatment	Hold Times	Constants					
			C_2	β	k	A'	β'	k_1'
900	Solution annealed and aged	-	0.466	0.487	0.936	410778	0.194	-0.010
1100	Solution annealed and aged	-	0.60	0.590	0.703	378392	0.225	0.068
1100	Solution annealed and aged	Zero and tension	0.514	0.566	0.685	422992	0.251	0.118
1100	Solution annealed and aged	Zero, tension, compression, and symmetrical	0.615	0.585	0.698	427594	0.248	0.108
1100	Solution annealed	Zero and tension	0.650	0.619	0.684	413276	0.244	0.096

Figures 2.10 and 2.11 represent plots of frequency-modified elastic and plastic strain ranges versus cycles to failure for solution-annealed material aged and nonaged, respectively.

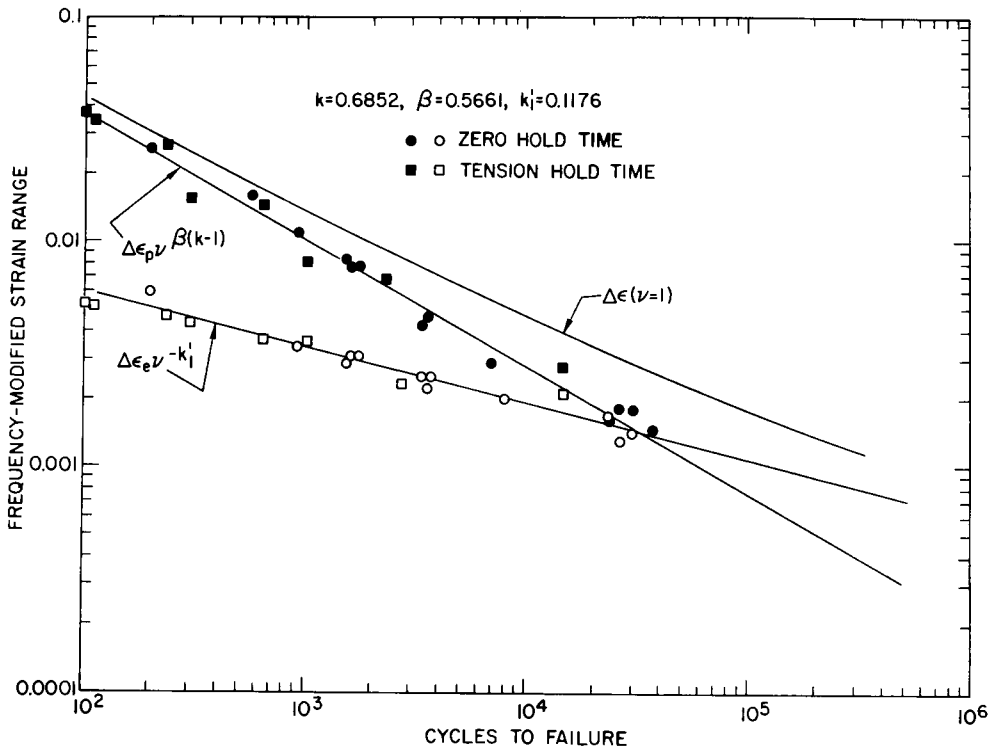

Fig. 2.10. Frequency-modified Elastic and Plastic Strain Range vs Cycles to Failure for Solution-annealed and Aged Type 304 Stainless Steel with Zero and Tension Hold Times at 1100°F. Neg. No. MSD-59370.

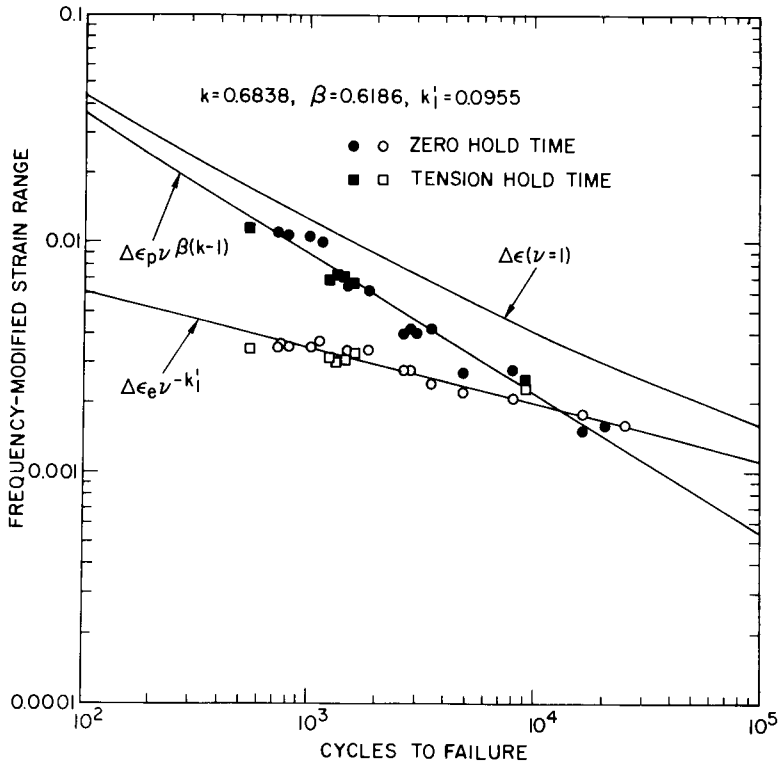

Fig. 2.11. Frequency-modified Elastic and Plastic Strain Range vs Cycles to Failure for Solution-annealed Type 304 Stainless Steel with zero and Tension Hold Times at 1100°F. Neg. No. MSD-59366.

A plot of frequency-modified elastic and plastic strain ranges versus cycles to failure for Type 304 stainless steel at 900 and 1100°F is shown in Fig. 2.12. As can be seen, the transition fatigue life N_t (the life at which the elastic and plastic strain ranges are equal) shifts to lower values with increasing temperature.

The frequency-modified equation has been used for fatigue-life prediction. For zero and tension hold times $\leq$1 hr, the predicted and actual fatigue lives are in agreement within a factor of 1.5 (Fig. 2.13). When the data obtained with compression and symmetrical hold times are also included in the analysis, the prediction becomes less accurate (Fig. 2.14). However, the predicted and actual fatigue lives are in agreement within a factor of two, except for one case.

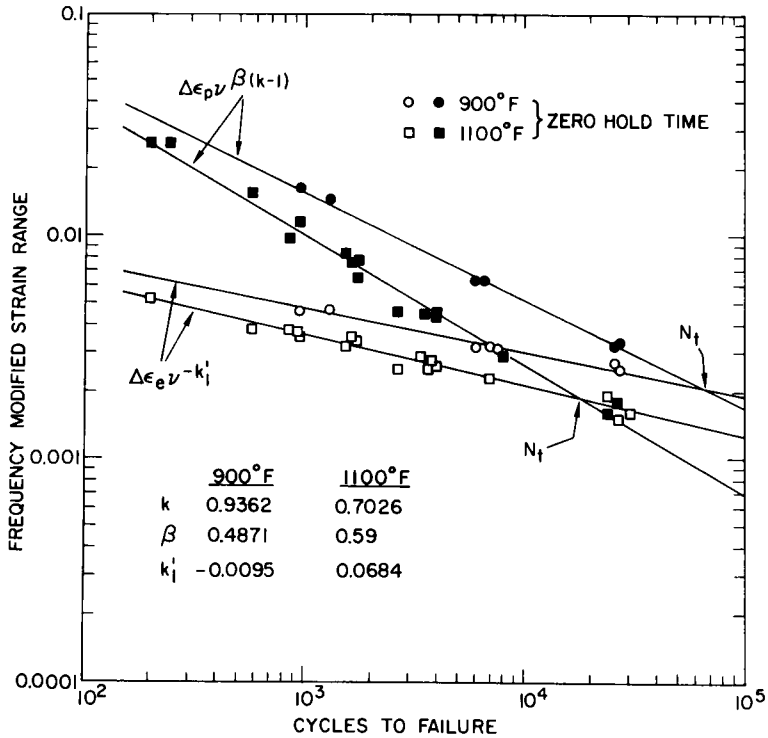

Fig. 2.12. Frequency-modified Elastic and Plastic Strain Range vs Cycles to Failure for Solution-annealed and Aged Type 304 Stainless Steel at 900 and 1100°F. N_t is transition fatigue life. Neg. No. MSD-59368.

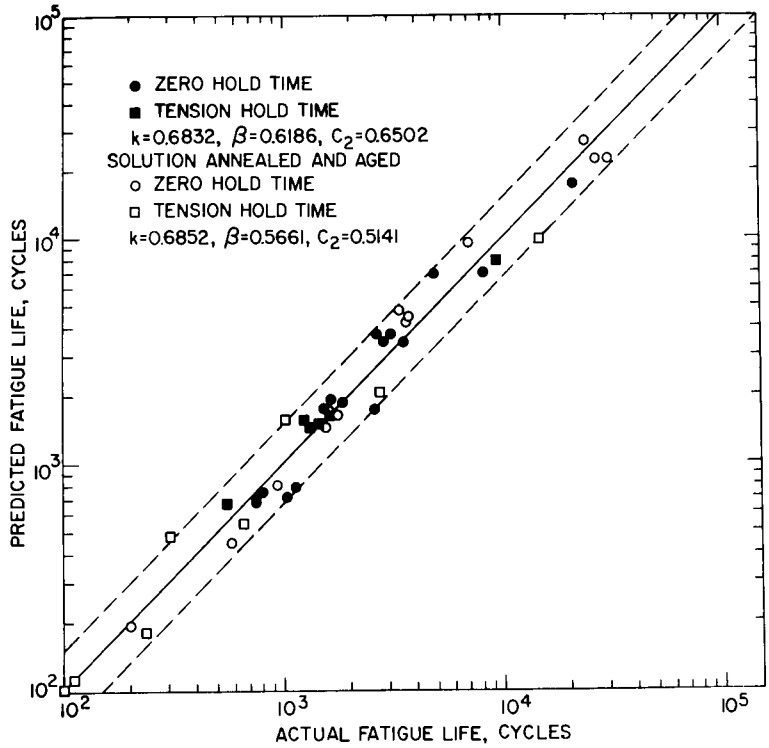

Fig. 2.13. Comparison of Actual and Predicted Fatigue Life with Hold Times for Type 304 Stainless Steel with Different Heat Treatments at 1100°F. Neg. No. MSD-59367.

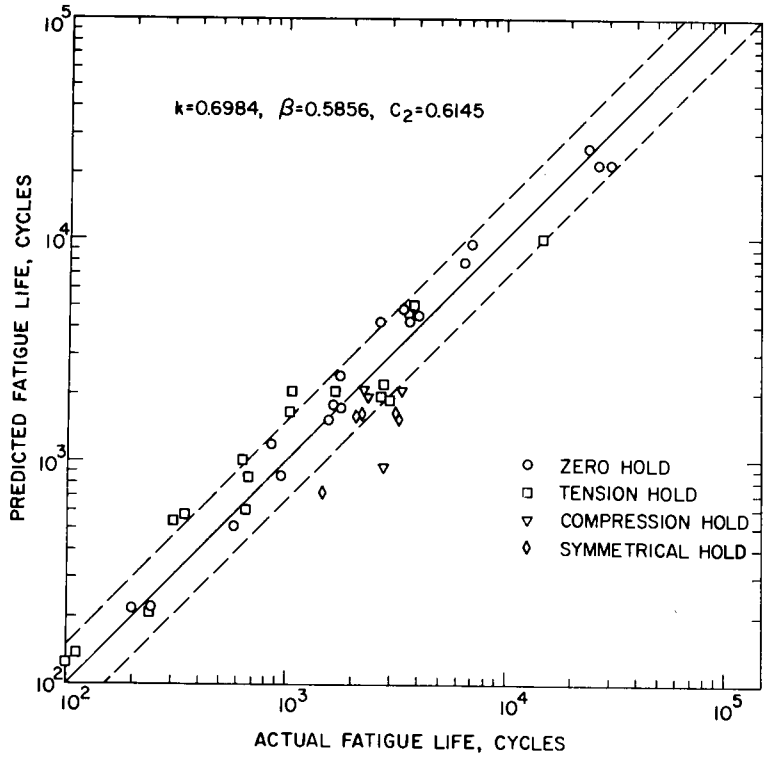

Fig. 2.14. Comparison of Actual and Predicted Fatigue Life with Hold Times for Solution-annealed and Aged Type 304 Stainless Steel at 1100°F. Neg. No. MSD-59369.

2.3 SODIUM EFFECTS ON LMFBR MATERIALS -- J. J. Weins and T. F. Kassner

2.3.1 Effect of Reduced Carbon and Nitrogen Content on the Creep Rupture Strength of Type 316 Stainless Steel

Flowing sodium is known to cause a reduction in the levels of both carbon and nitrogen in the stainless steel components in the relatively hot portions of a sodium system. In an effort to determine what effect this reduction might have on the mechanical properties of reactor materials, creep-rupture tests have been and are being conducted on 20% cold-worked material from a special heat of Type 316 stainless steel containing low carbon and nitrogen concentrations. The initial data, shown in Fig. 2.15, are compared with results obtained with FFTF heat V87210 of Type 316 stainless steel, which has a similar nitrogen concentration but a higher

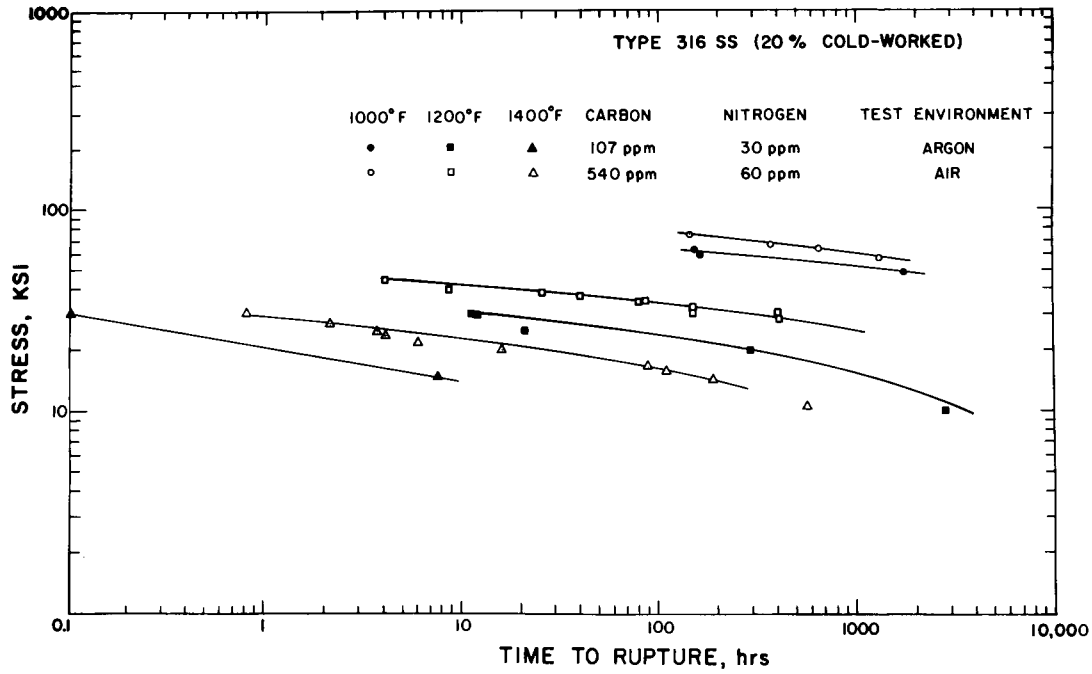

Fig. 2.15. The Effect of Chemistry on Stress Rupture of Type 316 Stainless Steel. Neg. No. MSD-59255.

carbon concentration. The compositions of the two materials are given in Table 2.2. The decrease in the stress-rupture properties of the modified material can be attributed to the lower concentration of nonmetallic elements rather than minor variations in the substitutional element composition. Tests of similar duration to those shown in Fig. 2.15 are in progress at temperatures between 593 and 760°C; longer term tests at 650°C are also being conducted at stress levels below 10 ksi to better evaluate the effect of thermal aging on the creep-rupture behavior.

The material under test is homogeneous with respect to chemistry and, therefore, will not be typical of piping sections. Since it is expected that the reduced levels of carbon and nitrogen in the piping sections will not be uniform, these data are therefore expected to represent a lower limit with respect to the effect of loss of carbon and nitrogen on creep-rupture properties.

Table 2.2. Composition of the FFTF and Modified Type 316 Stainless Steel (Composition in wt %)

Element	FFTF Heat V87210	Modified Heat
Cr	16.50	17.50
Ni	13.64	13.70
Mo	2.40	2.08
Mn	1.64	1.50
Si	0.44	<0.002
Cu	0.07	0.002
Co	0.04	<0.01
P	0.011	-
N	0.006	0.003
C	0.054	0.0107
B	0.0006	<0.01
S	0.006	-
Fe	Balance	Balance

REFERENCES

1. R. W. Weeks, D. R. Diercks, and C. F. Cheng, "ANL Low-cycle Fatigue Studies -- Program, Results, and Analysis," ANL-8009 (in press).

2. Argonne National Laboratory, Reactor Development Program Progress Reports (Fatigue Testing Reports) September 1970 through October 1973.

3. C. F. Cheng, C. Y. Cheng, D. R. Diercks, and R. W. Weeks, "Low-Cycle Fatigue Behavior of Type 304 and 316 Stainless Steel at LMFBR Operating Temperature," pp. 335-364 in Fatigue at Elevated Temperatures, ASTM STP-520 (1973).

4. C. Y. Cheng and D. R. Diercks, "Effects of Hold Time in Low-cycle Fatigue Behavior of AISI Type 304 Stainless Steel at 593°C," Met. Trans. 4(2), 615-617 (Feb 1973).

5. Masaki Kitagawa, "Hold-Time Effect in High Temperature Fatigue Fracture of Type 304 Stainless Steel," Trans. Am. Nucl. Soc. 15(2), 736-737 (Nov 1972).

6. R. W. Weeks, T. F. Kassner, and J. J. Weins, "The Influence of Sodium and Radiation on the Creep and Fatigue of Fast Reactor Components," presented at Intl. Conf. on Creep and Fatigue in Elevated Temperature Applications, Philadelphia, Pa., Sept 23-28, 1973.

7. C. F. Cheng and C. Y. Cheng, "Bilinear Representation of Stress-Strain Behavior of Type 304 and 316 Stainless Steel Cyclicly Deformed at 800-1200°F," presented at the 2nd Intl. Conf. on Structural Mechanics in Reactor Technology, Berlin, Germany, Sept 10-14, 1973 (to be published).

8. D. R. Diercks and W. F. Burke, "Elevated Temperature True-stress True-strain Tensile Tests on Type 304 Stainless Steel," submitted to 1974 Spring Meeting of the Pressure Vessel and Piping Division of ASME.

9. K. E. Horton, "Investigation of Thermal-Stress-Fatigue Behavior of Stainless Steels," EURAEC-1034, ATL-A-141 (1964), Advanced Technology Laboratories, Mountain View, California.

10. L. F. Coffin, Jr., Proc. Air Force Conf. on Fatigue and Fracture of Aircraft Structures and Materials, AFFDL TR 7D-144, pp. 301-312 (Sept 1970); and Met. Trans. 2, 3105 (1971).

3. HANFORD ENGINEERING DEVELOPMENT LABORATORY

Contribution not received in time for inclusion in this issue; it will be included in the subsequent report.

4. NAVAL RESEARCH LABORATORY

L. E. Steele

4.1 INTRODUCTION

The research program of the NRL, Metallurgy Division, Reactor Materials Branch, includes the study of the behavior of structural materials useful in reactor construction. This report is developed in support of the USAEC objective of compiling structural materials properties data for use in national reactor development programs. The NRL program is sponsored by the Office of Naval Research, the U. S. Atomic Energy Commission, and the U. S. Army Engineer Power Group. The unirradiated materials properties data developed in the course of research in the areas of high temperature materials, radiation damage, and fracture mechanics are contributed.

4.2 FATIGUE CRACK GROWTH IN TYPE 304 STAINLESS STEEL - D. J.Michel and H. H. Smith

4.2.1 Background

The resistance to fatigue crack growth in alloys and weldments intended for fast breeder reactor applications is being investigated. The effects of composition and microstructure are among the variables being considered at temperatures of primary liquid-metal fast-breeder reactor (LMFBR) interest. This report summarizes pertinent results concerning fatigue crack growth in Type 304 stainless steel plate material. [1-4]

4.2.2 Materials and Test Procedures

The chemical composition and tensile properties of the Type 304 stainless steel used in this work are given in Table 4.1. Fatigue crack growth rates on annealed and 25% cold-worked material were determined at 77, 800, and 1100 F (25, 47, and 593 C). Single-edge-notched specimens containing side grooves and oriented in the RW direction were

cycled at 10 cpm in cantilever bending under zero-to-tension loading to a constant maximum load. Induction heating was used for the elevated temperature tests. All data were analyzed to determine crack growth rate as a function of stress intensity at the crack tip. This analysis was applied since it has been shown by numerous investigators that growth rate (da/dN) and stress intensity factor range (ΔK) are related by a power law. This procedure allows the direct comparison of the fatigue crack growth resistance of materials and provides useful design data.

4.2.3 Results

The fatigue crack growth behavior of 304 stainless steel at 77 F (25 C) is shown in Fig. 4.1 for both the annealed and cold-worked conditions.[1-2] It is seen that the crack growth rates are nearly identical below a ΔK of about 45 ksi$\sqrt{\text{in.}}$ but differ slightly at higher values. The effect of cold-work is to reduce the crack growth rate, especially with higher values of ΔK. The correspondence of data points taken at the two load levels for each material indicate the validity of the stress intensity approach.

Figure 4.2 illustrates the fatigue crack growth behavior of annealed and 25% cold-worked Type 304 stainless steel at 800 F (427 C). The data[1-2] show that cold work produces a substantial increase in fatigue crack growth resistance at high ΔK values. At the early stage of crack growth, a higher ΔK was required in the cold-worked material than in the annealed material to produce crack growth.

At 1100 F (593 C), 25% cold work remains effective to improve fatigue crack growth resistance of Type 304 stainless steel at lower ΔK levels as shown in Fig. 4.3. The data[1] illustrate that the crack growth rate for a given ΔK value increases for both annealed and 25% cold-worked material with increasing temperature.

This effect is also seen in Fig. 4.4 where the crack growth data at 77, 800, and 1100 F for annealed material are plotted together.[3-4] In comparison with the 77 F results, the data at 800 and 1100 F exhibit crack growth curves having single power law relationships over narrower ΔK ranges. The slope of the curve, exponent m, is seen to be higher at

intermediate growth rates at 800 F than at 77 F, but decreased at 1100 F. Thus, the crack growth rates at high ΔK values are seen to be similar at both 800 and 1100 F and appreciably higher than at 77 F.

The effect of environment on fatigue crack growth resistance in annealed Type 304 stainless steel at 77 F (25 C) is shown in Fig. 4.5. For these experiments[4] a closed chamber containing a window for specimen observation was placed around the specimen test section. A continuous air flow was maintained during testing. The dry air had a frost point of -112 F (-80 C) and the humid air had a relative humidity of >90%. The results in Fig. 4.5 show that the crack growth rates were appreciably increased in humid air at low ΔK levels, slightly increased at intermediate ΔK levels (<55 ksi$\sqrt{\text{in.}}$), and not affected at high ΔK levels. The results indicate a lower ΔK threshold in humid air as compared to the dry air. The crack growth rates in room air, relative humidity from 48 to 62% during testing, are clearly within the growth rates in dry and humid air.

In summary, the fatigue crack growth results for Type 304 stainless steel indicate that crack growth rate is substantially controlled by the stress intensity factor range for a given material condition and that the crack growth rates increase with increasing temperature. It is recognized, however, that with increasing temperature the crack growth process becomes increasingly sensitive to variations in material composition and microstructure. These points are being addressed during other phases of the present fatigue crack growth investigations.

Table 4.1. Composition and Tensile Properties of Type 304 Stainless Steel

Chemical Composition

C	Mn	P	S	Si	Cr	Ni
0.048	1.48	0.025	0.015	0.52	18.57	9.45

Tensile Properties

	0.2% Yield Strength ksi	Tensile Strength ksi	Elongation %	Reduction in Area %
Annealed	37.0	83.0	57	72
Cold Rolled	74.0[a]	111.3[a]	10[b]	

[a] Determined from compression test

[b] Uniform elongation

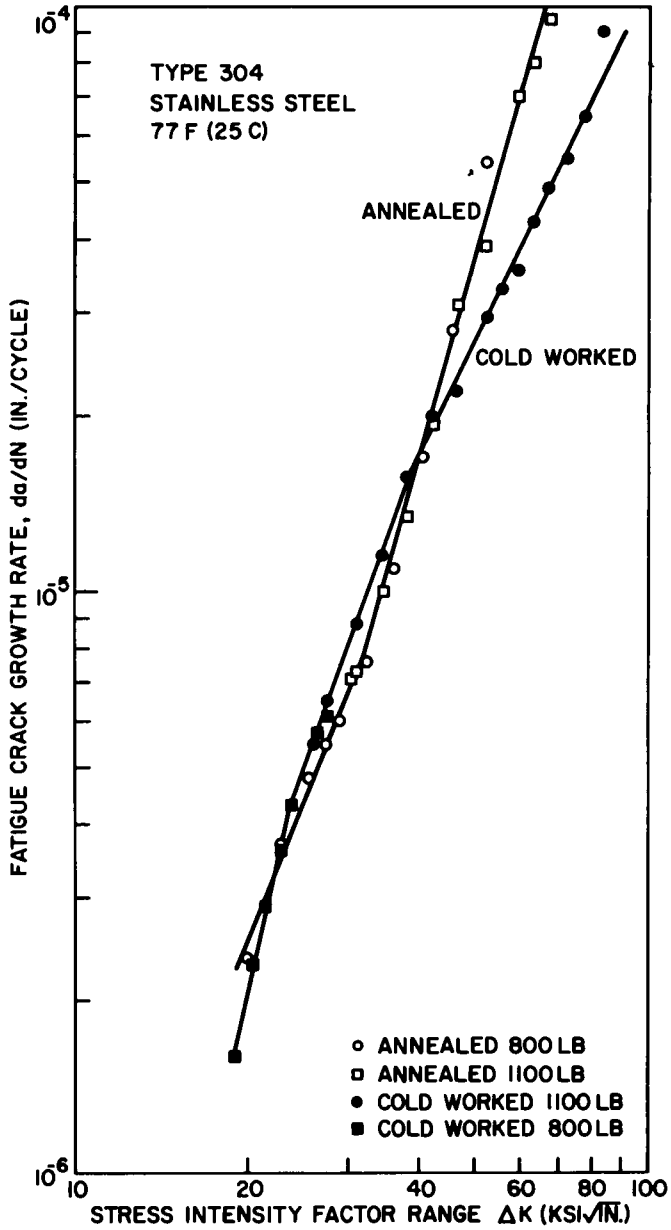

Fig. 4.1. Fatigue Crack Growth Characteristics of 25 Percent Cold-Worked and Annealed Type 304 Stainless Steel at 77 F (25 C).

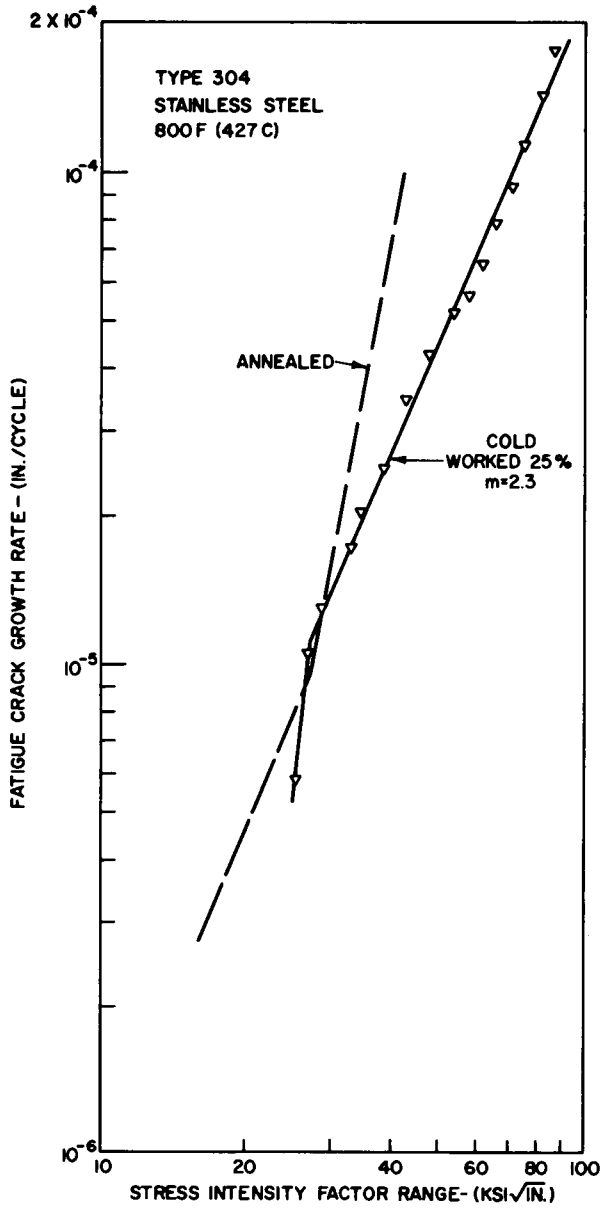

Fig. 4.2. Fatigue Crack Growth Characteristics of 25 Percent Cold-Worked and Annealed Type 304 Stainless Steel at 800 F (427 C).

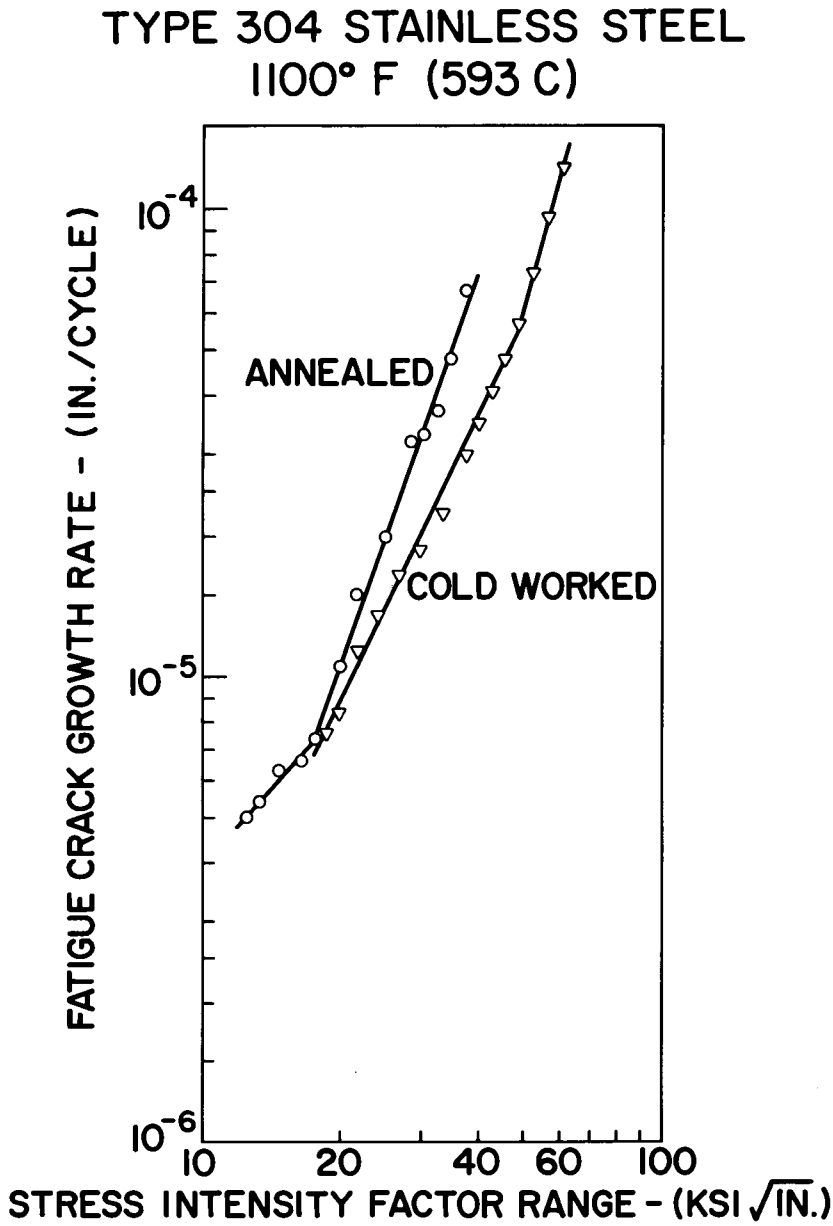

Fig. 4.3. Fatigue Crack Growth Characteristics of 25 Percent Cold-Worked and Annealed Type 304 Stainless Steel at 1100 F (593 C).

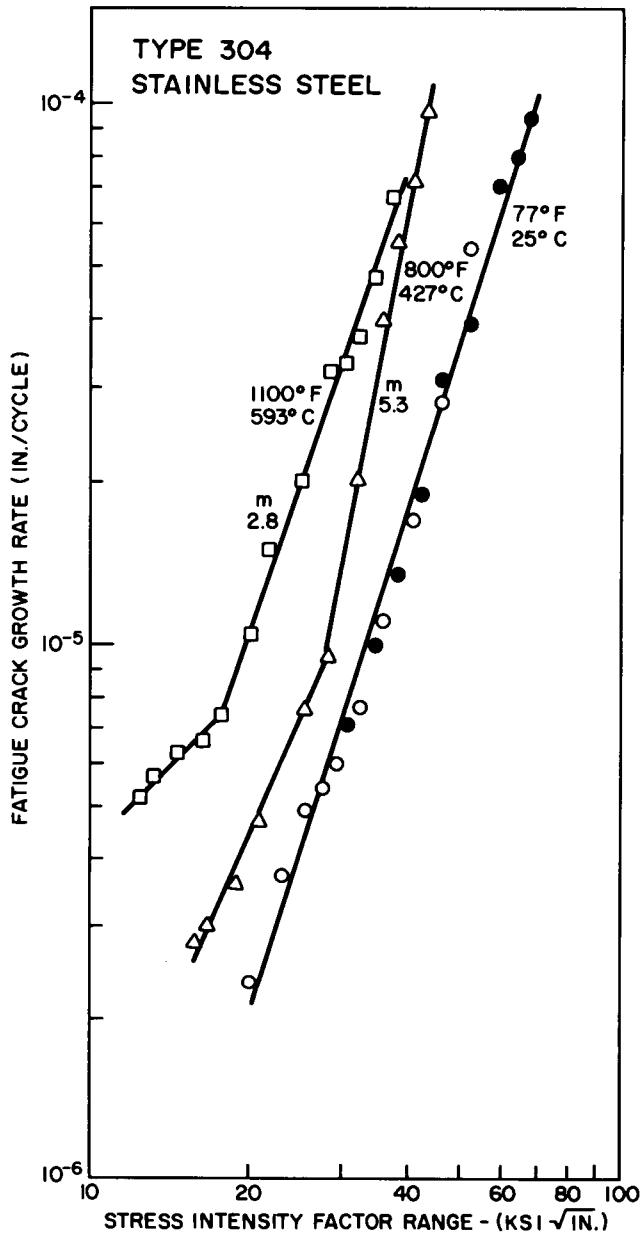

Fig. 4.4. Dependence of Fatigue Crack Growth Rate in Type 304 Stainless Steel at Several Temperatures on Stress Intensity Factor Range. Closed Symbols Represent Separate Tests.

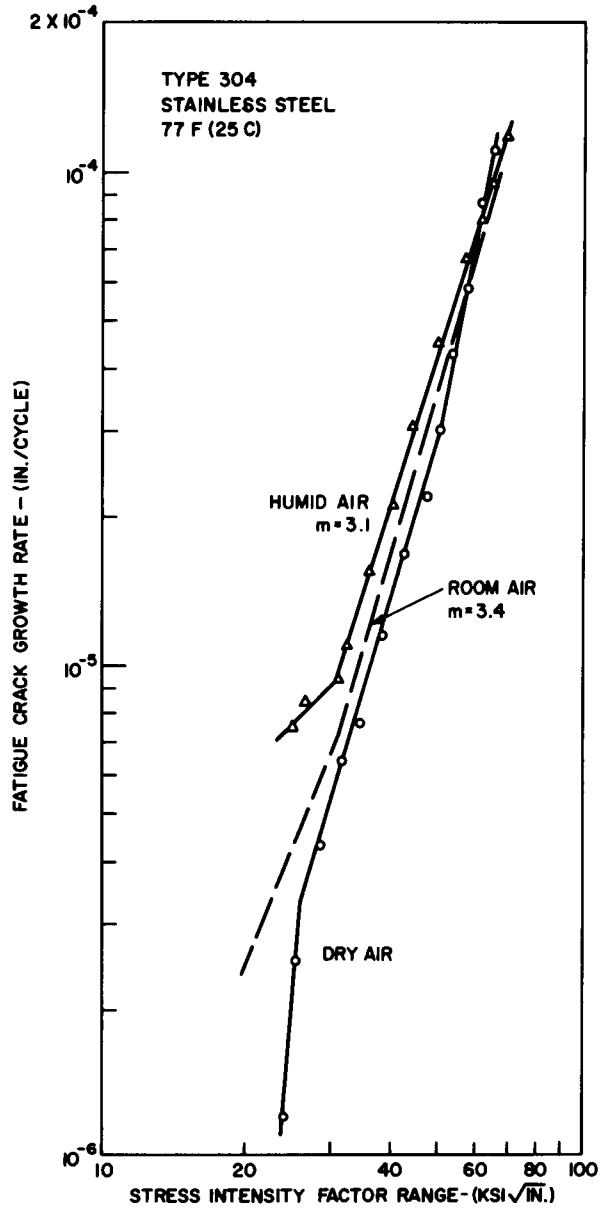

Fig. 4.5. Effect of Humidity on Crack Growth Rates in Type 304 Stainless Steel at 77 F (25 C).

4.3 J-INTEGRAL CHARACTERIZATION OF STAINLESS STEEL - F. J. Loss and R. A. Gray, Jr.

4.3.1 Background

The fracture toughness of austenitic stainless steel is being characterized in terms of the J Integral. The J-Integral concept[5-6] offers a promising means with which to express flaw instability in the elastic-plastic region in quantitative terms that are related to structural design parameters. The fact that the J Integral is applicable to cases of large scale plasticity, where linear elastic fracture mechanics analysis is invalid, provides the impetus for development of this technique. However, the theoretical promise of the J Integral must be demonstrated experimentally (i.e., validity of J as a material property). J-Integral characterizations also must be evolved for various structural alloys in terms of environmental conditions (temperature, radiation exposure, etc.) and metallurgical variables (chemistry, heat treatment, and cold working).

4.3.2 Preliminary Investigations

4.3.2.1 Materials and Specimen Types

Preliminary investigations of the J Integral have been undertaken using AISI Type 304 stainless steel (SS) plate and Type 308 SS weld metal. Tests have been conducted under slow loading used a notched three-point bend specimen having the dimensions: width (W) = 0.394 in., thickness (B) = 0.197 in., and length (L) = 2.165 in. Most specimens were fatigue precracked to give an a/W ratio of 0.3, where "a" is the total notch length. The details of the testing and J evaluation procedures are given in Reference 7.

4.3.2.2 Results

Table 4.2 presents the results of the J-Integral evaluations for the Type 304 plate and Type 308 weld metal under various conditions of notch preparation, temperature, cold work, and fluence. Chemical

compositions and mechanical properties are provided in Table 4.3.

The J-Integral values in Table 4.2 have been computed by two methods. Method 1 is an approximate procedure developed by Rice[8] and is based on the area (i.e., energy) of the specimen load versus midspan deflection record. Rice has shown that

$$J = \frac{2A}{B(W-a)} \qquad \text{Eq. 1}$$

where "A" is the area under the load versus deflection record up to the point of crack instability for a deeply notched beam in bending. Method 2 was devised by Bucci and coworkers[9] and uses the results from a load versus deflection record from one specimen to estimate the records for identical specimens having different crack lengths. These records are then used to compute J by means of a compliance calibration technique. The two described methods were applied to compute J at: (a) the point of maximum load on the specimen, and (b) the point of crack initiation. The point of crack initiation usually does not correspond to the maximum load on the specimen because of the phenomenon of slow, stable crack extension with rising load.

4.3.3 Conclusions

The results in Table 4.2 show general agreement between the two approximate methods of computing J. In some cases, however, a large difference is exhibited between the J values computed at the points of crack initiation and maximum load. It has been shown by others[10-11] that the J value at the point of maximum load is geometry dependent. Consequently, the structural applicability of J computed in this way requires further investigation and clarification. The value of J computed at the initiation of slow, stable crack extension may produce an overly conservative estimate of the material toughness. In other words, the structure may be limited to an applied J value equal to the J at crack initiation when, in fact, a much larger load could be tolerates.

Figure 4.6 presents a comparison of load versus deflection records for Type 304 SS in the annealed and cold-worked conditions. If it is

Table 4.2. Summary of J-Integral Values for SS Plates and Weld Metal

Code	Spec. No.	Material*	Notch† Prep.	Test Temp. (°F)	Method 1		Method 2	
					Crack Initiation (in.lb/in.^{2})	Max. Load	Crack‡ Initiation	Max. Load
P-10-54	1	I, A, WR	F	550	105	894	75-82	880-960
P-10-49	2	I, A, WR	F	550	-	548	-	530-600
P-10-33	3	I, CW, WR	F	550	247	366	190-215	310-340
P-10-36	4	I, CW, WR	F	550	177	222	160	215
P-10-45	5	U, CW, WR	F	550	-	325		
P-10-19	6	U, A, WR	F	550	-	2412		
P25-52	7	U, A, WR	P	RT	1682	7172		
P25-14	8	U, A, RW	P	RT	2085	9446		
P25-15	9	U, A, RW	M	RT	2287	8055		
P25-55	10	U, A, WR	P	1000	-	1765		
P25-7	11	U, A, RW	P	1000	-	2618		
P25-8	12	U, A, RW	M	1000	-	3347		
P26-7	13	U, Weld	P	RT	660	974 est.		
P26-5	14	U, Weld	P	1000	-	1045		

*304 SS or 308 SS weld
I - irradiated to fluence of 1.08×10^{21} n/cm^2 >0.1 MeV
U - unirradiated
A - annealed
CW - cold worked
RW and WR refer to specimen orientation

† F - fatigued
M - machined (60° tip angle)
P - machined(knife-pressed tip)

‡ Range of values for plane stress or plane strain calculations.

Table 4.3

Chemical Composition and Mechanical Properties

Type of Material	Composition, Weight Percent									
	C	Mn	P	S	Si	Ni	Cr	Mo	Co	Ta
304 SS Plate	0.050	1.48	0.028	0.016	0.53	9.53	18.57	0.7	-	-
308 S/A Weld	0.030	1.60	0.021	0.010	0.68	9.7	21.0	0.2	-	-

Mechanical Properties

	Unirrad. Annealed			Irrad. Annealed	Unirrad. Cold Worked			Irrad. Cold Worked		
304 SS Plate										
Temp. °F	RT	550	1000	550*	RT	550	1100	RT	550	1100
YS (ksi)	30	16.8	14	65	109	88.5	68.8	126.2	116.1	82.3
TS (ksi)	81.8	54.4	48	83	117	93.9	68.8	132.2	116.1	84.1
308 S/A Weld (Unirrad.)										
Temp. °F	RT		1000							
YS (ksi)	66		44							
TS (ksi)	107		60							

*Estimated

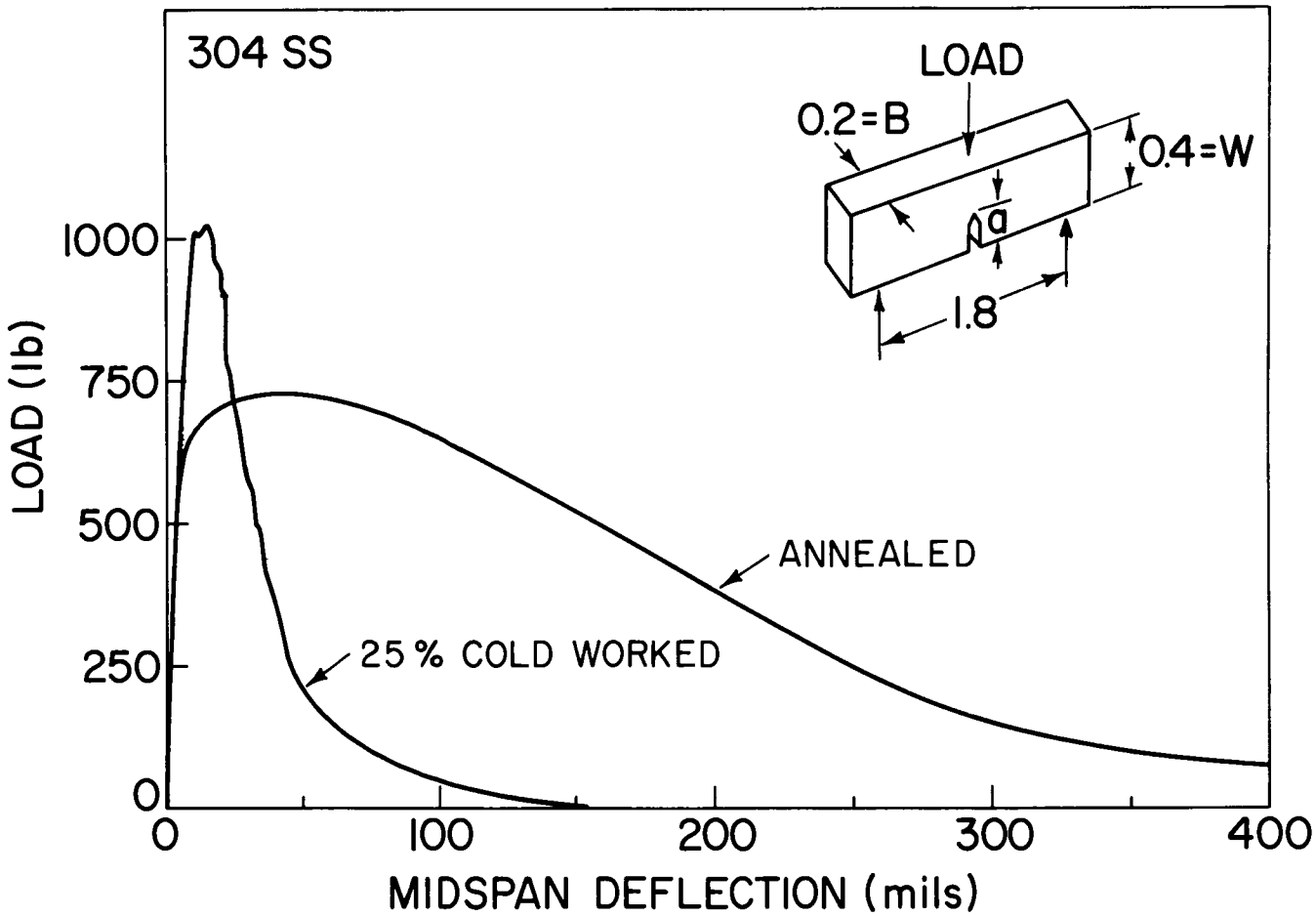

Fig. 4.6. Comparison of Load Versus Deflection Records for SS Specimens Irradiated at 535 F (279 C) to a Fluence of 1.08×10^{21} n/cm^2 >0.1 MeV and tested at 550 F (288 C).

assumed that J can be related to the area under each curve up to the point of maximum load (Eq. 1), then it is readily apparent that the J value of the annealed material is several times larger than that of the cold-worked material. Qualitative assessments of elastic-plastic toughness can thus be obtained directly from the areas associated with load versus deflection records. However, the factor of slow crack extension, occurring before maximum load, also must be taken into account. Research is continuing to define the nature of J with respect to crack extension and geometry dependence.

4.4. NOTCH DUCTILITY OF AUSTENITIC STAINLESS STEEL WELDMENTS - J. R. Hawthorne and H. E. Watson

4.4.1 Background

For most, if not all, nuclear system components, fracture resistance retention during service is a primary requirement. Consequently, a study[12] was undertaken to explore and compare the preirradiation and postirradiation notch toughness of austenitic stainless steel plates and of weld deposits representing different filler compositions and welding processes. Observations on Dynamic Tear (DT) and Charpy-V (C_v) notch ductility of the as-fabricated condition and of thermally aged conditions are reported here.

4.4.2 Materials

Six plates and three experimental weld deposits were evaluated and are identified by type, composition, and heat treatment condition in Tables 4.4 and 4.5. Welding parameters and procedures are given in Table 4.6. The submerged arc weldments conformed to specifications established by the AEC, Division of Reactor Development and Technology, and were fabricated by the Oak Ridge National Laboratory. The shielded metal-arc weldment was made with lime-coated electrodes by the Combustion Engineering Corporation (CE). Conformance to these specifications was not tested in this case since comparable weldments previously satisfied the requirements.

Table 4.4

Chemical Composition

Material	Thickness in.	Chemical Composition (Wt-%) C	Mn	P	S	Si	Cr	Ni	Mo	Cu	Co	Other
Type 308 S/A Weld	1	.03	1.6	.021	.010	.68	21.0	9.7	.02	-	-	B <.0006
Type 304 Base Plate	1	.06	1.6	.026	.014	.54	18.5	9.3	.07	.13	-	B <.0006
Type 316 S/A Weld	1	.06	2.1	.023	.009	.65	18.8	11.7	2.7	-	-	B <.0006
Type 316 Base Plate	1	.06	1.8	.014	.009	.45	17.4	13.4	2.7	-	-	B <.0006
Type 308 SMA Weld	2	.06	1.6	.036	.010	.54	19.4	9.4	.23	.14	-	Ti .04 Al <.01[a] Cb .01[a] V .09[a] B .007[a] N .041[a]
Type 304 Plate	3/4	.07	1.45	.015	.004	.57	18.1	9.9	.50	-	-	
Type 304L Plate	1/2	.03	1.48	.009	.023	.83	19.9	10.8	.19	.04[b]	.11[b]	
Type 316 Plate	3/4	.07	1.58	.020	.007	.30	17.8	13.4	2.55	-	-	
Type 316L Plate	3/4	.03	1.30	.009	.007	.44	17.8	13.5	2.65	-	-	

[a] CE determination (undiluted weld pad)

[b] USS determination

Table 4.5

- Heat Treatment Condition

Material	Yield Strength (ksi)[a] 75°F(24°C)	800°F(427°C)	Heat Treatment
Type 308 S/A Weld	66.0[b]	49.4[b]	Post-weld HT: 900°F(482°C) - 1 hr, FC
Type 304 Base Plate	37.0	24.0[b]	Pre-weld HT: 2000°F(1093°C) ±50°F(28°C) - 1 hr, WQ; PWHT (above)
Type 316 S/A Weld	50.9[b]	47.4[b]	Post-weld HT: 900°F(482°C) - 1 hr, FC
Type 316 Base Plate	44.1	28.6[b]	Pre-weld HT: 2000°F(1093°C) - 1 hr, WQ; PWHT (above)
Type 308 SMA Weld	62.8	[c]	None
Type 304 Plate	21.1	20.8	1900°F(1038°C), 3/4 hr, WQ (plate); 1950°F(1066°C), 1 hr, WQ (specimen blanks)
Type 304L Plate	21.5	19.6	1975°F(1080°C) ±25°F(14°C) - 1/2 hr, WQ
Type 316 Plate	20.3	21.9	1850°F(1010°C) - 1/2 hr, WQ (plate) 2000°F(1093°C) - 1/2 hr, WQ (specimen blanks)
Type 316L Plate	21.5	19.7	1900°F(1038°C) - 1/2 hr, WQ (plate) 2000°F(1093°C) - 1/2 hr, WQ (specimen blanks)

[a] Uniaxial tension tests except as noted
[b] Compression test
[c] Not available

Table 4.6

- Welding Materials and Parameters for Experimental Test Weldments

Material/ Parameter	Type 308 S/A Weldment	Type 316 S/A Weldment	Type 308 SMA Weldment
Base Metal	Type 304H plate (1-in. thick) GOC heat No. K44086	Type 316 plate (1-in. thick) Al heat No. 65808	Type 304 plate (2-in. thick)
Filler Metal	Type 308 (5/32-in. diam.) Arcos heat No. E1021T308	Type 316 (1/8-in. diam.) Unibrase heat No. 13811120	Type 308 (1/4-in. diam.) CE special electrode
Flux	Arcos S-4 (Lot 9D7F)	Arcos S-16 (Lot 1C9L)	Lime Coating
Backing	Type 304L (1/4 x 2 x L)	Type 316 (1/4 x 1 x L)	-
Joint	Single Vee (80 deg. incl. angle)	Single vee (90 deg. incl. angle)	Balanced double U, (5/8-in. rad., 7-1/2 deg. bevel)
Restraint	Full (mechanical)	Full (mechanical)	Full (mechanical)
Current	600 amp, ac	420 amp, ac	250 amp. dc
Voltage	33-35 v	30-32 v	24 v dcrp
Travel	18 ipm	12 ipm	8 ipm
Stickout	1-1/2 in.	1-1/4 in.	-
Interpass Temperature	<350°F (177°C)	<350°F (177°C)	<300°F (149°C)
Interpass Cleaning	Grinding, acetone, wire brush	Grinding, acetone, wire brush	Acetone, wire brush
Post-weld HT	900°F(482°C) - 1 hr, FC	900°F(482°C) -1 hr , FC	None

4.4.3 Specimen Location and Preparation

Tensile, standard C_v, and 5/8-in. DT test specimens were taken with their long dimension parallel to the primary rolling direction for base metal plates and perpendicular to the welding direction for weld deposits. The tensile specimens contained a 0.182-in. diam by 1-in. long gage section. The C_v and DT specimens had the notch oriented perpendicular to the plate or weldment surface. After machining, the DT specimen notch was sharpended using the pressed knife edge technique described in Reference 13.

4.4.4 Results

Observations on the notch ductility of the submerged arc and shielded metal arc weldments are illustrated in Figs. 4.7, 4.8, 4.9, and in Table 4.7. Data developed for unwelded plates are listed in Table 4.8.

4.4.4.1 As-Fabricated Notch Ductility

All plates produced high as-fabricated C_v notch toughness at elevated temperatures. In addition, notch toughness appeared relatively independent of temperature for the range of 75 F (24 C) to 900 F (482 C). This trend performance was confirmed by DT assessments of the 1-in. Types 304 and 316 plates. Average DT energy values for the plates were, respectively, 1300 ft-lb and 1700 ft-lb for temperatures to 900 F (482 C). In contrast to base metal performance, the three weld deposits exhibited a much lower preirradiation toughness. Average DT energy values for the Types 308 and 316 submerged arc welds and for the Type 308 shielded metal-arc weld were 690, 630, and 975 ft-lb, respectively.

Comparison of the preirradiation properties of the two Type 308 weld deposits (Table 4.7) denotes a superior product by the shielded metal-arc process. The higher preirradiation toughness of this weld, in particular, would promote a higher postirradiation toughness. It is noted, however, that the delta ferrite contents of the respective welds were not the same (15% for submerged arc versus 7% for shielded metal-arc). The Type 316 submerged arc weld deposit contained 7% delta ferrite comparable to the shielded metal arc weld.

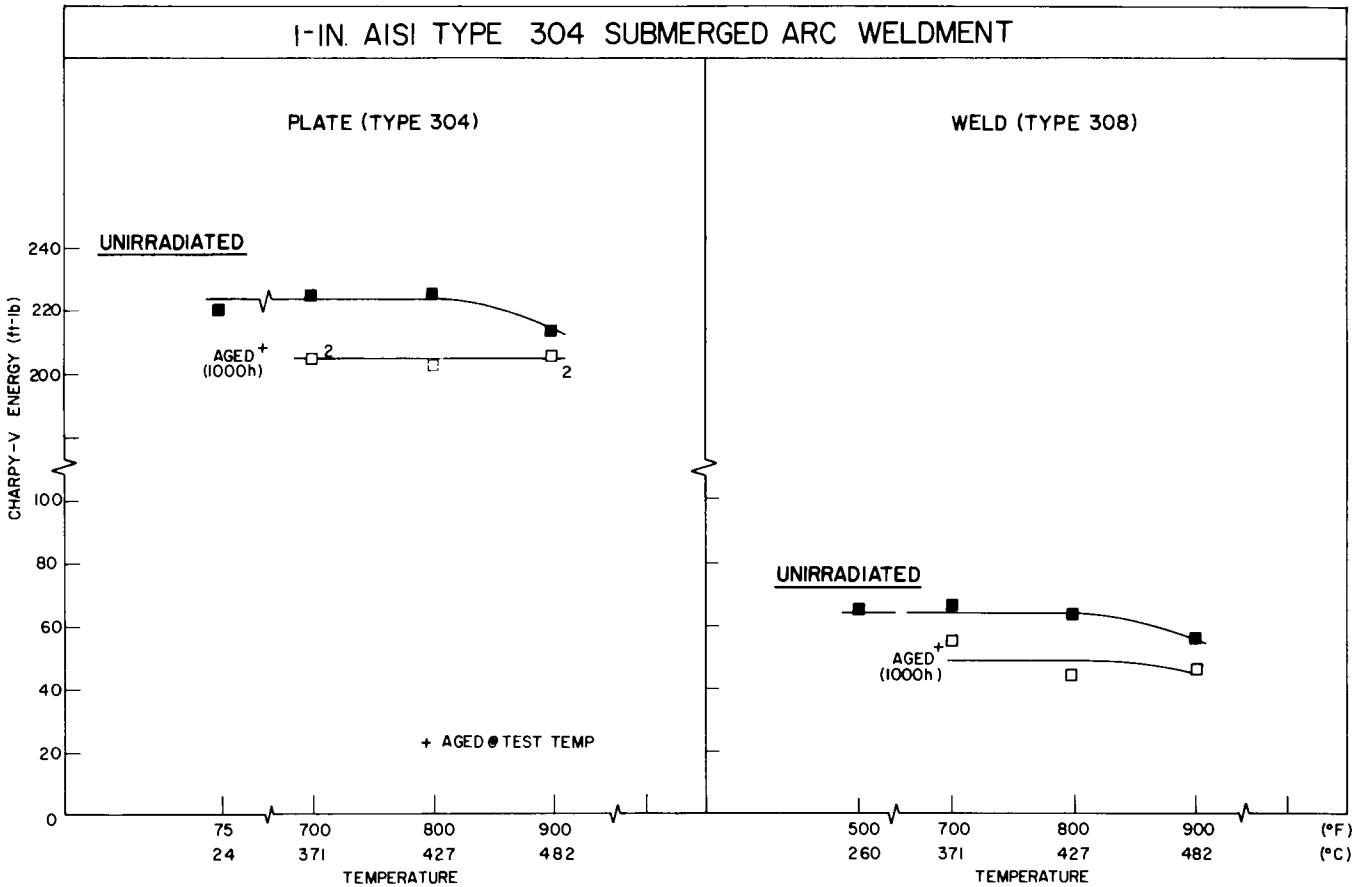

Fig. 4.7. Charpy-V Notch Ductility of the Type 304 Submerged Arc Weldment. Results for Thermal Aging of Unirradiated Specimens are Also Shown.

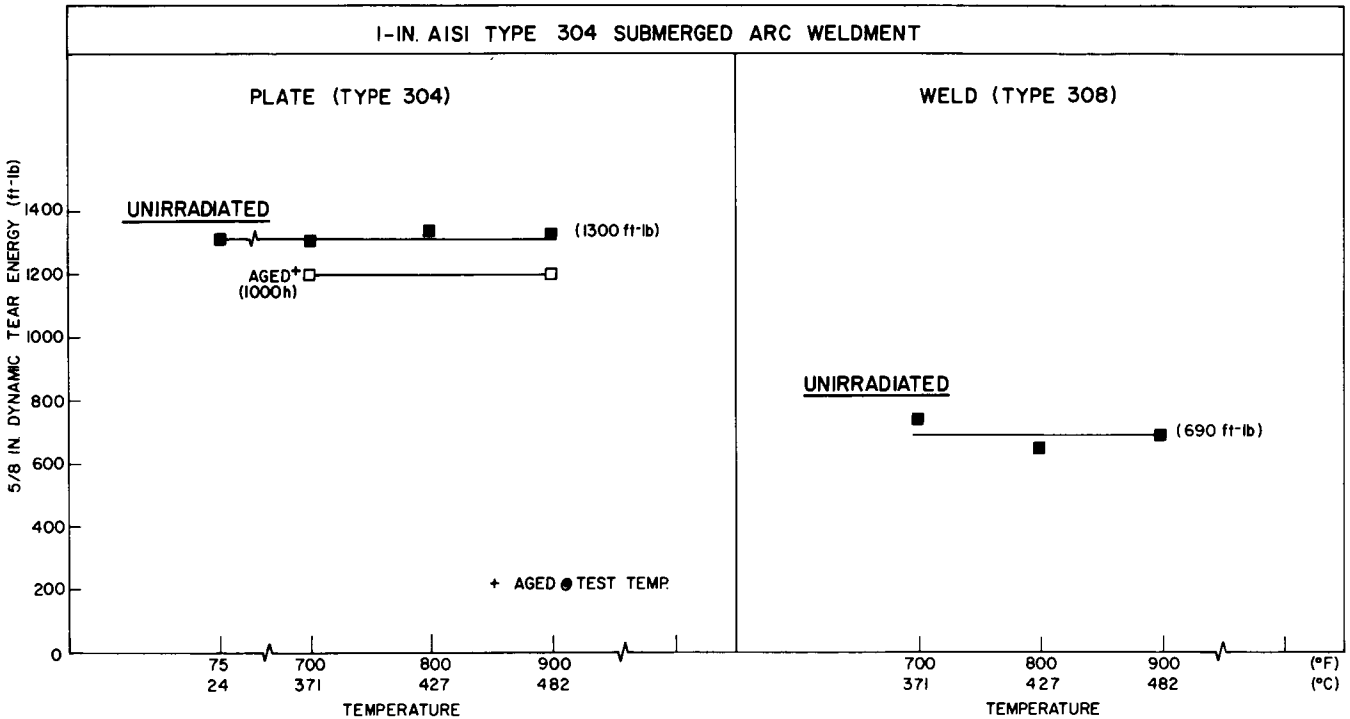

Fig. 4.8. Dynamic Tear Test Performance of the Type 304 Submerged Arc Weldment. Thermal Aging Response of the Base Plate is also Shown. Results Verify Charpy-V Indications for the Weldment Given in Fig. 4.7.

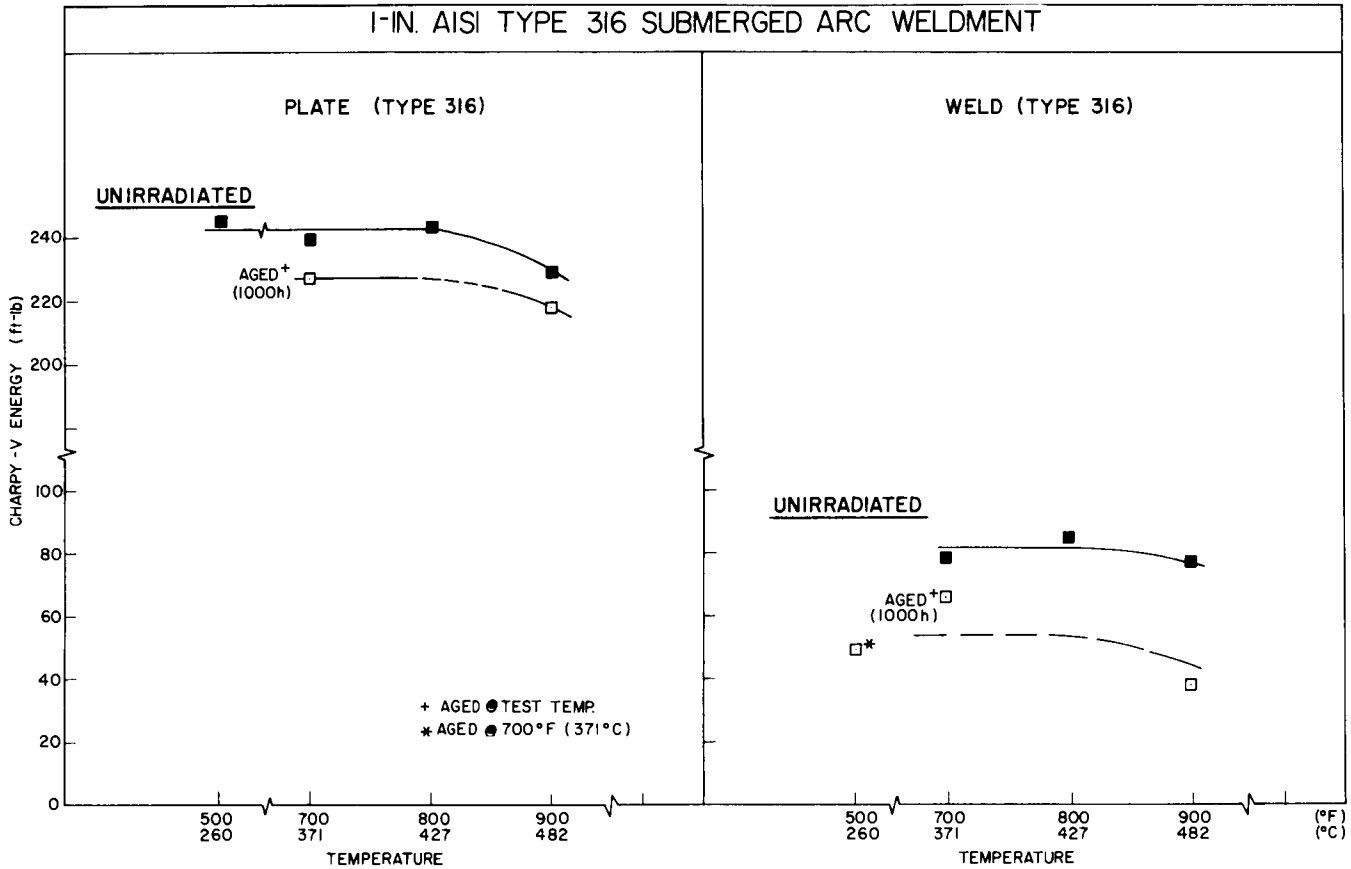

Fig. 4.9. Charpy-V Notch Ductility of the Type 316 Submerged Arc Weldment. Results for Thermal Aging of Unirradiated Specimens are Also Given. As-Fabricated Dynamic Tear Test Values for Plate and Weld Deposit were 1700 ft-lb and 630 ft-lb (average) for the Range 700 F (371 C) to 900 F (482 C).

Table 4.7

Properties Comparison of Experimental Type 308 Weld Deposits

	2-in. SMA Deposit	1-in. S/A Deposit
Yield Strength (ksi)	62.8	66.0[a]
Tensile Strength (ksi)	94.5	107.4[a]
DT Energy (ft-lb)		
700°F (371°C)	1030	740
800°F (427°C)	-	640
900°F (482°C)	920	700
Average	975	690
C_v Energy (ft-lb)		
700°F (371°C)	108	65
800°F (427°C)	-	61
900°F (482°C)	114	54
1100°F (593°C)	111	-
Average (700-900°F)	111	60
C_v Energy (ft-lb) Aged[b]		
700°F (371°C)	114[c]	55[d]
800°F (427°C)	-	44[d]
900°F (482°C)	92[c]	46[c]
Delta Ferrite (%)	7.2[e]	15

[a] Compression data
[b] Aged and tested at same temperature
[c] 2400 hr age, duplicate tests
[d] 1000 hr age
[e] Average 3 procedures

Table 4.8. Charpy-V Energy Absorption of Unwelded Type 304, 316, 304L and 316L Plates

Plate	Temperature (F)	Temperature (C)	C_v Energy (ft-lb)
304	700	371	154
	900	482	137
316	700	371	>180 ft-lb*[a]
	900	482	>180 ft-lb*[a]
304L	500	260	132, 138, 148
	600	316	141[a]
	700	371	160
	900	482	122
316L	500	260	>180 ft-lb
	700	371	>180 ft-lb
	1100	593	>180 ft-lb

*stalled test machine
[a] duplicate tests

4.4.4.2 Notch Ductility With Thermal Conditioning

Long term (1000 hr) thermal aging at 700 F (371 C) and at 900 F (482 C) produced some lowering (~20 ft-lb) in C_v energy absorption for both submerged arc weld deposits and for base metal plates (Figs. 4.7 and 4.9). A similar reduction was evident for the shielded metal-arc weld deposit when aged at 900 F (482 C) but not at 700 F (371 C). For the high toughness levels described, the decrease in plate toughness due to aging would be insignificant to in-service performance. However, for the weld deposits, a decrease with aging would appear quite important. Microstructure changes from either of the aging treatments were not detected by optical microscopy.

4.4.5 Summary of Observations

Primary observations from the data can be summarized as follows:

1. Significant differences in DT and C_v energy absorption between weld deposits (low) and plates (high) appear to be typical of weldments. Accordingly, weld deposit properties could be expected to govern the fracture resistance characteristics of welded stainless steel components.

2. The notch ductility of stainless steel weld deposits and plates is relatively independent of test temperature for the range 75 F to 900 F (24 C to 482 C).

3. Thermal aging at 700 F and 900 F (371 C and 482 C) for 1000 hr can produce a small reduction in DT and C_v notch ductility for both weld deposits and base metals. Microstructural changes with aging, however, were not observed.

4. Shielded metal arc weld deposits appear to offer higher preirradiation notch toughness than submerged arc weld deposits.

5. Delta ferrite content may be a critical factor governing the performance of weld deposits with and without neutron exposure.

4.5 NOTCH DUCTILITY AND STRENGTH PROPERTIES OF ADVANCED NiCrMo STEEL PLATES, FORGINGS AND WELDMENTS - J. R. Hawthorne

4.5.1 Background

A recent NRL study[14] has explored the radiation performance characteristics of several thick section NiCrMo steel plates, forgings, and weldments in anticipation of advanced reactor application. One phase of the investigation involved the development of preirradiation notch ductility and tensile properties to serve as baselines for radiation effects assessments and comparisons.

4.5.2 Materials

The chemical compositions, tensile strengths, and heat treatments of the materials studied are given by Tables 4.9 and 4.10. The plates, with one noted exception, were produced to ASTM Specification A543; the forgings were identified as ASTM Type A508-4 or as ASTM Type A508-5a. The submerged arc and electroslag weldments were produced using standard commercial equipment and procedures; however, filler metals in most cases were specially tailored for improved radiation embrittlement resistance using NRL specifications. NRL filler metal specifications primarily involved restrictions on certain residual element contents, notably copper and phosphorus. Welding parameters and procedures for individual welds are given in Table 4.11.

4.5.3 Notch Ductility of Plates and Forgings

The C_v notch ductilities of the A543 plates and A508 forgings, as heat treated (before irradiation), are illustrated in Figs. 4.10 to 4.12. Data describing material response to 550 F (288 C) thermal conditioning are also presented in selected figures. In general, very good notch ductility is indicated. The C_v upper shelf energy level of the materials typically exceeds 95 ft-lb and, except for plate 1, the C_v 30 ft-lb transition temperature lies below -100 F (-79 C). For the A543 plates, limited comparisons made of drop weight and C_v test results would suggest that the C_v 30 ft-lb transition provides a reasonable estimate of the drop weight nil-ductility transition (NDT) temperature of primary interest.

Table 4.9

Chemical Composition and Strength of the NiCrMo Plates, Forgings, and Weld Deposits

Identification	Type	Thickness (in.)	Yield Strength* (ksi)	Tensile Strength (ksi)	Chemical Composition (wt-%)										
					C	Mn	P	S	Si	Ni	Cr	Mo	Cu	V	Other
Plate 1†	A543-1	6	96.6	113.6	0.18	0.30	0.006	0.019	0.25	3.25	1.71	0.52	0.20	0.02	—
Plate 2†	A543-2	6	104.1	118.5	0.18	0.32	0.006	0.019	0.25	3.26	1.71	0.52	0.20	0.02	—
Plate 3	A543-2	5.5	100.5	116.5	0.18	0.31	0.004	0.010	0.22	3.00	1.56	0.42	0.12	0.004	0.030Al ¶
Plate 4	A543(mod)¶	4	109.0	120.7	0.10	0.79	0.005	0.011	0.28	3.36	0.90	0.41	0.04‡	0.09	—
Plate 5	A543-1	6	92.9	110.1	0.18	0.31	0.006	0.019	0.25	3.25	1.71	0.51	0.20	0.02	—
Plate 6(ref)#	A543-1	8	95.2	118.4	0.17	0.32	0.011	0.016	0.25	3.37	1.92	0.50	0.05	0.02	0.02Al
Forging 1	A508-4¶	23.5	84.5**††	102.0**††	0.15	0.34	0.007	0.011	0.21	3.47	1.72	0.48	0.10‡	0.01	—
Forging 2	A508-5a	62	107.5	124.4	0.26‡‡	0.31	0.007	0.014	0.05	3.40	1.81	0.47	0.07	0.08	—
Weld Deposit															
Subarc S/A 1	A543-1 (2-1/4NiMnMo filler)	6	102.2	110.4	(AD) 0.09	1.16	0.006	0.007	0.56	2.40	0.09	0.49	0.03	0.01	<0.01Al
					(FW) 0.09	1.63	0.005	0.008	0.51	2.30	0.06	0.57	0.02	0.01	—
					(BP)	(From same melt and ingot as plates 1 and 2 above)									
Subarc S/A 2	A543-2 (2-1/4Cr1MoNi filler)	6	116.4	130.0	(AD) 0.10	0.84	0.006	0.008	0.35	0.83	2.40	1.10	0.01	0.02	—
					(FW) 0.11	1.34	0.006	0.009	0.24	1.00	2.51	1.03	0.025	0.01	—
					(BP)	(Plate 1 above)									
Electroslag E/S 1	A543-2 (2-1/4Cr1Mo filler)	6	93.8	108.1	(AD) 0.14	0.46	0.006	0.018	0.20	2.22	2.10	0.68	0.16	0.02	—
					(FW) 0.06	0.60	0.007	0.019	0.18	0.12	2.70	0.96	0.02	0.02	—
					(BP)	(Plate 2 above)									
Electroslag E/S 2	NiCrMo¶¶ (2-1/4Cr1Mo filler)	3.5	87.8	102.8	(AD)¶0.09	0.43	0.012	0.018	0.10	1.43	1.83	0.54	0.08	< 0.01	0.022Al
					(FW)	(Same filler for E/S weld 1 above)									
					(BP)¶0.19	0.30	0.010	0.015	0.09	2.48	1.24	0.31	0.13	0.003	0.016Al
Electroslag E/S 3	A543-1 (2-1/4Cr1Mo filler;lot 2)	8	94.2	104.0	(AD) 0.11	0.42	0.008	0.016	0.12	1.27	2.35	0.71	0.04	—	—
					(FW)¶0.07	0.52	0.008	0.018	0.18	0.02	2.79	0.95	0.03	—	0.071Al
					(BP)	(Plate 6 above)									

* 0.2% offset.
† Plates 1 and 2 from same melt and ingot.
‡ NRL Determination.
¶ Chemical composition courtesy of supplier.
\# Reference plate from early commercial melt.
** Courtesy of supplier.
†† Specimen tangent to forging circumference.
‡‡ Out of specification.
AD = as deposited.
FW = filler wire.
BP = base plate.
¶¶ HY-80 plate.

Table 4.10

Heat Treatment of the Plates, Forgings, and Weld Deposits

Identification		Type	Thickness (in.)	Heat Treatment*
Plate	1	A543-1	6	Austenitized 1675°F(913°C) — 7.5 hr, WQ; Reaustenitized 1575°F(857°C) — 7.5 hr, WQ; Tempered 1160°F(627°C) — 6 hr, WQ; Stress relief annealed (SRA) 1050°F(566°C) — 2 hr, AC; Postweld SRA: 1135°F(613°C) — 6 hr, AC.
	2	A543-2	6	Same preweld heat treatment as plate 1; Postweld Heat Treatment: Austenitized 1675°F(913°C) — 6 hr, WQ; Reaustenitized 1575°F(857°C) — 6 hr, WQ; Tempered 1160°F(627°C) — 6 hr, WQ; SRA (first) 1100°F(593°C) — 6 hr, FC; SRA (second) 1160°F(627°C) — 6.5 hr, fan cooled†.
	3	A543-2	5.5	Austenitized 1650°F(899°C), WQ; Reaustenitized 1600°F(871°C), WQ; Tempered 1120°F(604°C), WQ.
	4	A543(mod)	4	Austenitized 1660°F(904°C) — 2 hr, WQ; Reaustenitized 1550°F(843°C) — 2 hr, WQ; Tempered 1180°F(638°C) — 2 hr, WQ.
	5	A543-1	6	Same preweld heat treatment as plate 1; Postweld Heat Treatment: SRA: 1145°F(619°C) — 6.5 hr, fan cooled.
	6	A543-1(Ref)	8	Austenitized 1650°F(899°C) — 8 hr heating and 2 hr hold, water quenched for 17 min; Reaustenitized 1500°F(816°C) — 8 hr heating and 2 hr hold, water quenched for 17 min; Tempered 1185°F(640°C) — 8 hr heating and 2 hr hold, water quenched cold.
Forging	1	A508-4	23.5	Heat treatment not available
	2	A508-5	62 (diam.)	Austenitized 1550°F(843°C) — 10 hr equalize and 30 hr hold, water (spray) quenched; Reheated to 1140°F(616°C) in 30 hr; Tempered 1140°F(616°C) — 10 hr equalize and 30 hr hold, AC.
Weld Deposit				
Subarc	S/A 1	A543-1 (2-1/4NiMnMo filler)	6	Postweld SRA: 1135°F(613°C) — 6.5 hr, fan cooled†.
	S/A 2	A543-2 (2-1/4Cr1MoNi filler)	6	Postweld SRA: 1135°F(613°C) — 6 hr, AC
Electroslag	E/S 1	A543-2 (2-1/4Cr1Mo filler)	6	Postweld Heat Treatment: see postweld heat treatment listed for plate 2 above.
	E/S 2	NiCrMo (2-1/4 Cr1Mo filler)	3.5	Postweld Heat Treatment: Austenitized 1675°F(913°C) — 3.5 hr, WQ; Reaustenitized 1575°F(857°C) — 3.5 hr, WQ; Tempered 1160°F(627°C) — 3.5 hr, WQ; SRA (single) 1100°F(593°C) — 3.5 hr, AC.
	E/S 3	A543-1 (2-1/4Cr1Mo filler)	8	Postweld Heat Treatment: Austenitized 1675°F(913°C) — 8 hr, WQ; Reaustenitized 1650°F(899°C) — 8 hr, WQ; Tempered 1200°F(649°C) — 8 hr, WQ; SRA (single) 1065°F(574°C) — 8 hr, AC.

* Austenitizing temperatures are ±25°F(15°C); tempering and stress relief temperatures are ±15°F(8°C) unless noted otherwise.

† Fan cooled — 1135°F(613°C) to 600°F(316°C) in 70 min.

WQ = quenched in agitated water.
AC = cooled in still air.
FC = furnace cooled.

Table 4.11

Welding Parameters and Procedures for Individual Welds

Parameter/Procedure	Submerged Arc Weld		Electroslag Weld		
	S/A 1	S/A 2	E/S 1	E/S 2	E/S 3
Base Plate	A543-1	A543-1	A543	NiCrMo (HY80)	A543
Weld Procedure	Tandem electrodes	Tandem electrodes	Twin electrodes*	Single electrode	Twin electrodes†
Filler Type (noncopper clad)	2-1/4NiMnMo (Arcos: IP 2915	2-1/4Cr1MoNi (Special; Arcos: 23706)	2-1/4Cr1Mo (Arcos: D1141 A521)	2-1/4Cr1Mo (Arcos: D1141 A521)	2-1/4Cr1Mo (Arcos: D2062 A521)
Electrode size	1/8 in. diam.	5/32 in. diam.	1/8 in. diam.	1/8 in. diam.	1/8 in. diam.
Flux	Linde 0091‡	Linde 0091‡	Arcos BV	Arcos BV (50%) Arcos V (50%)	Arcos BV
Joint Design	Double U; 2:1 ratio	Double U; 2:1 ratio	Square Edge; Gap 1-1/8 in. to 1-1/4 in.	Square Edge; Gap 1-1/4 in. to 1-5/8 in.	Square Edge; Gap 1-1/4 in. to 1-5/8 in.
Electrode Connection	Scott connection (ac-ac, 90° phase shift)	Scott connection (ac-ac, 90° phase shift)	ac	ac	ac
Current	550 amp (lead); 500 amp (trail)	550 amp (lead); 500 amp (trail)	600 amp (each wire)	600 amp	525-600 amp (each wire)
Voltage	25 V (lead) 30 V (trail)	25 V (lead) 30 V (trail)	50 V	50 V	36-38 V
Travel or Oscillation	31 ipm	31 ipm	2-in. with 5-s dwell	3/4-in. with 3-s dwell	2-5/8-in. with 3.5 s dwell
Slag Depth	—	—	2 in.	2 in.	1-3/4 in.
Preheat Temperature	300°F(149°C)	300°F(149°C)	none	none	none
Interpass Temperature (maximum)	300°F(149°C)	300°F(149°C)	—	—	—
Postweld Heat Treatment	1135°F(613°C)-6.5 hr fan cooled	1135°F(613°C)-6 hr still-air cooled	(see Table 2)	(see Table 2)	(see Table 2)

*Electrode spacing 3 in.

†Electrode spacing 4-3/8 in.

‡Flux (65 × 200) baked at 700°F(371°C) for 2 hr in 2-in.-deep pans prior to use.

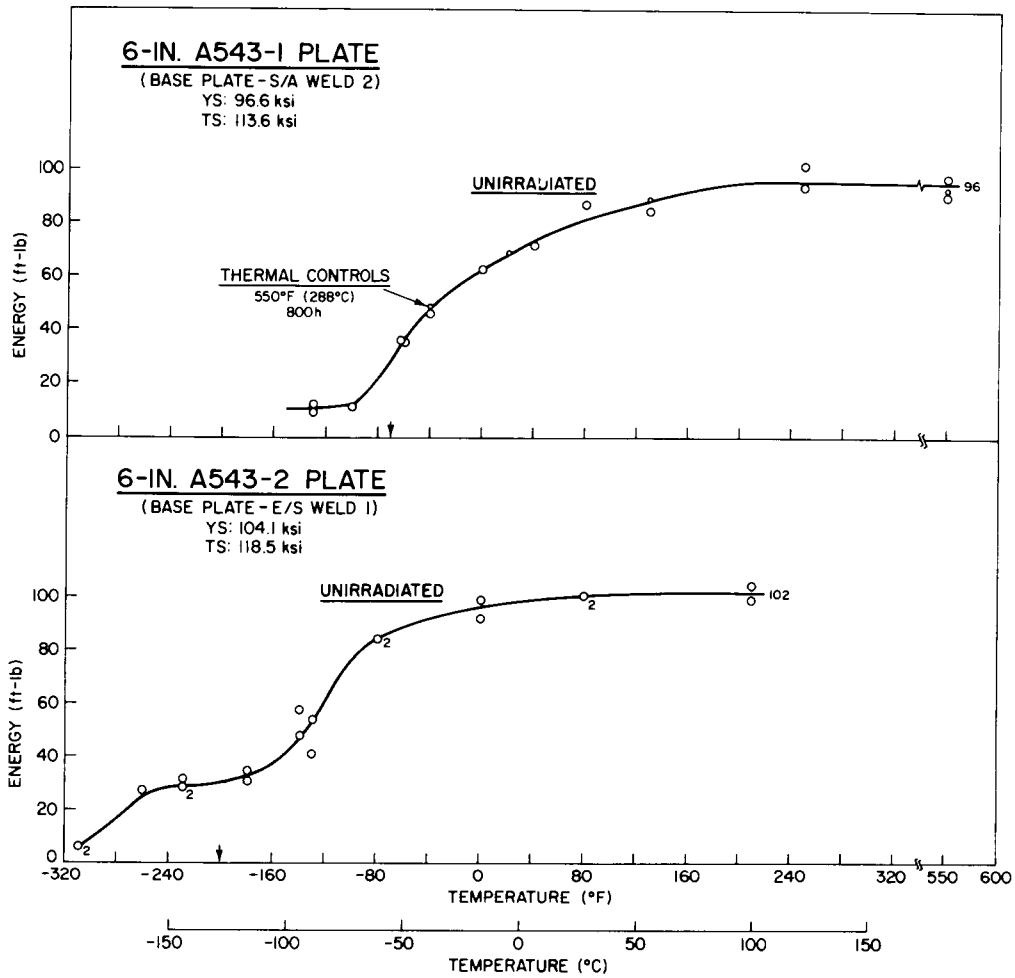

Fig. 4.10. Charpy-V Notch Ductility of Two A543 Plates from the Same Melt and Ingot (Quarter Thickness Position). Difference in Charpy-V Transition Behavior is Due to Dissimilar Heat Treatment Cycles and Post-weld Stress Relief Cooling Rates. Results of 550 F (288 C) Thermal Conditioning are also Indicated in the Upper Graph.

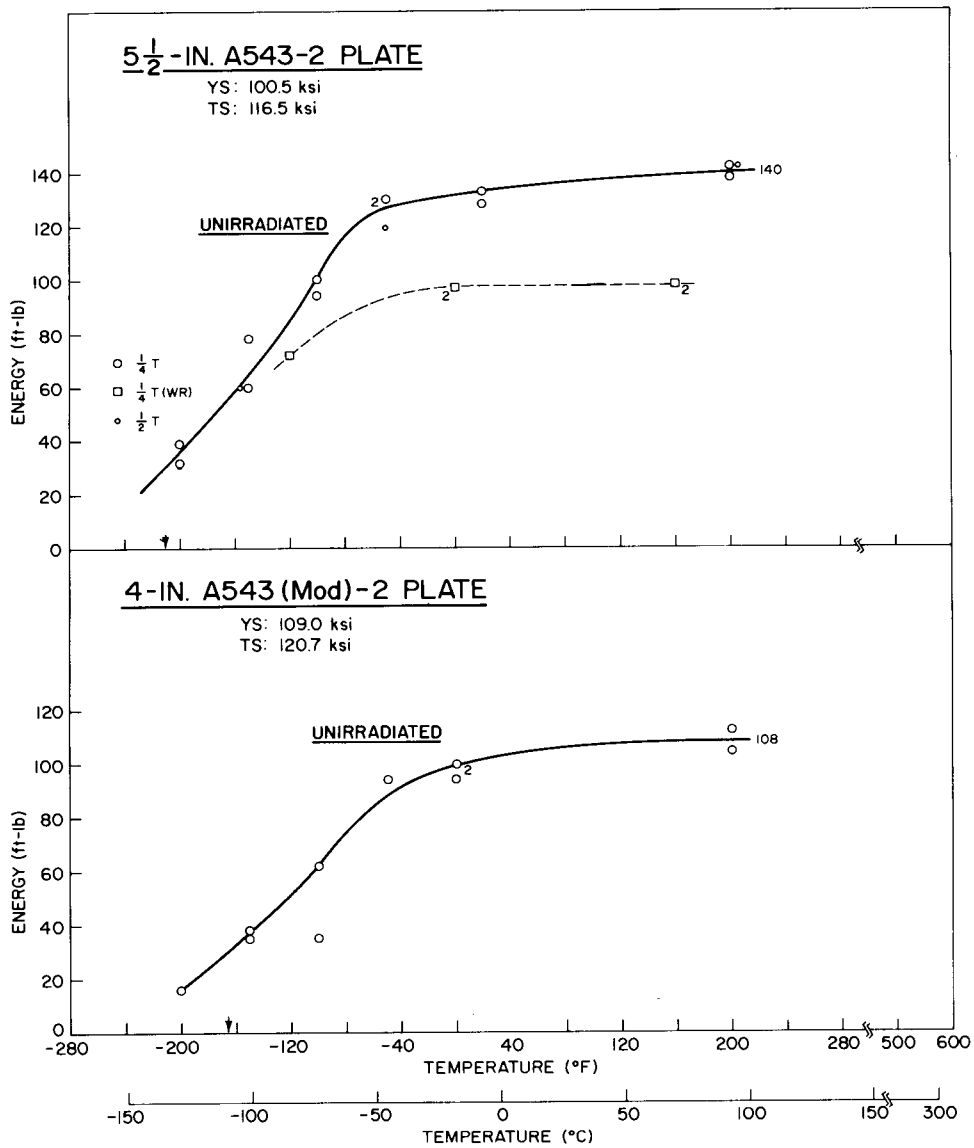

Fig. 4.11. Charpy-V Notch Ductility of Two A543 Class 2 Plates (Quarter Thickness Position).

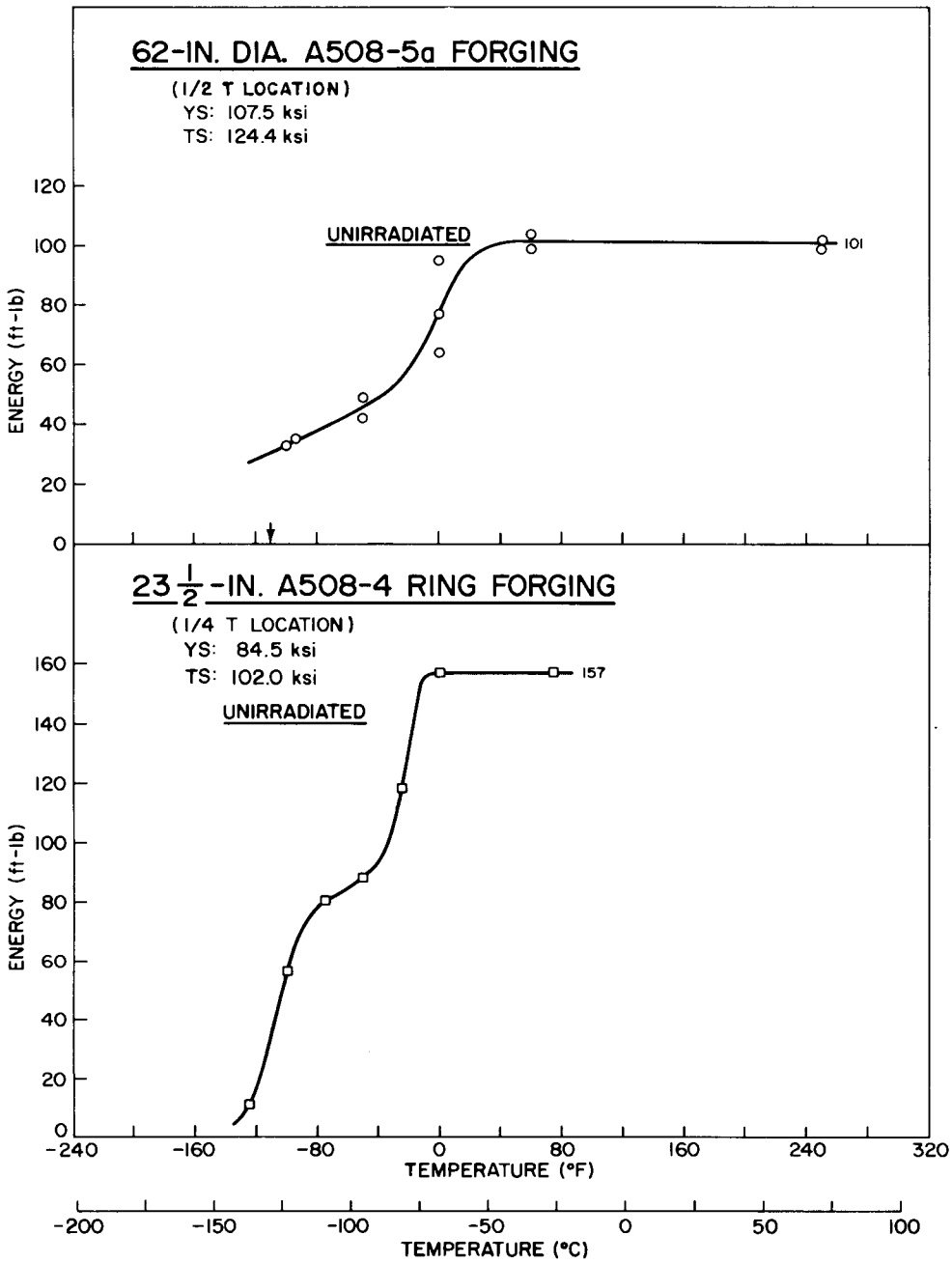

Fig. 4.12. Charpy-V Notch Ductility of Two A508 Forgings.

It is noted that plate 1 depicts a much poorer C_v 30 ft-lb transition than plate 2 even though both plates were from the same melt and ingot. The 130 F difference in transition temperature is believed to be the result of two factors: (a) a difference in cooling rate from postweld stress relief (still air cooled versus accelerated cooled), and (b) a difference in total austenitizing and quenching heat treatment cycles (two versus four cycles). Referencing the performance of plate 5 also of the same melt and ingot, a separation of the two effects can be made. For plate 5, two heat treatment cycles and an accelerated cool from postweld stress relief produced a -150 F (-101 C) transition temperature. Accordingly, the comparison suggests that the slow cooling and resultant temper embrittlement of plate 1 led to transition temperature elevation of 80 F (44 C) and that the higher number of heat treatment cycles (microstructure refinement) of plate 2 caused a transition temperature reduction of 50 F (28 C). Knowledge of full metallurgical history is thus most important for A543 materials.

4.5.4 Notch Ductility of Weld Metal

Observations on weld deposit notch ductility are given in Figs. 4.13 to 4.16. In Fig. 4.13, drop weight NDT and DT test performances of two submerged arc welds and of one electroslag weld are compared. Note that the toe of the DT curve approximates the NDT temperature for all three welds. In terms of both drop weight NDT and DT upper shelf energy level, submerged arc weld 1 (2-1/4 NiMnMo filler) showed much better notch toughness than submerged arc weld 2 (2-1/4 CrMoNi filler). However, this initial advantage of submerged arc weld 1 was found lost on irradiation at 550 F (288 C). The NDT performance of electroslag weld 1 also appeared better than that of submerged arc weld 2; however, differences in postweld heat treatment cooling rates are felt responsible. In Fig. 4.14, the NDT temperatures of both submerged arc weld deposits, like those of A543 plates, are shown to be approximated well by the C_v 30 ft-lb transition temperature.

Figure 4.15 illustrates results for one electroslag weld deposit for specimens taken at two positions on the quarter thickness plane.

Property differences in this case would reflect microstructure differences and impurities segregation during weld solidification. As noted, the centerline location offered much poorer notch toughness than the offset location.

4.5.5 Summary of Observations

Notch ductility observations, summarized in Table 4.12, denote a trend toward higher as-fabricated transition temperatures by weld deposits compared to either parent plates or forgings. However, it has been demonstrated elsewhere that the best preirradiation performance need not equate to best postirradiation performance. The results, nonetheless, point up the need for alternate weld filler metals that will match the low NDT performance of A543 and A508 materials.

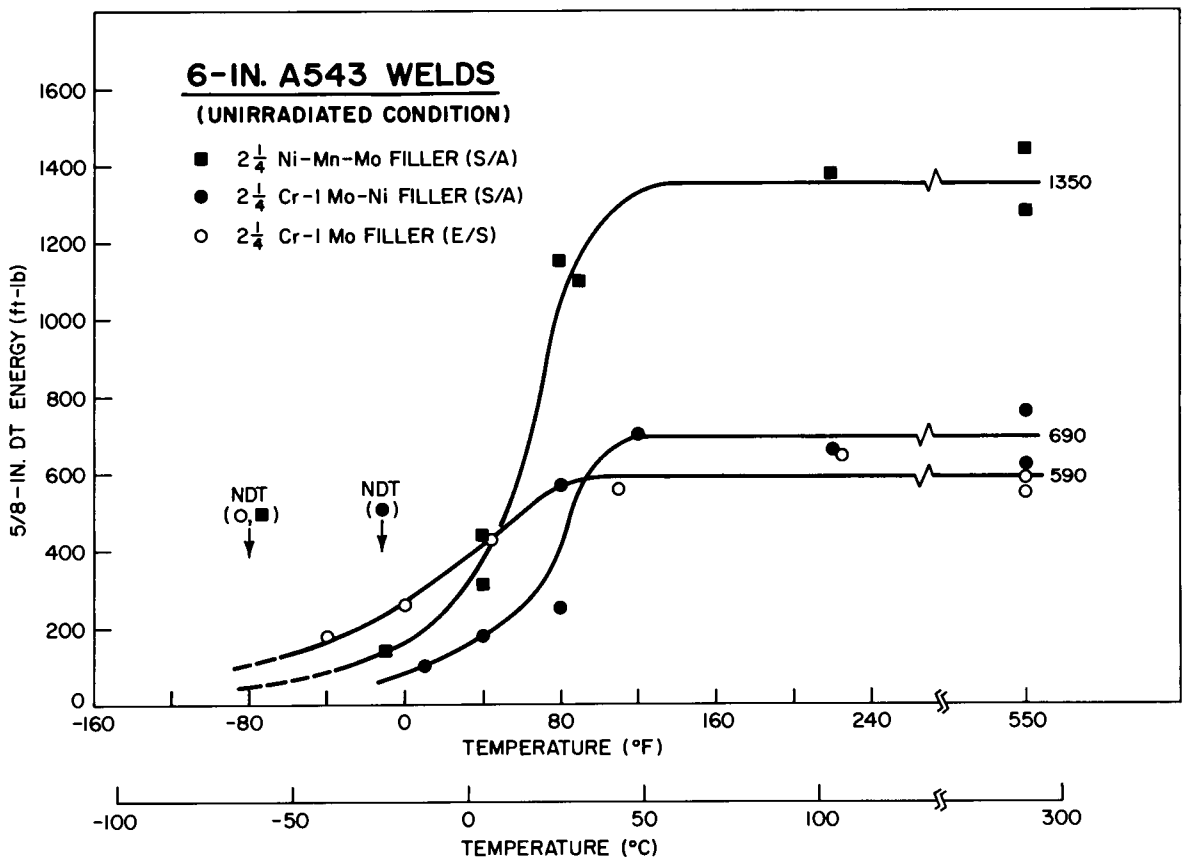

Fig. 4.15. Preirradiation Drop Weight and Dynamic Tear Test Performances of Three Representative Welds (Quarter Thickness Position). Best Overall Notch Ductility is Shown by Submerged Arc (S/A) Weld 1 (2-1/4 NiMnMo Filler). An A543-1 Reference Plate (Plate 6), by Comparison, Exhibited a -110 F (-79 C) Drop Weight NDT Temperature and a 550 ft-lb Dynamic Tear Upper Shelf Energy.

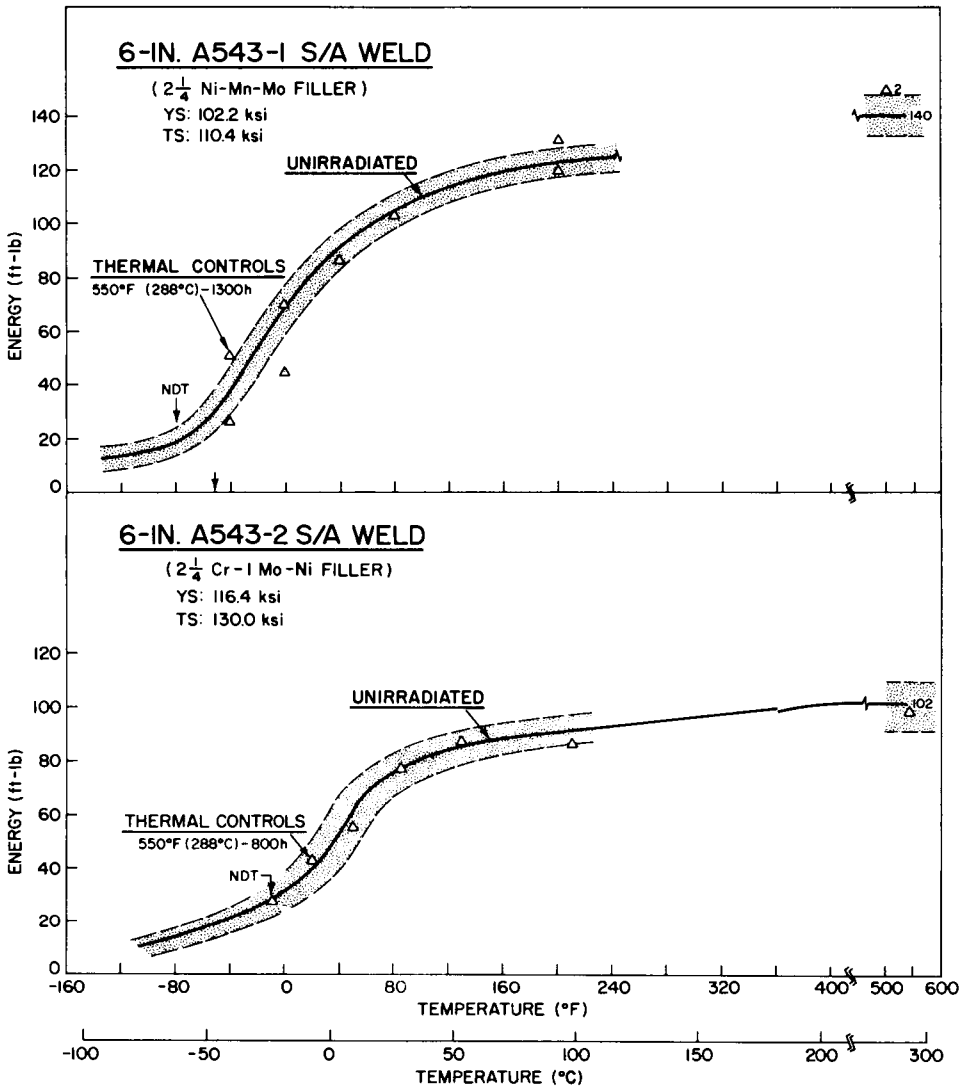

Fig. 4.14. Drop Weight NDT and Charpy-V Notch Ductility of Submerged Arc Welds 1 and 2. The Superior Notch Ductility of Weld 1 (Upper Graph) Relative to Weld 2 (Lower Graph) Appeared Lost on Irradiation Through Greater Radiation Embrittlement Sensitivity.

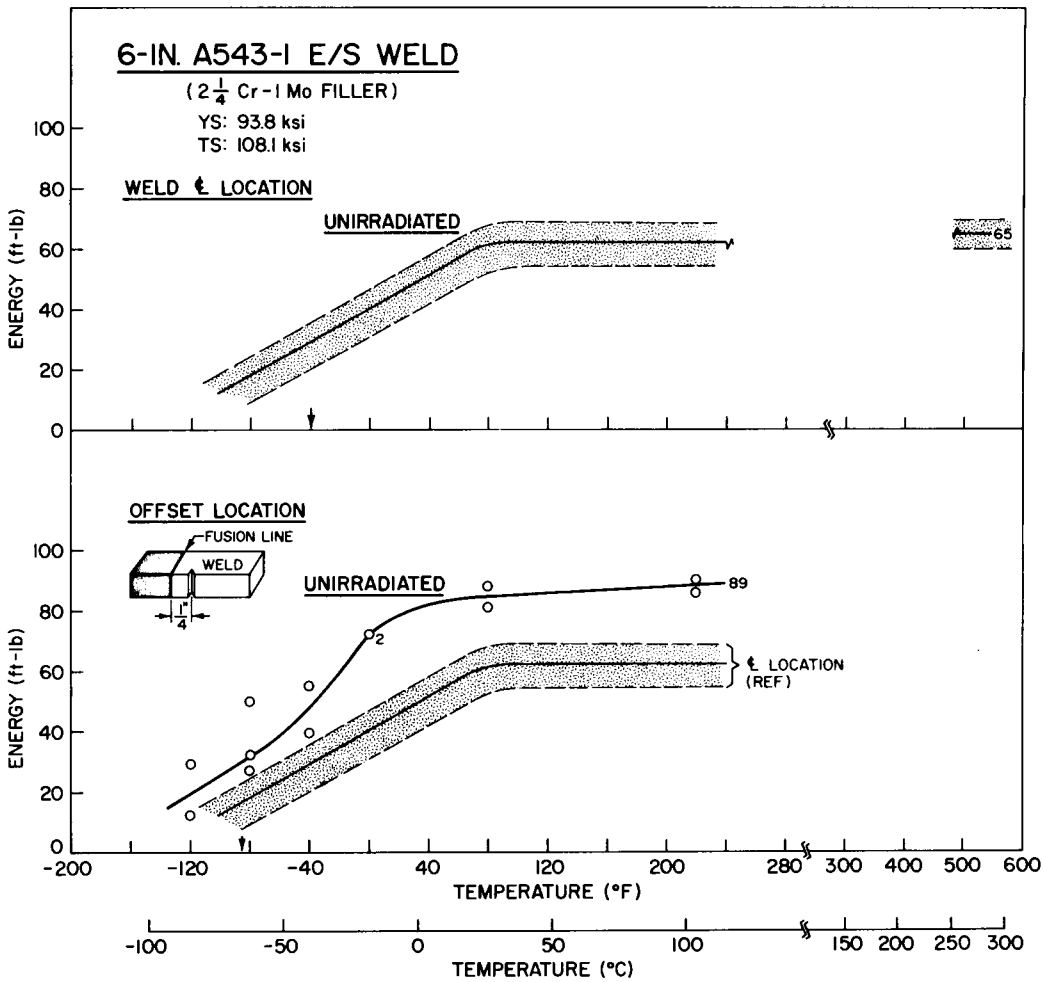

Fig. 4.15. Charpy-V Notch Ductility of Electroslag Weld 1 at Two Locations Across the Weld Width (Quarter Thickness Position). Poorer Performance is Indicated for the Weld Centerline Location (Upper Graph).

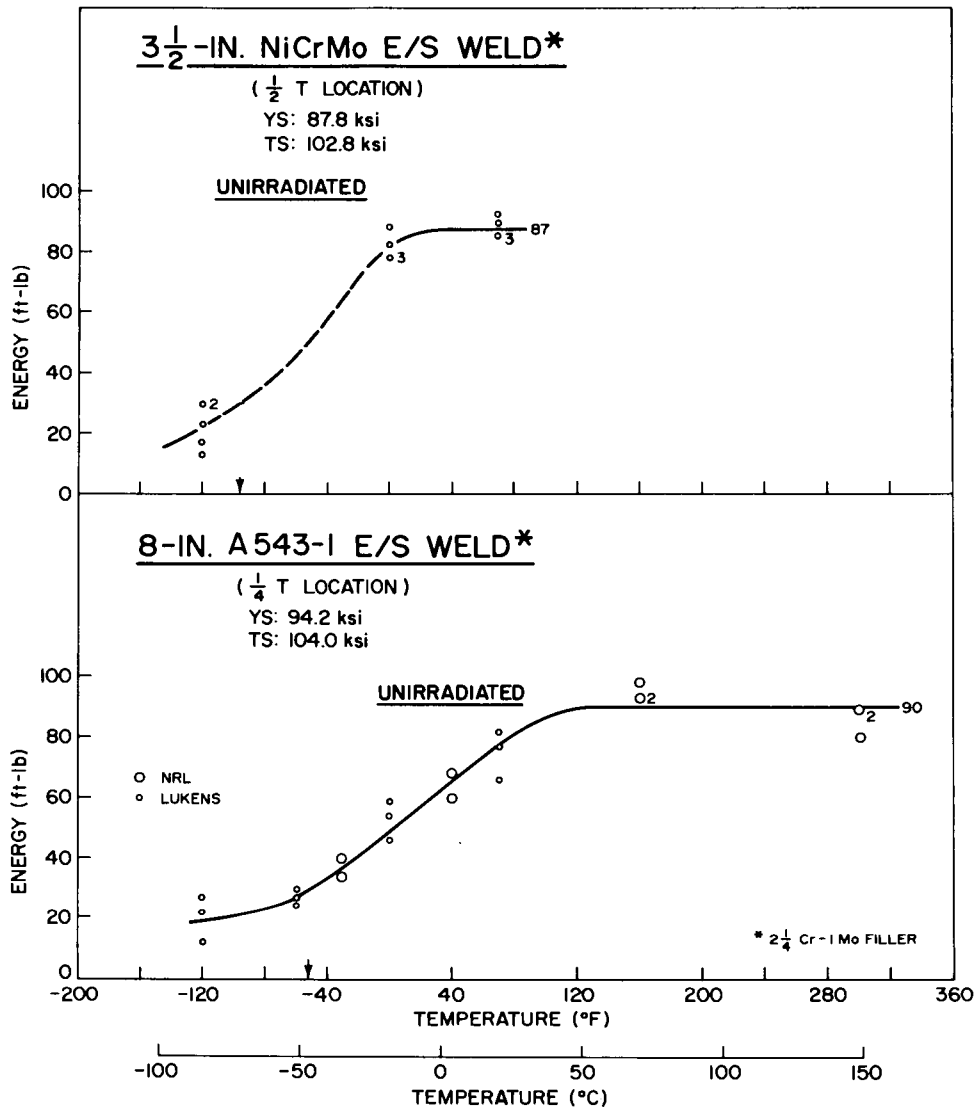

Fig. 4.16. Charpy-V Notch Ductility of Electroslag Weld 2 (Upper Graph) and of Electroslag Weld 3 (Lower Graph). Weld 2 Shared the Same Lot of Weld Wire as Weld 1 (Fig. 4.15).

Table 4.12

Summary of Notch Ductility Properties of the Plates, Forgings, and Weld Deposits

Identification		Type	C_v 30-ft-lb Temp.		C_v Upper Shelf	DT Upper Shelf*	Drop Weight NDT*	
			°F	°C	(ft-lb)	(ft-lb)	°F	°C
Plate	1	A543-1	− 70	− 57	96			
	2	A543-2	−200	−129	102			
	3	A543-2	−210	−134	140			
	4	A543 (mod)	−165	−109	108			
	5	A543-1	−150	−101	100	820	−140	−96
	6	A543-1 (ref.)	−130	− 90	72	550	−110	−79
Forging	1	A508-4	−115	− 82	157			
	2	A508-5a	−110	− 79	101			
Weld Deposit								
Subarc	S/A 1	A543-1 (2-1/4-NiMnMo filler)	− 50	− 46	140	1350	− 80	−62
	S/A 2	A543-2 (2-1/4-CrMoNi filler)	− 5	− 21	102	690	− 10	−23
Electroslag†	E/S 1	A543-1(C)	− 40	− 40	65	590	− 80	−62
		(O)	− 85	− 65	⩾ 89			
	E/S 2	NiCrMo	− 95	− 71	87			
	E/S 3	A543-1	− 50	− 46	90			

*5/8-in.-thick specimen.
†2-1/4 CrlMo filler
(C) = centerline location;
(O) = offset location.

4.6 REFERENCES

1. P. Shahinian, H. H. Smith, and H. E. Watson, in "Irradiation Effects on Reactor Structural Materials, QPR, 1 May-31 July 1971," Naval Research Laboratory, NRL Memorandum Report 2328, pp. 35-40; also Hanford Engineering Development Laboratory, HEDL-TME-71-116.
2. P. Shahinian, H. E. Watson, and H. H. Smith, "Fatigue Crack Growth in Selected Alloys for Reactor Applications," J. Materials 6(4):527-535 (1972).
3. P. Shahinian, H. H. Smith, and H. E. Watson, in "Irradiation Effects on Reactor Structural Materials, QPR, 1 Nov 1971-31 Jan 1972," Naval Research Laboratory, NRL Memorandum Report 2398, pp. 4-10; also Hanford Engineering Development Laboratory, HEDL-TME-72-27.
4. P. Shahinian, H. H. Smith, and H. E. Watson, "Fatigue Crack Growth Characteristics of Several Austenitic Stainless Steels at High Temperature," in Fatigue at Elevated Temperatures, ASTM STP 520, American Society for Testing and Materials, Philadelphia, Pa., 1973.
5. J. R. Rice, "A Path Independent Integral and the Approximate Analysis of Strain Concentration by Notches and Cracks," Trans. ASME, J. Appl. Mech., pp. 379-386 (June 1968).
6. J. R. Rice, "Mathematical Analysis in the Mechanics of Fracture," in Fracture, Liebowitz (ed.), Academic Press 2:191-311 (1968).
7. F. J. Loss and R. A. Gray, Jr., "J-Integral Characterization of Irradiated Stainless Steels," Naval Research Laboratory, NRL Report 7565, April 25, 1973.
8. J. R. Rice, P. C. Paris, and J. G. Merkle, "Some Further Results of J-Integral Analysis and Estimates," to be published.
9. R. C. Bucci, P. C. Paris, J. D. Landes, and J. R. Rice, "J Integral Estimation Procedures," in Fracture Toughness, Proceedings of the 1971 National Symposium on Fracture Mechanics, Part II, ASTM STP 514, American Society for Testing and Materials, Philadelphia, Pa., September 1972, pp. 40-69.
10. C. Z. Griffis and G. R. Yoder, "Application of the J Integral to Crack Initiation in a 2024-T351 Aluminum Alloy," NRL Report (pending publication).

11. J. D. Landes and J. A. Begley, "Test Results from J Integral Studies - An Attempt to Establish a J_{Ic} Testing Procedure," Seventh Annual Symposium on Fracture Mechanics, University of Maryland, August 1973 (to be published in ASTM STP symposium volume).

12. J. R. Hawthorne and H. E. Watson, "Notch Toughness of Austenitic Stainless Steel Weldments with Nuclear Irradiation," Welding J. Res.Supl. 52(6):255s-260s (1973).

13. E. A. Lange, P. P. Puzak, and L. A. Cooley, "Standard Method for the 5/8-inch Dynamic Tear Test," Naval Research Laboratory, NRL Report 7159, August 27, 1970.

14. J. R. Hawthorne, "Radiation-Embrittlement Resistance of Advanced NiCrMo Steel Plates, Forgings, and Weldments," NRL Report 7573, Naval Research Laboratory, September 13, 1973.

5. OAK RIDGE NATIONAL LABORATORY

5.1 INTRODUCTION

The objective of the Mechanical Properties of LMFBR Structural Materials Program is to collect mechanical property data and material behavior for LMFBR structural and component materials. Included in the scope of this effort are the following: (1) basic tensile, creep-, creep-rupture, and relaxation base-line data that are directly applicable to design criteria and methods for types 304 and 316 stainless steel reference heats and cyclic stress-strain tests performed with emphasis on loading and history effects, (2) find the variations in properties for several heats of types 304 and 316 stainless steel to allow establishment of minimum and average values of specific properties and the equation parameters required for design purposes. This work will include determination of property variation of samples from different mill products within a given heat of stainless steel.

In our Mechanical and Metallurgical Behavior of Weldments Program, we are evaluating the behavior of weldments in austenitic stainless steel at 370 to 750°C (700 to 1380°F) as a function of both welding process and the variables within a process for application to liquid-metal-cooled fast breeder reactor (LMFBR) vessels and components. The investigation covers both heavy-section weldments, which are applicable to reactor vessels as well as other components, and thinner section weldments, which are applicable to piping. Major portions of both the heavy-section and piping weldment studies are concerned with the development and evaluation (including the determination of elevated-temperature design data) of improved filler metals that contain controlled additions of minor elements for increased strength and ductility.

A limited effort is continuing to gain fundamental information on the welding of materials such as Incoloy 800, austenitic stainless steels, and ferritic steels that are used in critical nuclear components.

The LMFBR Steam Generator and Heat Exchanger Materials program has the broad responsibility for developing improved methods for fabricating and inspecting high-reliability components and for determining the

properties and behavior of the various materials of interest under typical service conditions. The development and evaluation of methods for producing bore-side welds, structural welds, and overlays is an important part of our program; simultaneously, nondestructive tests have to be developed to assure the required high quality of the as-fabricated component and assess the integrity of the component during service.

The service conditions include time, stress, and temperature for the base metals and weldments of interest. Because of the temperature requirements (>480°C, 900°F) for both the intermediate heat exchanger and the steam generator, creep, stress rupture, fatigue, and stress relaxation are all important considerations. As part of this study, we will develop design data to meet the existing ASME code requirements for components to operate in the creep regime.

The High-Temperature Structural Design Methods Program has as its goal the development of a verified high-temperature design technology applicable to the long-term operating conditions expected for LMFBR systems. Although the ultimate objective is to develop verified methods and criteria for reliably designing for high temperatures and long life, near-term efforts are largely concentrated on establishing and validating methods and criteria to be used, on an interim basis, for FFTF and LMFBR Demonstration Plant designs. The overall program is divided into a number of tasks that are being carried out with the participation and cooperation of industrial groups, universities, and design code bodies. Progress on the tasks involved with the generation of mechanical property data are described.

5.2 MECHANICAL PROPERTIES AND BEHAVIOR FOR STRUCTURAL MATERIALS — W. R. Martin

5.2.1 Base-Line Mechanical Property Testing of Reference Heat of Type 304 Stainless Steel

5.2.1.1 Creep Properties of the 2-in. Plate of Reference Heat — H. E. McCoy

The need for comprehensive mechanical property data on a single heat of type 304 stainless steel for use in developing constitutive equations for design purposes was recognized during the last few years. A large heat of type 304 stainless steel (designated heat 9T2796) was purchased in several product forms, and the testing began in 1972. The test program included creep tests to accurately define the strain-time response. The details of the averaging extensometer and associated electronics for creep testing were described previously.[1] We now have 19 lever-arm creep machines and two deadload machines equipped to do this caliber of testing.

The tests that have been completed and those that are in progress are given in Table 5.1. The tests have all been run on the 2-in.-thick plate, and samples were taken from the center line in the primary working direction. Test samples have a gage section 1/4 in. in diameter × 2.25 in. long and were reannealed 0.5 hr at 1093°C (2000°F) in argon. The test environment was air. The test matrix is given in Table 5.2. The numbers in parentheses are the test numbers and can be used to refer to Table 5.1. All the A priority tests are completed or in progress. Nine creep tests having B and C priorities in Table 5.2 remain to be started.

Some creep tests of about 1000 hr duration are needed to determine the primary creep behavior. The tests of A-1 priority are shown in Table 5.3, and nine remain to be started. There is some duplication of tests between Tables 5.2 and 5.3, so only a total of 13 tests remain to be started. These should all be started within the next few months.

Previously we had analyzed the strains that occurred when the tests in Table 5.1 were loaded. The additional data obtained during this report period have been added to Figs. 5.1 and 5.2. These correlations still hold except for the two tests loaded at 5000 psi, which do not follow the correlation in Fig. 5.2. However, the loading strains for these tests are about what would be expected from an elastic analysis.

Table 5.1. Creep Tests on Type 304 Stainless Steel Reference Heat 9T2796 2-in.-Thick Plate[a]

Test Number	Temperature °F	Temperature °C	Stress (psi)	Time in Test (hr)	Loading Strain (%)	Ratio of Creep Stress to Yield Stress[b]	Comments[c]
11595	800	427	20,000	3499	2.67	1.57	
11569	900	482	20,000	3621	3.27	1.70	
11675	900	482	16,000	2451	1.48	1.36	Discontinued
11693	900	482	14,000	2690	0.92	1.19	Discontinued
11830	900	482	12,000	1682	0.35	1.02	Discontinued
10489	1000	538	20,000	8564	3.80	1.80	
12250	1000	538	18,000	979	2.62	1.62	
11625	1000	538	16,000	3379	1.79	1.44	
10491	1000	538	14,000	8564	1.16	1.26	
11568	1000	538	12,000	3620	0.53	1.08	
11626	1000	538	10,000	3379	0.071	0.90	
11641	1000	538	8,000	3170	0.040	0.72	Discontinued
10853	1100	593	18,000	4545	2.84	1.65	Ruptured
10852	1100	593	16,000	6834	2.29	1.47	
10554	1100	593	14,000	8514	1.40	1.28	
11596	1100	593	12,000	3500	0.52	1.10	
10490	1100	593	10,000	8539	0.22	0.92	
11227	1100	593	8,000	5538	0.041	0.73	
10855	1200	649	16,000	304	2.41	1.57	Ruptured
10854	1200	649	14,000	761	1.60	1.37	Ruptured
11563	1200	649	12,000	2674	0.59	1.18	Ruptured
11226	1200	649	10,000	5503	0.18	0.98	
10851	1200	649	8,000	6810	0.044	0.78	
12255	1200	649	5,000	865	0.030	0.49	
10856	1300	704	10,000	568	0.067	0.90	Ruptured
11562	1300	704	10,000	653	0.12	0.90	Ruptured
11222	1300	704	8,000	2760	0.031	0.72	Ruptured
12254	1300	704	5,000	865	0.030	0.45	

[a]Annealed 0.5 hr at 1093°C (2000°F) before testing. All tests loaded at a strain rate of 0.005/min.

[b]Yield stresses used in this ratio were 12,700 psi at 427°C (800°F), 11,800 psi at 482°C (900°F), 11,100 psi at 538°C (1000°F), 10,900 psi at 593°C (1100°F), 10,200 psi at 649°C (1200°F), 11,100 psi at 704°C (1300°F).

[c]Unless other wise noted, tests in progress.

Table 5.2. Test Matrix for Uniaxial Creep of Type 304 Stainless Steel

Stress (psi)	Priority and Test Number[a] for Each Temperature, °F (°C)					
	800 (427)	900 (482)	1000 (528)	1100 (593)	1200 (649)	1300 (704)
2,000						C
3,000					C	B
5,000				C	C (12255)	A-1 (12254)
8,000			C (11641)	A-1 (11227)	A-1 (10851)	A-1 (11222)
10,000		C	C (11626)	A-1 (10490)	A-2 (11226)	A-1 (10856, 11562)
12,000		C (11830)	A-2 (11568)	B (11596)	B (11563)	
14,000	C	C (11693)	A-1 (10491)	A-1 (10554)	A-1 (10854)	
16,000	C	C (11675)	B (11625)	A-1 (10852)	A-1 (10855)	
18,000	C	C	B (12250)	A-1 (10853)		
20,000	A-2 (11595)	A-2 (11569)	A-1 (10489)			

[a]Test number refers to Table 5.1.

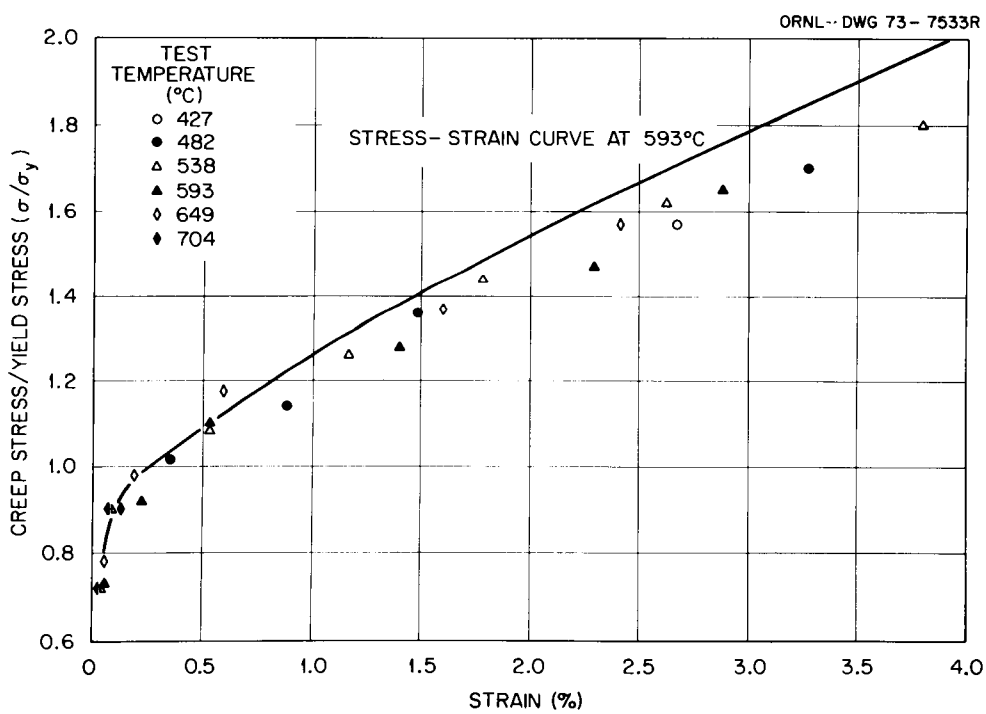

Fig. 5.1. Comparison of Strain on Loading With Stress Ratio for Type 304 Stainless Steel (Heat 9T2796) Annealed 0.5 hr at 1093°C (2000°F).

Table 5.3. Short-Time A-1 Priority Uniaxial Creep Tests of Type 304 Stainless Steel[a]

Stress (psi) and Loading $\dot{\varepsilon}$ (min^{-1})[b]	Temperature, °F (°C)					
	800 (427)	900 (482)	1000 (538)	1100 (593)	1200 (649)	1300 (704)
σ_1 = 3						1
σ_2 = 5				1	1 (12255)	1 (12254)
σ_3 = 8			1 (11641)	1 (11227)	1 (10851)	1 (11222)
σ_4 = 10, $\dot{\varepsilon}$ = 0.005		1	1 (11626)	1 (10490)	1 (11226)	1 (10856, 11562)
$\dot{\varepsilon}$ = 0.0005				1		
$\dot{\varepsilon}$ = 0.25				1		
σ_5 = 12		1 (11830)	1 (11568)	1 (11596)	1 (11563)	
σ_6 = 14	1	1 (11693)	1 (10491)	1 (10554)	1 (10854)	
σ_7 = 16, $\dot{\varepsilon}$ = 0.005	1	1 (11675)	1 (11625)	1 (10852)		
$\dot{\varepsilon}$ = 0.0005				1		
$\dot{\varepsilon}$ = 0.25				1		
σ_8 = 20	1 (11595)	1 (11569)	1 (10489)			

[a]Numbers in parentheses refer to test numbers in Table 5.1. Some of the same tests are also part of the long-term test matrix shown in Table 5.2.

[b]All tests loaded at a strain rate of 0.005/min unless noted otherwise.

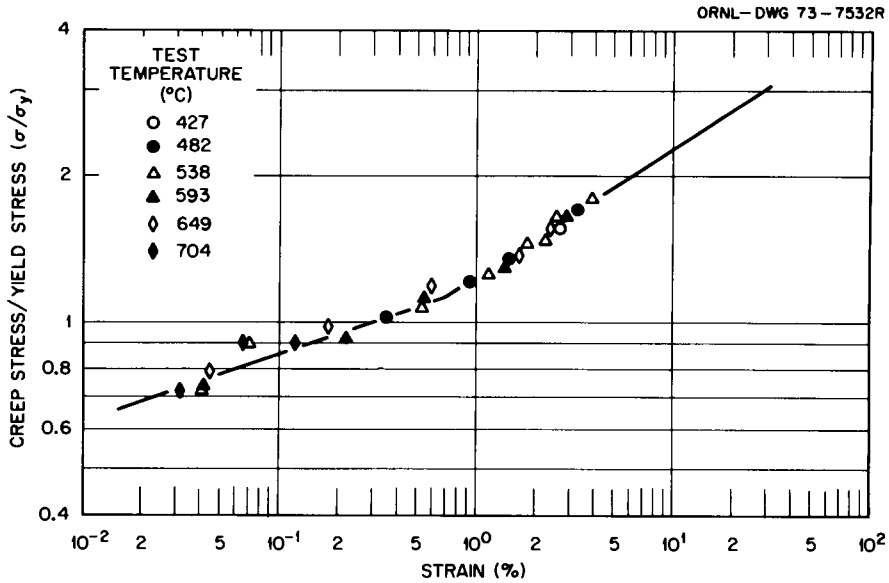

Fig. 5.2. Comparison of Strain on Loading With Stress Ratio in Type 304 Stainless Steel (Heat 9T2796) Annealed 0.5 hr at 1093°C (2000°F).

Seven tests have ruptured to date, and the results of these are summarized in Table 5.4. The results of these tests on reannealed 2-in.-thick plate are compared in Figs. 5.3 and 5.4 with those by Swindeman[2] for reannealed 1-in.-thick plate and 5/8-in.-diam bar. Generally, the 2-in.-thick plate seems to have slightly higher creep rates and shorter rupture lives, but the data are too few to support this conclusion unequivocally.

Table 5.4. Results of Stress-Rupture Tests on Type 304 Stainless Steel, Heat 9T2796, 2-in.-Thick Plate — Reannealed 0.5 hr at 1093°C (2000°F)

Test Number	Temperature		Stress (psi)	Loading Strain (%)	Minimum Creep Rate (%/hr)	Rupture Life (hr)	Creep Strain (%)	Reduction in Area (%)
	°C	°F						
10853	593	1100	18,000	2.84	0.000280	4545	5.9	14.9
10855	649	1200	16,000	2.41	0.0170	304	12.0	15.0
10854	649	1200	14,000	1.60	0.00816	761	13.0	17.3
11563	649	1200	12,000	0.59	0.00322	2674	13.4	19.0
10856	704	1300	10,000	0.067	0.0196	568	15.6	19.6
11562	704	1300	10,000	0.12	0.0253	653	22.5	23.0
11222	704	1300	8,000	0.031	0.00409	2760	16.4	15.6

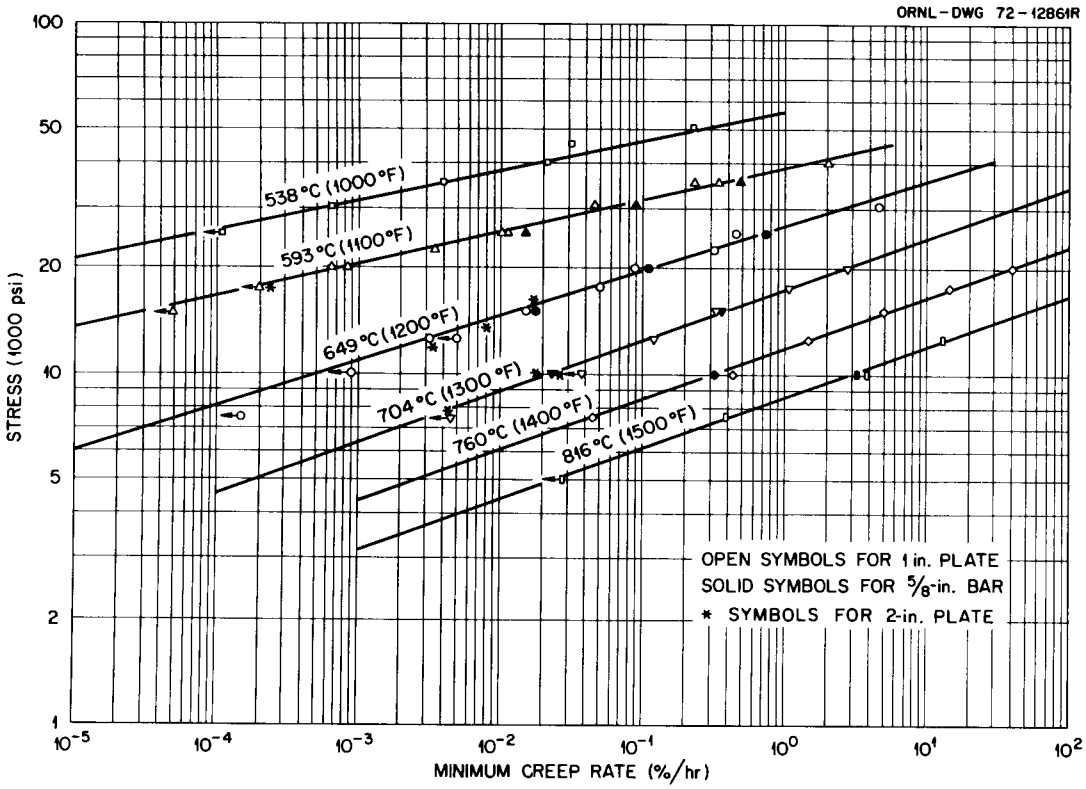

Fig. 5.3. Stress Versus Minimum Creep Rate for Type 304 Stainless Steel Heat 9T2796 [Reannealed 0.5 hr at 1093°C (2000°F)].

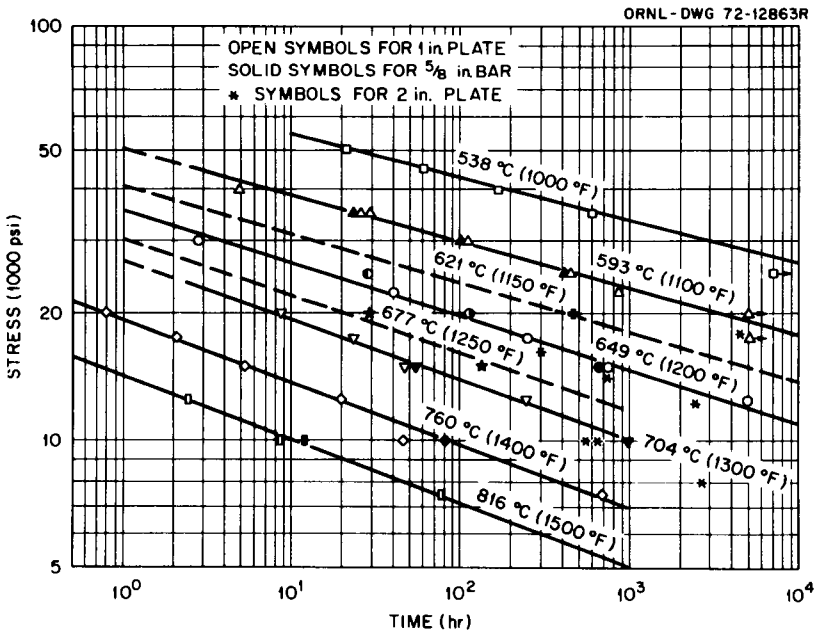

Fig. 5.4. Stress Versus Rupture Life for Type 304 Stainless Steel Heat 9T2796 [Reannealed 0.5 hr at 1093°C (2000°F)].

Most of the tests in progress have been plotted and some analysis has been made of the data. The strain-measuring instrumentation on each test includes a top dial gage that measures movement of the entire load train, a left dial gage and transducer that measures the movement of the left side of the extensometer, and a right dial gage and transducer that measures the movement of the right side of the extensometer. The transducer and dial gage measure the same movement and should give duplicate readings, but this has not always been the case. A computer program was written to analyze the data, and the package that we normally obtained included:

1. printout and plot of elongation vs time based on the top dial gage,
2. printout and plot of elongation vs time based on the average of the two dial gages on the extensometer,
3. printout, plot, and punched cards of elongation vs time based on the electronic average of the two transducers on the extensometer, and
4. a composite plot of the three above curves.

The computer plot for test 10491 is shown in Fig. 5.5. The test is still in progress.

For the sample configuration used, a strain of 0.05% corresponds to a change in length of 0.001125 in. There is considerable scatter in the top dial gage reading, as expected for such low strain values. Transducer readings were not made for the first 2000 hr of the test, but the extensometer and dial gage readings agree very well during the rest of the test. The data from tests 11569 and 11568 were fitted with an eight-constant polynomial equation. The estimates of standard error were 44 and 29 μin./in., respectively. This compares with values of 200 to 500 for nine long-term tests with nonaveraging extensometers.

The status plots for the long-term tests were used to construct the creep curves at 593°C (1100°F) and various stress levels (Fig. 5.6). The times to 0.1% strain were taken from most of the tests and used to construct Fig. 5.7. Smaller strains can be read from the individual plots, but the scatter is larger at smaller strains.

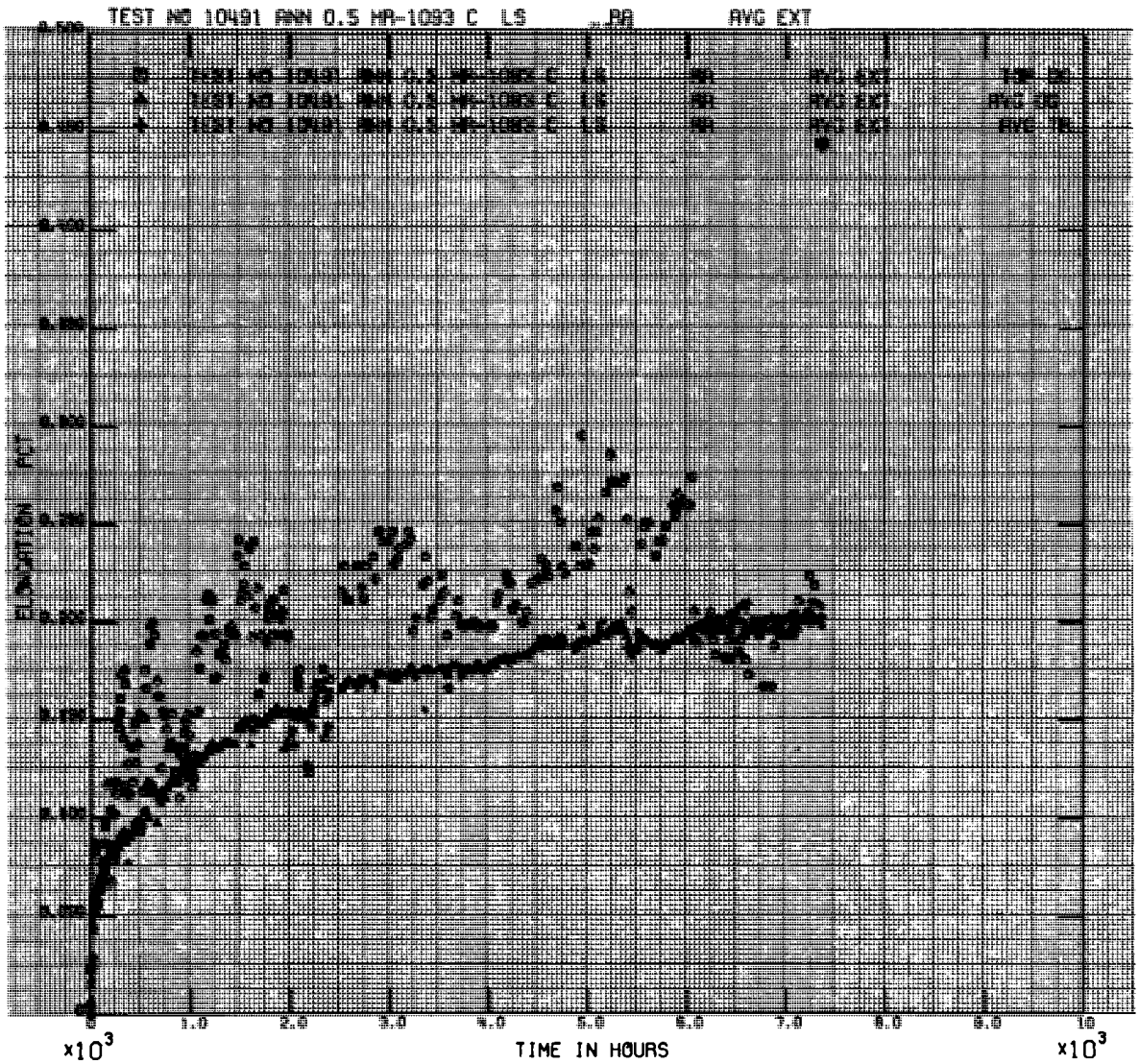

Fig. 5.5. Creep Curve for Type 304 Stainless Steel at 538°C (1000°F) and 14,000 psi, Heat 9T2796, 2-in. Plate, Reannealed 0.5 hr at 1093°C (2000°F) Before Testing.

5.2.1.2 Strain Rate Effect on the Tensile Properties of 2-in. Plate — H. E. McCoy

The type 304 stainless steel reference heat has been tensile tested in air over the temperature range of 25 to 704°C (77 to 1300°F) and at initial strain rates from 0.40 to 0.0004/min. The samples were all taken from the 2-in.-thick plate, and the gage length was parallel to the primary working direction. All samples were reannealed 0.5 hr in argon at 1093°C (2000°F) before testing. The gage section of the sample was 1.25 in. long × 0.250 in. in diameter. An averaging extensometer was joined to the center line of the specimen gage section and was used to measure the first few percent strain.

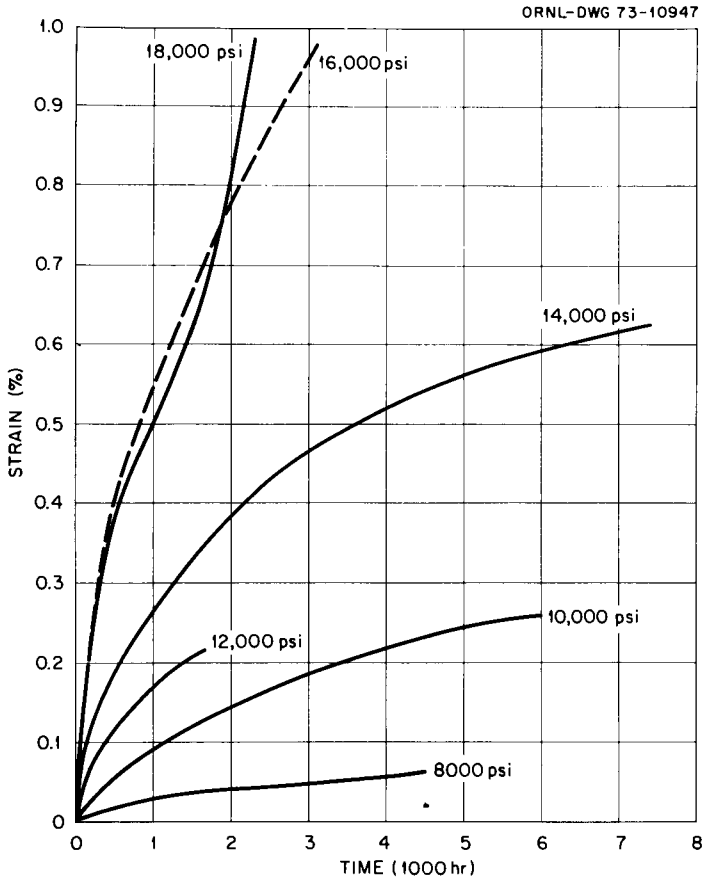

Fig. 5.6. Time to 0.1% Strain for Type 304 Stainless Steel, Heat 9T2796, 2-in.-Thick Plate, Reannealed 0.5 hr at 1093°C (2000°F).

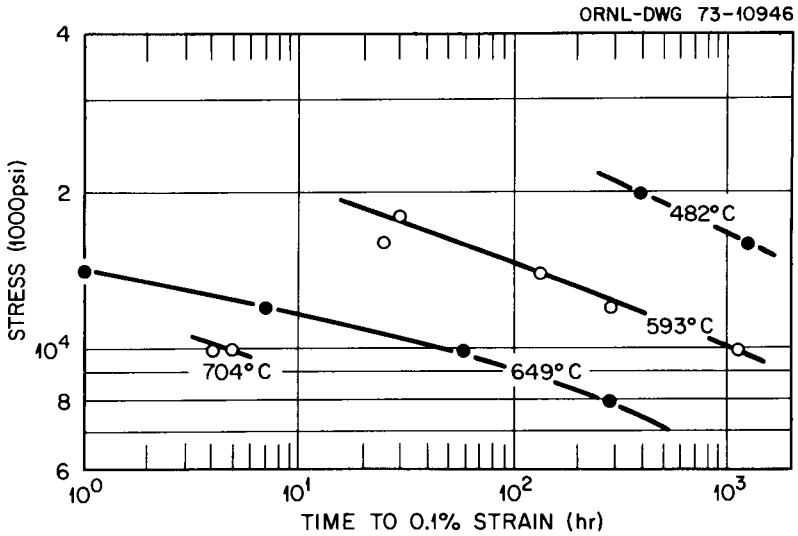

Fig. 5.7. Creep Curves at 593°C (1100°F) for Type 304 Stainless Steel, Heat 9T2796, 2-in. Plate, Reannealed 0.5 hr at 1093°C (2000°F).

The results of the tests are summarized in Table 5.5. The family of tensile curves in Fig. 5.8 illustrates the effects of temperature at a strain rate of 0.04/min. All the strength and ductility measures generally decreased with increasing temperature.

Strain rate had little effect on the yield stress (Fig. 5.9). However, the ultimate tensile stress was influenced by strain rate, particularly at the higher temperatures (Fig. 5.10). The rather random variations of ultimate tensile stress with strain rate at test temperatures of 25, 260, 427, and 482°C (77, 500, 800, and 900°F) are likely not significant. At 538 and 593°C (1000 and 1100°F), the ultimate tensile stress dropped off at the lowest strain rate of 0.0004/min. At 649 and 704°C (1200 to 1300°F) the ultimate tensile stress decreased progressively with decreasing strain rate. The reduction in area was likewise not very dependent upon strain rate at test temperatures of 25, 260, 427, and 482°C (Fig. 5.11). At 538°C (1000°F) the reduction in area dropped sharply at the lowest strain rate. At 593, 649, and 704°C (1100, 1200, and 1300°F) the reduction in area decreased progressively with decreasing strain rate.

The decrease in ultimate tensile stress with decreasing strain rate is likely due to the increasing tendency for creep or time-dependent

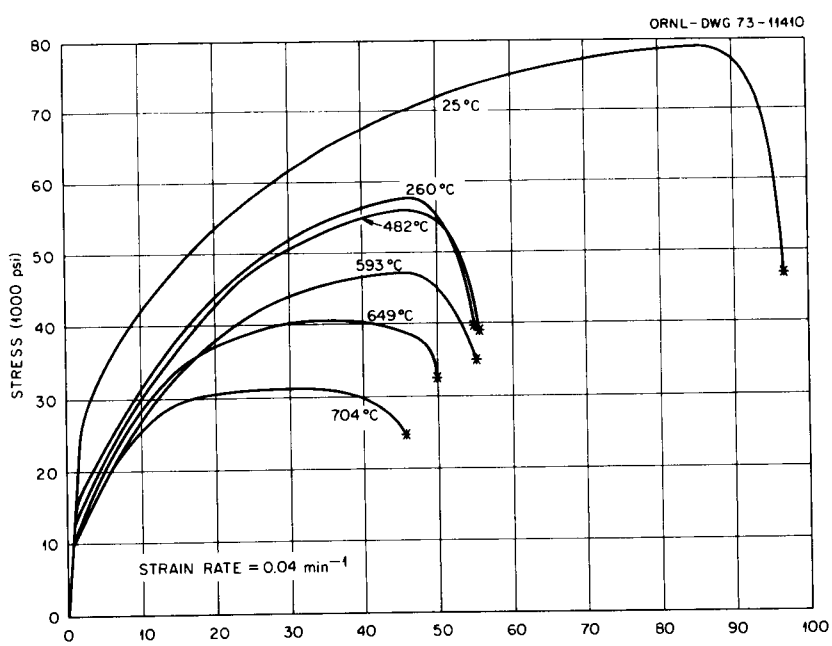

Fig. 5.8. Tensile Properties of Type 304 Stainless Steel Reference Heat 9T2796, 2-in. Plate, Annealed 0.5 hr at 1093°C (2000°F).

Table 5.5. Tensile Properties of Type 304 Stainless Steel (Heat 9T2796), 2-in.-Thick A 240 Plate Reannealed 0.5 hr at 1093°C (2000°F)

Temperature		Strain Rate	Stress, ksi[a]		Strain, %		Reduction in area
(°C)	(°F)	(min^{-1})	Yield	Ultimate	Uniform	Total	(%)
25	77	0.4	28.4	75.3	65.6	76.5	81.5
		0.04	25.8	78.1	85.6	91.4	83.0
			27.7	78.6	76.3	89.0	83.3
		0.004	26.7	80.0	85.2	102.0	85.1
			26.5	82.1	82.5	98.0	85.2
		0.0004	23.4	78.0	96.0	106.0	83.8
260	500	0.4	14.9	56.3	45.6	50.8	75.1
		0.04	14.7	57.2	47.2	51.2	73.3
		0.004	15.7	55.9	44.0	48.3	72.6
			15.8	59.3	47.7	49.9	63.7
		0.0004	13.2	59.1	52.3	53.4	71.6
427	800	0.4	12.3	55.8	45.6	47.3	66.9
		0.04	12.4	57.2	45.6	44.6	59.8
		0.004	12.5	60.2	45.9	52.2	63.8
			12.9	61.1	45.3	50.4	71.5
		0.0004	11.7	60.7	50.9	56.2	65.8
482	900	0.4	11.5	54.0	45.6	49.9	70.0
		0.04	12.2	55.8	46.4	51.5	71.4
		0.004	11.6	58.0	43.2	50.3	64.8
			12.0	57.0	47.5	54.7	58.9
		0.0004	11.1	56.6	51.8	56.8	63.7
538	1000	0.4	12.0	51.8	40.0	45.9	71.1
		0.04	10.9	47.4	48.0	51.9	71.1
		0.004	11.0	53.2	43.3	52.1	64.1
			11.2	54.1	39.4	52.5	67.3
		0.0004	10.2	47.7	46.3	46.2	41.1
593	1100	0.4	9.94	46.9	41.6	47.2	70.6
		0.04	10.1	46.7	48.0	49.6	63.3
		0.004	10.7	45.4	34.6	38.0	32.4
			11.0	45.7	32.8	45.4	43.2
		0.0004	10.2	36.8	28.8	31.8	32.3
649	1200	0.4	9.87	42.5	40.0	49.2	63.4
		0.04	10.4	40.2	36.0	48.3	49.2
		0.004	10.2	35.8	25.5	33.1	31.9
			10.2	41.0	28.0	37.0	33.4
		0.0004	9.80	26.4	20.2	30.9	26.2
704	1300	0.4	9.33	35.9	31.7	44.7	43.5
		0.04	9.60	31.2	28.8	42.8	41.9
		0.004	11.0	26.9	19.0	39.0	32.4
			11.1	26.8	19.4	40.0	33.8
		0.0004	10.1	18.9	10.1	29.2	24.4

[a]1000 psi.

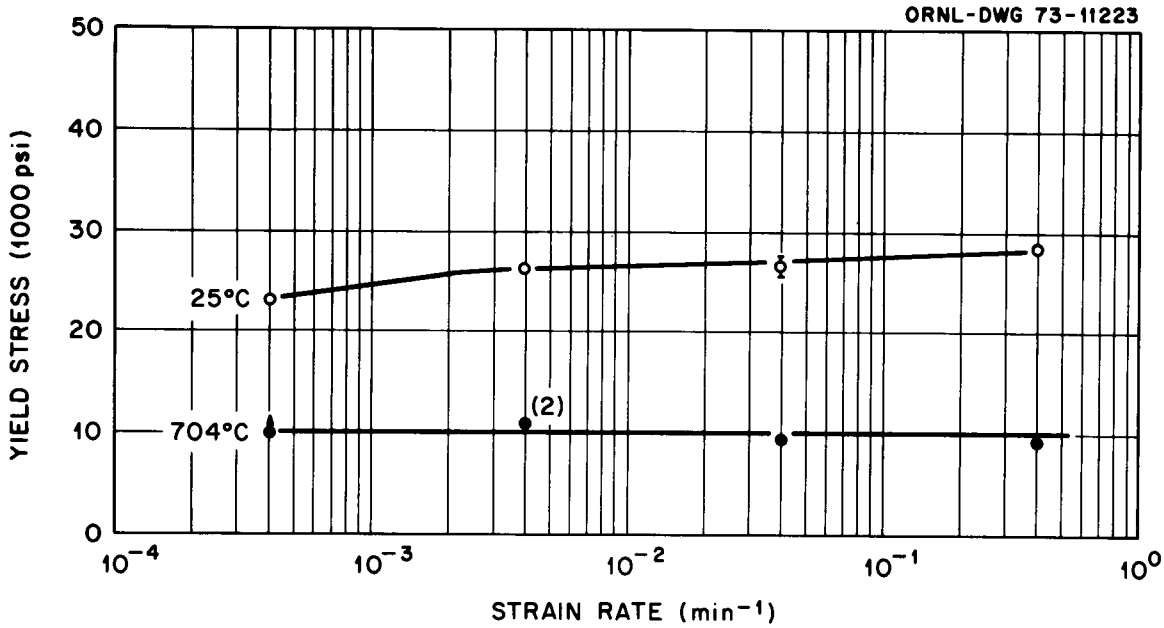

Fig. 5.9. Effect of Strain Rate on Yield Stress of Type 304 Stainless Steel, Heat 9T2796, Annealed 0.5 hr at 1093°C (2000°F).

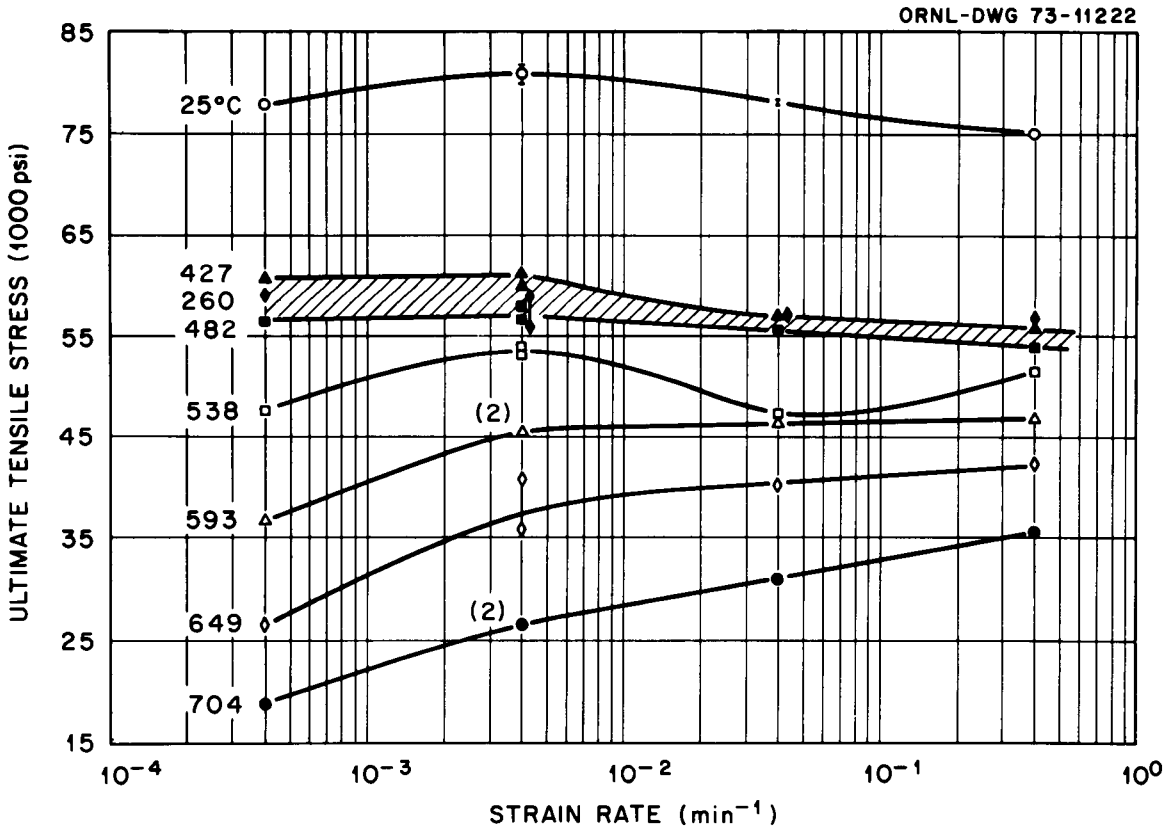

Fig. 5.10. Effect of Strain Rate on Ultimate Tensile Stress of Type 304 Stainless Steel, Heat 9T2796, Annealed 0.5 hr at 1093°C (2000°F).

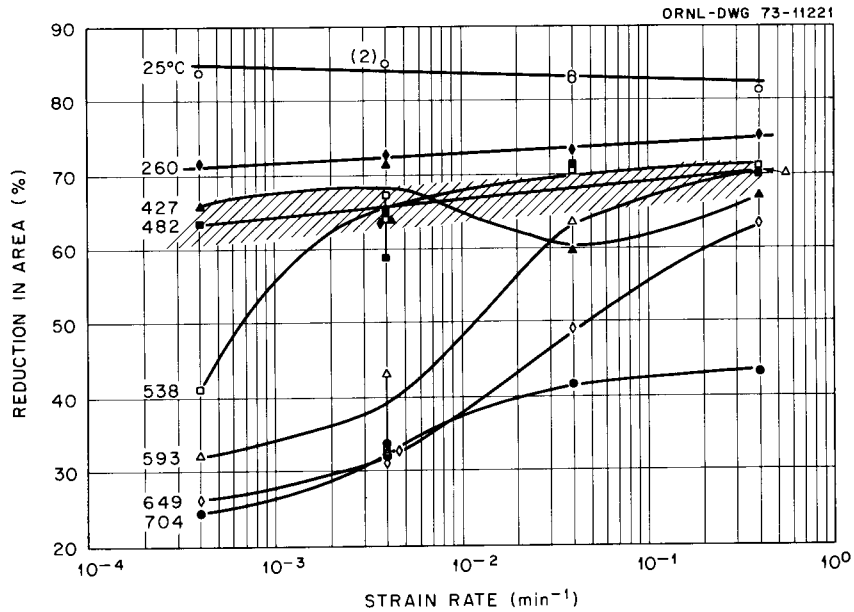

Fig. 5.11. Effect of Strain Rate on Reduction in Area of Type 304 Stainless Steel, Heat 9T2796, Annealed 0.5 hr at 1093°C (2000°F).

deformation to occur under these test conditions. The changes in reduction in area are likely associated with the transition from transgranular to intergranular fracture as the test temperature is increased and the strain rate decreased.

The yield and ultimate tensile stresses measured for heat 9T2796 are compared in Fig. 5.12 with the minimum values from the LMFBR Handbook. Note that the yield stress for this reannealed heat is below the "minimum value" at all test conditions. The ultimate tensile stress is above the minimum value of 75,000 psi at 25°C (77°F), but most of the measured values fall below

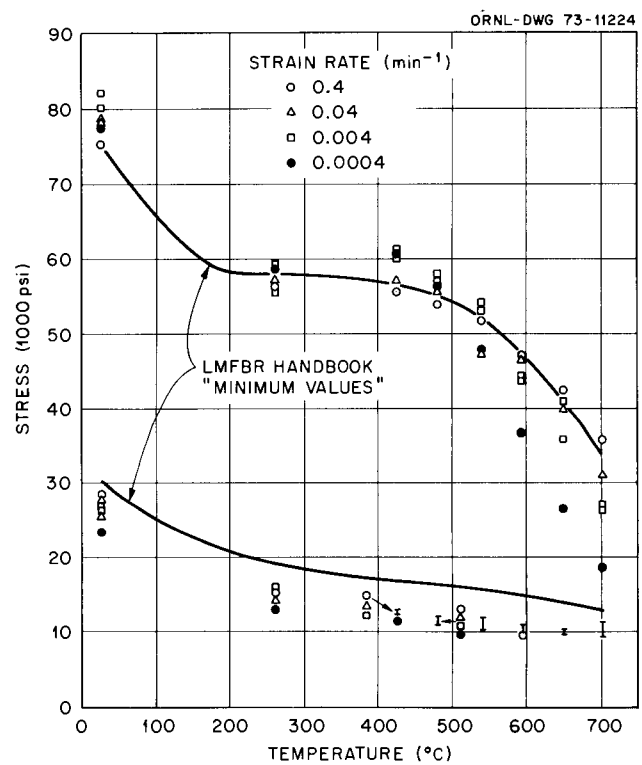

Fig. 5.12. Influence of Strain Rate on the Tensile Properties of Type 304 Stainless Steel, Heat 9T2796, Annealed 0.5 hr at 1093°C (2000°F). Upper curve, ultimate tensile stress; lower curve, yield stress.

the minimum handbook values at higher temperatures. The dependence of the ultimate tensile stress at 704°C (1300°F) on the strain rate is apparent.

5.2.1.3 Variation of Properties of Reference Heat with Product Form (Plate, Bar, and Pipe) — H. E. McCoy

In the present study 12 products from a single heat of type 304 stainless steel were tested in tension at 25 and 593°C (77 and 1100°F) and under stress-rupture conditions at 593°C (1100°F) to investigate variations with product. Material was tested in the as-received condition and after reannealing 0.5 hr at 1093°C (2000°F). Ideally, one would correlate the property variations with the fabrication sequences used in making the products, but the needed details of fabrication are not available. However, the properties obtained in this study are useful since they were obtained on a large number of products from a single heat of material and, therefore, illustrate the variations that result only from fabrication and heat treatment.

The products included in this study were fabricated from one 90-ton electric-arc-melted heat of type 304 stainless steel. Each product is briefly described in Table 5.6. The 12 products were of three basic forms: (1) plate from 3/8 to 2 in. thick, (2) bar from 1 3/4 to 4 1/2 in. in diameter, and (3) pipe (or tubing) from 2 1/2 to 8 5/8 in. (8 in. nominal) OD. Applicable ASTM and RDT standards are indicated in Table 5.6. Generally, the two standards differ only in that the RDT standard requires closer control of composition and additional inspection.

Hardness was measured before and after reannealing. A large range was noted for each as-received product, likely reflecting nonuniform working. After reannealing, the R_B hardness of all products decreased to the range 63 to 69.

A sample of each product was examined metallographically before and after reannealing. An oxalic acid etch was used to reveal the grain structure, and comparative grid charts were used to determine the ASTM grain size. The grain size of the as-received products ranged from 1–3 to 6–7 and that of the reannealed products from 1–2 to 4.

Each product was analyzed for carbon, oxygen, and nitrogen. Carbon and nitrogen concentrations averaged 0.052 and 0.045%, respectively.

Table 5.6. Information on Several Product Forms of Type 304 Stainless Steel, Heat 9T2796

Product Form	Specification	Hardness, R_B		Grain Size, ASTM No.		Chemical Composition,[b] %		
		Initial	Reannealed[a]	Initial	Reannealed	C	O	N
Plate, 3/8 in. thick	RDT M5-1T(A 240)	86	63	5-6	3-4	0.045	0.0033	0.041
Plate, 1/2 in. thick	RDT M5-1T(A 240)	73	66	5-6	3	0.052	0.0075	0.046
Plate, 3/4 in. thick	RDT M5-1T(A 240)	66	65	5-6	3	0.051	0.011 0.014	0.048 0.044
Plate, 1 in. thick	RDT M5-1T(A 240)	70	65	1-3	1-3	0.048 0.050	0.0020	0.039 0.031
Plate, 2 in. thick	RDT M5-1T(A 240)	69	65	1-3	1-2	0.055	0.0086	0.040
Bar, 1 3/4 in. diam	RDT M7-3T(A 479)	81	65	5-6	3	0.052	0.0062	0.048
Bar, 2 in. diam	RDT M7-3T(A 479)	89	65	5-6[c] 6-7[d]	3	0.053	0.0049	0.048
Bar, 4 1/2 in. diam	RDT M7-3T(A 479)	67	67	2-3[c] 3-5[d]	3	0.051	0.0062	0.049
Pipe, 4 in. sched 160	ASTM A 376	73	63	5-6	4	0.052	0.0089	0.051
Pipe, 8 in. sched 40	ASTM A 376	73	69	5-6	2	0.056	0.018 0.019	0.042 0.042
Tube, 2 1/2 in. OD × 5/8 in. wall (hot reduced)	RDT M7-3T(A 479)	88	65	6-7	3	0.051	0.0053	0.050
Tube, 2 1/2 in. OD × 5/8 in. wall (cold drawn)	RDT M3-3T(A 376)	74	67	3-6	3	0.050	0.0046	0.047

[a]0.5 hr at 1093°C (2000°F).

[b]Four product forms were analyzed for trace elements, and the following levels apply to all four: <0.01% Ag, 0.05% Al, <0.01% B, <0.01% Ba, <0.005% Be, <0.02% Bi, <0.1% Ca, <0.1% Cd, 0.3% Co, 0.3% Cu, 0.01% Mg, <0.1% Nb, <0.02% Pb, <0.05% Pt, <0.02% Sn, <0.1% Sr, 0.05% Ta, <0.02% Ti, 0.03% V, <0.1% W, <0.2% Zn, <0.05% Zr, <0.05% Ge, <0.05% Ga. The concentrations of other alloying additions are 1.22% Mn, 0.029% P, 0.012% S, 0.47% Si, 18.5% Cr, 9.58% Ni, 0.10% Mo.

[c]Longitudinal plane.

[d]Transverse plane.

Variations of both elements were within the limits of analytical error, except in the 1-in.-thick plate, which had a lower nitrogen content. Oxygen concentrations varied significantly among the various products.

5.2.1.3.1 Room-Temperature Properties. The results of tensile tests at 25°C (77°F) on the 12 products in the as-received and reannealed conditions are given in Table 5.7. Samples were taken parallel, perpendicular, and at 45° to the primary working direction for the plate products, but no significant variation was found and the data are presented without identification of orientation. Samples made from the 4 1/2-in.-diam bar were oriented parallel or perpendicular to the working direction, but no difference in properties was noted. All other products were sampled parallel to the primary working direction.

The initial portions of the stress-strain curves at 25°C (77°F) are shown in Fig. 5.13 for the as-received products and in Fig. 5.14 for reannealed specimens. Typical stress-strain curves are shown, and the 0.2% offset yield stresses are indicated. Although there is considerable variation in the yield stress, the parallel curves indicate that the different products had similar work-hardening characteristics. Reannealing reduced the magnitude of the yield stress as well as the range observed for the various products.

The yield stresses of the plate products are shown in Fig. 5.15. Several significant observations can be made for the plate products.

1. Yield stress of the as-received material decreased with increasing plate thickness.

2. Yield stress after reannealing was the same for all plate thicknesses.

3. Variations in yield stress within for each plate were greater for the as-received product than for reannealed plate.

4. All the reannealed samples and several of the as-received had yield stresses less than the 30,000 psi minimum required by the ASTM A 240 specification.

The hardnesses in Table 5.6 follow the same trends noted in Fig. 5.15. for the yield stresses. The hardness and yield stress for the as-received plate generally decreased as the plate thickness increased. Reannealing

Table 5.7. Tensile Properties of Type 304 Stainless Steel (Heat 9T2796) at 25°C (77°F)[a]

Product	Yield Stress, ksi		Ultimate Tensile Stress, ksi		Fracture Strain, %		Reduction in Area, %	
	As Received	Annealed[b]	As Received	Annealed	As Received	Annealed	As Received	Annealed
Plate, 3/8 in. thick	41.2	25.0	89.4	82.6	75.2	85.8	82.5	84.9
	45.4		89.2		70.5		71.7	
Plate, 1/2 in. thick	29.3	25.2	87.0	85.0	79.8	81.1	73.0	75.0
	30.1	25.9	87.9	85.1	80.5	82.8	81.9	82.5
	32.9	26.2	87.0	83.7	81.8	84.0	82.5	82.7
Plate, 3/4 in. thick	34.4	26.0	85.9	83.5	80.0	79.0	82.6	81.3
	29.3	26.1	85.2	83.4	77.0	81.0	76.0	76.6
	29.4	25.3	83.8	81.9	85.2	88.1	80.5	83.5
Plate, 1 in. thick	32.4	26.4	84.0	84.7	70.0	85.0	80.0	85.5
	29.2		81.6		95.0		82.0	
Plate, 2 in. thick	26.5	26.0	78.8	82.9	91.0	88.0	85.2	82.3
	27.7		80.6		85.0		84.6	
Bar, 1 3/4 in. diam	42.0	26.6	85.6	83.1	80.9	88.7	83.5	84.2
	42.3	27.0	85.2	82.7	77.9	86.1	83.5	83.9
	41.6		85.2		79.5		82.3	
	44.5	25.2	86.4	82.9				
Bar, 2 in. diam	45.0	25.2	89.8	82.4	78.4	85.4	82.9	84.7
	40.0	23.7	88.1	81.9	76.8	82.6	80.8	83.8
	50.8	25.2	89.9	84.3	75.2	84.1	82.9	84.0
	48.9				74.6		80.9	
Bar, 4 1/2 in. diam	46.7	26.5	82.8	83.6	85.0	77.0	84.3	82.0
	30.8	26.1	82.4	86.8	85.0	84.0	84.6	82.6
	29.7		83.5		83.5		69.6	
Pipe, 8 in. sched 80	30.3	26.0	85.4	82.9	82.0	88.0	82.2	82.3
		26.5		83.0		80.0		82.6
Pipe, 4 in. sched 160	31.7	26.7	84.5	82.9	84.0	85.0	83.3	83.6
	32.3	26.5	84.6	82.8	83.0	87.0	83.3	83.1
Tube, 2 1/2 in. OD × 5/8 in. hot reduced	57.2	23.6	96.0	81.4	70.8	87.5	81.1	84.9
	57.0	23.2	93.3	81.3	71.8	88.9	83.2	85.7
		23.7		81.4		88.9		84.9
Tube, 2 1/2 in. OD × 5/8 in. cold drawn	32.2	25.6	86.5	84.0	78.4	80.0	83.1	83.3
	32.2	25.1	86.5	83.6	78.3	82.0	82.8	84.3
		25.6		84.3		80.8		83.5

[a]Strain rate of 0.004/min to 5% strain, 0.04/min to failure.

[b]Annealed 0.5 hr at 1093°C (2000°F) in argon.

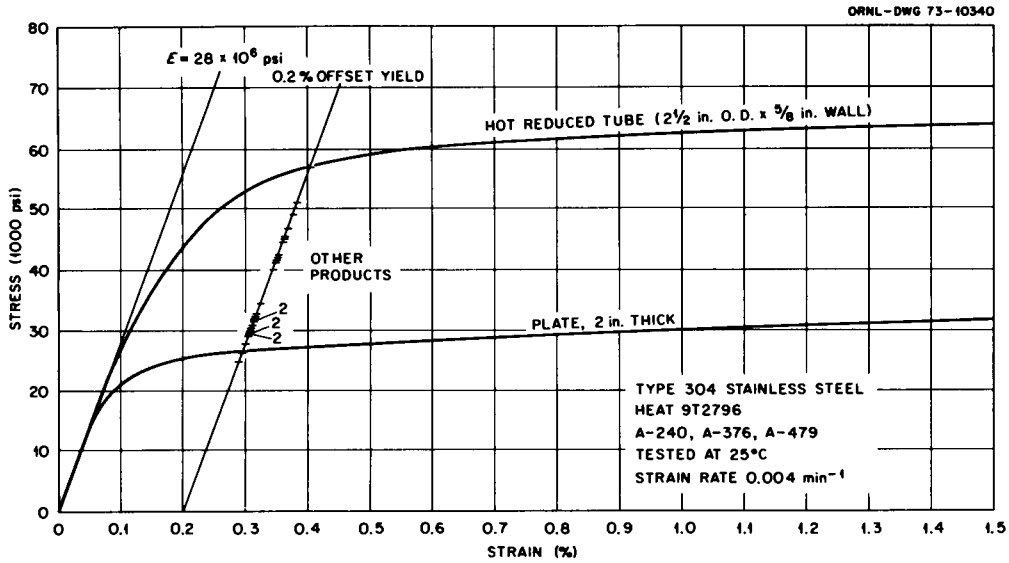

Fig. 5.13. Stress-Strain Response at 25°C (77°F) of Various Type 304 Stainless Steel Products in the As-Received Condition.

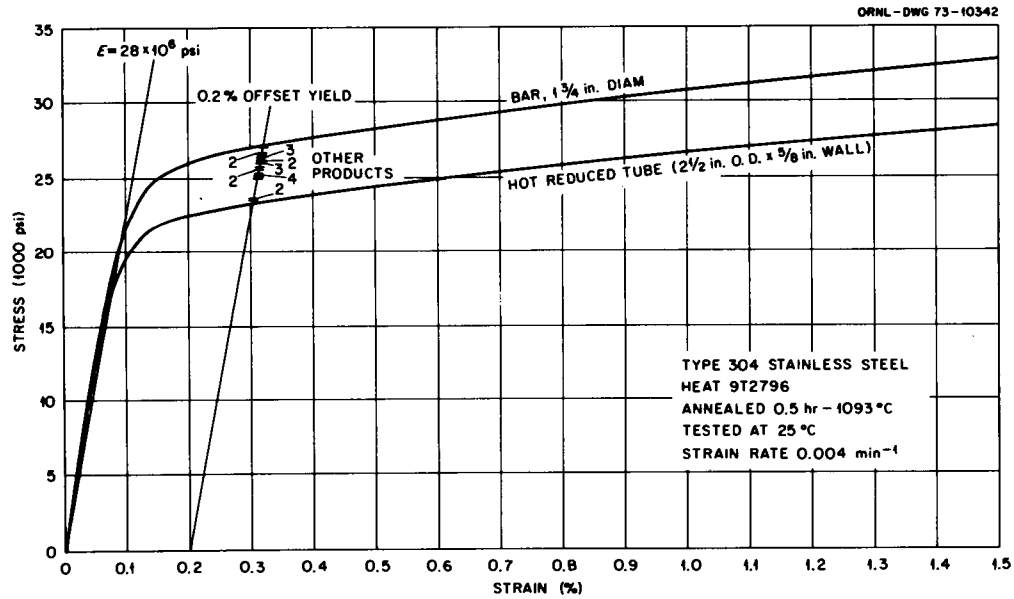

Fig. 5.14. Stress-Strain Response at 25°C (77°F) of Various Type 304 Stainless Steel Products After Reannealing 0.5 hr at 1093°C (2000°F).

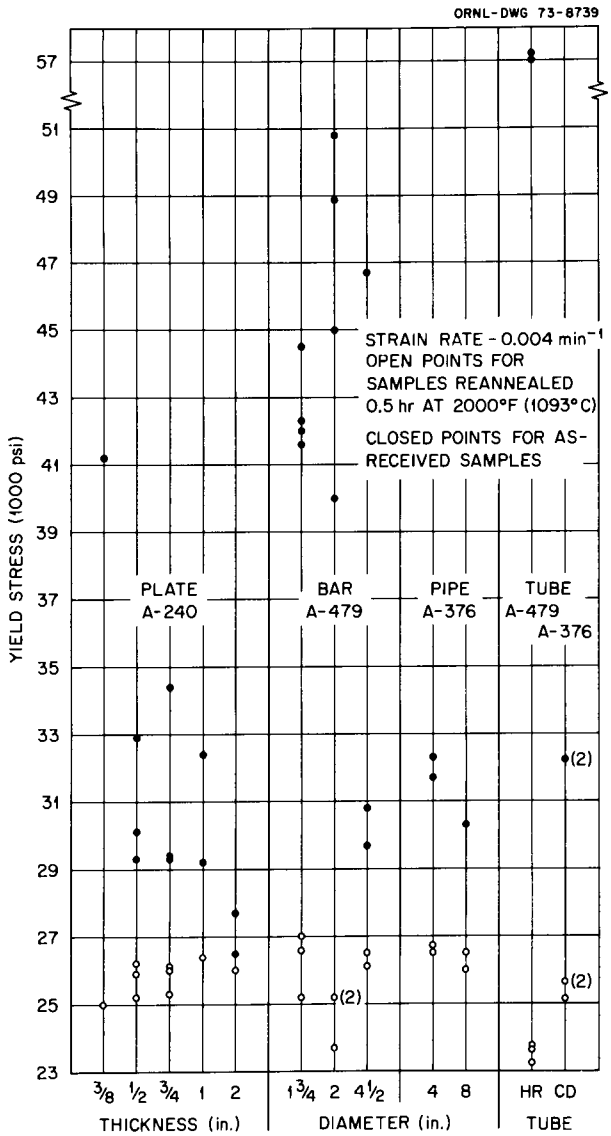

Fig. 5.15. Yield Stress at 25°C (77°F) of Several Products of a Single Heat of Type 304 Stainless Steel.

resulted in a hardness of about 65 and an average yield stress of 25,800 psi for all plates. Hardness measurements reflected non-uniformity of working also in that the individual measurements on as-received samples had about a 15-point spread, whereas those for reannealed samples had a spread of 5 points or less.

The plates under discussion were rolled from slabs varying in thickness from 3 3/4 to 6 1/2 in. The slabs were soaked at 1220 to 1245°C (2225 to 2275°F) and rolled through multiple passes to obtain the final thicknesses. The final pass temperatures for the 3/8-, 1/2-, 3/4-, 1-, and 2-in.-thick plates were 675, 865, 880, 915, and 1010°C (1250, 1590, 1620, 1675, and 1850°F), respectively. The plates were given a final anneal at 1065°C (1950°F) for 25 to 70 min, water quenched, cleaned, and roller-leveled.

Several factors were likely important in determining the properties of the plates. These include the amount of work in the plates before annealing, the grain size before annealing, the temperature-time history during the final 1065°C (1950°F) anneal, and the amount of working as a result of roller leveling the plates after annealing. However, the details of the above are not known, and one can only assume that they were typical of commercial practice. Thus, the differences in properties are representative of what would be observed in commercial products.

Yield stresses of the bar products shown in Fig. 5.15 illustrate the following points: (1) the yield stress of as-received material was much higher than that of reannealed product; (2) the yield stress of the as-received material was very nonuniform for each product (e.g., it varied from 29,700 to 46,700 psi for the 4 1/2-in.-diam bar); (3) reannealing resulted in an average yield stress of 25,700 psi and much smaller variations in strength; and (4) there was no systematic variation of yield stress from one bar product to another in either the as-received or reannealed conditions.

No fabrication details are available for the bar products, but the yield strength data (Fig. 5.15) and the hardness values (Table 5.6, p. 95) indicate that the as-received products contained considerable residual cold work. The spread in the yield stresses and the hardness measurements for the as-received products indicate that residual cold work was nonuniform. Reannealing reduced hardness to about 65 and increased grain size to ASTM No. 3.

The hot-reduced (HR) tubing was fabricated by gun drilling a bar. In the as-received condition the yield stress and hardness were higher than those of the bar products. Reannealing reduced the yield stress to an average value of 23,500 psi, reduced the hardness to 65, and increased the grain size to ASTM No. 3. We have no explanation for the yield stress of this product being about 2000 psi lower after reannealing than that of the other rod products.

The yield stresses of two pipe products and one thick-walled tube, all produced to ASTM Standard A 376 (given in Fig. 5.15) show the following significant features;

1. The yield stress in the as-received condition was about equal for all three products, with an average value of 31,700 psi.

2. After reannealing the yield stress had decreased to an average value of 26,200 psi.

The R_B hardnesses for the three products in the as-received condition are in excellent agreement, the measurements being 73, 73, and 74. Reannealing resulted in hardness values of 63, 69, and 67.

Only the yield stress has been discussed this far, but several other tensile properties are listed in Table 5.7. These other properties were

less sensitive to fabrication variables than the yield stress. For example, the yield stress of the as-received products varied from 26,500 to 57,200 psi, a variation about the mean of ±37%. The ultimate tensile stress varied from 78,000 to 96,000 psi, a variation about the mean of only ±10%. The tensile stresses of the reannealed products fell in the range 81,300 to 86,800 psi. This range is smaller but within that of the as-received products. Generally, high ultimate tensile stresses were associated with high yield stresses. The fracture strains of the as-received products varied from 70 to 95% and those of the reannealed products from 77 to 89%. These values are all quite high and considerably above the specified minimum of 40%. Again, the range for the reannealed samples is smaller and contained within the range for the as-received materials. Measured reductions in area were quite high, ranging from 70 to 85% for as-received material and from 75 to 86% for the reannealed material. Based on the accuracy of the measurement and the reproducibility from specimen to specimen, none of the variation in ductility measures is thought to be significant.

5.2.1.3.2 Elevated-Temperature Properties. The results of tensile tests on the 12 products at 593°C (1100°F) are summarized in Table 5.8. The initial portions of the stress-strain curves for the reannealed products are shown in Fig. 5.16. The yield stresses are shown in Fig. 5.17. Most of the tests at 593°C (1100°F) were performed on reannealed rather than as-received products. The only as-received plate tested was the 3/8-in.-thick plate, which has a yield stress about twice that of the reannealed material. As-received bar, pipe, and tubing products had yield stresses of 15,000 to 17,000 psi except for the gun-drilled hot-reduced tubing, which had a yield stress of 35,500 psi. The reannealed products had an average yield stress of 10,900 psi, with all but six tests giving values in the range of 10,200 to 11,700 psi. The yield stress of the 1 3/4-in.-diam bar fell above this range and that of the 2-in.-diam bar and hot-reduced tube fell below. Since the hardnesses, grain sizes, and chemical analyses of these two products in the reannealed condition were almost identical, we have no explanation for the difference in yield strengths.

Table 5.8. Tensile Properties of Type 304 Stainless Steel Heat 9T2796 at 593°C (1100°F)[a]

Product	Condition	Stress, ksi		Fracture Strain (%)	Reduction in Area (%)
		Yield	Ultimate		
Plate, 3/8 in. thick	As received	23.5	51.7	42.3	69.8
	Annealed[b]	10.4	48.9	49.6	68.5
Plate, 1/2 in. thick	Annealed[b]	10.7	49.4	46.8	61.6
		11.0	50.1	48.2	67.8
		11.5	48.9	48.2	65.9
Plate, 3/4 in. thick	Annealed[b]	10.5	50.6	50.0	72.9
		10.8	50.4	49.1	63.2
		10.2	47.6	51.7	65.7
Plate, 1 in. thick	Annealed[b]	11.1	46.5	37.5	51.5
Plate, 2 in. thick	Annealed[b]	10.7	45.4	38.0	32.4
		11.0	45.7	45.4	43.2
Bar, 1 3/4 in. diam	Annealed[b]	13.1	48.8	49.4	65.8
		12.9	48.6	49.2	67.6
Bar, 2 in. diam	Annealed[b]	9.53	48.8	45.5	66.7
		9.51	48.8	50.5	68.3
Bar, 4 1/2 in. diam	As received	14.8	47.0	43.3	61.6
	Annealed	10.6	47.7	52.1	68.7
		10.8	48.1	53.7	70.7
		10.6	46.7	43.3	61.9
		10.8	46.3	43.9	60.6
Pipe, 8 in. sched 80	As received	15.9	49.5	50.6	65.9
	Annealed	11.2	49.2	53.9	68.9
Pipe, 16 in. sched 160	As received	16.6	49.5	50.6	65.9
	Annealed	11.7	49.5	54.3	68.5
		11.7	49.5	56.3	68.7
Tube, 2 1/2 in. OD × 5/8 in. (hot reduced)	As received	35.5	47.1	42.9	56.9
	Annealed	9.55	48.4	48.7	65.3
		9.44	49.3	54.0	69.8
Tube, 2 1/2 in. OD × 5/8 in. (cold drawn)	As received	15.5	52.0	44.4	66.9
	Annealed	11.4	50.9	44.2	69.2
		10.8	50.7	46.2	70.2
		10.6	50.6	47.7	66.2

[a]Strain rate of 0.004/min to 5% strain, 0.04/min to failure.

[b]Annealed 0.5 hr at 1093°C (2000°F) in argon.

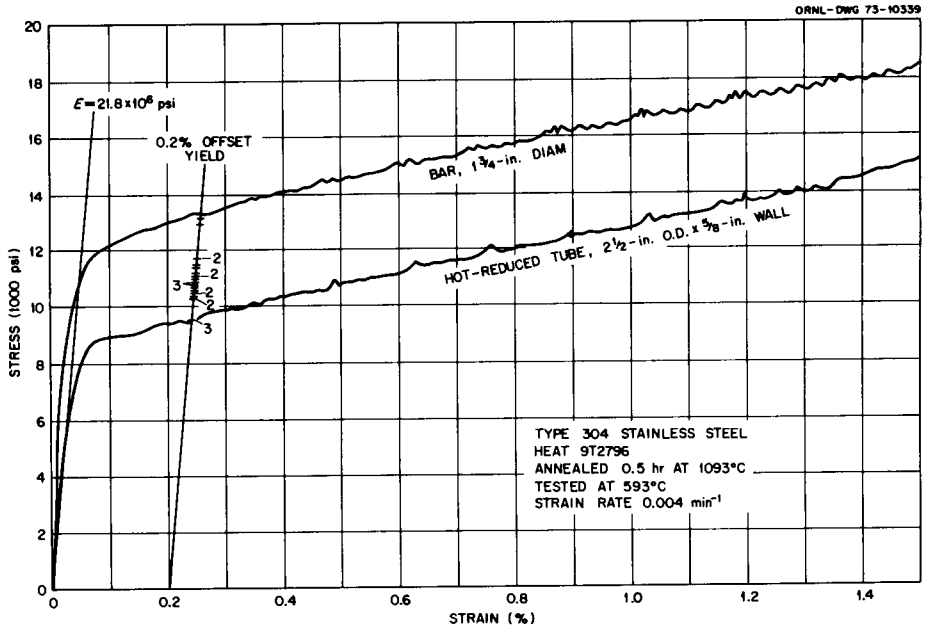

Fig. 5.16. Stress-Strain Curves at 593°C (1100°F) for Several Type 304 Stainless Steel Products Reannealed 0.5 hr at 1093°C (2000°F).

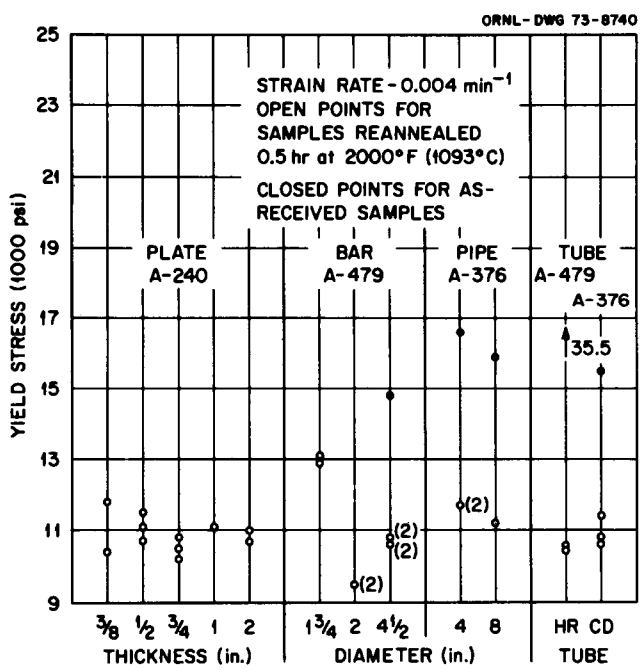

Fig. 5.17. Yield Stress at 593°C (1100°F) of Several Products of a Single Heat of Type 304 Stainless Steel.

The other tensile properties showed less variation than did the yield strengths. The ultimate tensile strength of the as-received samples varied from 47,000 to 52,000 psi and that of the reannealed material from 45,400 to 50,900 psi. The strength of the reannealed 1- and 2-in.-thick plates fell on the low side of this range. The fracture strains varied from 40.8 to 44.4% for the as-received samples and from 37.5 to 56.3% for the reannealed material. The reduction in area ranged from 56.9 to 69.8% for the as-received samples and from 32.4 to 72.9% for the reannealed material. The 1- and 2-in.-thick plates had lower ductility (fracture strain and reduction in area) than the other products. The slight differences in tensile strength and ductility for the two plates compared with the other products are likely due to the larger grain size of the plates.

Twelve products in the reannealed condition were stress-rupture tested at 593°C (1100°F), and the results are listed in Table 5.9 and shown in Figs. 5.18 and 5.19. The complete creep curves obtained at 25,000 psi are shown in Fig. 5.20. These data have been analyzed statistically, and we conclude that the properties of any one product

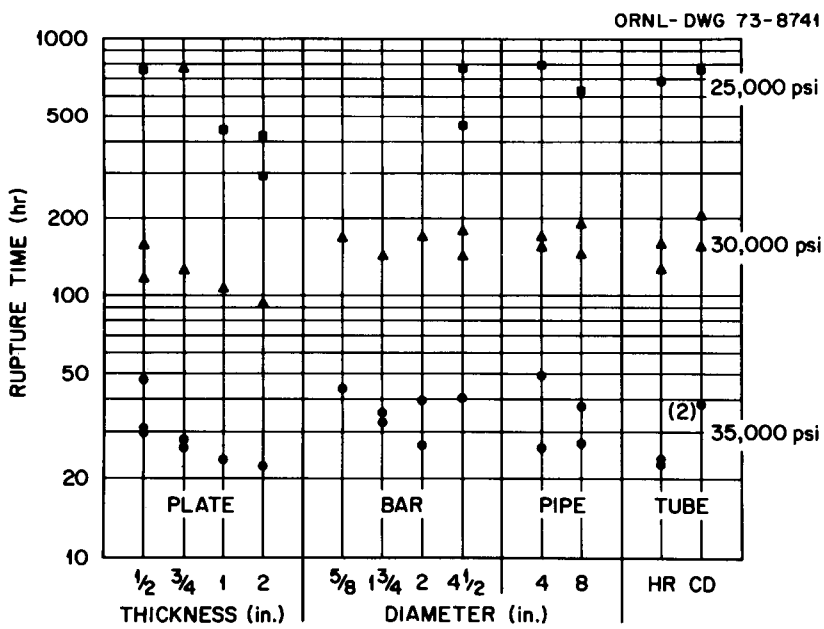

Fig. 5.18. Stress-Rupture Properties at 593°C (1100°F) of Several Products of a Single Heat of Type 304 Stainless Steel Reannealed 0.5 hr at 1093°C (2000°F).

Table 5.9. Stress-Rupture Properties of Type 304 Stainless Steel at 593°C (1100°F)[a]

Product	At 35,000 psi			At 30,000 psi			At 25,000 psi		
	Rupture Life (hr)	Minimum Creep Rate (%/hr)	Creep Strain (%)	Rupture Life (hr)	Minimum Creep Rate (%/hr)	Creep Strain (%)	Rupture Life (hr)	Minimum Creep Rate (%/hr)	Creep Strain (%)
Plate, 3/8 in. thick	14.9	0.34	14.9	150.7	0.055	15.6	527.3	0.013	10.2
Plate, 1/2 in. thick	47.6	0.33	23.4	158.2	0.090	20.8	759.3	0.013	19.8
	29.9	0.55	22.8						
	30.9	0.49	30.0	117.0	0.13	23.8			
Plate, 3/4 in. thick	26.1	0.32	13.9	123.9	0.043	9.4	769.6	0.0065	11.8
	28.0	0.26	11.9						
Plate, 1 in. thick	23.5	0.41		107.1	0.10	17.4	440.1	0.011	16.0
Plate, 2 in. thick	22.2	0.37	16.2	92.8	0.078	11.4	423.3	0.0080	4.4
							291.0	0.010	7.4
Bar, 5/8 in. diam	43.7	0.35		168.8	0.061				
Bar, 1 3/4 in. diam	32.5	0.33	20.4	142.5	0.066	14.7	600.7	0.011	14.0
	35.4	0.29	19.3						
Bar, 2 in. diam	39.5	0.28	16.7	169.0	0.058	17.1	614.4	0.0084	12.8
	26.8	0.33	15.2						
Bar, 4 1/2 in. diam	40.2	0.33	19.6	140.2	0.070	15.7	765.9	0.0072	12.6
				178.8	0.12	31.2	457.8	0.021	18.1
Pipe, 8 in. sched 20	37.4	0.29	15.4	187.8	0.041	11.1			
	27.0	0.30		143.7	0.057	15.7	630.4	0.011	13.6
Pipe, 4 in. sched 160	26.0	0.56	29.2	168.5	0.055	16.0			
	49.6		20.1	153.4	0.080	28.3	785.9	0.0074	13.0
Tube, 2 1/2 in. OD	23.9	0.41	17.6	126.6	0.056	10.3			
× 5/8 in. hot reduced	22.7	0.36	12.4	159.2	0.034	11.1	690.7	0.0076	11.1
Tube, 2 1/2 in. OD	38.7	0.25	17.2	203.3	0.038	13.6			
× 5/8 in. cold drawn	38.3	0.28	13.2	154.9	0.053	12.5	758.4	0.0064	12.2

[a]Reannealed 0.5 hr at 1093°C (2000°F).

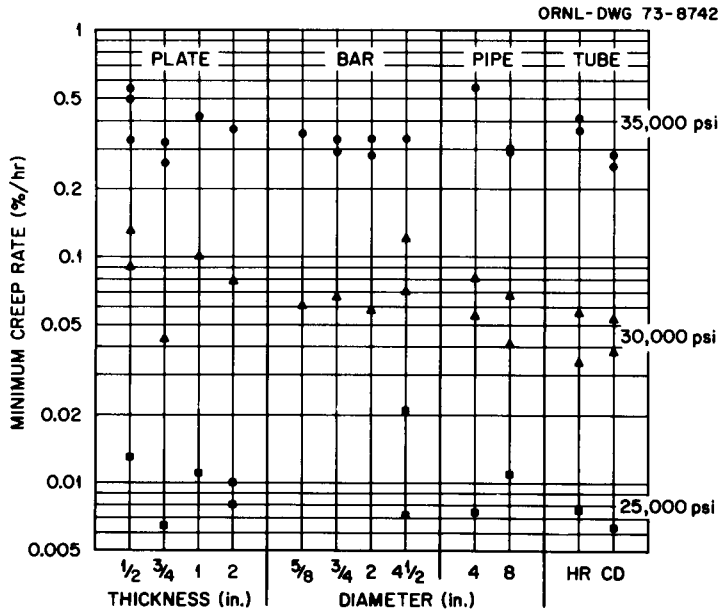

Fig. 5.19. Minimum Creep Rate at 593°C (1100°F) of Material Reannealed 0.5 hr at 1093°C (2000°F).

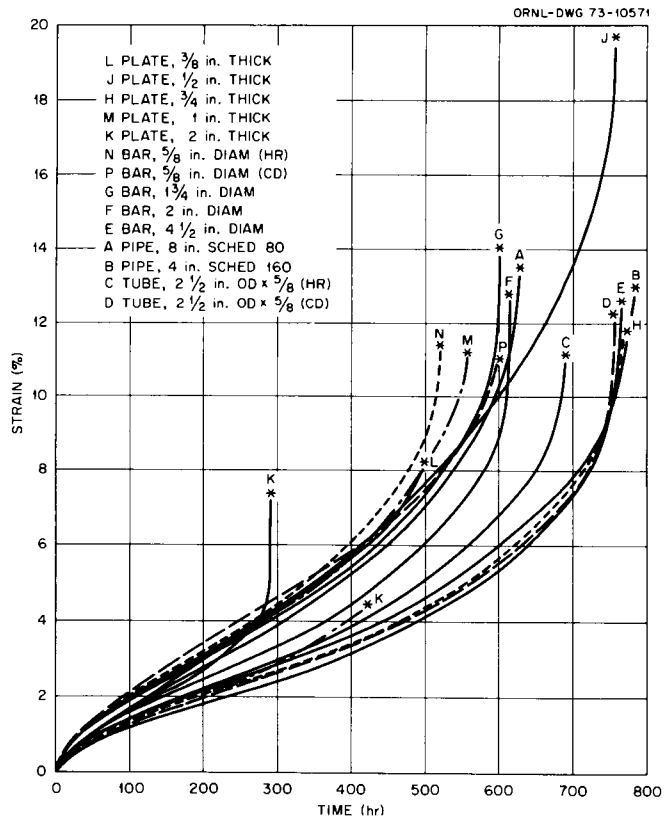

Fig. 5.20. Creep Curves for Type 304 Stainless Steel (Heat 9T2796) Annealed 0.5 hr at 1093°C (2000°F) and Tested at 593°C (1100°F) and 25,000 psi.

were not significantly different from those of another. Some of the property variations may be significant, but the degree of reproducibility of tests on "identical samples" made it impossible to conclude that the properties of different products were significantly different. The creep properties agree reasonably well with those compiled by Smith[3] but tend to fall on the weak side of the scatter band.

5.2.2 Heat-to-Heat Variation Study of Type 304 Stainless Steel

Applications of current interest, such as LMFBRs, require the use of stainless steels at temperatures where time-dependent deformation occurs. Accurate analytical techniques must be developed for designing such systems, and their development and use require that the stress-strain-time interactions be known for the structural material of interest. It is recognized that the properties of type 304 stainless steel may vary from heat to heat, and it is the purpose of the present program to define this variation and to relate it, where possible, to the metallurgical characteristics (chemical composition, grain size, etc.) of the heats. This program currently involves 16 heats of type 304 stainless steel, and test results have been published in this report series over the past year. The chemical composition and other pertinent information are given in Table 5.10.

5.2.2.1 Tensile and Short-Term Creep Tests — H. E. McCoy

The first phase of testing for each heat of material in this program includes tensile tests in the as-received and reannealed conditions at room temperature, 427, 593, and 649°C (800, 1100, and 1200°F), and creep tests in the as-received and reannealed conditions at test conditions of 593°C (1100°F) and 35,000 and 30,000 psi. The tensile tests have been completed, and the yield and ultimate tensile strengths are listed in Table 5.11. The range of yield strengths observed for the as-received material is shown in Fig. 5.21. All the values are above the minimum in ASME Code Case 1331-8. The yield strengths after reannealing are shown in Fig. 5.22. The values are lower than those obtained in the as-received condition, and many values fall below the 1331-8 minimum. Thus, these

Table 5.10. Type 304 Stainless Steel Heats Being Investigated In the Heat-to-Heat Variation Program

Heat	Sample	Content, wt %																		Product[a] Size (in.)	Grain Size
		C	N	P	B	O	H	Ni	Mn	Cr	Si	Mo	S	Ti	Cu	Co	Pb	Sn	Ta + Cb		
544086	086-14	0.050	0.045	0.025		0.0091	0.0005	9.46	1.23	18.4	0.53	0.2	0.016	0.01	0.10	0.05	0.01	0.02	0.08	1	3
337187	187-7	0.058	0.034	0.021		0.0034	0.0006	9.27	0.97	18.1	0.42	0.03	0.010	0.01	0.07	0.05	0.01	0.02	0.08	1 1/2	2
337330	330-8	0.068	0.031	0.018		0.0042	0.0005	9.43	0.83	18.2	0.59	0.07	0.008	0.03	0.15	0.05	0.01	0.02	0.08	1 1/8	5.5
300380	380-24	0.063	0.068	0.018		0.0260	0.0009	8.30	0.97	18.4	0.55	0.07	0.010	0.03	0.10	0.05	0.01	0.02	0.08	2 3/8	2.5
600414	414-23	0.073	0.058	0.016		0.0190	0.0004	9.52	0.94	18.7	0.69	0.1	0.015	0.03	0.10	0.05	0.01	0.02	0.08	2 3/8	2.5
55697	697-7	0.057	0.034	0.016		0.0150	0.0005	9.38	0.91	18.5	0.50	0.05	0.037	0.01	0.10	0.05	0.01	0.02	0.08	5/8 bar	2.5
9T2796R	796	0.047	0.031	0.029		0.0110	0.0006	9.58	1.22	18.5	0.47	0.1	0.012	0.01	0.10	0.05	0.01	0.02	0.08	5/8 bar	3
R22926	926-6	0.053	0.041	0.020		0.0084	0.0007	9.79	1.16	19.0	0.68	0.1	0.025	0.01	0.07	0.05	0.01	0.02	0.08	2	3.5
X23283	283-1	0.043	0.025	0.018	0.0003	0.0140	0.0009	9.12	1.32	18.2	0.45	0.3	0.020	0.027	0.14	0.05	0.01	0.01	0.02	3/4	3
346845	845-1	0.057	0.024	0.023	0.0002	0.0092	0.0013	9.28	0.92	18.4	0.53	0.1	0.006	0.033	0.11	0.07	0.01	0.01	0.03	2 3/4	3
346544	544-7	0.063	0.019	0.023	0.0002	0.0081	0.0006	9.12	0.99	18.4	0.47	0.2	0.006	0.036	0.12	0.05	0.01	0.01	0.02	2	3
60551	551-1	0.043	0.027	0.022	0.0010	0.0220	0.0013	9.40	1.20	18.5	0.59	0.3	0.018	0.037	0.25	0.08	0.01	0.01	0.02	5 × 7 bar	3
345866	866-8	0.044	0.022	0.023	0.0002	0.0096	0.0010	8.98	1.51	18.5	0.47	0.2	0.007	0.031	0.13	0.04	0.01	0.01	0.02	3	3
X22807	807-1	0.029	0.021	0.024	0.0005	0.0100	0.0012	9.67	1.26	18.8	0.50	0.2	0.023	0.025	0.11	0.03	0.01	0.01	0.02	2 1/2	2
346779	779-1	0.065	0.023	0.024	0.0002	0.0056	0.0009	9.46	0.94	18.1	0.47	0.2	0.005	0.035	0.16	0.02	0.01	0.01	0.02	2 1/2	3
8043813	813	0.062	0.033	0.040	0.0003			8.95	1.87	17.8	0.48	0.32	0.004							1	4

[a]Product form is plate unless specified otherwise.

Table 5.11. Summary of Tensile Properties on Several Heats of Type 304 Stainless Steel

Heat[a]	Condition[b]	25°C (77°F)		427°C (800°F)		593°C (1100°F)		649°C (1200°F)	
		Yield Stress (ksi)	Tensile Stress (ksi)	Yield Stress (ksi)	Tensile Stress (ksi)	Yield Stress (ksi)	Tensile Stress (ksi)	Yield Stress (ksi)	Tensile Stress (ksi)
086	A 240	34.7	93.8	23.0	63.5	16.4	51.3	18.9	42.5
	1065°C	29.2	90.4	15.4	63.1	13.4	51.4	12.3	42.2
187	A 240	31.5	90.4	21.6	60.9	17.5	48.7	15.1	40.2
	1065°C	26.1	86.5	13.5	59.4	11.8	48.0	10.9	38.4
330	A 240	37.0	93.8	25.7	64.9	20.9	52.8	22.1	43.1
	1065°C	30.7	91.8	17.6	63.5	14.9	52.2	13.8	41.1
380	A 240	40.7	90.2	21.1	65.7	18.1	54.5	20.6	47.1
	1065°C	35.4	88.1	17.7	63.9	14.1	52.8	14.0	43.1
414	A 240	34.0	88.7	18.5	63.9	15.4	50.5	18.5	44.2
	1065°C	30.3	86.5	15.8	63.1	13.2	52.5	13.8	43.4
796	A 240	42.4	89.7	27.2	63.1	23.6	51.7	21.0	42.3
	1065°C	30.2	85.9	12.4	61.0	13.8	59.9	13.9	43.6
926	A 240	36.1	88.9	22.3	62.6	19.1	52.0	16.9	40.1
	1065°C	29.0	87.4	15.3	50.7	13.4	50.5	12.6	41.8
283	A 240	35.1	89.6	20.0	61.9	16.9	50.5	16.7	41.8
	1065°C	28.0	87.1	14.4	61.6	11.6	51.5	11.6	43.1
697	A 240	37.0	89.7	20.5	60.0	17.3	48.9	17.5	40.7
	1065°C	25.8	86.5	14.4	60.1	11.9	48.3	11.7	39.0
845	A 240	35.9	88.7	26.0	63.2	20.3	51.8	18.6	43.0
	1065°C	29.7	87.1	18.0	65.4	13.8	52.2	12.7	41.1
544	A 240	32.8	91.4	22.9	64.3	18.8	52.2	18.0	42.9
	1065°C	31.3	89.2	17.0	63.8	13.3	52.0	14.0	42.6
551	A 240	36.3	85.4	23.4	62.2	17.9	50.1	18.6	42.5
	1065°C	29.5	84.5	17.1	61.7	14.7	52.5	12.8	43.8
866	A 240	44.2	92.1	27.0	59.5	16.2	47.2	14.7	38.2
	1065°C	28.5	90.1	17.7	59.3	11.3	48.5	10.7	40.4
807	A 240	33.2	83.4	19.1	56.6	17.9	45.2	16.4	38.3
	1065°C	27.0	81.1	14.3	57.2	13.0	47.9	11.3	39.3
779	A 240	35.0	87.4	20.2	62.1	21.3	50.7	21.9	42.8
	1065°C	30.5	86.1	16.6	61.9	15.2	52.8	14.1	43.1
813	A 240	31.0	92.4	20.0	61.7	15.2	50.1	16.2	41.3
	1065°C	29.6	87.8	14.8	62.9	11.9	51.3	11.4	43.5

[a]Last three digits of number in Table 5.10.

[b]As received per specification A 240 or reannealed 0.5 hr at 1065°C (1950°F).

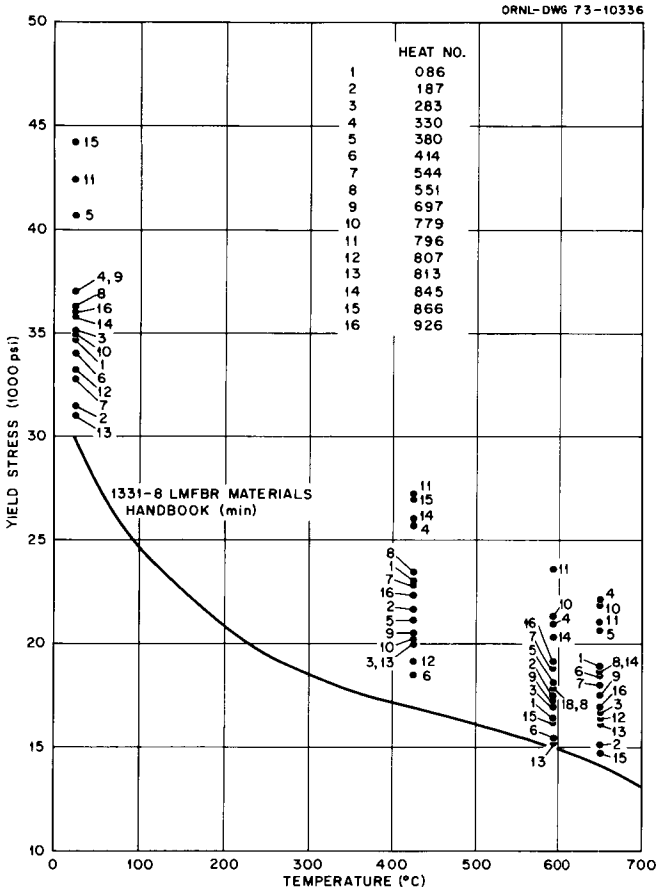

Fig. 5.21. Comparison of the Observed Yield Stress of As-Received Type 304 Stainless Steel with the 1331-8 Minimum.

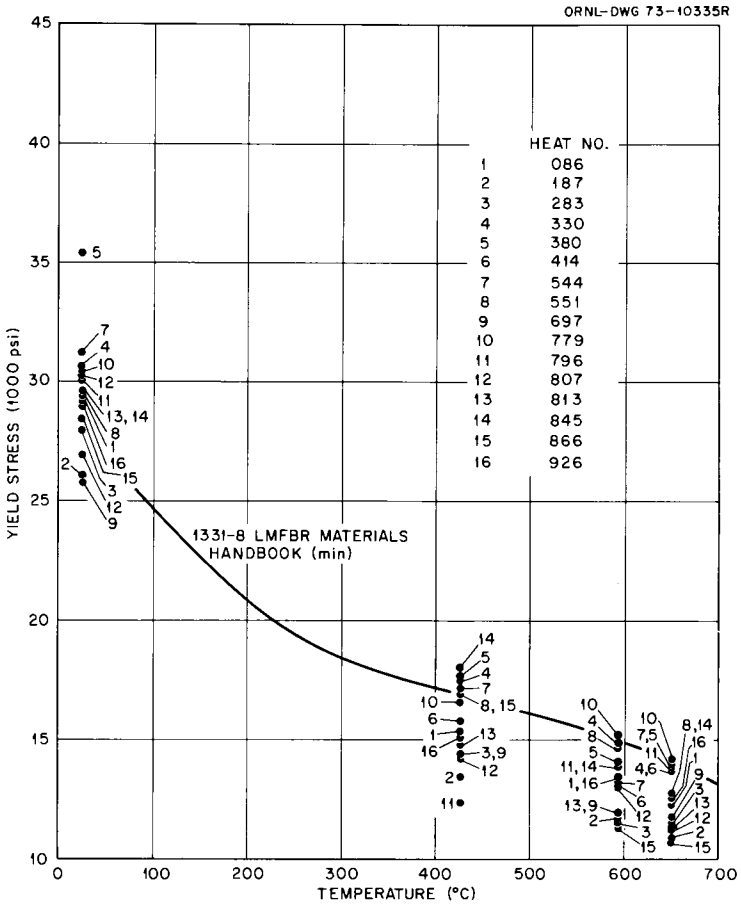

Fig. 5.22. Comparison of the Observed Yield Stress of Reannealed (0.5 hr at 1065°C, 1950°F) Type 304 Stainless Steel with the 1331-8 Minimum.

materials in their fully annealed condition would not satisfy the minimum strength expectations.

Typical stress-strain curves to 1.5% strain are shown in Fig. 5.23 for 25°C (77°F) and Fig. 5.24 for 593°C (1100°F). The various heats of material have similar strain hardening behavior, and the curves are parallel.

The results of creep-rupture tests at 593°C (1100°F) on these same materials are shown in Table 5.12. The range of properties is quite large. At a stress level of 35,000 psi the rupture life of the reannealed material varied from 18 hr for heat 807 to 721 hr for heat 813. The corresponding minimum creep rates were 0.97 and 0.011%/hr.

The results of these mechanical property tests, material availability, and other factors were used to choose three heats for further study. These heats are 807 (weakest), 544 (medium strength), and 845 (near strongest). More detailed testing is already in progress on the reference heat, 9T2796 (2-in.-thick plate).

5.2.2.2 Long-Term Creep Tests — H. E. McCoy

Several long-term creep tests are in progress on some of the heats. The results of eight of these tests at 17,000 psi and 593°C (1100°F) are shown in Fig. 5.25. Heat 697 does not exhibit any measurable primary creep, and the curve for heat 414 in the A 240 condition has an unusual shape. These tests are still in progress.

5.2.2.3 Statistical Analysis of Type 304 Stainless Steel Creep-Rupture Data — D. O. Hobson and T. L. Hebble*

A large body of type 304 stainless steel creep-rupture data was collected from several sources. These sources included data used by Smith[3] in his analysis and data collected by Blackburn,[4] by Williams,[5] and by investigators at ORNL. We analyzed 407 data points. Because of a general lack of knowledge about the test conditions and quality of the test results, an all-inclusive analysis was made to determine the expected values of stress and rupture time and the lower two-sided

---

*Mathematics Research Staff.

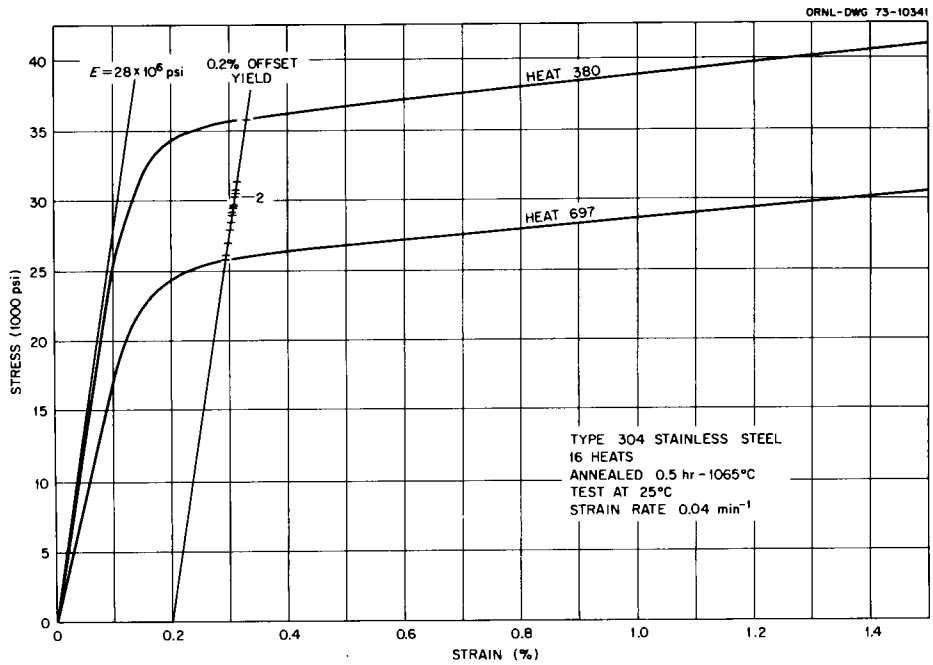

Fig. 5.23. Stress-Strain Curves for Several Heats of Type 304 Stainless Steel Tested at 25°C (77°F) After Reannealing 0.5 hr at 1065°C (1950°F).

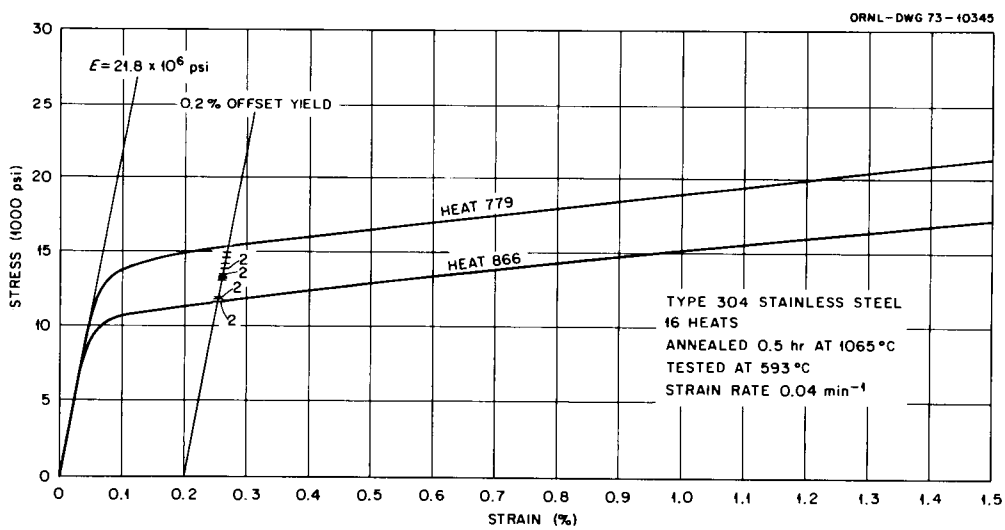

Fig. 5.24. Stress-Strain Curves for Several Heats of Type 304 Stainless Steel Tested at 593°C (1100°F) After Reannealing 0.5 hr at 1065°C (1950°F).

Table 5.12. Stress-Rupture Results at 593°C (1100°F) for Various Heats of Type 304 Stainless Steel

Heat	Rupture Life, hr				Minimum Creep Rate, %/hr			
	As Received[a]		Reannealed[b]		As Received[a]		Reannealed[b]	
	35 ksi	30 ksi	35 ksi	30 ksi	35 ksi	30 ksi	35 ksi	30 ksi
086	52.7	331.8	78.0	428.1	0.20	0.014	0.13	0.025
187	18.3	120.5	25.8	92.7	0.50	0.056	0.29	0.088
330	56.0	355.3	70.1 91.2	254.1	0.13	0.014	0.086 0.13	0.024
380	168.1	738.4	102.8 323.3	741.5	0.022	0.0023	0.046 0.017	0.0034
414	325.9	1958.6[c]	119.5 415.6	1795.7	0.012	0.0012[c]	0.025 0.012	0.0024
697	46.0	412.6 406.4	24.0	195.0	0.15	0.027	0.34	0.049
796	286.7	274.2 281.4	43.7	168.8	0.044	0.045	0.35	0.061
926	332.5		639.5[d]		0.035		0.015[d]	
283	70.9	331.6	60.8	290.4	0.23	0.035	0.22	0.038
845	287.0	1459.6	247.7	1275.4	0.035	0.0029	0.048	0.0044
544	66.3	431.0	62.1	356.1	0.19	0.017	0.19	0.022
551	189.6	1507.5	257.4 299.4	1788.5	0.068	0.0067	0.041 0.038	0.0037
866	33.8	162.3	42.9 25.2	121.0	0.70	0.13	0.68 0.75	0.17
807	16.8	143.2	18.1 35.8	96.4	1.1	0.15	0.97 0.70	0.16
779	80.1	599.3	82.8	280.4	0.10	0.010	0.096	0.021
813	284.2	2765.6	721.0	2298.8[e]	0.033	0.0023	0.011	

[a]Specification A 240, A 479, or A 276.

[b]0.5 hr at 1065°C (1950°F).

[c]29 ksi.

[d]Average for five tests with results 613.7 hr, 0.016%/hr; 699.1, 0.013; 585.8, 0.016; 673.7, 0.015; 625.1, 0.016. Two short-life results were excluded from the average.

[e]Discontinued without rupture.

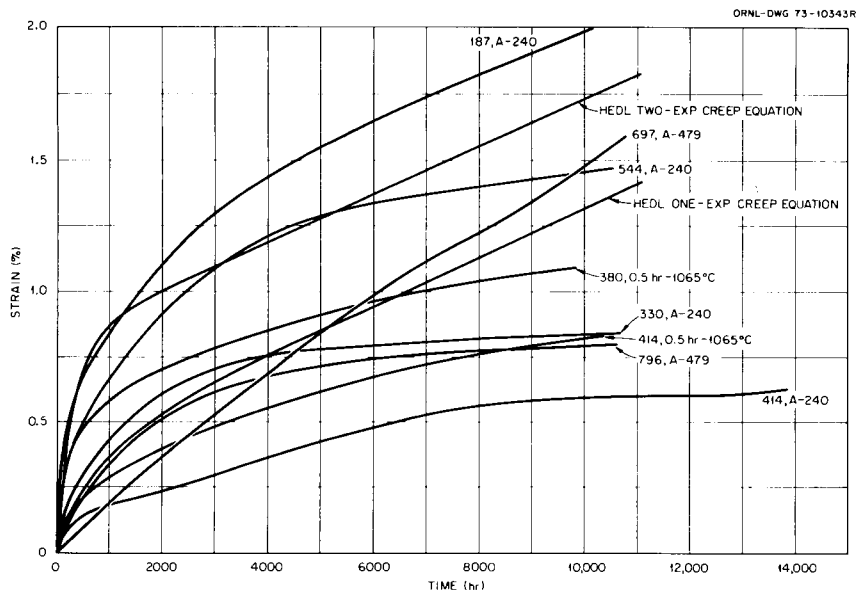

Fig. 5.25. Creep Behavior of Several Heats of Type 304 Stainless Steel Tested at 17,000 psi at 593°C (1100°F).

tolerance limits on them. No attempt was made to distinguish among product forms, chemical compositions, or heat treatments; the data were simply gathered into one population group.

The data were analyzed by using three different models, each a function of two independent variables. Two models are first-order polynomials with interaction. One assumes log σ to be the dependent variable; the other assumes that log t is the dependent variable.

$$\log \sigma = A_0 + A_1(T + 460) + A_2 \log t + A_{12}(T + 460) \log t \ , \qquad (1)$$

$$\log t = B_0 + B_1(T + 460) + B_2 \log \sigma + B_{12}(T + 460) \log \sigma \ , \qquad (2)$$

where σ is in ksi, T in °F, and t in hours. In three dimensions the surfaces have curvature; however, when one independent variable is held constant, the relationship between the remaining variables is linear.

The third model used a quadratic form of the Larson-Miller relationship.

$$\log \sigma = \alpha_0 + \alpha_1 P + \alpha_2 P^2 \ , \tag{3}$$

where

$P = (C + \log t)T$, and

C = Larson-Miller parameter.

The method of least squares was used to estimate the unknown coefficients in all three models. The lower bound for the three models is defined to be the lower central tolerance limit ($\lambda = 0.95$, $P = 0.90$) about the expected value obtained from an assumed mathematical model. Thus, with a confidence level of 0.95, 95% of the observed values are expected to be greater than the lower limit. The actual tolerance limit is based on the Bonferroni inequality and is explained in greater detail by Lieberman and Miller.[6] This limit is simultaneous in all levels of temperature and time. That is, the lower limit can be calculated repeatedly for different levels of the independent variables without affecting the level of confidence. Estimates of coefficients for each model (i.e., the equations for the expected values of the dependent variables) are given in Table 5.13.

Table 5.13. Coefficients of the Equations for Computing Expected Values of the Dependent Variable

Equation	$(A,B,\alpha)_0$	$(A,B,\alpha)_1$	$(A,B,\alpha)_2$	$(A,B)_{12}$	C
(1)	3.9043	-1.4019×10^{-3}	0.10572	−1.2538	
(2)	43.18	−0.01857	−15.47	0.004879	
(3)	1.0827	7.554×10^{-5}	-1.6059×10^{-9}		23.6

A direct comparison of Eqs. (1) and (3) is given in Table 5.14. The basis for comparison is the set of values for minimum stress to rupture given[7] in Code Case 1331-8. Additional values for 3×10^5 hr are taken from another source.[8] The sets of bracketed numbers are those in which the result from Eq. (1) is within 10% of the 1331-8 code

Table 5.14. Comparison of Calculated Rupture Stresses with Present Design Values

Temperature (°C)	Temperature (°F)	Value Source	Rupture Stress, ksi, for Various Lives in hr: 10	30	100	300	1000	3000	10^4	3×10^4	10^5	3×10^5
427	800	Design[a]							57.0	51.0	44.3	39.0
		Eq. (1)							57.1	52.1	47.1	42.9
		Eq. (3)							42.6	41.0	39.1	37.3
454	850	Design					56.5	50.2	45.4	40.0	34.7	30.5
		Eq. (1)					56.4	51.6	46.7	42.5	28.2	34.7
		Eq. (3)					42.4	40.7	38.8	36.9	34.8	32.9
482	900	Design			55.5	51.5	46.9	41.2	36.1	33.0	27.2	24.1
		Eq. (1)			54.6	50.9	46.5	42.4	38.2	34.6	31.0	28.1
		Eq. (3)			42.5	40.7	38.7	36.8	34.6	32.6	30.3	28.2
510	950	Design	54.2	51.0	48.1	43.0	38.0	33.5	28.8	24.9	21.2	18.3
		Eq. (1)	51.8	48.8	45.5	42.2	38.3	34.8	31.2	28.2	25.2	22.7
		Eq. (3)	42.8	41.2	38.9	36.9	34.7	32.6	30.2	28.1	25.9	23.7
538	1000	Design	50.0	44.5	39.8	35.0	30.9	26.5	22.9	19.7	16.6	14.0
		Eq. (1)	44.0	41.1	37.9	34.9	31.5	28.5	25.5	22.9	20.4	18.4
		Eq. (3)	39.5	37.4	35.1	32.9	30.5	28.3	25.9	23.7	21.4	19.5
566	1050	Design	41.9	37.0	32.9	28.9	25.0	21.6	18.2	15.5	13.0	11.0
		Eq. (1)	37.3	34.5	31.6	28.9	26.0	23.4	20.8	18.7	16.6	14.8
		Eq. (3)	35.8	33.6	31.1	28.8	26.3	24.0	21.7	19.6	17.5	15.7
593	1100	Design	35.2	31.0	27.2	23.9	20.3	17.3	14.5	12.3	10.2	8.6
		Eq. (1)	31.6	29.1	26.3	23.9	21.3	19.1	16.9	15.1	13.4	11.9
		Eq. (3)	31.9	29.6	27.0	24.7	22.2	20.1	17.9	16.0	14.1	12.5
621	1150	Design	29.5	26.0	22.5	19.3	16.5	13.9	11.6	9.6	8.0	6.6
		Eq. (1)	26.7	24.3	21.8	19.7	17.5	15.6	13.7	12.2	10.8	9.6
		Eq. (3)	28.1	25.6	23.0	20.8	18.5	16.5	14.5	12.8	11.2	9.8
649	1200	Design	24.7	21.5	18.6	15.9	13.4	11.1	9.2	7.6	6.2	5.0
		Eq. (1)	22.5	20.3	18.1	16.2	14.3	12.7	11.1	9.8	8.6	7.6
		Eq. (3)	24.2	21.8	19.4	17.3	15.1	13.4	11.6	10.1	8.7	7.5
677	1250	Design	20.7	17.9	15.4	13.0	10.8	8.9	7.3	6.0	4.9	4.0
		Eq. (1)	18.9	16.9	14.9	13.2	11.6	10.2	8.9	7.8	6.8	5.9
		Eq. (3)	20.6	18.3	16.0	14.2	12.3	10.7	9.1	7.9	6.6	5.6
704	1300	Design	17.4	15.0	12.7	10.5	8.8	7.2	5.8	4.8	3.8	3.1
		Eq. (1)	15.8	14.0	12.3	10.8	9.4	8.2	7.0	6.1	5.3	4.6
		Eq. (3)	17.2	15.2	13.1	11.5	9.8	8.4	7.1	6.0	4.9	4.1

[a]Code Case 1331-8.

case value. In general, this model gives better agreement with 1331-8 than does Eq. (3) (the Larson-Miller). The higher temperature, longer time (extrapolated) stress values, although exceeding the 10% criterion, are relatively close as far as actual numerical difference is concerned.

Equation (1) used in the comparison discussed above was based on stress as the dependent variable, with the tolerance limits applied to stress. Since stress and temperature are really the major independent variables in a creep test one should examine time as the dependent variable, as given by Eq. (2). This was done for the larger population at 407 observations described earlier, and the results are given in Table 5.15. The italicized values are the lower two-sided tolerance limits on rupture time. The expected values are in regular type.

We are presently examining the problem of choosing and handling the dependent variable in these analyses. Because of the manner in which the experiments were carried out, time is necessarily the dependent variable. Many analyses presently in use, however, consider stress as the dependent variable. This problem needs to be resolved because the regression of time on stress and temperature yields different results than does the regression of stress on time and temperature.

5.2.3 Exploratory Studies on Type 304 Stainless Steel in Support of Structural Design Methods — R. W. Swindeman

5.2.3.1 Tensile Testing of Reference Heat 9T2796 1-in. Plate

The results of a series of tensile tests on 1-in. plate of type 304 stainless steel (heat 9T2796) were reported internally. More recently, tensile data were reported for tests that were not continued to failure.[9,10] These and additional data collected this quarter are summarized in Table 5.16. All specimens were reannealed at 1093°C (2000°F) for 0.5 hr in argon before testing.

The tests reported in Table 5.16 represent about 60% of our tensile test matrix. Emphasis has been placed on the nominal 0.005/min strain rate since this represents the maximum rate expected for transients in

Table 5.15. Expected Rupture Life (Roman Type) and Lower Tolerance Limits (Italics) for Type 304 Stainless Steel

Temperature		Rupture Life, hr,[a] for Various Stress Values in ksi									
(°C)	(°F)	5	10	15	20	25	30	35	40	45	50
371	700									264025.8	93908.8
								147419.0	*38755.3*	*11686.5*	*3941.1*
399	750								243224.6	78815.4	28762.8
							205731.6	*47423.8*	*12940.8*	*4033.9*	*1401.7*
427	800							245009.9	70549.8	23527.5	8809.6
							63398.3	*15242.1*	*4315.0*	*1389.6*	*497.2*
454	850						278854.6	68790.4	20463.7	7023.3	2698.2
						96305.8	*19518.8*	*4891.9*	*1435.7*	*477.2*	*175.7*
482	900						75404.0	19314.0	5935.7	2096.5	826.4
					179562.6	*28222.3*	*6000.4*	*1566.4*	*476.0*	*163.1*	*61.7*
510	950					97660.8	20389.7	5422.7	1721.7	625.8	253.1
					49703.0	*8255.2*	*1839.8*	*499.5*	*156.8*	*55.2*	*21.4*
538	1000				162712.1	25259.5	5513.5	1522.5	499.4	186.8	77.5
				125348.2	*13726.2*	*2406.6*	*561.2*	*157.9*	*51.0*	*18.4*	*7.3*
566	1050				39855.4	6533.2	1490.9	427.5	144.9	55.8	23.7
				32386.9	*3775.2*	*696.8*	*169.1*	*48.9*	*16.1*	*5.9*	*2.4*
593	1100			93667.1	9762.4	1689.8	403.1	120.0	42.0	16.6	7.3
			155824.1	*8333.6*	*1029.8*	*198.4*	*49.3*	*14.4*	*4.8*	*1.8*	*0.7*
621	1150			21388.6	2391.2	437.1	109.0	33.7	12.2	5.0	2.2
			36805.9	*2127.8*	*275.8*	*54.1*	*13.4*	*3.9*	*1.3*	*0.5*	*0.2*
649	1200		97046.0	4884.0	585.7	113.0	29.5	9.5	3.5	1.5	0.7
			8618.3	*534.6*	*70.7*	*13.6*	*3.4*	*1.0*	*0.4*	*0.1*	*0.1*
677	1250		20073.6	1115.3	143.5	29.2	8.0	2.7	1.0	0.4	0.2
		190978.1	*1984.9*	*129.7*	*16.9*	*3.2*	*0.8*	*0.3*	*0.1*	*0.0*	*0.0*
704	1300		4152.1	254.7	35.1	7.6	2.2	0.7	0.3	0.1	0.1
		36826.4	*442.5*	*29.6*	*3.8*	*0.8*	*0.2*	*0.1*	*0.0*	*0.0*	*0.0*

[a]Values for upper left blank region are too long to be meaningful.

Table 5.16. Summary of Tensile Tests Performed on Type 304 Stainless Steel Heat 9T2796, 1-in. Plate Reannealed at 1093°C (2000°F)

Specimen	Temperature (°C)	Temperature (°F)	Strength, ksi 0.2% Yield	Strength, ksi Ultimate	Uniform Elongation (%)	Fracture Stress (ksi)	Fracture Strain (%)	Reduction in Area (%)	Eq. (4)[a] k (ksi)	Eq. (4)[a] m	Eq. (5)[b] σ_0 (ksi)	Eq. (5)[b] k' (ksi)	Eq. (5)[b] m'	Strain Rate (min^{-1})
RP165	593	1100	9.88	34.2	17.0	14.1	20.6[c]	23.4	63.07	0.314	8.470	130.6	0.732	0.00009
RP113	593	1100	10.2											0.00009
RP114	593	1100	11.2											0.00009
RP175	Room		23.9	81.5	79.9	48.9	95.0	84.5	131.9	0.309	21.7	174.6	0.722	0.0004
RP174	427	800	12.1	62.9	41.2	44.4	50.0	72.0	112.4	0.387	10.1	178.1	0.726	0.0004
RP20	538	1000	11.3	52.8	35.7	31.0	42.5[c]	41.0						0.0005
RP195	593	1100	12.1	39.4			27.0	30.0[d]	72.40	0.298	9.71	119.4	0.624	0.0004
RP115	593	1100	11.2											0.00045
RP116	593	1100	10.0											0.00045
RP21	649	1200	11.2	30.6	44.0		57.5[c]	34.5[d]						0.0005
RP197	704	1300	11.0	20.3	9.8	4.5	49.0	33.0	36.31	0.189				0.0004
RP10	Room		26.4	84.7	76.7	48.8	85.0[c]	85.5		0.279	25.0		0.788	0.005
RP176	Room		25.7	83.4	80.3	51.5	95.0	84.4	131.9	0.291	24.1	178.1	0.737	0.004
RP66	Room		24.8											0.0045
RP66	Room		24.8											0.005
RP181	93	200	21.0	67.7	60.0	41.4	78.0	85.4	109.1	0.293	19.0	156.4	0.703	0.004
RP183	204	400	16.5	61.5	39.8	39.7	52.0	75.0	98.7	0.316	14.9	176.3	0.776	0.004
RP11	316	600	14.2	63.0	39.5	45.4	47.0[c]	73.5	100.7	0.353	13.5	198.1	0.843	0.005
RP185	316	600	15.9	62.6	42.3	42.8	52.0	72.1	98.7	0.322	14.6	178.1	0.790	0.004
RP12	427	800	13.0	62.1	37.9	43.5	45.0[c]	70.5	115.8	0.404	12.0	219.7	0.848	0.005
RP187	427	800	12.9	61.8	39.7	46.5	50.0	63.3	101.7	0.360	11.55	187.2	0.786	0.004
RP88	427	800	12.1											0.0045
RP132	427	800	12.8											0.005
RP13	482	900	12.2	59.4	40.4	41.2	48.0[c]	70.0	110.2	0.401	11.0	192.9	0.800	0.005
RP189	482	900	11.8	59.5	39.6	43.4	48.0	67.1	99.7	0.373	10.5	181.2	0.786	0.004
RP128	482	900	11.3											0.005
RP14	538	1000	11.6	55.8	39.9	39.2	50.5[c]	68.0	104.8	0.403				0.005
RP190	538	1000	10.5	54.5	39.6	40.6	45.0	54.0[d]	93.9	0.377	9.26	164.4	0.763	0.004
RP127	538	1000	11.7											0.005
RP15	593	1100	11.1	46.5	35.7	30.8	37.5[c]	51.5[d]	93.0	0.380	10.00	169.4	0.783	0.005
RP192	593	1100	10.5	45.2	28.8	37.6	38.0	41.2[d]	80.8	0.346	9.03	140.1	0.711	0.004
RP91	593	1100	10.2											0.0045
RP131	593	1100	10.0											0.005
RP16	641	1200	10.5	37.1	23.6	16.5	34.0[c]	26.0[d]	78.4	0.357				0.005

Table 5.16. (Continued)

Specimen	Temperature (°C)	Temperature (°F)	Strength, ksi 0.2% Yield	Strength, ksi Ultimate	Uniform Elongation (%)	Fracture Stress (ksi)	Fracture Strain (%)	Reduction in Area (%)	Eq. (4)[a] k (ksi)	Eq. (4)[a] m	Eq. (5)[b] σ_0 (ksi)	Eq. (5)[b] k' (ksi)	Eq. (5)[b] m'	Strain Rate (min^{-1})
RP179	649	1200	11.6	36.3	24.4	27.5	42.0	38.5	68.2	0.301	8.04	94.8	0.546	0.004
RP17	704	1300	10.9	27.8	16.0	12.3	41.0[c]	40.5[d]	57.5	0.281				0.005
RP180	704	1300		26.2	18.6	18.3	50.0	40.0	49.5	0.244				0.004
RP161	760	1400	10.0	18.7	11.1	5.0	54.0	37.8	33.5	0.191				0.004
RP177	Room		27.3	83.4	70.6	47.8	88.0	83.8	128.0	0.274	25.6	174.6	0.722	0.04
RP178	427	800	14.6	60.5	38.1	42.0	49.0	74.5	99.7	0.336	12.8	169.4	0.740	0.04
RP18	538	1000	11.7	55.2	33.5	36.0	41.0[c]	70.0						0.05
RP193	593	1100	11.2	49.3	34.0	32.6	46.0	66.4	85.8	0.350	9.77	153.3	0.749	0.04
RP92	593	1100	10.1											0.045
RP96	593	1100	10.2											0.045
RP19	649	1200	10.4	42.1	30.6	30.0	43.5[c]	29.0						0.05
RP184	704	1300	10.0	32.9	21.4	4.0	48.0	40.3	62.9	0.304	7.66	93.9	0.588	0.04
RP182	593	1100	11.2	49.9	31.8	33.8	46.0	74.1	90.2	0.357	9.49	153.3	0.722	0.4
RP93	593	1100	10.3											0.45
RP95	593	1100	11.6											0.45
RP94	593	1100	11.8											4.5

[a]Constants for $\bar{\sigma} = k\bar{\varepsilon}_p^{\,m}$.

[b]Constants for $\bar{\sigma} = k'\bar{\varepsilon}_p^{\,m'} + \sigma_0$.

[c]Elongation in 8 times gage diameter.

[d]Failed at extensometer contact point.

fast breeder reactors. Tests at higher strain rates were included so that monotonic data could be gathered at rates that overlap those used in strain cycling and fatigue testing programs. High-rate data also helped in separating time-dependent and time-independent inelastic deformation. Similarly, low rates were of interest because they provided conditions under which creep could occur during testing, and the information from such tests could be used to verify methods of separating strain components.

One group of tests reported in Table 5.16 was performed under servo-controlled conditions and was discontinued at about 0.5% strain. These data were collected to assist in a detailed analysis of yielding around the knee of the flow curve.[10]

Another group of tests, for which only yield stresses are reported in Table 5.16, was discontinued at 5% total strain. More detailed information about these test results will be forthcoming when our tensile data are bilinearized according to recommended procedures.[11]

The bulk of the test results were processed to provide the usual tensile properties such as yield, ultimate, and fracture stresses and strains. Other information contained in Table 5.16 is concerned with the "strength coefficient," k, and the "work-hardening coefficient," m. These constants were obtained by fitting true stress—true strain data to the Holloman[12] equation:

$$\overline{\sigma} = k\overline{\varepsilon}_p^{\,m} , \tag{4}$$

where $\overline{\sigma}$ is true stress and $\overline{\varepsilon}_p$ is true plastic strain. Similarly, values were calculated for the Ludwik[13] equation:

$$\overline{\sigma} = k'\overline{\varepsilon}_p^{\,m'} + \sigma_0 , \tag{5}$$

where k', m', and σ_0 are material constants.

At 593°C (1100°F) the influence of strain rate on tensile properties has been examined over the range 0.0001 to 5/min. As indicated in Table 5.16, the yield stress was not very sensitive to rate, but the ultimate strength and elongation decreased with decreasing rate. The contribution of creep to the tensile deformation at 593°C (1100°F) can be demonstrated by plotting both creep and tensile data on the same graph. In Fig. 5.26 the ultimate strengths are plotted against the applied strain rates, while the applied creep stresses are plotted against the corresponding minimum creep rates. The two types of data could be blended reasonably well into a single curve. At high rates the curve appears to be approaching a rate-independent value.

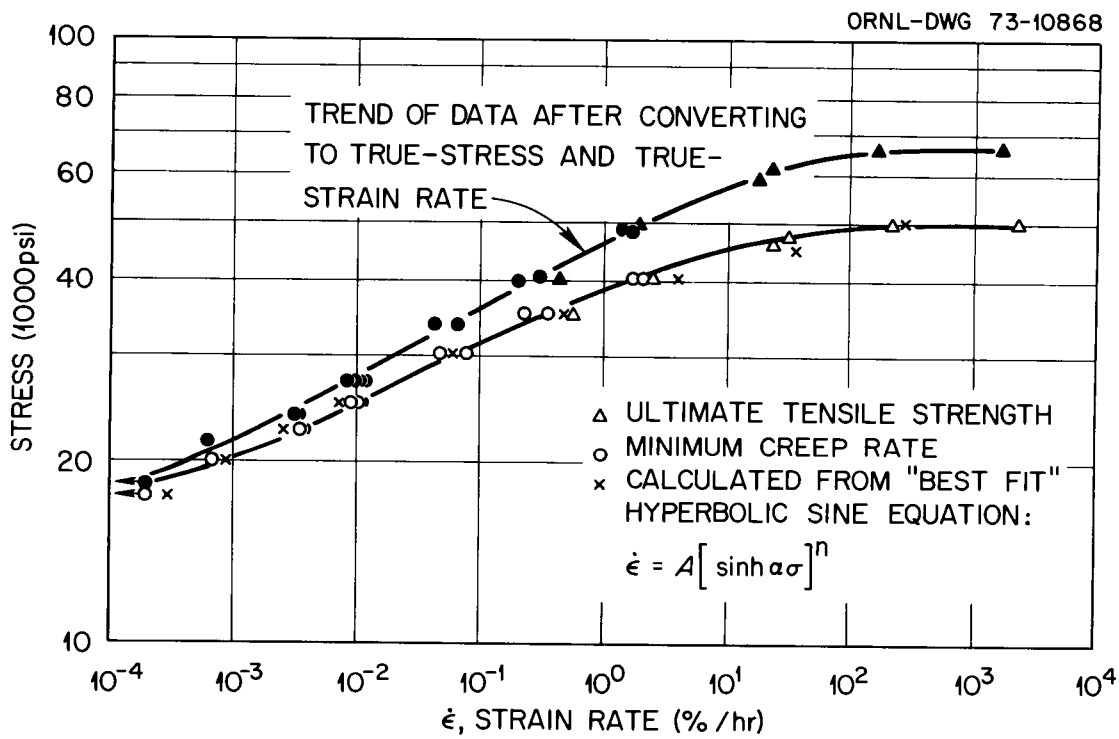

Fig. 5.26. Stress vs Strain Rate Plot Constructed from Tensile and Creep Data for Type 304 Stainless Steel (Heat 9T2796) at 593°C (1100°F); 1-in. Plate Reannealed at 1093°C (2000°F).

5.2.3.2 Creep Testing of 5/8-in.-diam Bar and 1-in. Plate of Type 304 Stainless Steel (Heat 9T2796)

More data have been collected concerning the influence of thermomechanical history on creep behavior of type 304 stainless steel (heat 9T2796). A group of specimens machined from 5/8-in.-diam HRAP (hot rolled and pickled) bar (Item 18) were tested at 593°C (1100°F) and 25,000 psi. The results obtained to date are summarized in Fig. 5.27. Included are three curves obtained on specimens reannealed at 1093°C (2000°F) for 0.5 hr in argon (RR 35, RR 62, and RR 55). Another curve represents a specimen reannealed at 1093°C (2000°F) in a Sen-Pak envelope (RR 100). Compared with these four curves are data for the same material (5/8-in.-diam HRAP bar) collected during the course of another research program. These curves, for specimens BWC 3 and BWR 3, represent results obtained by Babcock & Wilcox[14] in their investigations of creep damage. The six curves differ appreciably. Rupture lives vary from 430 to 947.5 hr for specimens reannealed at 1093°C (2000°F). As suggested by the metalographic studies performed at B & W, part of the answer for variability in the creep-rupture response of the 5/8-in.-diam bar could be due to variability in grain size.

The influence of plastic strain on the creep behavior of reannealed type 304 stainless steel 1-in. plate is being examined. The first test group involved high-stress creep tests on specimens strain cycled at either room temperature or 593°C (1100°F). Longer time tests in this group are still in progress, and the results are compared with reannealed material in Fig. 5.28. The results of these lower stress tests differ from results obtained[15] at stresses of 25,000, 30,000, and 35,000 psi. At low stresses, there appears to be more creep hardening in the precycled specimens than in the specimens tested after only reannealing. However, the initial creep rates are similar. Thus, it appears that the influence of precycling increases with decreasing stress and increasing testing times. Relative to the heat-to-heat variability of creep data, however, the differences in the creep curves shown in Fig. 5.28 are rather small.

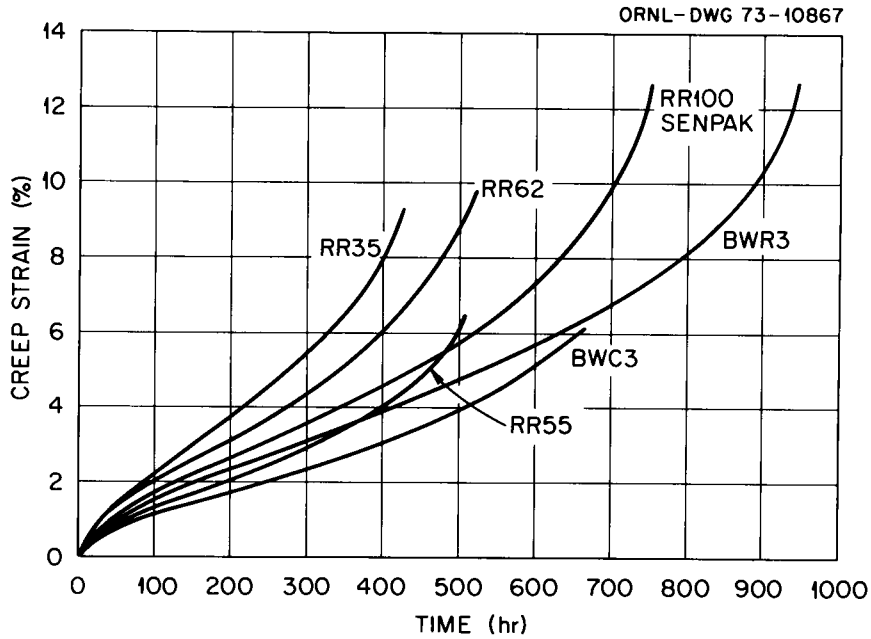

Fig. 5.27. Variation in the Creep Response of Type 304 Stainless Steel (Heat 9T2796) 5/8-in.-diam Bar. Reannealed at 1093°C (2000°F) in argon or Sen-Pak envelopes.

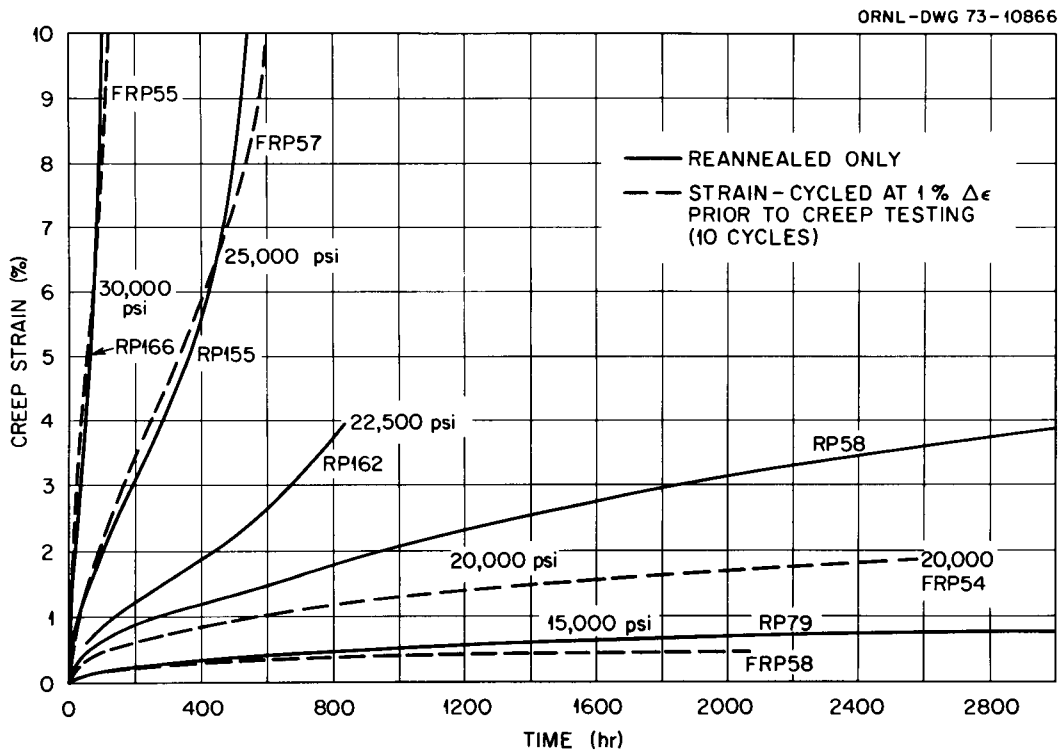

Fig. 5.28. Creep Curves Showing the Effect of Small Amounts of Cyclic Cold Work on the Subsequent Creep of Type 304 Stainless Steel at 593°C (1100°F). Heat 9T2796 1-in. plate reannealed at 1093°C (2000°F).

The constant-load exploratory creep testing series on reannealed type 304 stainless steel 1-in. plate (heat 9T2796, Item 7) is about 70% complete. Sufficient data exist to construct isochronous stress-strain curves to 5000 hr for 538, 593, and 649°C (1000, 1100, and 1200°F). These curves are provided in Fig. 5.29. Compared with these curves are data replotted from the ASME Boiler and Pressure Vessel Code Case 1331-8. The code case curves are supposed to represent an "average" heat of type 304 stainless steel in the mill-annealed condition. It is quite obvious that our reannealed material (heat 9T2796) is weak relative to what the code considers typical or average.

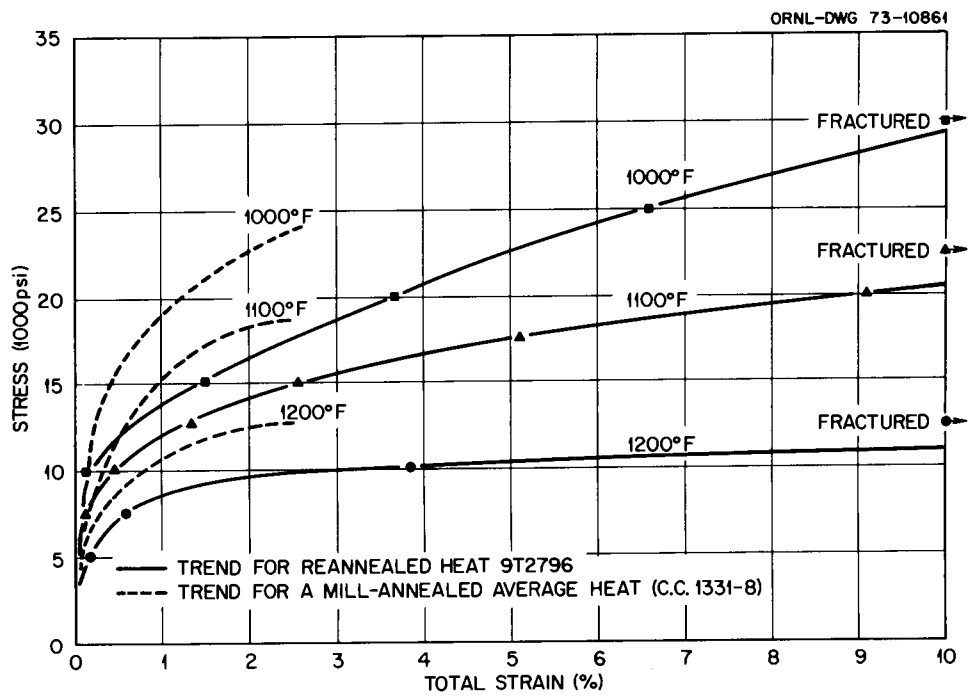

Fig. 5.29. Isochronous Stress-Strain Curves at 5000 hr for Type 304 Stainless Steel. Heat 9T2796 1-in. plate reannealed at 1093°C (2000°F).

5.2.3.3 Relaxation Testing of 1-in. Plate — Reference Heat

Two relaxation tests were performed at 538°C (1000°F) during the last quarter on reannealed type 304 stainless steel (reference heat 9T2796 1-in. plate). The results from these tests, which were started at 30,000 and 40,000 psi, are represented in Fig. 5.30. Also included are data from tests reported earlier.[16] The curves represent the

maximum range of starting stresses that we plan to cover. Additional testing at this temperature will involve duplicate tests and repetitive loading tests. Constant-load creep data covering times and stresses similar to the relaxation test series are provided in Fig. 5.31. These data can be used to analyze the relaxation behavior.

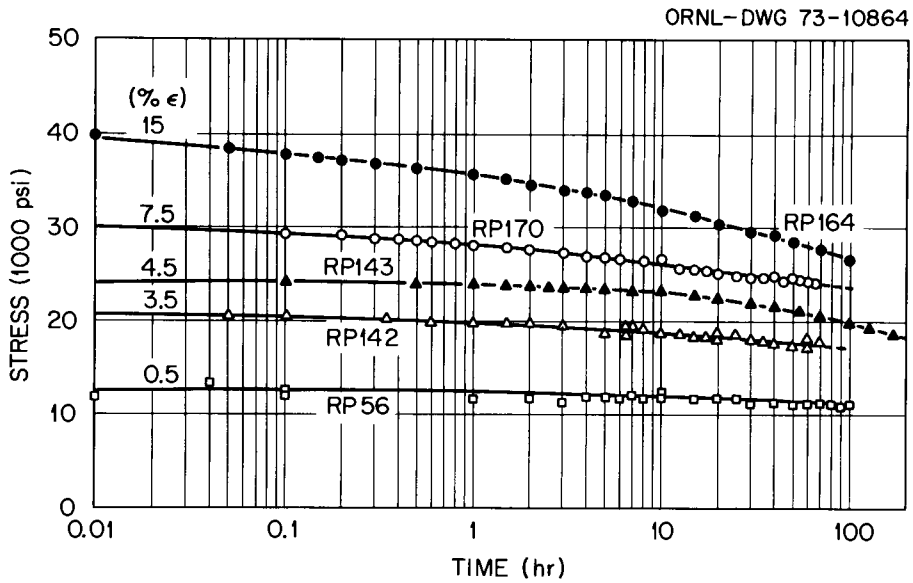

Fig. 5.30. Relaxation Curves for Type 304 Stainless Steel at 538°C (1000°F). Heat 9T2796 1-in. plate reannealed at 1093°C (2000°F).

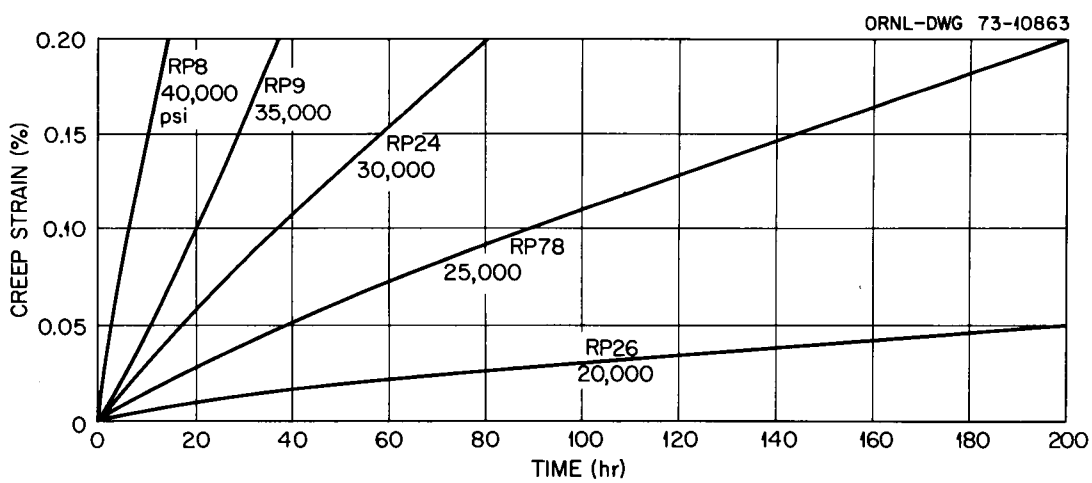

Fig. 5.31. Creep Curves for Short Times and Low Strains for Type 304 Stainless Steel at 538°C (1000°F). Heat 9T2796 1-in. plate reannealed at 1093°C (2000°F).

5.2.3.4 Creep-Plasticity Interaction of 1-in. Plate — Reference Heat

Investigation of the deformation behavior of type 304 stainless steel (reference heat, 9T2796) under conditions of interspersed strain cycling and creep are under way. Our initial studies are intended to explore for areas where meaningful information can be gathered. Some of our preliminary findings at 593°C (1100°F) are summarized in Fig. 5.32. Specimen FRP 68 was strained in tension to 0.59% (curve OA) and then compressed to −0.55% (AB). It was then reloaded toward tension. When the strain neared −0.1% (BC) the control mode was switched to load and the specimen was crept for one week at 15,000 psi. After the week, when the strain near zero (CD), strain-cycling was resumed. We observed that the flow stress (at E) increased to a value near what we would expect had the creep strain segment (CD) been introduced by strain cycling. This implies that the creep strain hardening is approximately equivalent to "instantaneous" plastic strain hardening for the particular conditions we selected. A second hysteresis loop was introduced (EFGH) and essentially repeated the original strain limits. When the loop was completed, the stress was reduced from 20,500 to 15,000 psi (HI) and the control mode was switched to constant load again. After about one week the specimen crept to about 0.07% (IJ). When strain cycling was resumed (JKL), we observed that the flow stress decreased. We can conclude from this response that creep strain can have either hardening or softening influences and the sign of the flow stress change depends on the prior history. The results shown here agree qualitatively with response reported by Jaske[17] for similar testing conditions.

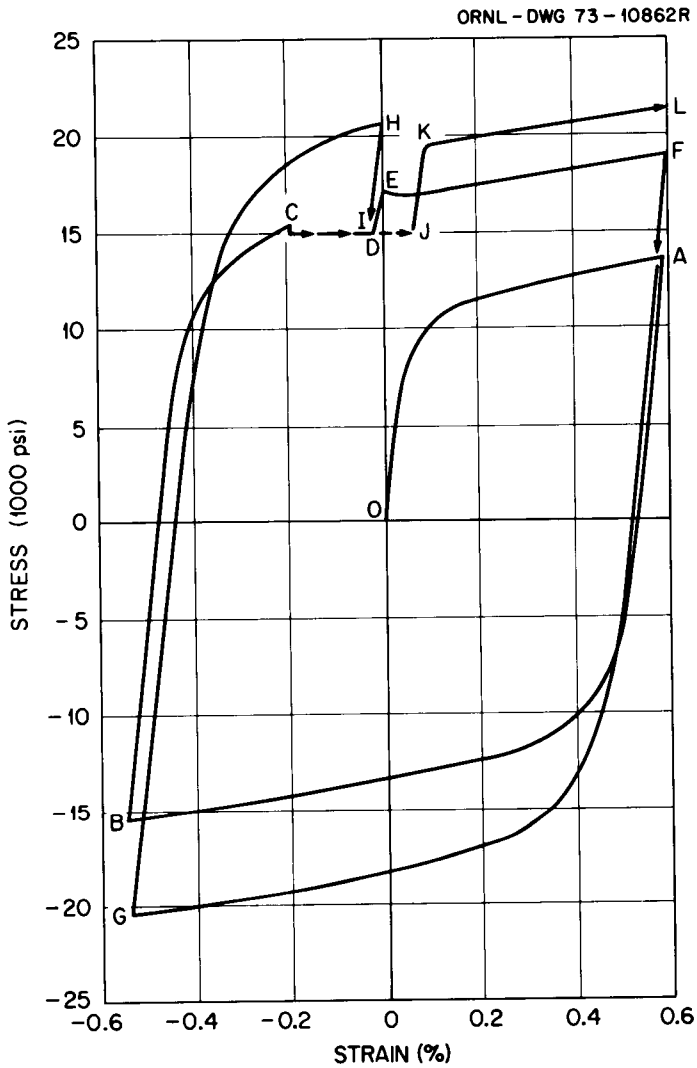

Fig. 5.32. Influence of Creep Strain on the Cyclic Stress-Strain Behavior of Type 304 Stainless Steel at 593°C (1100°F). Heat 9T2796 1-in. plate reannealed 1093°C (2000°F). Specimen FRP 68.

5.2.4 Variation in the Mechanical Properties of Type 316 Stainless Steel — H. E. McCoy

Three heats of 0.5-in.-thick type 316 stainless plate are being tested to determine the variation in their mechanical properties. The chemical analyses and other information are given in Table 5.17.

Tensile tests at a strain rate of 0.04/min were run at 25, 427, 593, and 649°C (77, 500, 1100, and 1200°F) on samples in the A 240 condition and after reannealing 0.5 hr at 1065°C (1950°F). The results of these tests are summarized in Table 5.18. The properties of heats 2P3212 and 500613 were about equal, but heat 377686 was stronger. Reannealing reduced the yield strength slightly for all heats and test conditions.

In Fig. 5.33 the yield strengths of these three heats of type 316 stainless steel are compared with the minimum expected values from Code Case 1331-8. The yield strengths of all heats in the as-received (A 240) condition were above the minimum expected values. After reannealing the yield stress of heat 2P3212 was slightly below the minimum at test temperatures above 427°C (800°F). The yield strength of heat 377686 was about double the minimum expected value.

The strength of heat 377686 is quite outstanding. Except for one tensile stress value at 25°C (77°F) the yield and tensile stress values for this heat fall above those compiled by Smith.[3] Reference to Table 3.20 shows that heat 377686 is different from the other two heats in several aspects. Its grain size is smaller, and the concentrations of nitrogen, boron, and niobium are higher. Further tests will be performed in an effort to determine the reason for the superior strength of this heat.

Table 5.17. Type 316 Stainless Steel Being Studied in the Heat-to-Heat Variation Program

Heat[a]	377686	500613	2P3212
Vendor	Allegheny Ludlum	Carlson	USS
Grain size, ASTM			
As received	8	5–6	5–6
Reannealed[b]	8		5–6
Chemical composition,[c] %			
Carbon	0.053	0.063	0.055
Nitrogen	0.079	0.042	0.053
Phosphorus	0.023	0.023	0.026
Boron	0.010	0.0002	0.0002
Oxygen	0.0066	0.015	0.0076
Hydrogen	0.0005	0.0002	0.0008
Nickel	13.3	12.9	13.4
Manganese	1.60	1.65	1.41
Chromium	17.2	16.4	17.3
Silicon	0.55	0.72	0.55
Molybdenum	2.2	2.2	2.4
Sulfur	0.007	0.024	0.012
Titanium	0.037	0.041	0.035
Copper	0.13	0.19	0.09
Cobalt	0.03	0.08	0.07
Lead	0.0007	0.007	0.0007
Niobium	0.15	0.005	0.002

[a]All materials procured as 1/2-in.-thick plate in the A 240 condition.

[b]0.5 hr at 1065°C (1950°F).

[c]Tin <0.01%, tantalum <0.001%.

Table 5.18. Tensile Strength Properties of Type 316 Stainless Steel[a]

Heat, Condition	Test Temperature (°C)	Test Temperature (°F)	Stress, ksi: Yield	Stress, ksi: Ultimate Tensile	Strain, %: Uniform	Strain, %: Total	Reduction in Area (%)
2P3212 A 240	25	77	36.8	86.6	60.7	72.0	73.0
	427	800	20.5	80.6	45.0	48.0	77.8
	593	1100	19.2	66.3	44.0	49.0	60.4
	649	1200	18.0	52.7	34.4	63.7	65.2
500613 A 240	25	77	37.8	86.5	54.4	69.0	67.0
	427	800	20.8	71.9	50.4	47.6	58.9
	593	1100	18.1	63.2	45.6	45.5	53.9
	649	1200	18.1	54.1	36.0	54.0	56.1
377686 A 240	25	77	53.4	100.3	38.8	57.0	69.0
	427	800	32.3	81.3	35.2	43.6	59.1
	593	1100	30.2	75.0	35.2	46.5	59.5
	649	1200	29.7	64.8	32.0	46.0	62.8
2P3212 annealed[b]	25	77	34.8	85.0	56.8	72.0	72.9
	427	800	17.2	68.6	49.5	49.8	61.9
	593	1100	14.5	60.6	49.6	51.0	60.7
	649	1200	14.2	50.7	40.0	59.5	64.8
500613 annealed[b]	25	77	35.1	85.7	64.0	72.4	65.8
	427	800	19.2	71.5	49.7	52.8	55.8
	593	1100	16.3	63.5	45.6	53.9	53.9
	649	1200	16.1	53.1	36.0	56.4	53.7
377686 annealed[b]	25	77	53.3	100.5	38.8	58.0	70.2
	427	800	32.6	79.6	44.6	45.0	56.8
	593	1100	28.8	72.6	38.4	48.8	60.5
	649	1200	28.0	62.3	36.0	54.3	60.2

[a]Strain rate of 0.04/min.

[b]0.5 hr at 1065°C (1950°F).

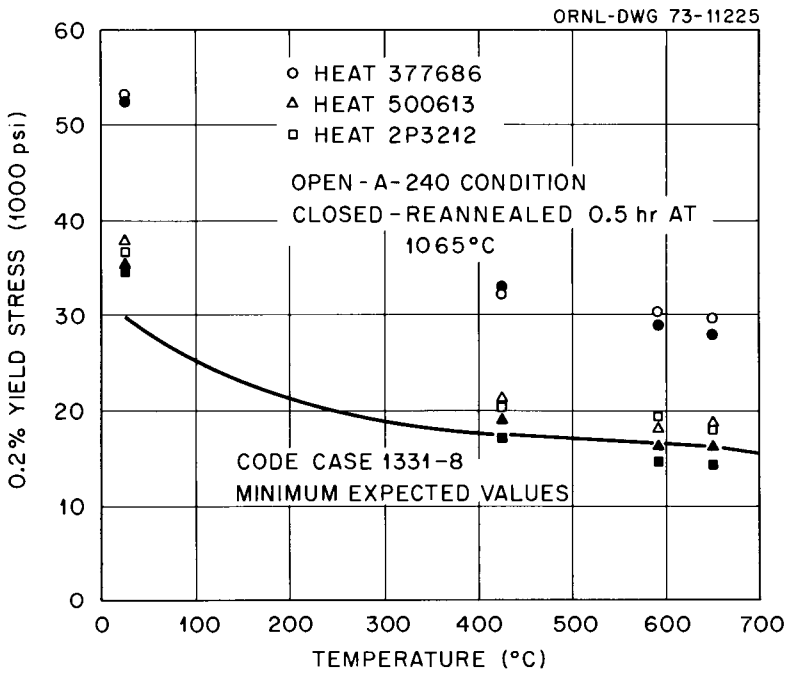

Fig. 5.33. Comparison of the Yield Stresses of Several Heats of Type 316 Stainless Steel.

5.3 MECHANICAL AND METALLURGICAL BEHAVIOR OF WELDMENTS FOR LMFBR — P. Patriarca, G. M. Slaughter, and W. R. Martin

5.3.1 Welding Development and Mechanical Testing of the Weldments for Stainless Steel Components

5.3.1.1 Creep and Tensile Properties of SMA Type 316 CRE Stainless Steel Weld Metal — R. T. King, R. G. Berggren, and B. McNabb, Jr.

Coated 5/32-in.-diam type 316 stainless steel electrodes of batch COEB were obtained from Combustion Engineering, Chattanooga. The chemical compositions of the electrode coatings had been modified to produce controlled amounts of the residual elements B, P, and Ti in the finished welds and were used to make 1/2-in.-thick type 316 stainless steel plate welds that were intended to be similar to welds in an LMFBR piping system. The joint configuration was a 75° V-groove with a 1/16-in. root face and a 3/32-in. root opening. The chemical composition of the weld metal is given in Table 5.19 as determined by analysis at ORNL. The finished welds were designated V40, V41, V42, and V43 in a series of simulated LMFBR piping welds.

Test specimen blanks were cut with center lines 3/16 in. below the weld surface. Buttonhead test specimens having a 0.125-in.-diam × 1.125-in.-long gage section parallel to the welding direction were machined from the blanks. Some specimens were tested in air on an Instron tensile machine at 0.005 in./min crosshead speed (0.0044/min strain rate) at 25, 482, 593, and 649°C (77, 900, 1100, and 1200°F) without extensometers on the specimen gage length. Creep tests were performed in air at 649°C (1200°F) at stresses that produced rupture times from 0.4 to 5930 hr. One specimen is now under test at 593°C (1100°F) and 50,000 psi stress; another specimen remains to be creep tested at 482°C (900°F).

Table 5.19. Chemical Composition of As-Deposited Type 316 CRE Stainless Steel Weld Metal

Element	Composition (wt %)	Element	Composition (wt %)
Cr	18.62	Si	0.49
Ni	11.27	S	0.009
Mo	2.12	Mn	1.83
C	0.049	Co	0.03
B	0.007	Cu	0.04
P	0.045	Nb	0.01
Ti	0.06	N	0.02

The results of the tensile tests are given in Table 5.20. The basis for deriving allowable stresses for austenitic type 316 stainless steel at elevated temperatures in the creep range in Section III of the *ASME Boiler and Pressure Vessel Code*, Code Case 1331, is the lower of 0.9 × yield stress at temperature or (1.1/3) × ultimate stress. These values are tabulated for CRE type 316 stainless steel weld metal in Table 5.21, and they are always greater than the allowable stresses for base metal. At room temperature, where allowable stresses are governed by one-fourth the tensile stress and two-thirds the yield stress considerations, the weld metal "computed allowable stresses" still exceed the allowable stresses for base metal. Uniform strains were always about 19% or greater, total strains always exceeded 26%, and reductions of area were always greater than 45%. However, the anisotropy of deformation previously observed for type 308 CRE stainless steel weld metal also occurs in this weld metal, as evidenced by the ratios of maximum to minimum diametral strains at failure.

Results from creep tests at 649°C (1200°F) are given in Table 5.22. All of the strains that occurred before fracture are creep strains that do not include the initial loading strains. However, since most tests were performed at stresses below the 0.2% offset yield stress, the loading strains are relatively small. The total elongations were

Table 5.20. Tensile Stress-Strain Behavior of Type 316 CRE Stainless Steel Weld Metal

Test Temperature		Specimen	Instron Chart Measurements						Reduction of Area (%)	Diametral Strain, %					
			Strength,[a] ksi[b]				Strain,[a] %			At Fracture			Away from Fracture		
(°C)	(°F)		Apparent Elastic Limit	0.2% Offset Yield	Ultimate	Fracture	Uniform	Total		Minimum	Maximum	Ratio	Minimum	Maximum	Ratio
25	75	V42-02	36.4	42.7 42.9	113.9 149.0	99.2 215.4	30.8 27	39.1 78	53.9	37.1	27.5	1.35	20.2	8.5	2.4
482	900	V42-03	36.1	41.5 41.5	69.7 86.5	55.0 104.4	24.1 22	28.1 64	82.1	37.0	18.9	2.0	10.8	6.8	1.6
593	1100	V42-04	32.8	39.8 39.9	57.0 68.1	43.5 81.3	19.6 18	26.9 63	46.5	35.8	19.0	1.9	14.9	4.5	3.3
649	1200	V40-01	27.6	34.6 34.7	50.0 59.5	35.3 76.1	19.0 17	29.4 77	53.6	38.2	26.2	1.46	14.9	6.9	2.16

[a]First number given is engineering value; second is true.

[b]1000 psi.

Table 5.21. Comparison of Allowable Stresses for Type 316 CRE Stainless Steel Weld Metal with Similar Values for Base Metal

Test Temperature		Specimen	Allowable Stress, ksi		
(°C)	(°F)		0.9 × Yield Stress	(1.1/3) × Ultimate Strength	Allowable for Type 316
25	75	V42-02	38.4[a]	41.8[a]	25.0[b]
482	900	V42-03	37.3	25.5	15.6[c]
593	1100	V42-04	35.8	20.9	14.7[c]
649	1200	V40-01	31.1	18.3	14.5[c]

[a]For proper comparison at temperatures below the creep range, the allowable stresses in Section III, *ASME Boiler and Pressure Vessel Code*, 1971 ed., are the minimum of: (1) one-fourth the minimum specified tensile strength (= 28.5 ksi for weld metal) and (2) two-thirds the minimum specified yield strength (= 28.4 ksi for weld metal).

[b]S values for plate and seamless pipe, Table 1-7.2 in Section III, *ASME Boiler and Pressure Vessel Code*, 1971 ed.

[c]Taken from Fig. 3b, S_{mt} plot, ASME Code Case 1331-7.

calculated from measurements made by mating the fractured halves. All the total fracture strains were greater than 12%, and the smallest measured reduction of area was 54.9%. Although the reductions of area did not decrease with increasing rupture time, the total elongations did decrease.

The fracture surfaces of specimens V41-03 (0.4 hr rupture time) and V40-02 (5930.3 hr rupture time) were examined by scanning electron microscopy. They were covered with dimples that are indicative of a relatively ductile fracture, and the fracture morphology does not appear to be related to the microstructure of the welds. The surface features that have been associated with internal interphase separations and low ductility were not present.

Table 5.22. Creep Properties of Type 316 CRE Stainless Steel Weld Metal at 649°C (1200°F)

Specimen	Stress (ksi)	Strain, %			Approximate Minimum Creep Rate (%/hr)	Reduction of Area (%)	Time, hr, to Various Events						
		First Stage[a]	First Plus Second Stage[a]	Total[b]			End First Stage	End Second Stage	Fracture	0.5% Strain	1% Strain	2% Strain	Tertiary Creep
V40-02	25[c]	>0.19	>0.21	15.8	9.3×10^{-6}	61.9	5(?)	2150	5930.3	~3000	~4500	~5250	2500
V40-04	28[c]	0.21	0.67	16.6	6.7×10^{-4}	68.6	25	715	1472.5	~470	~840	~1190	830
V40-03	30[d]	0.34	0.57	12.6	1.5×10^{-3}	64.5	15	165	552.6	~130	~320	~450	300
V41-02	32.5[e]	0.63	1.17	20.9	4.2×10^{-3}	62.8	12.5	140	360.7	~2.0	~110	~230	200
V42-01	34[e]	~1.46	~3.2	27.6	5.2×10^{-2}	61.2	~10	~44	104.7	~1.0	~3.5	~20	~60
V41-03	35[e]	<2	~6	27.5	~29	54.9	<0.01	~0.15	0.4	~0.03	~0.05	~0.09	~0.155

[a]Strains are creep strains and do not include initial loading strain.

[b]Total strain is from post-test measurement on specimen and therefore includes loading strain.

[c]Step-loaded dead load test, no extensometer.

[d]Lever arm machine, no extensometer.

[e]Lever arm machine, extensometer located on grips, not gage.

A particularly important result from the creep testing is that the amount of strain sustained before third-stage creep decreased markedly with increasing rupture time or decreasing stress. At 35,000 psi stress, the specimen strained about 6% before the onset of third-stage creep, whereas less than 1% strain occurred before third-stage creep for specimens tested below 30,000 psi.

We may gain some perspective on the rupture time behavior of the type 316 CRE stainless steel weld metal by comparing it with the behavior of type 316 stainless steel base metal. To this end, we plotted in Fig. 5.34 the average and 95% upper and lower one-sided confidence limits (±1.645 standard deviations, assuming known mean and standard deviation values) from Blackburn's[18] analysis of type 316 stainless steel data against the Larson-Miller parameter, $(T + 460)(20 + \log_{10} t_r)$. ($T$ is temperature in °R and t_r is rupture time in hr.) It is not strictly valid in that Blackburn did not report an analysis of type 316 stainless steel data at 482°C (900°F), and we arbitrarily extrapolated his results to 482°C (900°F). Limits are drawn, bounded on the upper side by 95% confidence limits for 100,000-hr rupture, and on the lower side by 95% lower confidence limits for 10-hr rupture in one region and for 100,000-hr rupture in another region.

The rupture time data for the type 316 CRE stainless steel weld metal are shown in Fig. 5.35 and compared with these limits. The weld metal has longer rupture times than most type 316 stainless steel base metal at low stresses. The Blackburn analysis does not treat rupture times less than 10 hr, so a valid comparison cannot be made with expected base metal values for the 0.4-hr weld metal rupture datum.

5.3.2 High-Temperature Structural Design Data for Austenitic Stainless Steel Weldments

5.3.2.1 Characterization of FFTF Vessel Test Welds: SMA Type 308 (CRE) Stainless Steel Welds — R. T. King and G. M. Goodwin

We are investigating the properties and structure of type 304 stainless steel welds with controlled residual elements (CRE) made to

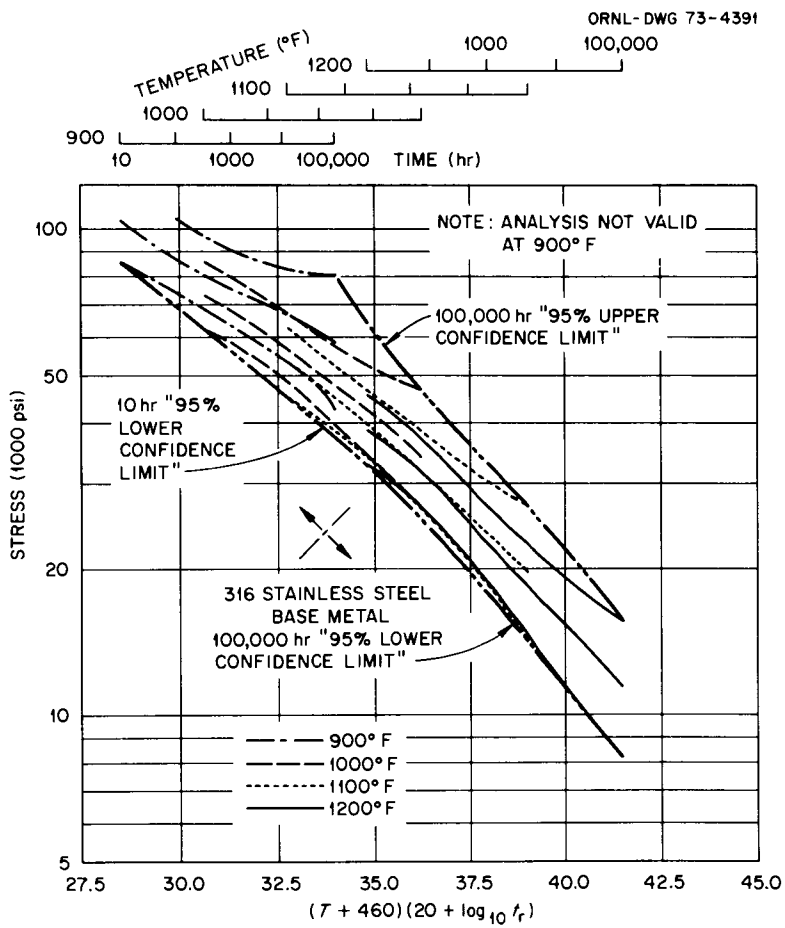

Fig. 5.34. Blackburn's Stress-Rupture Analysis of Type 316 Stainless Steel.

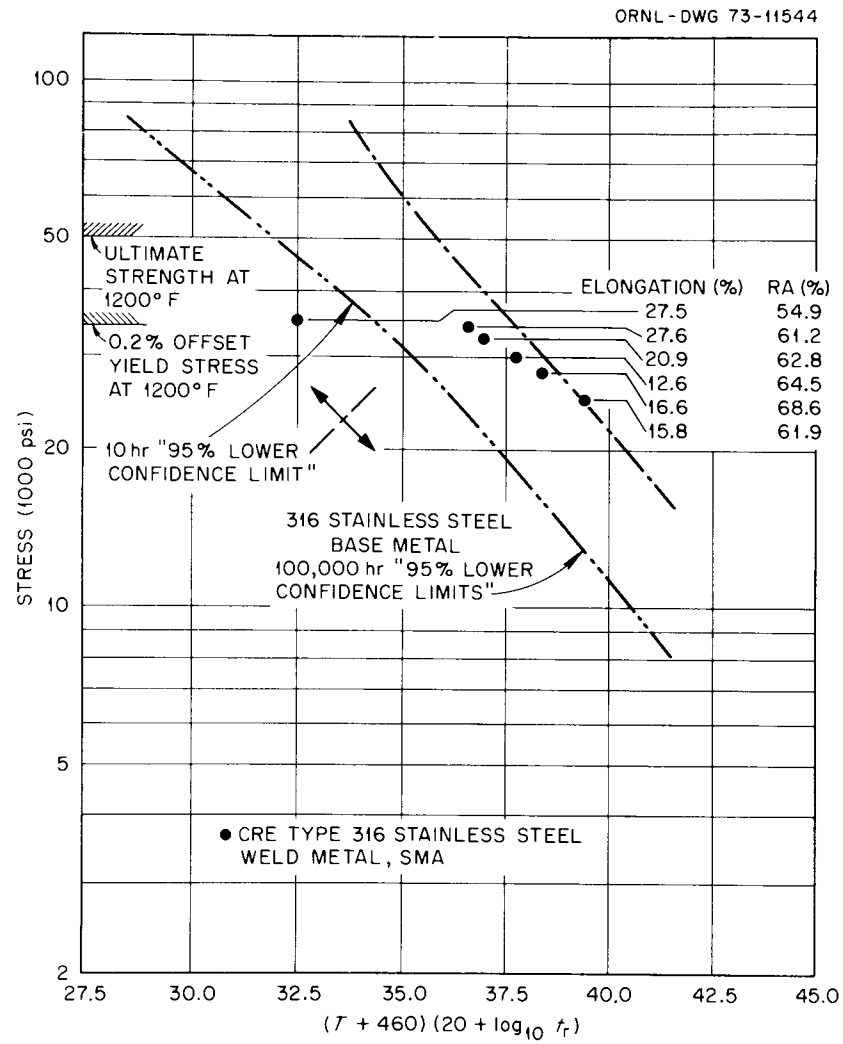

Fig. 5.35. Stress-Rupture Behavior of Type 316 CRE Stainless Steel Weld Metal.

simulate the seam and girth welds of the Fast Flux Test Facility (FFTF) vessel. The welds were produced by Combustion Engineering, Inc., of Chattanooga, Tenn. Sections of 2 3/8-in.-thick type 304 stainless steel plates were welded together; these plates are from two heats of steel used in the FFTF vessel, Carlson Heat 600414-1A (heat 1) and Carlson Heat 300380-1A (heat 2). The vendor's chemical analyses of the plates are given in Table 5.23. Several batches of 1/4-in. CRE type 308 stainless steel welding rods were needed to fabricate the FFTF vessel, and test welds made with six of these weld rod batches (batches 1, 2, 4, 6, 9, and 10) are represented in our study to date. In addition, test welds were also made with standard lime-coated type 308 stainless steel electrodes to compare the properties of welds made with lime-coated electrodes (batches 7 and 12) with the properties of welds made with CRE electrodes. The deposit analyses reported by Combustion Engineering, Inc., for the various batches of electrodes are given in Table 5.24.

Table 5.23. Chemical Composition of Type 304 Stainless Steel Plates Used in FFTF Vessel Test Weld Study

Element	Amount Present, wt %, in Carlson Heat	
	600414-1A (Heat 1)	300380-1A (Heat 2)
C	0.061	0.058
Mn	1.48	1.60
P	0.016	0.016
S	0.014	0.011
Si	0.64	0.55
Cr	18.88	18.68
Ni	9.56	8.44

Because two heats of base plate material and at least nine batches of welding rod will eventually be represented in this program, we have

Table 5.24. Chemical Composition of Type 308 Stainless Steel Deposited Weld Metal

Lot Number	Batch Number	Si	S	P	Mn	C	Cr	Ni	Mo	Cb	Ti	Co	Cu	B	V	N_2
LOEJ	1	0.46	0.009	0.043	1.90	0.068	19.72	9.86	0.16	Cb + Ta <0.01	0.06	0.07	0.11	0.007	0.08	0.048
LBHJ	2	0.60	0.009	0.042	1.87	0.061	20.10	10.14	0.24	Cb + Ta <0.01	0.06	0.07	0.17	0.007	0.10	0.042
AAPA	3	0.55	0.009	0.042	1.91	0.060	20.09	10.05	0.23	Cb + Ta <0.01	0.06	0.07	0.16	0.007	0.10	0.041
CAEA	4	0.52	0.016	0.043	1.95	0.066	19.73	9.88	0.25	0.01	0.06	0.07	0.16	0.007	0.09	0.039
DACA	5	0.60	0.016	0.042	1.82	0.061	20.04	9.83	0.12	Cb + Ta <0.01	0.06	0.17	0.15	0.007	0.07	0.046
HBEA	6	0.56	0.005	0.040	1.83	0.064	19.70	9.61	0.07	Cb + Ta <0.01	0.06	0.03	0.04	0.007	0.07	0.030
IBCA	7	0.45	0.009	0.019	1.84	0.063	19.50	9.64	0.06	Cb + Ta <0.01	0.01	0.01	0.03	0.001	0.06	0.026
ICJA	8	0.54	0.005	0.040	1.76	0.060	19.48	9.62	0.27	Cb + Ta <0.01	0.07	0.04	0.18	0.007	0.08	0.046
JADA	9	0.49	0.004	0.044	1.91	0.061	19.70	9.63	0.24	Cb + Ta <0.01	0.06	0.07	0.16	0.007	0.09	0.042
JAFA	10	0.37	0.004	0.044	1.90	0.060	19.81	9.77	0.12	Cb + Ta <0.01	0.06	0.17	0.15	0.007	0.07	0.046
ABHB	11	0.46	0.007	0.043	1.77	0.060	19.50	9.48	0.20	Cb + Ta <0.01	0.06	0.06	0.11	0.007	0.09	0.041
IBJB	22	0.30	0.010	0.026	1.90	0.063	19.82	9.85	0.23	Cb + Ta 0.01	0.01	0.05	0.12	0.001	0.07	0.039

developed a code to specify the weld rod batch and heats of plate which were joined to make a given test weld. The code is of the form:

Weld Rod Batch Number:Heat Number-Heat Number. Thus, a test weld of type 6:2-2 indicates that weld rod batch 6 was used to join two plates of heat 2 (Carlson Heat 300380-1A).

5.3.2.2 Tensile Properties of As-Welded SMA Type 308 (CRE) Stainless Steel FFTF Vessel Test Welds — R. T. King, J. K. Alley, and B. McNabb, Jr.

The SMA test welds were made by manually joining 15 × 20 × 6-cm-thick sections of the stainless steel plates along the 20-cm length with 0.635-cm-diam coated electrodes. The welding current and voltage were 300 A DCRP (direct current, reverse polarity) and 45 V. A both-sides U-groove joint design was used, and constraints prevented the plates from flexing about the weld. The root pass was deposited, excess base metal was removed to assure a full penetration weld, and the grooves were filled with weld metal deposited in about 35 to 40 passes. The final weld is nearly hourglass shaped and almost symmetrical about the midplane of the plate, and it is two passes wide everywhere except at the root.

Because we had found that the room temperature hardness of the weldments varied through the thickness of the weld, tending to be relatively soft near the surface of the test plates, we segregated the specimens according to their distance from the weld test plate surface. All weld metal specimens prepared with their gage lengths parallel to the welding direction, with their center lines located 0.48 cm (0.19 in.) below the surface, were designated L1-type specimens (longitudinal-Level 1). Specimens located 1.42 cm (0.56 in.) below the surface were designated type L2, and specimens located 2.39 cm (0.94 in.) below the surface were designated type L3. Accuracy of locating center lines of gage lengths is probably ±0.1 cm. Fig. 5.36 illustrates the locations from which these specimens were cut. Each set of longitudinal specimens prepared according to this scheme yields no more than four type L1, four type L2, and two type L3 specimens, and no more than three such sections can be prepared from each weld test plate.

In order to conserve material, the specimens for this program were fabricated by joining gage blanks of the weld metal using a low heat input welding process to type 304 stainless steel specimen end pieces and machining to the dimensions shown in Fig. 5.37.

The tensile tests were performed on an Instron tensile testing machine using a system which has the demonstrated capability of holding test temperatures to ±3°C (±37.4°F) at 600°C (1112°F).

Tests have been performed in air at 25, 93, 204, 371, 427, 482, 565, and 640°C (75, 200, 400, 700, 800, 900, 1050, and 1200°F). The 0.004/min strain rate receives primary emphasis in the test matrix because it is as close to the 0.005/min strain rate requested for ASTM Code Case 1331-5 qualification of materials as can be achieved using the Instron machine and the 1.25-in. gage length needed for extensometer measurements of strain on a 1-in. section of the gage. These measurements are supplemented by other tests at 0.04, 0.016, and 0.0004/min to demonstrate the effect of changing strain rate on measured properties.

In addition to obtaining the usual chart of load-vs-crosshead travel from the Instron load cell and drive system, we measured the strain which occurred in a 1-in. section of the gage length using an averaging extensometer fitted with two LVDT sensors. A separate plot of specimen deformation vs load as determined by a second load cell in the loading train was also made on an x-y recorder. The extensometer stress-strain curve is the more useful and accurate at small strains (we use it for strains <0.2%, although it is good to about 5% strain), but because the extensometer does not remain in place at higher strains and because the extensometer electronic system is nonlinear at large strains, we rely on the Instron chart at larger strains.

The data obtained from the averaging extensometer were reduced only to obtain the proportional limit and 0.2% offset yield stress values.

The data obtained from the Instron are processed by a BASIC-language program, MOD21, on the DEC PDP-10 time-sharing computer at ORNL. The program treats all of the observed elastic deflection as testing stand and load train deflection and computes the engineering and true stress and strain values at the apparent proportional limit, the 0.2%

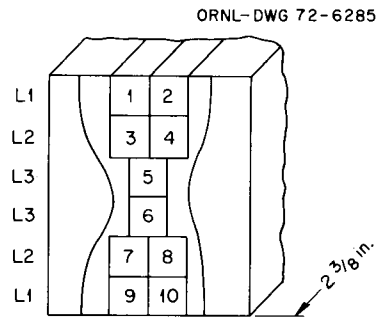

Fig. 5.36. Positions from Which Longitudinal, All-Weld-Metal Specimens Were Prepared from FFTF Vessel Test Welds. Hourglass region denotes weld metal.

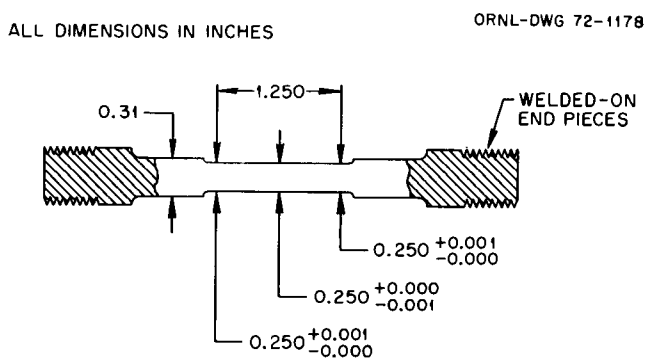

Fig. 5.37. Weld Test Specimens.

offset yield, the ultimate point, and the fracture point. The true fracture stress is based on an after-test measurement of the fracture diameters. For this anisotropic material, the fracture area is computed as though the projection of the fracture area were an ellipse. As a measure of the anisotropic behavior of the material, we also compute the diametral strain along the major and minor axes of the elliptical fracture surface. Because the deformation that occurs while the specimen necks down locally may differ considerably from uniform deformation, we have also measured the diametral strains at arbitrary points away from the necked-down region to compare with the fracture strains. All of these results are recorded in Tables 5.25 and 5.26.

Statistical analyses of these data are in progress to determine whether there are significant differences between CRE and conventional filler metal, or significant differences between electrode batch and base metal combinations for CRE filler metal welds. Graphical representations and interpretations of this data set, minus only a few tests, have been published.[19]

5.3.2.3 Tensile Properties of Aged SMA Type 308 CRE Stainless Steel FFTF Vessel Test Welds — R. T. King, E. Bolling, and B. McNabb, Jr.

In addition to testing as-received weld metal from the FFTF vessel test welds, we are also exploring the effects of aging on this material (see Section 5.3.2.1, this report). Our weld metal aging program for mechanical properties specimens includes the temperatures of 482, 593, and 649°C (900, 1100, and 1200°F). The aging program for microscopic structural studies includes 343 and 427°C (650 and 800°F) also, with the intent that mechanical properties specimens might be aged at these temperatures at a later date if significant microstructural changes are observed. Aging times to 20,000 hr are involved in the program, and longer times may eventually become desirable. This range of aging conditions is consistent with the anticipated operating temperatures of the FFTF vessel and the need to examine specimens aged at temperatures near 649°C (1200°F), where certain transformation reactions, including sigma phase formation, occur relatively rapidly.

Table 5.25. Tensile Properties of FFTF Vessel Test Weld Longitudinal All-Weld Metal Specimens at 0.004/min Strain Rate

Test Temp (°C)	Specimen Type: Location/Weld Block	Specimen Number	Instron Chart Measurements: Apparent Elastic Limit (ksi)	0.2% Offset Yield Stress (ksi) (Eng/True)	Strength: Ultimate (ksi) (Eng/True)	Strength: Fracture (ksi) (Eng/True)	Strain: Uniform (%) (in./in.) (Eng/True)	Strain: Total (%) (in./in.) (Eng/True)	Reduction of Area (%)	Diametral Strain: At Fracture (%) (max/min)	At Fracture (ratio)	Away from Fracture (%) (max/min)	Away from Fracture (ratio)	Extensometer Measurements: Elastic Limit (ksi)	0.2% Offset Yield Stress (ksi)
593 (1100°F)	L1/ 4:2-2	FF-49-2	26.7	32.8/32.9	51.0/60.4	41.9/82.4	18.4/0.17	31.4/0.68	49.2	29.3/28.1	1.0	14.9/6.1	2.4	18.98	33.04
	6:2-2	21-21	26.7	31.3/31.4	44.2/52.7	23.6/73.6	19.4/0.18	35.6/1.14	67.8	44.6/42.2	1.1	11.6/3.2	3.6	19.00	30.80
	9:1-1	43-2	24.6	32.4/32.5	47.5/57.5	30.7/66.8	21.2/0.19	37.0/0.78	54.0	40.2/25.0	1.6	16.1/6.5	2.5	20.91	31.88
	2:1-1	27-2	26.7	32.2/32.2	49.5/59.9	33.8/63.8	21.0/0.19	33.1/0.63	47.0	32.6/22.1	1.5	12.5/5.7	2.2	16.4	31.47
	7:1-1	18-2	17.4	26.7/26.7	42.0/51.5	29.7/65.1	22.6/0.20	37.9/0.78	54.4	36.6/28.6	1.3	16.1/7.3	2.2	18.45	26.24
	1:1-1	25-2	21.6	27.4/27.5	45.0/56.4	33.0/86.1	25.3/0.23	42.0/0.96	61.7	42.0/34.4	1.2	18.4/6.4	2.9	18.8	27.3
	10:1-1	48-2	21.9	29.2/29.2	45.3/55.0	33.1/95.3	21.4/0.19	37.2/1.06	65.2	47.2/35.5	1.3	18.1/6.5	2.8	19.1	29.0
	10:1-1	48-12	24.5	29.9/29.9	43.9/54.1	29.6/73.9	23.4/0.21	43.8/0.91	60.0	44.3/29.9	1.5	20.7/9.5	2.2	17.3	29.2
	L2/ 4:2-2	49-4	29.8	37.6/37.6	50.4/58.8	47.3/95.6	16.5/0.15	28.3/0.70	50.5	30.0/29.2	1.0	10.5/5.5	1.9	24.19	38.60
	6:2-2	21-23	30.8	37.4/37.5	45.7/51.9	33.9/77.0	13.5/0.13	31.0/0.82	56.0	36.5/30.9	1.2	18.2/8.1	2.2	27.77	37.02
	9:1-1	43-4	38.1	39.8/39.9	47.3/54.2	34.2/75.0	16.4/0.14	35.3/0.78	54.4	34.9/30.1	1.2	16.4/8.4	2.0	34.94	39.05
	2:1-1	27-4	26.8	37.5/37.6	50.6/59.3	41.2/72.5	17.3/0.16	26.0/0.56	43.1	30.0/19.5	1.5	10.7/7.0	1.5	17.51	37.08
	7:1-1	18-4	30.9	35.6/35.7	44.3/50.0	30.9/52.9	12.9/0.12	30.1/0.54	41.5	25.6/21.6	1.2	12.5/4.3	2.9	22.7	36.6
	1:1-1	25-4	29.4	37.8/37.9	46.6/53.2	32.2/80.9	14.2/0.13	34.1/0.92	60.2	41.9/32.3	1.3	21.9/7.8	2.8	22.48	37.40
	10:1-1	88-3	32.6	40.9/41.0	46.4/51.9	33.7/74.7	11.7/0.11	29.6/0.80	54.9	40.4/26.1	1.5	17.1/5.5	3.1	28.6	40.6
	L3/ 4:2-2	49-6	31.7	38.4/38.5	49.9/57.3	37.9/69.6	14.9/0.139	26.8/0.61	45.5	34.2/19.0	1.8	15.4/6.5	2.35	22.31	37.69
	6:2-2	21-26	32.6	39.9/40.0	47.2/51.7	32.6/75.8	9.4/0.09	26.5/0.84	57.0	41.6/27.9	1.5	9.6/4.8	2.0	21.78	38.45
	9:1-1	43-6	30.2	39.4/39.5	50.2/56.5	33.8/61.3	12.5/0.12	30.4/0.60	44.9	28.6/29.4	1.2	12.5/5.3	2.4	20.67	37.80
	2:1-1	27-6	33.9	41.1/41.2	49.5/55.3	36.0/66.5	11.7/0.11	27.4/0.62	45.9	30.3/22.9	1.3	7.6/3.4	2.2	23.6	39.56
	7:1-1	18-6	32.7	38.1/38.2	45.2/49.8	32.7/79.4	10.0/0.10	34.0/0.89	58.8	39.1/32.7	1.2	16.3/7.8	2.1	25.53	37.98
	1:1-1	25-6	33.1	40.8/40.9	49.3/54.6	33.1/74.6	10.8/0.10	28.6/0.81	55.6	41.9/25.8	1.6	15.7/5.6	2.8	20.7	40.4
	10:1-1	48-6	31.1	39.1/39.2	47.4/53.0	29.0/76.6	11.7/0.11	32.3/0.97	62.2	43.9/33.5	1.3	19.3/8.1	2.4	16.6	38.8
649 (1200°F)	L1/ 6:2-2	21-11	22.4	28.9/29.0	34.6/37.0	21.9/64.1	7.0/0.068	40.0/1.07	65.8	49.2/34.7	1.4	16.5/5.2	3.1	17.60	27.32
	L2/ 4:2-2	49-8	25.8	33.7/33.7	39.9/42.2	25.8/66.8	5.6/0.05	33.1/0.95	61.4	44.2/32.1	1.4	13.9/6.3	2.2	20.79	36.37
	6:2-2	21-24	27.2	32.7/32.7	36.7/37.9	23.9/50.8	3.06/0.03	32.4/0.75	52.9	33.6/29.1	1.1	10.3/1.8	5.7	19.59	32.16
	2:1-1	27-8	30.7	35.2/35.2	39.1/40.4	20.5/47.7	3.4/0.03	36.1/0.85	57.1	41.9/27.9	1.5	11.8/5.0	2.4	15.34	33.95
	10:1-1	48-8	23.6	32.7/32.8	38.1/40.2	24.0/54.6	5.5/0.05	38.5/0.82	56.0	41.1/27.0	1.5	13.7/6.9	2.0	21.94	32.29
	L3/ 6:2-2	84-15	26.4	33.0/33.1	35.8/36.8	23.6/70.9	2.8/0.028	34.6/1.10	66.8	53.7/32.0	1.6	14.1/5.4	2.6		33.0

*Chart stopped during test.

Table 5.26. Tensile Properties of FFTF Vessel Test Weld Longitudinal All-Weld Metal Specimens, Weld Combination 6:2.2

Test Temp (°C)	Strain Rate (in./in./min)	Specimen Type/Number	Instron Chart Measurements: Apparent Elastic Limit (ksi)	0.2% Offset Yield Stress (ksi) (Eng/True)	Strength: Ultimate (ksi) (Eng/True)	Strength: Fracture (ksi) (Eng/True)	Strain: Uniform (%) (in./in.) (Eng/True)	Strain: Total (%) (in./in.) (Eng/True)	Reduction of Area (%)	Diametral Strain: At Fracture (%) (max/min)	At Fracture (ratio)	Away from Fracture (%) (max/min)	Away from Fracture (ratio)	Extensometer Measurements: Elastic Limit (ksi)	0.2% Offset Yield Stress (ksi)
25 (75°F)	0.016	L1/FF-21-1	44.9	54.4/54.5	91.5/137.3	87.6/177.6	50.0/0.41	58.0/0.71	50.6	39.7/21.0	1.9	10.9/6.6	1.7	*	52.1
		L2/ 21-3	56.1	61.5/61.6	95.3/135.1	91.1/169.9	41.8/0.35	47.8/0.62	46.4	30.9/22.8	1.4	16.9/7.3	2.3	34.9	59.4
		L3/ 21-5	58.4	65.2/65.3	95.0/134.2	88.3/162.0	41.4/0.36	47.7/0.61	45.5	33.6/19.4	1.7	19.3/5.6	3.4	51.75	60.6
482 (900°F)	0.04	L1/ 21-19	30.2	36.0/36.1	61.4/79.0	45.5/119.3	28.8/0.25	37.3/0.96	61.8	41.5/35.1	1.2	13.3/3.6	3.7	22.8	34.9
		L2/ 17-23	36.2	42.4/42.5	65.5/76.6	50.7/103.9	22.5/0.20	29.9/0.72	51.2	34.3/26.2	1.3	12.0/3.2	3.7	38.3	41.9
	0.0004	L1/ 21-12	23.6	33.1/33.2	65.5/84.2	52.5/115.8	28.5/0.25	36.0/0.79	54.7	40.3/25.8	1.6	16.7/4.0	3.9	20.7	32.5
		L2/ 17-28	37.6	45.7/45.8	62.4/73.5	44.8/98.0	17.9/0.16	25.3/0.70	50.1	36.2/23.2	1.6	10.0/2.8	3.6	29.1	45.2
565 (1050°F)	0.04	L1/ 21-9	26.1	31.0/31.0	53.8/66.9	39.8/103.2	30.4/0.26	38.5/0.95	61.4	40.3/35.5	1.1	14.2/4.5	3.2	21.7	30.3
		L2/ 21-14	31.2	39.6/39.7	53.5/64.0	41.9/97.0	19.5/0.18	27.8/0.84	56.7	40.1/28.8	1.4	11.6/5.6	2.1	24.6	38.5
	0.0004	L1/ 21-10	22.4	28.9/28.9	41.2/48.8	22.8/51.2	18.4/0.17	49.3/0.92	60.2	44.4/30.2	1.5	22.2/6.8	3.2	18.8	29.7
		L2/ 21-17	31.5	37.3/37.4	43.8/49.0	28.5/73.2	11.8/0.11	33.7/0.94	61.0	40.7/34.7	1.2	13.3/3.2	4.1	28.0	38.1
		L3/ 17-15	36.6	43.1/43.2	53.3/62.7	38.5/82.0	17.7/0.16	27.4/0.76	53.1	39.4/24.4	1.6	9.9/1.8	5.4	24.4	41.1
593 (1100°F)	0.04	L1/ 84-1	22.2	27.7/27.7	45.2/56.8	33.8/74.7	25.8/0.23	37.2/0.79	54.7	42.2/24.3	1.7	14.3/4.0	3.6	12.1	26.9
		21-29	22.6	28.9/29.0	46.5/58.0	32.9/70.8	24.5/0.22	35.9/0.77	53.6	36.7/27.7	1.3	22.7/8.7	2.6	18.4	28.2
		L2/ 84-7	33.5	38.4/38.5	46.3/56.5	34.2/82.5	22.1/0.20	35.8/0.88	58.5	44.3/27.9	1.6	16.7/4.7	3.6	23.7	38.4
	0.0004	L1 21-22	22.6	28.2/28.3	37.4/41.2	19.5/59.4	10.2/0.10	41.0/1.11	67.2	52.2/34.5	1.5	20.5/8.0	2.5	20.7	26.8
		L2 17-14	25.7	39.3/39.4	41.1/42.3	22.6/51.2	3.1/0.03	35.9/0.82	55.9	41.0/26.9	1.5	16.9/8.4	2.0	23.6	36.5
649 (1200°F)	0.04	L1/ 17-11	20.6	26.4/26.5	39.2/47.7	28.0/75.1	21.7/0.20	42.4/0.99	62.7	42.3/35.2	1.2	18.9/6.5	2.9	12.3	25.3
		L2/ 84-4	29.2	33.7/33.7	36.2/42.2	27.6/71.8	7.8/0.075	38.0/0.95	61.5	42.1/34.1	1.2	18.5/7.0	2.7	17.6	33.1
	0.0004	L1/ 17-12	22.6	27.9/28.0	30.9/31.9	15.7/49.8	3.0/0.03	46.7/1.15	63.4	48.4/39.5	1.2	29.8/17.3	1.7	20.7	27.5
		L2/ 84-3	25.0	30.7/30.8	32.4/32.7	16.2/47.2	1.1/0.01	31.1/1.07	65.5	48.0/35.3	1.4	9.1/3.3	2.7	17.9	30.3

*Could not be defined due to coarse output scale used in test.

Entire test weld pieces of 6:2-2 welds that have been described previously were aged to prepare mechanical properties specimens. The test specimens were then cut from the aged blocks and prepared in a manner identical to that used to prepare as-welded specimens.

The tensile data for aged longitudinal all-weld-metal specimens are summarized in Table 5.27. Only L1 (surface) and L2 (intermediate location) specimens were tensile tested after aging; because the L3 (root pass) specimens are in short supply, they were not tested immediately. Data for comparable as-welded specimens are given for comparison in Table 5.27. The range of values for different combinations of weld metal and base metal is shown for those test conditions at which several tests were run. Preliminary statistical analysis of data for as-welded specimens indicated that the different combinations did not have significantly different properties, so the ranges of values probably reflect only normal scatter of data. Values for aged specimens that lie below or above the observed ranges of values or values for as-welded weld metal are italicized in the table. The statistical significance of this approach to assessing changes due to aging has not been established.

Whenever aging produced a change in either strength or ductility, those properties were usually reduced. The greatest effect of aging occurred at 482°C (900°F), where large changes in ultimate and fracture strength and in uniform and total elongation were observed. The tensile stress-strain curves for L1 and L2 specimens aged 4000 hr and tested at 482°C (900°F) are shown in Fig. 5.38(a) and (b), respectively. These results are not in conflict with similar results recently obtained[20] on the same weld metal in tests performed at 516°C (960°F) at HEDL.

Microstructural instability during thermal aging at 482°C (900°F) has been observed in the ORNL aging program. The microstructure of as-welded material consisted of about 5 to 7% ferrite distributed in an austenite matrix. The austenite-ferrite phase boundaries were decorated with an $M_{23}C_6$ precipitate. After aging for 10,000 hr at 482°C (900°F), the $M_{23}C_6$ precipitate phase was replaced by another phase. Selected area electron diffraction patterns taken from these precipitates show that the phase on the austenite-ferrite boundaries is probably the M_3C phase. In addition, the interior of the ferrite grains contained

Table 5.27. Comparison of the Tensile Properties of Aged and As-Welded CRE Type 308 Stainless Steel Weld Metal[a]

Aging and Test Temperature		Specimen		Instron Chart Measurements[c]						Reduction of Area (%)	Diametral Strain, %						Extensometer Measurements, ksi	
				Strength, ksi				Strain, %			At Fracture			Away From Fracture				
(°C)	(°F)	Type	Condition[b]	Apparent Elastic Limit	0.2% Offset Yield	Ultimate	Fracture	Uniform	Total		Max	Min	Ratio[a]	Max	Min	Ratio[a]	Elastic Limit	0.2% Offset Yield Stress
482	900	L1	As welded, low	26.3	32.7	62.5	46.6	26.5	34.3	42.8	29.7	19.3	1.3	13.4	3.6	1.8	15.52	31.5
					32.8	81.4	98.6	23	56									
			As welded, high	30.0	37.0	67.0	56.4	32.5	38.9	55.7	41.1	29.0	1.6	19.5	7.6	4.2	24.19	37.0
					37.1	85.9	116.7	28	81									
			Aged 4000 hr	25.7	32.9	*54.6*	46.9	*20.7*	*26.3*	44.6	31.2	20.4	1.5	*12.8*	6.0	2.1	*13.3*	31.5
					33.0	*65.9*	*84.7*	*19*	59									
482	900	L2	As welded, low	33.1	43.1	62.7	50.7	19.6	26.7	42.6	28.6	21.0	1.4	10.4	4.2	2.0	17.6	42.6
					43.2	75.7	96.4	18	57									
			As welded, high	37.3	44.9	66.9	56.0	24.3	31.4	52.7	41.9	25.8	1.7	16.0	8.0	3.8	34.3	44.7
					45.0	83.2	114.7	22	81									
			Aged 4000 hr	*28.3*	*43.0*	*56.1*	*48.1*	*10.4*	*18.1*	*41.0*	29.8	*17.0*	1.7	*7.1*	*2.3*	3.1	25.5	42.7
					43.1	*61.9*	*81.5*	*9.9*	*53*									
593	1100	L1	As welded, low	21.6	27.4	43.9	23.6	18.4	31.4	49.2	29.3	22.1	1.0	11.6	3.2	2.2	16.4	27.3
					27.5	52.7	63.8	17	68									
			As welded, high	26.7	32.8	51.0	41.9	25.3	43.8	67.8	47.0	42.2	1.6	20.7	9.5	3.6	20.9	31.9
					32.9	60.4	95.3	23	114									
			Aged 4000 hr	24.3	31.0	45.5	33.5	*13.8*	*29.5*	53.0	34.9	28.1	1.2	13.4	5.8	2.3	*16.2*	30.4
					31.0	51.7	71.3	*13*	76									
593	1100	L2	As welded, low	26.8	37.4	45.7	32.2	11.7	26.0	43.1	30.0	19.5	1.0	10.5	5.5	1.5	17.5	37.0
					37.4	51.9	52.9	0.11	56									
			As welded, high	38.1	40.9	50.6	47.3	17.3	34.1	60.2	41.9	32.3	1.5	21.9	8.4	3.1	34.9	40.6
					40.9	59.3	95.6	16	92									
			Aged 4000 hr	32.3	38.6	48.0	37.2	*9.2*	27.4	48.6	33.1	23.9	1.4	11.9	6.8	1.8	*17.2*	37.0
					38.7	52.4	*72.4*	*8.8*	67									
649	1200	L1	As welded	22.4	28.9	34.6	21.9	7.0	40.0	65.9	49.2	34.7	1.4	16.5	5.2	3.1	17.6	27.32
					29.0	37.0	64.1	6.8	7									
			Aged 1000 hr	26.2	31.1	38.9	23.7	8.0	*35.0*	*60.0*	*43.1*	*31.1*	1.4	*11.8*	*4.6*	*2.6*	19.7	30.6
					31.2	42.0	*59.4*	7.7	92									
			Aged 4000 hr	31.6	33.9	39.0	28.2	*5.0*	44.5	*57.8*	*40.4*	*30.1*	*1.3*	*13.3*	6.1	2.2	23.6	33.7
					33.9	40.9	66.9	*4.9*	*86*									
649	1200	L2	As welded, low	23.6	32.7	36.7	20.5	3.06	32.4	52.9	33.6	27.0	1.1	10.3	1.8	2.0	19.6	32.2
					32.7	37.9	47.7	3	75									
			As welded, high	30.7	35.2	39.9	25.8	5.6	38.5	61.4	44.2	32.1	1.5	13.9	6.9	5.7	21.9	36.4
					35.2	42.2	66.8	5	95									
			Aged 1000 hr	*22.4*	*27.6*	37.4	22.4	*9.9*	*50.6**	56.3	43.3	25.7	*1.7**	*17.6*	*9.6**	1.8	*18.0*	*27.9*
					27.6	41.0	51.3	*9.4**	82									
			Aged 4000 hr	25.5	*31.8*	39.1	25.5	5.5	*42.6**	54.5	37.3	28.0	1.3	12.8	5.9	2.1	*14.0*	*31.9*
					31.9	41.2	56.0	5.4	79									

[a]Values for aged specimens below the range for as-welded specimens are shown in italics. Values above the range are in italics and marked with *.

[b]Where data are available from more than one specimen, the low and high extreme values are given. The diametral strain ratios are the extremes for ratios for individual specimens, not ratios of the extreme values for all specimens.

[c]First number given is engineering value; second is true.

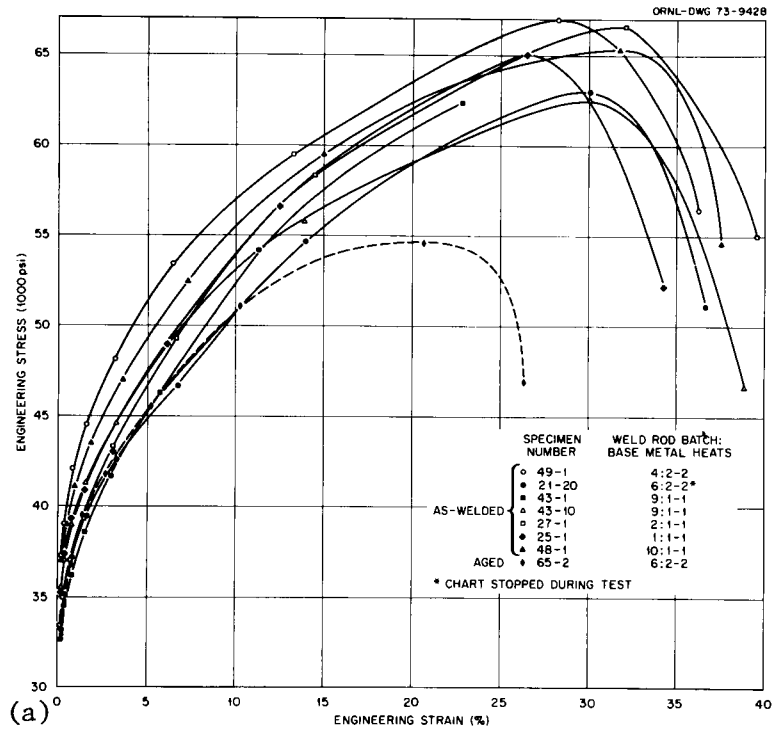

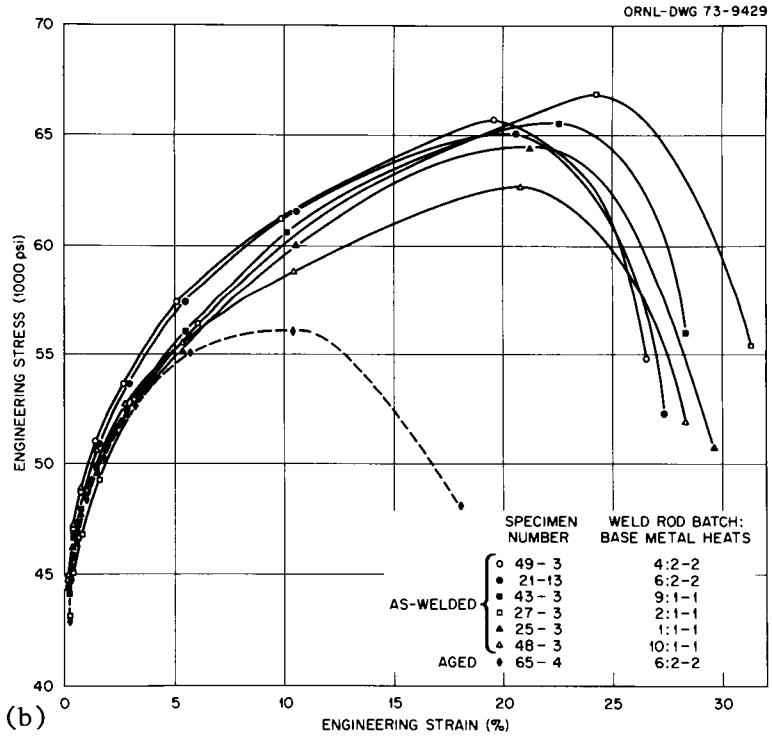

Fig. 5.38. Effect of Aging 4000 hr at 482°C (900°F) on the Tensile Stress-Strain Behavior of Type 308 CRE Weld Metal at 482°C (900°F). (a) L1 specimens. (b) L2 specimens.

a precipitate phase that was not present in the as-welded structure. The precipitate in the ferrite has a platelet morphology, and it has been identified as M_6C. It has not yet been established whether any of these precipitates play an important role in the property changes that occurred as a result of aging.

Aging for 4000 hr at 593°C (1100°F) reduced the uniform strain of the L1 and L2 specimens of CRE weld metal; the other apparent changes may not be significant. The microstructures of aged specimens are being studied.

Aging L1 specimens for 1000 and 4000 hr at 649°C (1200°F) produced some apparent changes in properties. However, since we have data from only one as-welded specimen, the significance of these apparent changes cannot be ascertained. Several L2 as-welded specimens were tested and produced ranges of values for comparison with the data for L2 specimens aged for 1000 and 4000 hr. Aging L2 specimens at 649°C (1200°F) apparently reduced the yield strength and increased both the uniform and total elongations. Microstructural studies of specimens aged at 649°C (1200°F) have shown that ferrite in the CRE weld metal transforms to sigma phase rather sluggishly at this temperature, while $M_{23}C_6$ carbide precipitates dissolve. After 4000 hr, for example, large regions of ferrite should still be present. The effect of these phase transformations on tensile properties are not well understood; other factors may also influence tensile properties.

A few creep tests have also been performed on aged specimens of CRE type 308 stainless steel weld metal. The results of these tests are summarized in Table 5.28. The greatest effect of aging observed to date is the reduction of rupture time at 482°C (900°F). This observation is consistent with the reduction of ultimate strength caused by aging for 4000 hr at 482°C (900°F).

Aging of weld sections for times up to 20,000 hr for both mechanical properties and microscopic investigations is still in progress. Some of this material might be aged for even longer times, should the data indicate a need for continued aging studies.

Table 5.28. Comparison of the Creep Behavior of As-Welded and Aged Type 308 CRE Weld Metal

Aging and Testing Temperature (°C)	(°F)	Specimen Type	Specimen Condition	Stress (ksi)	Rupture Time (hr)	Total Elongation (%)
482	900	L1	As-welded	55	913.8	29.6
				55	873.0	36.2
			Aged 4000 hr	55	0	26.8
		L2	As-welded	50	2394.6	27.9
			Aged 4000 hr	50	630.5	29.6
593	1100	L1	As-welded	33	73.3	35.8
			Aged 4000 hr	33	181.6	42.05
		L2	As-welded	33	610.2	23.9
			Aged 4000 hr	33	480.7	29.6

5.4 MECHANICAL PROPERTIES OF STEAM GENERATOR MATERIAL

5.4.1 The Effect of Carbon on the Mechanical Properties of 2 1/4 Cr-1 Mo Steel — R. L. Klueh

We have now completed our work, and a report was issued[21] on the studies of microstructure, room-temperature hardness, tensile properties, and creep-rupture properties for 2 1/4 Cr-1 Mo steel with 0.009, 0.030, 0.120, and 0.135% C. The 0.120 and 0.135% C contents are typical values for a commercial steel. Studies were made on steels in the annealed [furnace cooled from 927°C (1700°F)], normalized [air cooled from 927°C (1700°F)], and normalized-and-tempered [1 hr at 704°C (1300°F)] conditions. The important results can be summarized as follows:

1. In the annealed condition, the major phase of each steel was proeutectoid ferrite. As the carbon content increased, the amounts of spherical carbide and pearlite increased. Additionally, the annealed commercial plate (0.135% C) contained bainite.

2. When normalized, the steels contained progressively more granular bainite with increasing carbon content. The 0.009 and 0.030% C steels contained 1 to 2 and 15 to 20%, respectively, the balance proeutectoid ferrite.

The 0.120 and 0.135% C steels were both entirely bainite. After tempering, the only microstructural changes noted were the large amounts of precipitate formed, especially in the bainite.

3. For all heat treatments, there was little difference in the hardness for the 0.009 and 0.030% C steels. Similarly, there was little difference in the hardness of the normalized and the normalized-and-tempered 0.120 and 0.135% C steels, although in the annealed condition, the bainite present in the 0.135% C steel made it somewhat harder. As expected, the 0.120 and 0.135% C steels were considerably harder (in all conditions) than the other two.

4. With the exception of the room-temperature yield strength, where the smaller grain size for the 0.030% C steel made it stronger, the 0.009 and 0.030% C steels, which were primarily proeutectoid ferrite, had similar yield strengths over the range 25 to 565°C at a nominal strain rate of 0.02/min. This was true for both the annealed and normalized-and-tempered conditions. Ultimate tensile strengths, which are affected by the amounts of pearlite or bainite present in the microstructures, were always larger for the 0.030% C steel. The tensile properties of the 0.135% C steel were always greater than those for the 0.120% C steel, but both were in good agreement with studies by other investigators on 2 1/4 Cr-1 Mo steel with commercial carbon contents. Tests of the normalized-and-tempered steels at 371, 454, 510, and 565°C (700, 850, 950, and 1050°F) were made at three different strain rates. Reducing the nominal strain rate from 0.02 to 0.0008/min had little effect on yield and tensile strengths, but a change to 0.00008/min significantly decreased the strengths, an effect that increased with temperature and carbon content.

5. Creep-rupture properties were determined at 454, 510, and 565°C (850, 950, and 1050°F). At 565°C (1050°F), the properties for the 0.009 and 0.030% C steels were similar (a slight advantage for the 0.030% C steel); likewise, the properties for the two high-carbon steels were similar (a slight advantage for the steel with 0.135% C). At 454 and 510°C (850 and 950°F), however, the properties of the 0.030% C steel approached those of the 0.120 and 0.135% C steels; the properties for

the 0.009% C steel were considerably below those of the other three steels at both temperatures. The effect of carbon content on the creep-rupture behavior was qualitatively explained in terms of the known precipitation reactions that occur in 2 1/4 Cr-1 Mo steel.

5.4.2 Mechanical Properties of Overlaid Stainless Steel Forgings — R. L. Klueh and D. A. Canonico

We previously reported on the hardness and metallography of the 30-in.-diam type 304 stainless steel forging overlaid with type 308 stainless steel weld metal.[22] Microhardness traverses showed a uniform hardness through the weld metal but a considerable hardness gradient in the underlying forging, which indicated that the overlaying process affected the forging immediately below the fusion line.

Our initial room-temperature tensile tests substantiate the hardness measurements. Table 5.29 lists the room-temperature properties of the type 308 stainless steel at two levels in the overlay. They are substantially the same, as would be expected from the hardness measurements. However, there are differences in the underlying type 304 stainless steel. Immediately below the interface the yield and tensile stresses of the type 304 stainless steel are much higher than those of the forging at a distance from the interface and also exceed those of the type 308 stainless steel weld metal (Table 5.29). The 68,000-psi yield and 97,000-psi tensile strengths are somewhat above those given by Simmons and Van Echo[23] and Smith[24] in their compilations of properties for "annealed" and "wrought" type 304 stainless steel (product forms in the Simmons and Van Echo compilation included bar, plate, and sheet, and the Smith compilation included bar, plate, and pipe). According to Swindeman,[25] yield stresses of reannealed type 304 run from 24 to 32 ksi; vendor annealed (which obviously contain cold work) from 30 to 50 ksi; and vendor cold drawn, above 50 ksi.

We have also completed tensile tests over the range room temperature to 649°C (1200°F) on the forging that was unaffected by the overlay (i.e., specimens were taken greater than 2 in. from the overlay-forging fusion line). Specimens were taken in the axial, radial, and tangential orientations. Tests for all three orientations were made at a nominal strain

Table 5.29. Room Temperature Tensile Properties at Various Locations of the Overlaid Intermediate Heat Exchanger Forging

Specimen[a] Location (in.)	Strength, ksi		Total Elongation (%)	Reduction in Area (%)
	Yield	Tensile		
	Type 308 Stainless Steel			
1/4 below surface	63.7	89.4	38	60.3
3/8 below surface	64.2	90.9	41	43.3
	Type 304 Stainless Steel			
1/4 below interface	68.7	97.4	51	50.0
3 below interface	41.7	85.7	67	74.2

[a]All specimens are in the radial direction.

rate of 0.04/min (0.05 in./min crosshead speed), and additionally, axial specimens were tested at strain rates of 0.004 and 0.0004/min. The results are shown in Table 5.30.

In general, the properties fall within the scatter band of data given by Simmons and Van Echo[23] and Smith[24] for "annealed" and "wrought" type 304 stainless steel, respectively. Figure 5.39 shows the 0.2% yield and ultimate tensile stresses and Fig. 5.40 shows the elongation and reduction in area as functions of temperature for the three orientations at the 0.04/min strain rate. At room temperature, the tangential specimen has the highest strength and the lowest ductility, with very little difference in the properties of the tangential and axial specimens. However, in the range 538 to 649°C (900 to 1200°F), the radial specimens consistently have the highest yield stress, followed by the tangential, and then the axial. The ultimate tensile stresses, on the other hand, showed essentially no variation. Considering the inherent scatter in elongation and reduction in area measurements, we conclude that there is no variation of ductility with orientation at the elevated temperatures, though the tangential specimen exhibited a considerably reduced ductility at room temperature.

Table 5.30. Tensile Properties of Type 304 Stainless Steel Forging in Three Orientations

Temperature (°C)	Temperature (°F)	Nominal Strain Rate[a] (min^{-1})	Stress, ksi: 0.2% Offset Yield	Stress, ksi: Ultimate Tensile	Total Elongation (%)	Reduction in Area (%)
			Axial Orientation			
25	77	0.04	40.5	89.5	77.9	73.4
427	800	0.04	24.5	64.5	46.9	60.1
482	900	0.04	24.2	65.9	42.8	57.1
538	1000	0.04	23.8	63.0	46.0	60.7
593	1100	0.04	23.0	47.9	42.7	62.9
649	1200	0.04	22.0	50.2	39.9	62.6
482	900	0.004	24.7	71.1	46.6	56.5
593	1100	0.004	24.2	55.8	40.7[b]	41.8
649	1200	0.004	22.5	46.0	52.6[b]	46.8
482	900	0.0004	25.0	69.7	44.3[b]	54.3
593	1100	0.0004	22.3	50.5	28.2[b]	27.3
649	1200	0.0004	20.0	39.6	26.8[b]	29.3
			Radial Orientation			
25	77	0.04	42.0	85.7	63.4	74.0
427	800	0.04	28.3	64.0	39.3	56.2
482	900	0.04	33.1	65.5	42.8	60.9
538	1000	0.04	32.2	62.8	39.5	64.6
593	1100	0.04	30.8	58.4	41.3	62.5
649	1200	0.04	29.2	49.4	46.2	60.8
			Tangential Orientation			
25	77	0.04	50.5	88.1	36.6	53.4
427	800	0.04	30.3	68.2	45.8	63.2
482	900	0.04	28.9	66.4	41.6	57.2
538	1000	0.04	27.8	62.8	44.8	63.7
593	1100	0.04	24.8	47.9	42.9	60.2
649	1200	0.04	26.2	49.5	48.2	56.9

[a]0.05 in./min crosshead speed.

[b]Fractured at gage mark.

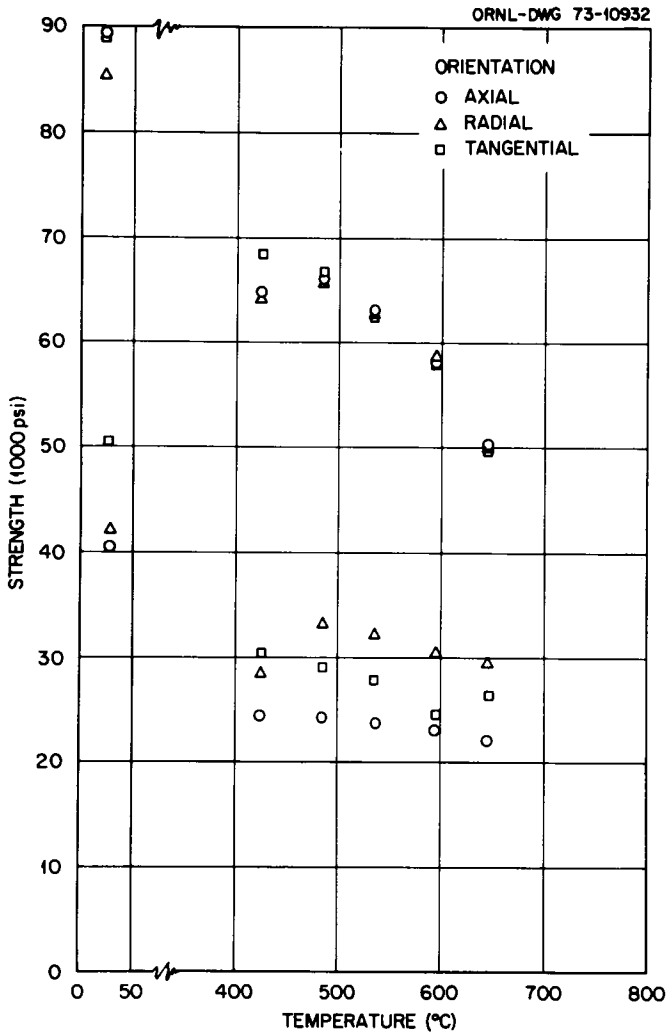

Fig. 5.39. The Effect of Temperature on the Yield Strength (Lower Points) and Ultimate Tensile Strength (Upper Points) of a Type 304 Stainless Steel Forging; Three Orientations Were Tested.

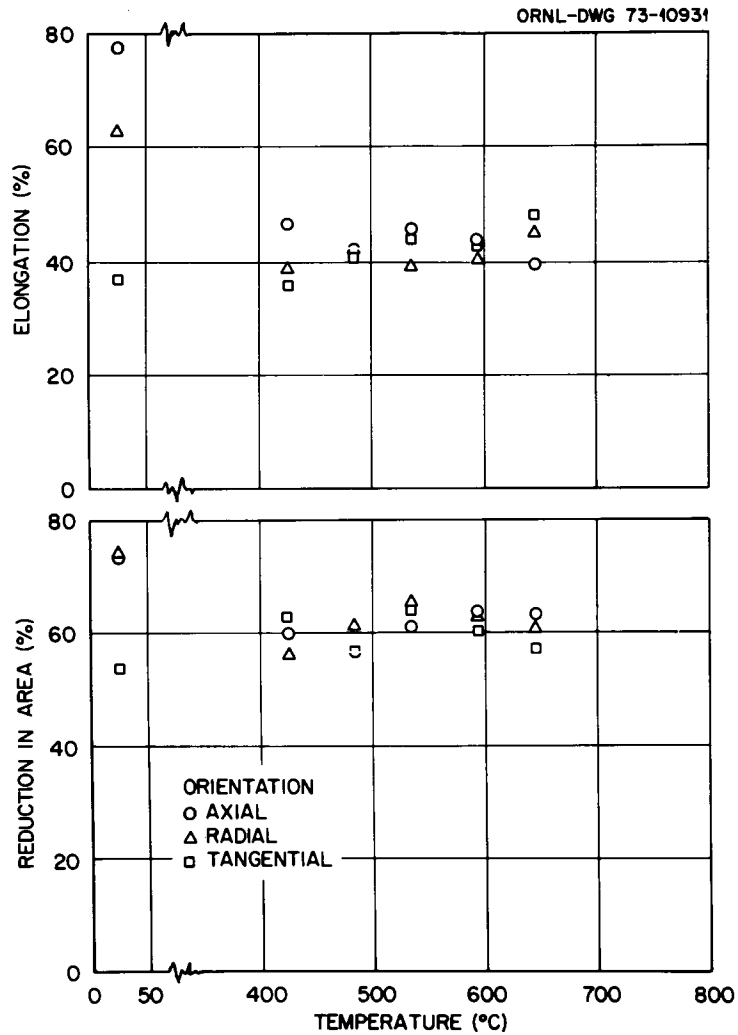

Fig. 5.40. The Effect of Temperature on the Elongation and Reduction in Area of a Type 304 Stainless Steel Forging: Three Orientations Were Tested.

When the strain rate for the axial specimens over the range 427 to 659°C (800 to 1200°F) was decreased, there was little effect on yield stress — perhaps a slight decrease at 0.0004/min at 649°C (1200°F). However, as shown in Fig. 5.41, the ultimate tensile stress progressively decreased with decreasing strain rate and increasing temperature. Figure 5.42 shows that the elongation and reduction in area paralleled the ultimate tensile stress.

Visual observations indicated that all specimens (all orientations) tested at 0.04/min formed a neck and failed transgranularly. A similar failure mode was noted for the axial specimen tested at 482°C (900°F) and 0.004/min. The remainder of the axial specimens at 0.004/min and all the specimens at 0.0004/min displayed a flat fracture with no neck formation, and in all cases, cracks (apparently along grain boundaries) were readily visible on the specimen surface. During the next quarter, selected specimens will be examined metallographically.

5.4.3 Mechanical Properties of 9 Cr-1 Mo Steel — P. L. Rittenhouse

There is interest in 9 Cr-1 Mo steel as a backup material for nuclear steam generator construction. Since this material is currently qualified for nuclear use only to 371°C (700°F) (Section III of the ASME Code), we undertook to determine whether presently available data were sufficient to allow qualification to higher temperatures as in ASME Code Case Interpretation 1331-8. Our review, analysis, and treatment of tensile, creep, and stress-rupture data for 9 Cr-1 Mo steel have now been completed.

5.4.3.1 Elevated-Temperature Tensile Properties

The specification of the time-independent stress intensity limits (S_m's) in the ASME Code requires the determination of minimum yield and tensile strengths. In our review of tensile properties of 9 Cr-1 Mo, we have obtained data from 24 heats of material. However, only for seven of these were strength data given at temperatures above room temperature

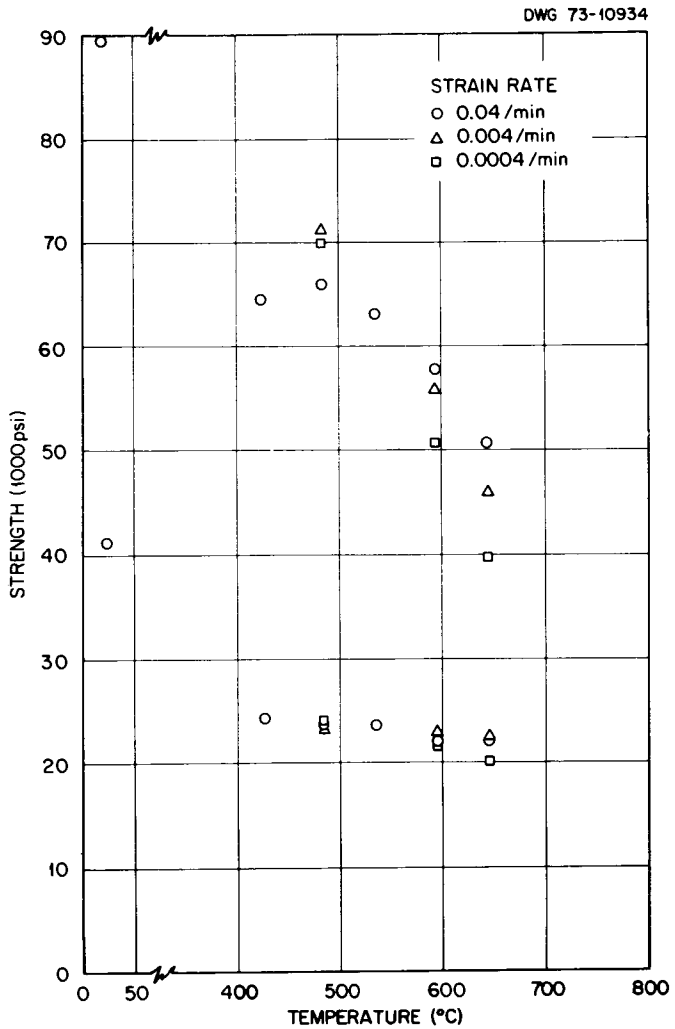

Fig. 5.41. The Effect of Temperature and Strain Rate on the Yield Strength (Lower Points) and Ultimate Tensile Strength (Upper Points) of a Type 304 Stainless Steel Forging; the Axial Orientation Was Tested.

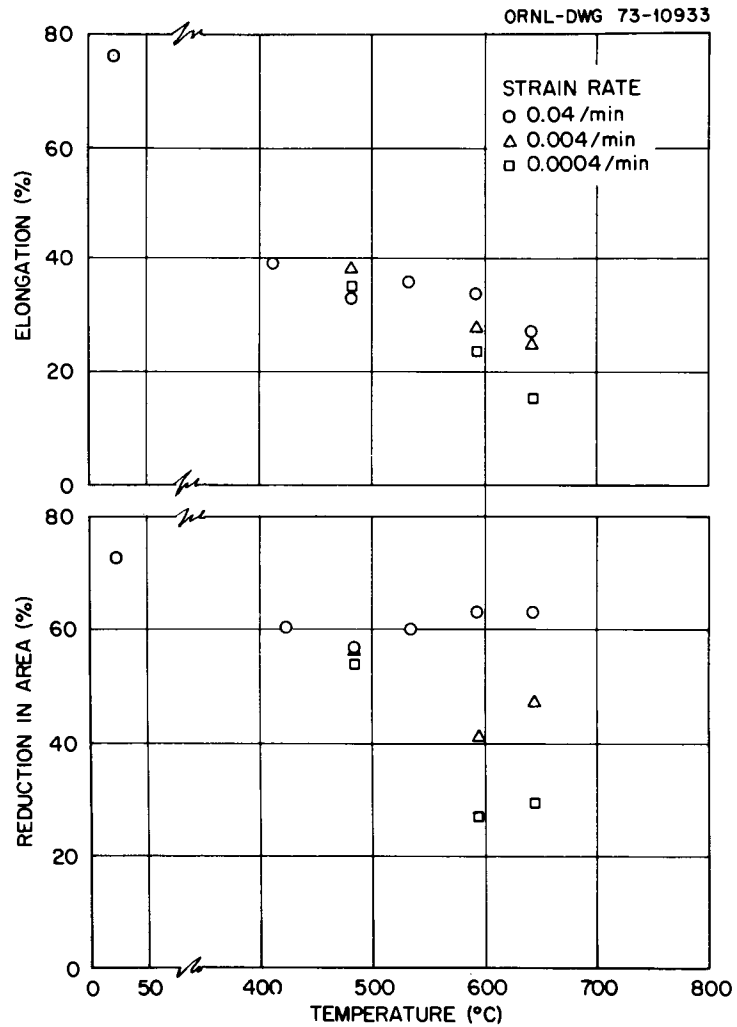

Fig. 5.42. The Effect of Temperature and Strain Rate on Elongation and Reduction in Area of a Type 304 Stainless Steel Forging; the Axial Orientation Was Tested.

(RT). These data are shown in Figs. 5.43 (0.2% offset yield strength) and 5.44 (ultimate tensile strength). The dashed line in Fig. 5.43 represents our judgment as to the "minimum" yield strength and, from RT to 538°C (1000°F), is identical to that in Section III of the ASME Code. Similarly, the dashed line in Fig. 5.44 is our recommended "minimum" ultimate tensile strength. Note that this minimum curve neglects the ORNL data[26] because we do not believe that these data, obtained using a very low strain rate (0.005/min), are applicable to the determination of ultimate tensile strength at high temperatures.

Because of the limited data base available, statistical analysis techniques were not employed to generate curves of minimum yield and tensile strength. Additional testing on other lots of material would be required to confirm the conservatism of our minimums.

5.4.3.2 Creep and Stress Rupture

We earlier[26] reported average stresses (determined with the Larson-Miller technique) to cause (1) rupture, (2) 1% total strain, and (3) tertiary creep as a function of time from 10 to 300,000 hr and temperature from 371 to 704°C (700 to 1300°F). Tables 5.31, 5.32, and 5.33 give minimum or lower bound values of stress associated with these three items. The lower bound is defined to be the lower central tolerance limit ($\lambda = 0.95$, $P = 0.90$) about the expected stress obtained from the assumed (Larson-Miller in this case) mathematical model. Thus, with a confidence level of 95%, 95% of all observed stresses are expected to be greater than the lower limit. The actual tolerance limit is based on the Bonferroni inequality and is explained in greater detail by Lieberman and Miller.[27]

Figure 5.45, a plot of the logarithm of stress to initiate tertiary creep against the Larson-Miller parameters ($P = CT + T \log t$ with T in °R and t in hours), illustrates the procedure for obtaining the minimum stresses. The solid line is the Larson-Miller representation of the expected value of stress for given time-temperature combinations; the dashed line represents the lower tolerance limit on this correlation. The minimum value of stress to initiate tertiary creep for all combinations of time and temperature yielding a given value of P is that stress given by the intersection of P with the lower tolerance limit.

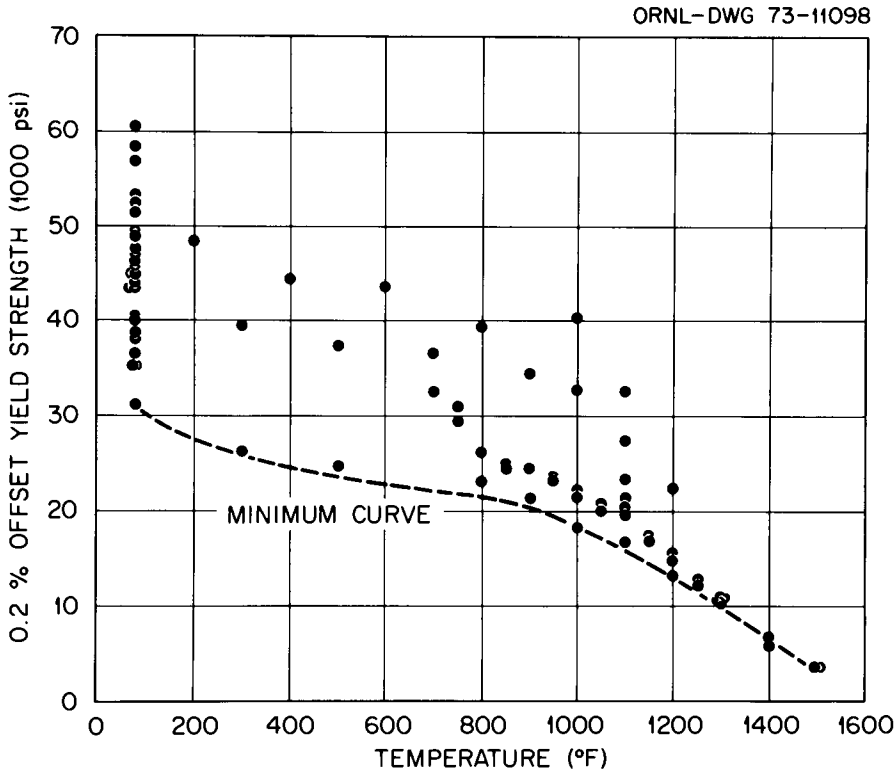

Fig. 5.43. Yield Strength (0.2% Offset) Data for 9 Cr-1 Mo Steel. Data from 24 lots of material are represented, but elevated-temperature data were given only for seven of these lots.

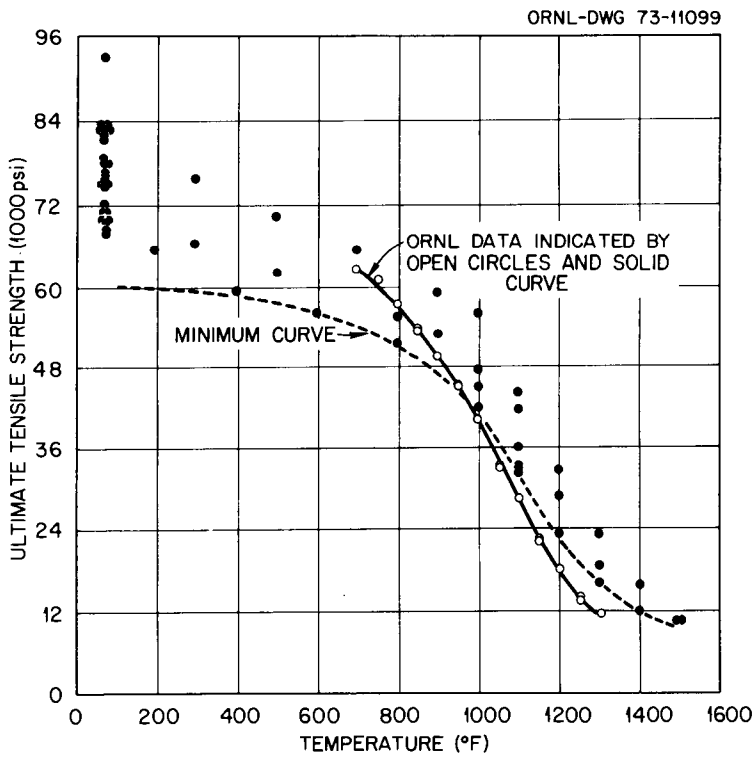

Fig. 5.44. Ultimate Tensile Strength Data for 9 Cr-1 Mo Steel. Data from 24 lots of material are represented, but elevated temperature data were given only for seven of these lots.

Table 5.31. Minimum Values of Stress to Rupture

Temperature		Stress Values, ksi, for Various Rupture Times in hr									
(°C)	(°F)	10	30	100	300	1000	3000	10,000	30,000	100,000	300,000
371	700	53.5	52.1	50.4	48.7	46.7	44.9	42.7	40.7	38.4	36.4
399	750	49.9	48.1	46.0	44.0	41.8	39.6	37.3	35.1	32.7	30.6
427	800	45.6	43.5	41.2	38.9	36.5	34.2	31.7	29.5	27.1	25.0
454	850	40.9	38.6	36.0	33.7	31.1	28.8	26.4	24.2	21.9	19.9
482	900	36.0	33.5	30.9	28.5	26.0	23.7	21.3	19.3	17.2	15.4
510	950	31.0	28.5	25.9	23.6	21.1	19.0	16.8	15.0	13.1	11.6
538	1000	26.2	23.8	21.2	19.0	16.8	14.9	13.0	11.4	9.8	8.6
566	1050	21.7	19.4	17.0	15.0	13.1	11.4	9.8	8.5	7.2	6.2
593	1100	17.6	15.5	13.4	11.7	10.0	8.69	7.3	6.2	5.2	4.3
621	1150	14.0	12.1	10.3	8.9	7.5	6.3	5.3	4.4	3.6	3.0
649	1200	10.9	9.4	7.8	6.6	5.5	4.6	3.7	3.0	2.4	2.0
677	1250	8.4	7.1	5.8	4.9	3.9	3.2	2.6	2.1	1.6	1.3
704	1300	6.4	5.3	4.3	3.5	2.8	2.2	1.7	1.4	1.0	0.8

Table 5.32. Minimum Values of Stress to Produce 1.0% Total Strain in Given Times

Temperature		Stress Values, ksi, for Various Times in hr[a]									
(°C)	(°F)	10	30	100	300	1000	3000	10,000	30,000	100,000	300,000
371	700	22.3	22.8	23.2	23.5	23.6	23.6	23.5	23.2	22.8	22.3
399	750	23.4	23.6	23.6	23.6	23.3	23.0	22.4	21.8	21.0	20.2
427	800	23.6	23.5	23.2	22.8	22.2	21.5	20.6	19.7	18.6	17.5
454	850	23.2	22.7	22.0	21.3	20.3	19.3	18.2	17.0	15.7	14.5
482	900	22.0	21.2	20.2	19.1	17.9	16.7	15.3	14.0	12.6	11.3
510	950	20.2	19.1	17.8	16.5	15.1	13.8	12.3	11.0	9.6	8.5
538	1000	17.9	16.6	15.1	13.7	12.2	10.8	9.4	8.3	7.1	6.1
566	1050	15.3	13.9	12.3	10.9	9.4	8.2	7.0	6.0	5.1	4.3
593	1100	12.6	11.1	9.6	8.3	7.1	6.1	5.1	4.3	3.6	3.0
621	1150	10.0	8.6	7.3	6.2	5.2	4.4	3.6	3.0	2.4	2.0
649	1200	7.7	6.5	5.4	4.6	3.7	3.1	2.5	2.0	1.6	1.2
677	1250	5.8	4.8	4.0	3.3	2.6	2.1	1.6	1.3	1.0	0.7
704	1300	4.3	3.5	2.8	2.3	1.8	1.4	1.0	0.8	0.6	0.4

[a]The small increases in stress value with time at 371°C (700°F) and 399°C (750°F) are the result of using the parametric analysis and statistical treatment outside the range of experimental data.

Table 5.33. Minimum Values of Stress to Initiate Tertiary Creep in Given Times

Temperature		Stress Values, ksi, for Various Times in hr[a]									
(°C)	(°F)	10	30	100	300	1000	3000	10,000	30,000	100,000	300,000
371	700	27.8	28.5	29.1	29.6	30.0	30.2	30.4	30.4	30.2	29.9
399	750	29.6	30.0	30.2	30.4	30.3	30.2	29.8	29.4	28.8	28.1
427	800	30.4	30.4	30.2	29.9	29.4	28.8	28.1	27.2	26.2	25.1
454	850	30.0	29.6	29.0	28.3	27.4	26.4	25.2	24.1	22.7	21.4
482	900	28.6	27.8	26.8	25.7	24.4	23.2	21.7	20.3	18.7	17.3
510	950	26.3	25.1	23.7	22.4	20.8	19.4	17.7	16.2	14.6	13.1
538	1000	23.2	21.8	20.2	18.6	17.0	15.4	13.7	12.2	10.8	9.5
566	1050	19.8	18.2	16.4	14.8	13.1	11.6	10.1	8.9	7.7	6.7
593	1100	16.0	14.4	12.7	11.1	9.7	8.5	7.3	6.3	5.4	4.6
621	1150	12.4	10.9	9.4	8.2	7.0	6.0	5.1	4.4	3.6	3.1
649	1200	9.4	8.1	6.9	5.9	5.0	4.2	3.5	2.9	2.4	1.9
677	1250	6.9	5.9	4.9	4.2	3.4	2.0	2.3	1.8	1.4	1.1
704	1300	5.0	4.2	3.4	2.8	2.2	1.8	1.4	1.1	0.8	0.6

[a]The small increases in stress value with time at 371°C (700°F) and 399°C (750°F) are the result of using the parametric analysis and statistical treatment outside the range of experimental data.

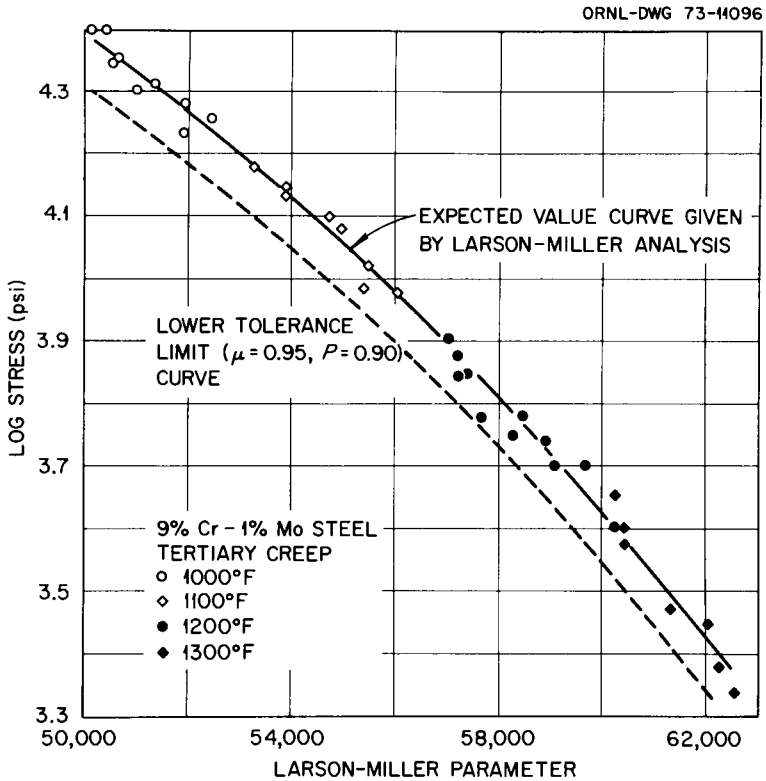

Fig. 5.45. Larson-Miller Plot of Stress to Initiate Tertiary Creep in 9 Cr-1 Mo Steel. This figure shows the available experimental data for the initiation of tertiary creep, the expected value curve (solid line) determined in the Larson-Miller analysis, and the lower tolerance limit (dashed line).

Figure 5.46 is given as an example of our Larson-Miller analysis results. In this figure the expected value curve (stress for a given time to rupture) for 649°C (1200°F) is shown relative to the experimental data taken at that temperature. The minimum values of stress for a given rupture time, as shown by the lower tolerance limit, fall slightly below the scatter of the data. In general, comparison of data with the predicted expected and minimum values is quite good at all temperatures. However, we have no data for comparison with predictions below 482°C (900°F) and few data from tests as long as 10,000 hr at any temperature. Therefore, we have reservations as to the reliability of predictions of expected values of stress outside the data range, especially at the lower temperatures.

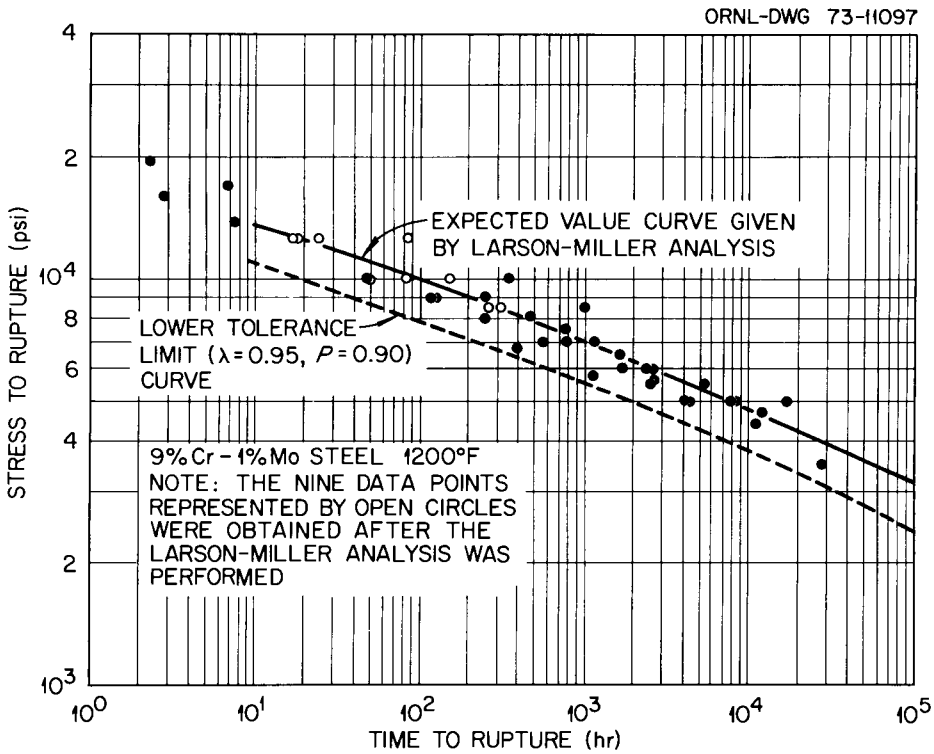

Fig. 5.46. Stress-Rupture Plot for 9 Cr-1 Mo Steel at 649°C (1200°F). This figure shows the experimental values of stress and time to rupture and the expected value and lower tolerance limit curves derived from the Larson-Miller treatment.

5.4.3.3 Stress Intensity Limits

The selection of values of S_m, the time-independent stress intensity limit used in Section III of the ASME Code, is normally based on the lesser of two-thirds of the minimum yield strength and one-third of the ultimate strength. Our recommendations for S_m as a function of temperature from 371 to 704°C (700 to 1300°F) are given in Table 5.34. The values in this table were developed with the minimum strength curves shown in Figs. 5.43 and 5.44. Values of S_m at temperatures below 371°C (700°F) [and, indeed, true below 538°C (1000°F)] may be taken as given in Section III of the ASME Code.

Table 5.34. Values of S_m for 9 Cr-1 Mo

Temperature (°C)	Temperature (°F)	S_m (ksi)	Basis
371	700	14.7	(2/3)YS[a]
399	750	14.5	(2/3)YS[a]
427	800	14.2	(2/3)YS[a]
454	850	13.8	(2/3)YS[a]
482	900	13.3	(2/3)YS[a]
510	950	12.8	(2/3)YS[a]
538	1000	12.2	(2/3)YS[a]
566	1050	11.3	(2/3)YS[a]
593	1100	10.3	(1/3)UTS[b]
621	1150	9.0	(1/3)UTS[b]
649	1200	7.4	(1/3)UTS[b]
677	1250	6.3	(1/3)UTS[b]
704	1300	5.3	(1/3)UTS[b]

[a]YS, 0.2% offset yield strength.

[b]UTS, ultimate tensile strength.

The time-dependent stress intensity limit (S_t) used in the Code is presently selected as the least of the following:

1. two-thirds of the minimum stress to cause rupture,
2. 80% of the minimum stress to initiate tertiary creep,
3. the minimum stress to cause 1% total strain.

Table 5.35 gives, for temperatures from 371 to 704°C (700 to 1300°F) and times from 10 to 300,000 hr, values of S_t chosen on the basis of the three factors above. In each case the limiting factor (i.e., rupture, tertiary creep, or 1% strain) is indicated. Notice that at the lower temperatures the S_t values are generally based on the minimum stress to a total of 1% strain. As temperature and time are increased, the minimum stress to rupture becomes controlling. Finally, at the highest temperatures, the stress to 1% strain is again controlling. Only in a few instances [i.e., relatively short times at 677 and 704°C (1250 and 1300°F)] does tertiary creep dominate.

5.4.3.4 Conclusions

We believe that the S_m (based on minimum yield and tensile strength) and S_t (based on the appropriate creep and rupture properties) values for 9 Cr-1 Mo have been specified with sufficient conservatism to assure that their use would not compromise design. However, in the former case, the determination of proper statistical minimum values of yield and tensile strength would require testing additional lots of material. In connection with S_t, our confidence in the values of stress to 1% strain and to tertiary creep would be greatly increased by additional data from carefully conducted creep experiments, especially at the lower temperatures.

5.5 HIGH-TEMPERATURE DESIGN — W. L. Greenstreet, J. M. Corum, and C. E. Pugh

5.5.1 Characterization of Product Form — H. E. McCoy

The large heat of type 304 stainless steel (Heat 9T2796) was purchased in several product forms. Creep and tensile tests are being run to determine the variation in mechanical properties with product form. Some of the results were presented previously,[28] and portions are still in progress.

Table 5.35. Temperature and Time-Dependent Stress Intensity Limits (S_t's)[a] for 9 Cr-1 Mo

Temperature		S_t, ksi, for Various Times in hr									
(°C)	(°F)	10	30	10^2	3×10^2	10^3	3×10^3	10^4	3×10^4	10^5	3×10^5
371	700	23.7ε	23.7ε	23.7ε	23.7ε	23.7ε	23.7ε	23.7ε	23.7ε	23.7ε	23.7ε
399	750	23.7ε	23.6ε	23.6ε	23.5ε	23.3ε	23.0ε	22.5ε	21.8ε	21.0ε	20.2ε
427	800	23.6ε	23.5ε	23.2ε	22.8ε	22.2ε	21.5ε	20.6ε	19.7εr	18.1r	16.7r
454	850	23.2ε	22.7ε	22.0ε	21.3ε	20.3ε	19.2r	17.6r	16.1r	14.6r	13.3r
482	900	22.0ε	21.2ε	20.2ε	19.0r	17.3r	15.8r	14.2r	12.9r	11.5r	10.3r
510	950	20.2ε	19.0r	17.3r	15.7r	14.1r	12.7r	11.2r	10.0r	8.7r	7.7r
538	1000	17.5r	15.9r	14.1r	12.7r	11.2r	9.9r	8.7r	7.6r	6.5r	5.7r
566	1050	14.5r	12.9r	11.3r	10.0r	8.1r	7.6r	6.5r	5.7r	4.8r	4.1r
593	1100	11.7r	10.3r	8.9r	7.8r	6.7r	5.7r	4.9r	4.1r	3.5r	2.9r
621	1150	9.3r	8.1r	6.9r	5.9r	5.0r	4.2r	3.5r	2.9r	2.4εr	2.0εr
649	1200	7.3r	6.3r	5.2r	4.4r	3.7εr	3.1εr	2.5εr	2.0εr	1.6εr	1.2ε
677	1250	5.5c	4.7rc	3.9rc	3.3εr	2.6εr	2.1εr	1.5ε	1.3ε	1.0ε	0.7ε
704	1300	4.0c	3.4c	2.7c	2.2c	1.7ε	1.4εc	1.0ε	0.8ε	0.6ε	0.4ε

[a]Symbol following stress value indicates limiting parameter (i.e., ε indicates S_t is based on 100% of stress to achieve 1% total strain; r, 2/3 of minimum stress to rupture; c, 80% of stress to initiate tertiary creep). In some cases two criteria gave the same value.

Ten of the twelve product forms and some of their properties are listed in Table 5.36. Two of the product forms, 3/8- and 1-in.-thick plates, have just been included in this program. The grain sizes of the various products varied from ASTM 1 to 7, with some of the products having a wide variation within themselves. Tensile tests have been run at room temperature for five of the product forms in the as-received and reannealed conditions. The stress-strain curves to 2% strain are shown in Fig. 5.47 for the as-received material and in Fig. 5.48 for the reannealed material. The yield stress of the as-received products varied from 26,500 to 34,400 psi, but the work-hardening rates appear the same after a few tenths of percent strain. The yield stress of the reannealed material varied from 26,000 to 27,700, and the curves to 2% strain almost superimpose (Fig. 5.48).

The results of chemical analyses for C, O, and N are given in Table 5.36. The carbon content varied from 0.050 to 0.056% and the nitrogen content from 0.040 to 0.051%. The quoted reproducibility for each analysis is ±5%; the carbon values fall within this range and the values for nitrogen have a span of about ±10%. The oxygen values varied from 0.0046 to 0.0089 for eight of the products, and values of 0.018 and 0.011 were noted for two products. Check analyses indicated concentrations of 0.019 and 0.014%, respectively. Thus, the oxygen concentrations in the product forms indicate variations far outside the ±5% reproducibility of the analysis. Metallographic studies in progress should indicate whether the inclusion count is significantly different for the product forms.

The stress-rupture properties at 593°C (1100°F) for reannealed samples are shown in Fig. 5.49 for seven product forms. Three stress levels were involved, and samples were taken from several locations and orientations within each product. The results obtained to date do not indicate a large difference in the rupture life due to variables of product form, specimen location, or specimen orientation. The rupture life of the 2-in. plate does seem to be slightly shorter, but the difference is not great.

The minimum creep rates for these same products are shown in Fig. 5.50. The differences among different product forms seem quite small and random.

Table 5.36. Information on Several Product Forms of Type 304 Stainless Steel, Heat 9T2796

Product Form	Specification	Hardness, R_B		Initial ASTM Grain Size	Yield Stress[b] at 25°C ksi		Chemical Composition, %[c]		
		Initial	Annealed[a]		Initial	Annealed	C	O	N
Pipe, 8-in. sched 80	A-376	73	69	5-6	30.3	26.0 26.5	0.056	0.018 0.019	0.042 0.042
Pipe, 4-in. sched 160	A-376	73	63	5-6	31.7 32.3	26.7 26.5	0.052	0.0089	0.051
Bar, 4 1/2 in. diam	A-479	67	67	2-3[d] 3-5[e]	30.8	26.5 26.1	0.051	0.0062	0.049
Bar, 2 in. diam	A-479	89	65	5-6[d] 6-7[e]			0.053	0.0049	0.048
Bar, 1 3/4 in. diam	A-479	81	65	5-6			0.052	0.0062	0.048
Plate, 1/2 in. thick	A-240	73	66	5-6			0.052	0.0075	0.046
Plate, 3/4 in. thick	A-240	65	65	5-6	34.4	26.0	0.051	0.011 0.014	0.048 0.044
Plate, 2 in. thick	A-240	59	66	1-3	27.7 26.6	27.7	0.055	0.0086	0.040
Tube, 2 1/2 in. O.D. × 5/8 in. wall (H.R.)	A-213	88	65	6-7			0.051	0.0053	0.050
Tube, 2 1/2 in. O.D. × 5/8 in. wall (C.D.)	A-213	74	67	3-6			0.050	0.0046	0.047

[a]1/2 hr at 1093°C (2000°F).

[b]Strain rate of 0.004/min. All samples parallel with the primary forming direction.

[c]Four product forms were analyzed for trace elements and the following levels apply to all four forms; <0.01% Ag, <0.05% Al, <0.01% B, <0.01% Ba, <0.005 Be, <0.02% Bi, <0.1% Ca, <0.1% Cb, <0.1% Cd, 0.3% Co, 0.3% Cw, 0.01% Mg, <0.02% Pb, <0.05% Pt, <0.02% Sn, <0.1% Sr, 0.05% Ta, <0.02% Ti, 0.03% V, <0.1% W, <0.2% Zr, <0.05% Zr, <0.05% Ge, <0.05% Ga. The concentrations of other alloying additions are 1.22% Mn, 0.029% P, 0.012% S, 0.47% Si, 18.5% Cr, 9.58% Ni, 0.10% Mo.

[d]Longitudinal plane.

[e]Transverse plane.

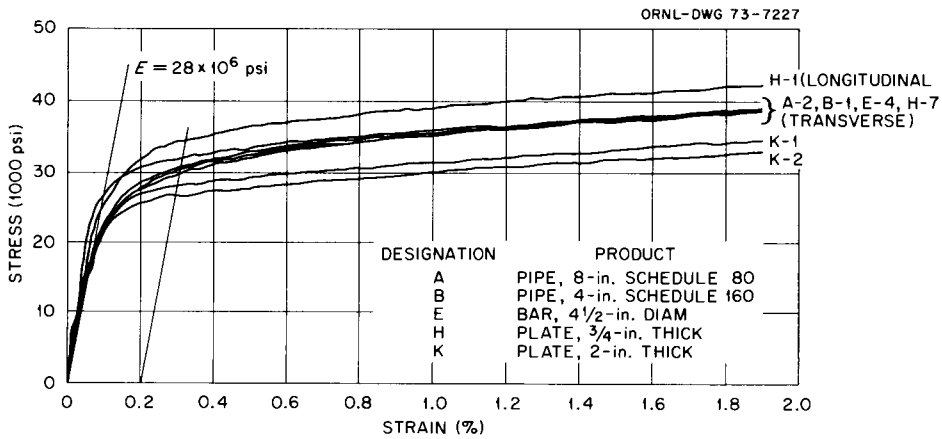

Fig. 5.47. Stress-Strain Properties at Room Temperature of Several Product Forms of Type 304 Stainless Steel Heat 9T2796. As received.

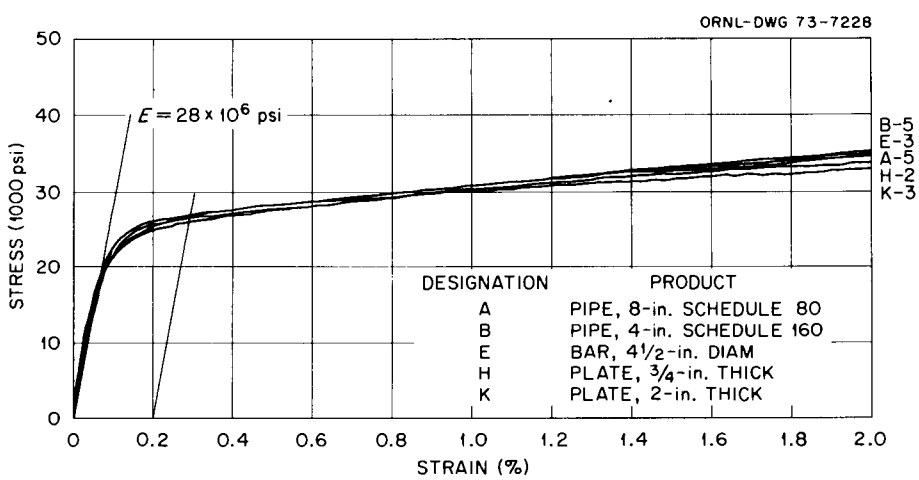

Fig. 5.48. Stress-Strain Properties at Room Temperature of Several Product Forms of Type 304 Stainless Steel Heat 9T2796. Annealed 0.5 hr at 1093°C (2000°F).

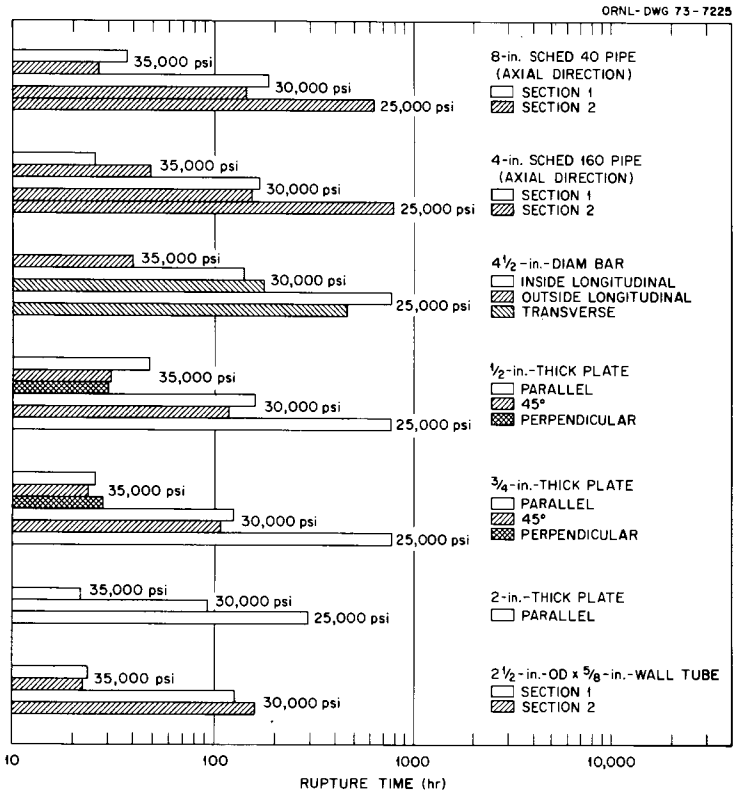

Fig. 5.49. Stress-Rupture Properties of Several Product Forms of Type 304 Stainless Steel (Heat 9T2796) at 593°C (1100°F) After Reannealing 0.5 hr at 1093°C (2000°F).

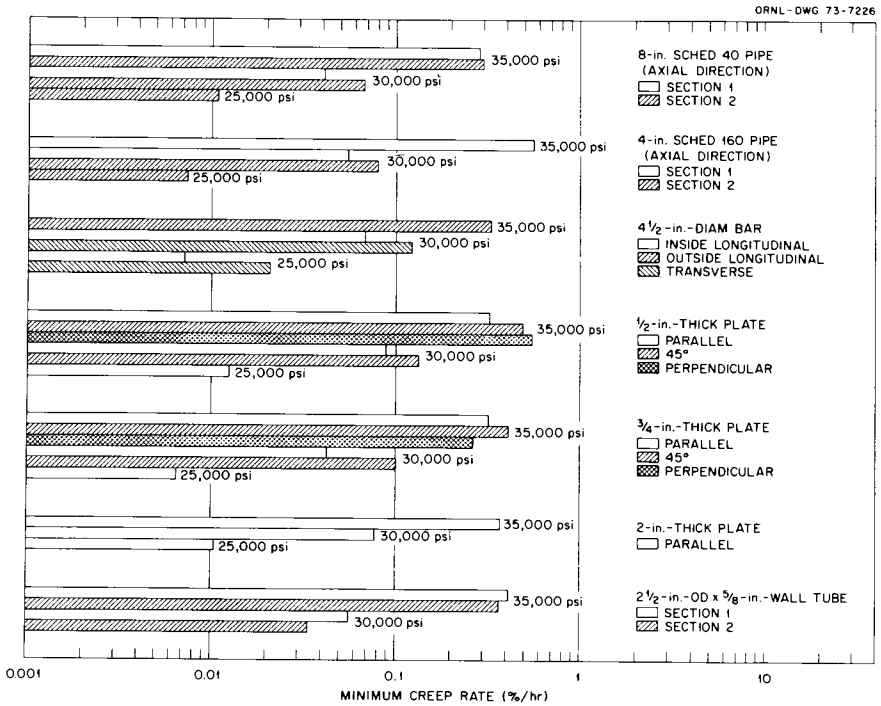

Fig. 5.50. Creep Properties of Several Product Forms of Type 304 Stainless Steel (Heat 9T2796) at 593°C (1100°F) After Reannealing 0.5 hr at 1093°C (2000°F).

The 2-in. plate that seemed weaker based on the rupture time (Fig. 5.49) does not appear different from the other products on the basis of minimum creep rate.

5.5.2 Exploratory Testing to Identify Behavioral Features — R. W. Swindeman

5.5.2.1 Stress-Strain Testing

Several tensile tests were performed on type 304 stainless steel (Heat 9T2796 plate) for the purpose of exploring the inelastic behavior at relatively low strains. We reported earlier[29] that between the 0.1% inelastic offset strain and the uniform strain at the ultimate the Ludwik equation excellently represents the true stress—true strain behavior for laboratory reannealed material. Not included in this representation were inelastic offset strains in the zero to 0.1% range, and these, of course, are often the most commonly experienced strain levels in design analysis. A tracing of a yield curve obtained at 1100°F (593°C) is shown in Fig. 5.51. This, and several other curves which cover the temperature range from 800 to 1100°F (427 to 593°C) are shown in Fig. 5.52. All tests were performed under servo-controlled conditions at a strain rate of 0.005/min. Low-load cycling showed that the extensometer turn-around error and sensitivity corresponded to strain values less than 10^{-5}. We observed that the elastic limit of the curves was difficult to detect. Assuming the static modulii values provided in the ASME Code Case 1331 to be correct, we found, as indicated in Fig. 5.51, that the 10^{-5} offset stresses were between 5,000 and 8,000 psi. Deviations from linearity developed gradually until stresses neared 10,000 psi. Above this stress the strain-hardening rate (tangent modulus) rapidly changed and approached a near-constant value, which was maintained for several percent strain. Sometimes, however, we observed a short strain interval in which the yield curve was horizontal. This occurred between 0.05 and 0.1% total strain. We have seen this behavior before, in the "preliminary" heat (Heat 8043813) of type 304 stainless steel. The inelastic deformation below the knee of the yield curve could be the result of several causes. Among them are the usual anelastic

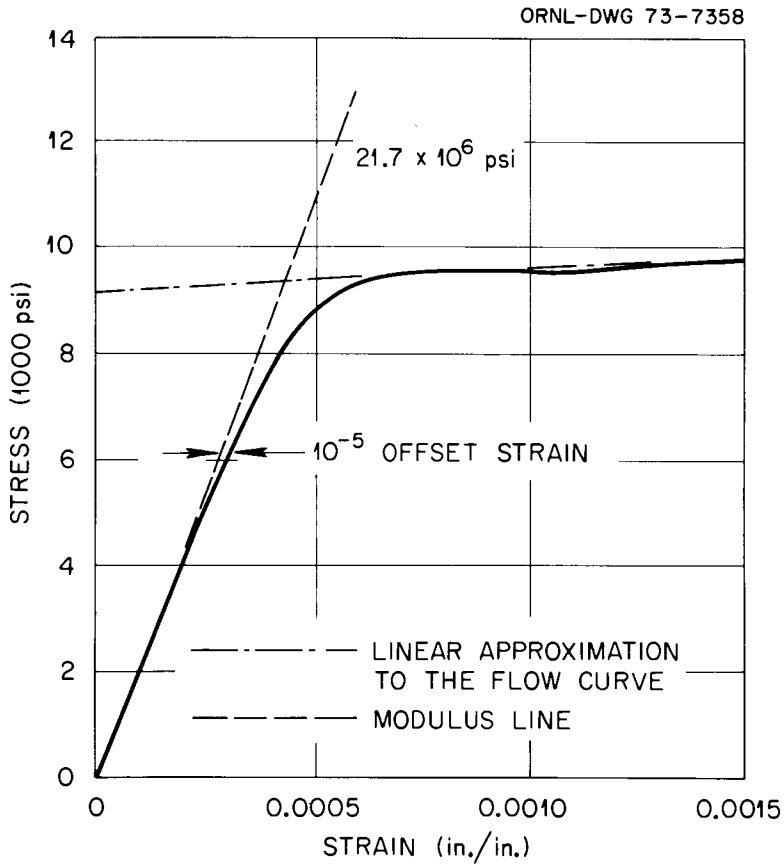

Fig. 5.51. Tensile Yield Curve for Type 304 Stainless Steel at 1100°F (593°C). Heat 9T2796 1-in.-thick plate reannealed at 2000°F (1093°C) for 0.5 hr and tested at 0.005/min. under servo control. Specimen 7RP-131.

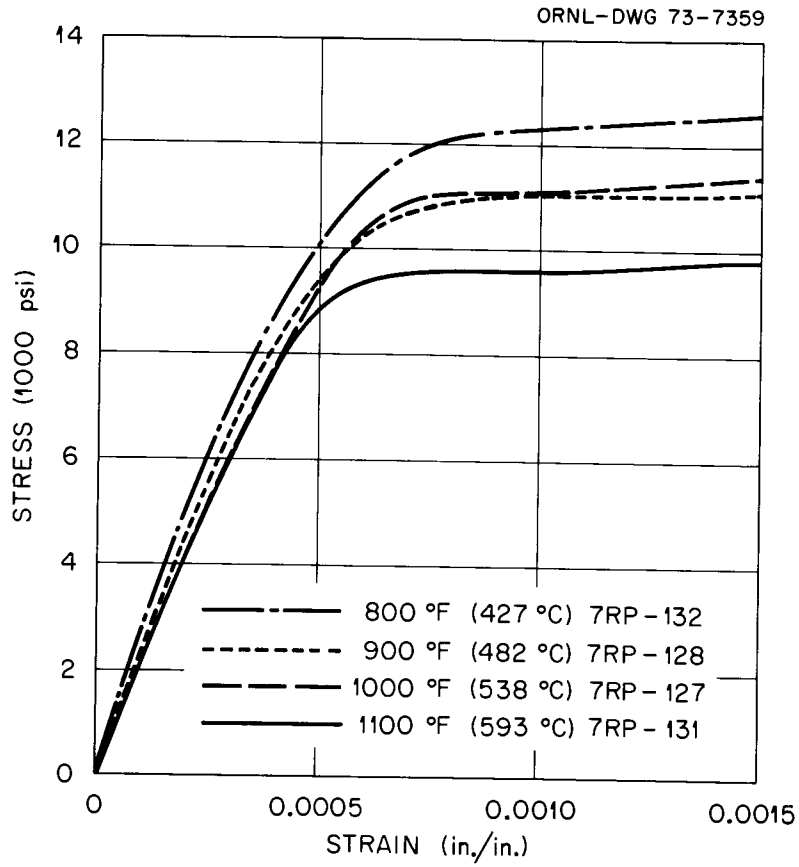

Fig. 5.52. Tensile Yield Curves for Type 304 Stainless Steel at 800, 900, 1000, and 1100°F (427, 482, 538, and 593°C). Heat 9T2796 1-in.-thick plate reannealed at 2000°F (1093°C) for 0.5 hr and tested at 0.005/min. under servo control.

strain, which is recoverable, and true microyielding, which is not recoverable. Microyielding could result from eccentric loading, residual stress due to handling of the specimens, or the movement of favorably oriented mobile dislocations. At the present time data are not sufficient to either identify the cause or quantify the stress dependence of these strains, although they do not appear to exceed the elastic components.

5.5.2.2 Creep Testing

Testing is under way to examine the influence of thermal and mechanical variables on the creep-rupture response of type 304 stainless steel (Heat 9T2796). We reported earlier[30] that the reannealing temperature was not a very important variable for the case of 1-in. plate, especially when the reannealing temperature was in the 1950 to 2050°F (1065 to 1110°C) range. Likewise, the cooling rate effect was not pronounced except for a very slow rate, which greatly improved the ductility and the rupture life.

These studies are continuing, with reduced emphasis, and two other product forms are being included. Currently, attention is being given to the influence of cyclic deformation on subsequent creep behavior at 1100°F (593°C). Several specimens reannealed at 2000°F (1093°C) were subjected to ten cycles at room temperature over a 1% strain range. This treatment raised the yield strength from a nominal 26,000 to about 34,000 psi, which is more typical of type 304 stainless steel plate in the A-240 condition. Creep tests were then initiated at 1100°F (593°C) and over the stress range from 15,000 to 35,000 psi. The results obtained to date are summarized in Fig. 5.53, where they are compared with the minimum-creep-rate and rupture-life trend curves developed from tests on reannealed material. The data suggest that small amounts of cold work do not greatly influence the subsequent steady-state minimum creep rate behavior or rupture properties. Not shown here, of course, is the significant difference in the loading strains. The reannealed material, for example, had a yield stress of about 11,000 psi at 1100°F (593°C), but the precycled material yielded near 17,500 psi. The similarity in creep properties of the two conditions may, in fact, be due to the influence of loading strains. We have seen that the "warm work," which is associated with the loading of reannealed specimens to

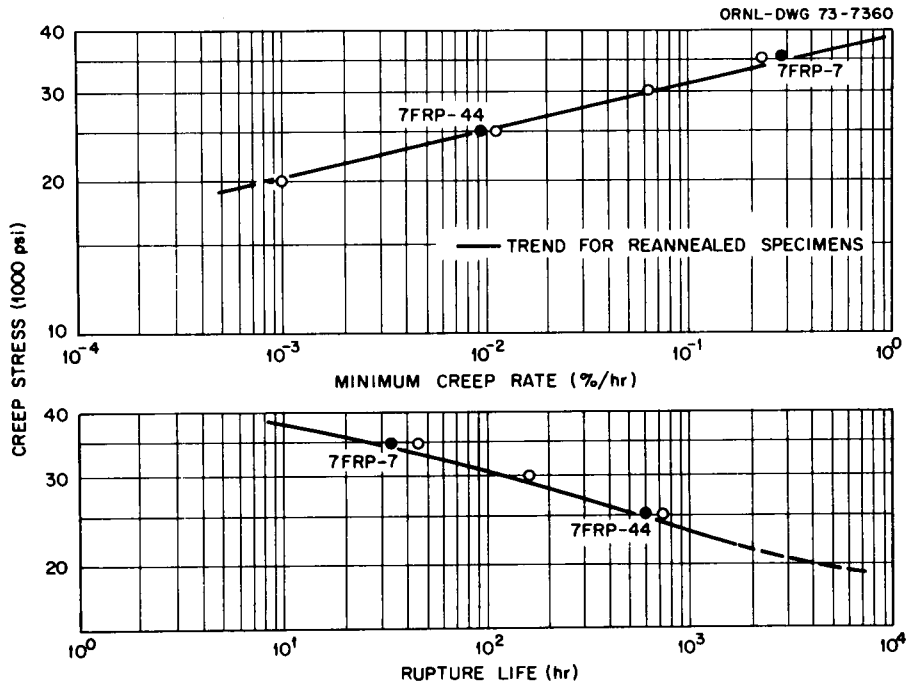

Fig. 5.53. Influence of Cyclic Deformation on the Minimum Creep Rate and Rupture Life of Type 304 Stainless Steel at 1100°F (593°C). Heat 9T2796 1-in.-thick plate reannealed at 2000°F (1093°C). Open symbols are for specimens precycled at room temperature and 1% strain range. Closed symbols are for specimens precycled at 1100°F (593°C); specimen 7FRP-7 at 2% and specimen 7FRP-44 at 0.6% strain range.

very high stresses (≧30,000 psi), actually depresses initial creep rate for a short period.[31] We have also found that large plastic strain pulses introduced during creep at a very high stress (≧30,000 psi) also depress creep for a short while. Conversely, in these present investigations small precycling strains increased the primary creep at high and intermediate stresses. Similarly, small plastic strain pulses can also accelerate creep at intermediate stresses (15,000–20,000 psi), at least for a short time.[32] Two data are included in Fig. 5.53 which show that the influence of precycling at 1100°F (593°C) is similar to precycling at room temperature.

5.5.2.3 Relaxation Testing

No relaxation tests were performed in the last quarter. The results obtained from earlier testing periods are still being studied. Some previously unreported results of interest involve multiple loadings and plots of behavior patterns at 1100°F (593°C) and are included in Fig. 5.54. The relaxation hardening was fairly gradual for this heat of type 304 stainless steel (Heat 9T2796). In other words, each reloading to the original stress, after a period of relaxation, produced a curve slightly above the previous curve. Such behavior, of course, we expected. The slow increase in the resistance to relaxation implied by these results is in qualitative agreement with the relatively slow rate of hardening that we have observed under single-stress creep conditons for this heat of type 304 stainless steel. Some checks were also made to see if relaxation rates after reloadings which included a large plastic strain (about 0.2%) were different than after small reloading plastic strains (less than 0.1%). We observed no meaningful trend. At first glance, this behavior conflicts with our previous observation, based on creep data, that plastic strain pulses accelerate creep rates for a short interval at intermediate stresses.[32]

5.5.2.4 Creep-Plasticity Testing

Our machine to study creep-plasticity interactions was placed in operation. The first testing involved a number of strain-cycling experiments to check capability relative to the servo-controlled electro-hydraulic machine. Results are summarized in Fig. 5.55, which plots the stress range against strain range for the tenth cycle at several temperatures. The performance was satisfactory, and we are now in a position to begin interspersing creep and cyclic plasticity over time periods extending to at least 2000 hr.

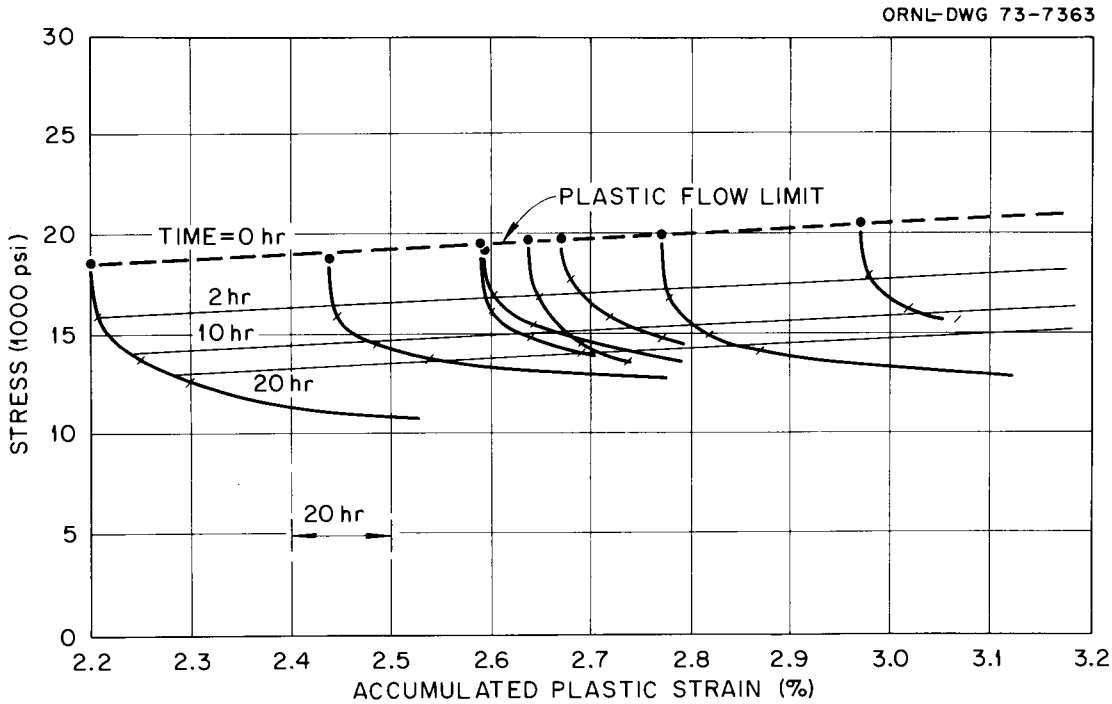

Fig. 5.54. The Influence of Repetitive Loading into the Plastic Strain Range on the Relaxation Strength of Type 304 Stainless Steel at 1100°F (593°C). Heat 9T2796 (1-in.-thick plate) reannealed at 2000°F (1093°C). Specimen 7RPT-8.

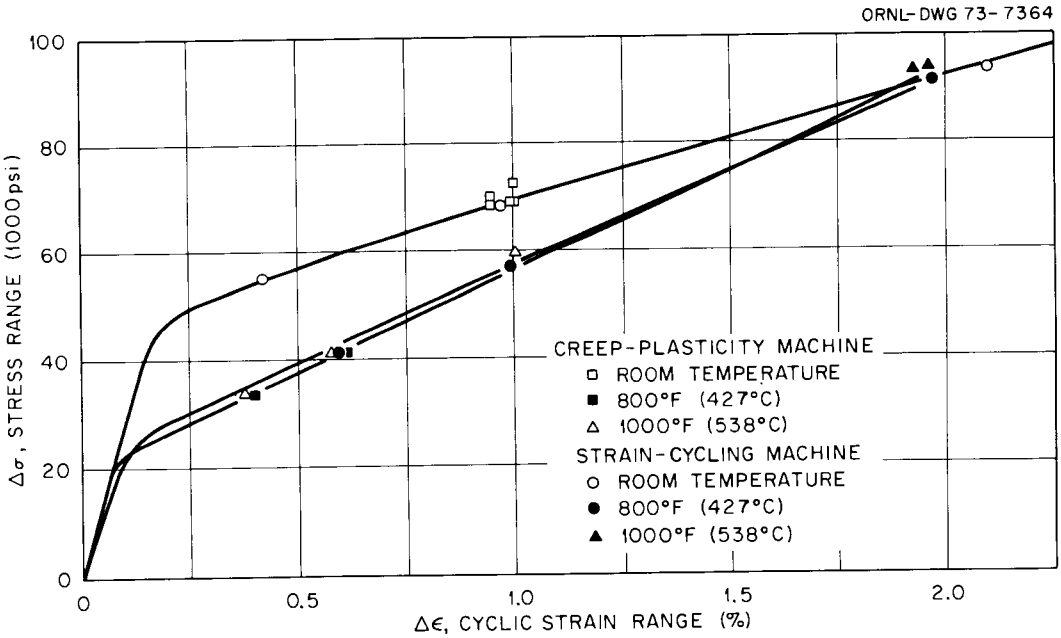

Fig. 5.55. Comparison of the Tenth Cycle Hardening Data Obtained on Different Machines for Type 304 Stainless Steel. Heat 9T2796 1-in.-thick plate reannealed at 2000°F (1093°C).

5.5.3 Investigations of Creep Failure Under Uniaxial and Multiaxial Conditions — C. C. Schultz, Babcock & Wilcox

The status of the constant load, step load, and interrupted uniaxial tests are shown in Tables 5.37, 5.38, and 5.39, respectively.

The first three specimens for the interrupted uniaxial tests (19.5 ksi) have been loaded. These tests are identified as BWI-1, BWI-2, and BWI-3. Tests BWI-1 and BWI-3 both experienced unexplained steps between the final load increment and the initial creep data point (time, 2 hr).

The initial tubular rupture specimen was loaded in simple tension. During loading an oil seal in the axial load system failed. Repairs have been made and the specimen will be reloaded, as the specimen should not have incurred damage.

Test BWC-5B (20 ksi), which was originally anticipated to rupture in 2,000 to 4,000 hr, has finally begun tertiary creep. Consideration of more recent data led to an estimate of 7,500 hr for rupture at 20 ksi.

A B & W sponsored program was initiated to rectify the apparent difference in creep strain data as obtained from the two types of testing machines being used. A threaded rupture machine specimen (9R-2A) is being tested with four DCDT's over the 2-in.-gage length and a single DCDT and dial gage over the full-load train. From the results to date, it can be concluded that the strain occurring outside of the gage length is not sufficient to explain the differences seen thus far between the two types of machines. No conclusion can be reached with respect to specimen bending, which will be the next area of consideration.

Table 5.37. Status of Uniaxial Rupture Tests — Type 304 Stainless Steel (Heat 9T2796) 593°C (1100°F)

Test No.	Specimen No.	Stress (ksi)	Total strain on loading[a] (%)	Time to secondary creep (hrs)	Minimum creep rate (%/hr)	Time to tertiary creep (hrs)	Intercept creep strain (%)	Test time[d] (hrs)	Fracture elongation[e] (%)	Reduction in area (%)
BWC-1	7-15	30	4.7					187 R	19.0	30.5
BWR-1	7-1	30	---					138 R	21.5	32.9
BWC-2	2-22	28	5.8	40	0.016	195	0.50	227 R	13.0	20.4
BWR-2	2-1	28	---	40	0.022	230	0.65	368 R	16.5	29.0
BWR-13	7-13	28	---	60	0.023	215	0.88	276 R	16.5	18.9
BWC-9	7-25	28	3.8	85	0.021		1.16	415 R	18.3	25.2
BWC-3[h]	7-28	25	3.8	80	0.0065	500	0.45	667 R	12.7	12.0
BWR-3	7-8	25	---	100	0.0079	585	0.71	948 R	17.0	23.2
BWC-4	2-28	22	3.7	175	0.0014	1,400	0.60	2,130 R	10.7	13.7
BWR-4	7-7	22	---	160	0.0030	1,170	0.72	2,026 R	12.5	16.6
BWC-5[f]	2-15	20	---					--- D		
BWC-5B	2-16	20	1.8					8,800 I		
BWR-5[i]	2-14	20	---					4,842 D		
BWR-6	7-14	19	---					9,000 I		
BWR-9	7-11	18	---					8,000 I		
BWR-11[g]	2-12	17	---					94 D		
BWR-11	2-10	17	---					8,200 I		
BWR-7	2-4	16	---					8,700 I		

[a]All specimens were step-loaded at 1.87 ksi increments, except test BWC-5B, which was step-loaded at 1.49 ksi increments. Loading curves on BWR series include load train displacements, thus not reported.

[b]Time to tertiary creep based on the 0.2% offset from the minimum rate line.

[c]Intercept creep strain does not include the elastic and initial plastic components.

[d]R = rupture; D = discontinued; I = in test.

[e]Elongation over 3 inches in BWC series; over 2 inches in BWR series.

[f]Temperature excursion to 1300°F prior to loading. Replaced by Test No. BWC-5B.

[g]Temperature excursion at 1300°F at 94 hours. Replaced by Test No. BWR-11B.

[h]Failure occurred near end of gage length.

[i]Temperature excursion to 1380°F at 4,842 hours. Terminated.

Table 5.38. Status of Uniaxial Step Load Rupture Tests — Type 304 Stainless Steel (Heat 9T2796) 593°C (1100°F)

Test No.	Specimen No.	Stress (ksi)	Total strain on loading (%)	Time to secondary creep (hrs)	Minimum creep rate (%/hr)	Time to tertiary creep[a] (hrs)	Intercept creep strain[b] (%)	Time at load[c] (hrs)	Fracture elongation[d] (%)	Reduction in area (%)
BWC-6	2-17	16						3,871		
		25						136		
		20						4,660 I		
BWR-10	2-11	16						3,871		
		25						136		
		20						4,660 I		
BWC-7	2-18	17						3,699		
		25						136		
		20						4,660 I		
BWR-8	2-5	17						3,703		
		25						136		
		20						4,660 I		
BWLF-5	2-25	20						503		
		25						198		
		20						4,050 I		
BWC-8	7-16	18						5,071		
		25						136		
		20						2,800 I		
BWR-12	7-12	18						5,071		
		25						136		
		20						2,800 I		

[a]Time to tertiary creep based on the 0.2% offset from the minimum rate line.

[b]Intercept creep strain does not include the elastic and initial plastic components.

[c]R = rupture; D = discontinued; I = in test.

[d]Elongation over 3 inches in BWC series; over 2 inches in BWR series.

Table 5.39. Status of Uniaxial Interrupted Tests — Type 304 Stainless Steel (Heat 9T2796) 593°C (1100°F)

Test No.	Specimen No.	Stress (ksi)	Time at load (hrs)
BWI-1	4-6	19.5	1,780
BWI-2	5-6	19.5	1,780
BWI-3	6-6	19.5	1,780

5.6 REFERENCES

1. H. E. McCoy, *Fuels and Materials Development Program Quart. Progr. Rep. Mar. 31, 1973,* ORNL-TM-4250, pp. 89–92.
2. R. W. Swindeman, *Fuels and Materials Development Program Quart. Progr. Rep. Dec. 31, 1972,* ORNL-TM-4105, pp. 4.19–4.35.
3. G. V. Smith, *An Evaluation of the Yield, Tensile, Creep, and Rupture Strengths of Wrought 304, 316, 321, and 347 Stainless Steels at Elevated Temperature, ASTM Data Ser. Publ.* DS 5 S2, American Society for Testing and Materials, Philadelphia, 1969.
4. L. D. Blackburn, "Isochronous Stress-Strain Curves for Austenitic Stainless Steels," pp. 15–48 in *The Generation of Isochronous Stress-Strain Curves,* ed. by A. O. Schaefer, American Society of Mechanical Engineers, New York, 1972.
5. W. L. Williams, "Parameter and Long Life Creep-Rupture Tests of Type 304 Steel," pp. 351–59, ASM Publ. D8-100, American Society for Metals, Metals Park, Ohio, 1968.
6. G. J. Lieberman and R. G. Miller, Jr., "Simultaneous Tolerance Intervals in Regression," *Biometrika* 50: 155–68 (1963).
7. Case 1331-8, *Interpretations of ASME Boiler and Pressure Vessel Code,* American Society of Mechanical Engineers, New York, 1972.
8. Letter, R. A. Moen (HEL) to P. M. Brister (Chairman ASME Subgroup on Strength) Feb. 8, 1973.
9. R. W. Swindeman and R. D. Waddell, Jr., "Characterization of the ORNL Reference Heat (No. 9T2796) of Type 304 Stainless Steel," *High-Temperature Structural Design Methods for LMFBR Components Quart. Progr. Rep. Sept. 30, 1972,* ORNL-TM-4058, pp. 137–47.
10. R. W. Swindeman, "Tensile Testing," *High-Temperature Structural Design Methods for LMFBR Components Quart. Progr. Rep. June 30, 1973,* ORNL-TM-4356 (in press).
11. C. E. Pugh et al., *Currently Recommended Constitutive Equations for Inelastic Design Analysis of FFTF Components,* ORNL-TM-3602, pp. 15–27.
12. J. H. Holloman, "Tensile Deformation," *Trans. AIME* 162: 268 (1945).
13. P. Ludwik, *Elemente der Technologischen Mechanik,* Springer, Berlin, 1970.

14. C. C. Schultz, "Investigations of Creep Failure under Uniaxial and Multiaxial Conditions," *High-Temperature Structural Design Methods for LMFBR Components Quart. Progr. Rep. Sept. 30, 1972,* ORNL-TM-4058, pp. 20–31.

15. R. W. Swindeman, "Creep Testing," *High-Temperature Structural Design Methods for LMFBR Components Quart. Progr. Rep. June 30, 1973,* ORNL-TM-4356 (in press).

16. R. W. Swindeman, "Relaxation Testing," *High-Temperature Structural Design Methods for LMFBR Components Progress Report October 1972 through March 1973,* ORNL-TM-4089, pp. 220–24.

17. C. E. Jaske, "Creep-Plasticity Interaction Tests," *High-Temperature Structural Design Methods for LMFBR Components Progress Report October 1972 through March 1973,* ORNL-TM-4089, pp. 231–39.

18. L. D. Blackburn, "Isochronous Stress-Strain Curves for Austenitic Stainless Steels," pp. 15–48 in *The Generation of Isochronous Stress-Strain Curves,* ed. by A. O. Schaefer, American Society of Mechanical Engineers, New York, 1972.

19. R. T. King, J. K. Alley, and E. Bolling, *Fuels and Materials Development Program Quart. Progr. Rep. Mar. 31, 1973,* ORNL-TM-4250, pp. 139–51.

20. A. L. Ward, Private Communication, August 1973.

21. R. L. Klueh, *Effect of Carbon on the Mechanical Properties of 2 1/4 Cr-1 Mo Steel,* ORNL-4922 (November 1972).

22. R. L. Klueh and D. A. Canonico, *Fuels and Materials Development Program Quart. Progr. Rep. June 30, 1973,* ORNL-TM-4355, pp. 25–32.

23. W. F. Simmons and J. A. Van Echo, *The Elevated-Temperature Properties of Stainless Steels, ASTM Data Ser. Publ.* DS 5-S1, American Society for Testing and Materials, Philadelphia, 1965.

24. G. V. Smith, *An Evaluation of the Yield, Tensile, Creep, and Rupture Strengths of Wrought 304, 316, 321, and 347 Stainless Steels at Elevated Temperatures, ASTM Data Ser. Publ.* DS 5 S2, American Society for Testing and Materials, Philadelphia, 1969.

25. R. W. Swindeman, Private Communication.

26. P. L. Rittenhouse, *Fuels and Materials Development Program Quart. Progr. Rep. June 30, 1973,* ORNL-TM-4355, pp. 59–68.

27. G. J. Lieberman and R. G. Miller, Jr., "Simultaneous Tolerance Intervals in Regression," *Biometrika* 50: 155–68 (1963).

28. H. E. McCoy, Jr., *Fuels and Materials Development Program Quart. Progr. Rep. Mar. 31, 1973,* ORNL-TM-4250, pp. 89–98.

29. R. W. Swindeman and R. D. Waddell, Jr., *Fuels and Materials Development Program Quart. Progr. Rep. Dec. 31, 1971,* ORNL-TM-3703, p. 195.

30. R. W. Swindeman, *Fuels and Materials Development Program Quart. Progr. Rep. Mar 31, 1973,* ORNL-TM-4250, pp. 110–23.

31. R. W. Swindeman, *Fuels and Materials Development Program Quart. Progr. Rep. Dec. 31, 1972,* ORNL-TM-4105, p. 4.26.

32. R. W. Swindeman, *High-Temperature Structural Design Methods for LMFBR Components Quart. Progr. Rep. Mar. 31, 1972,* ORNL-TM-3845, p. 95.

6. WESTINGHOUSE ADVANCED REACTORS DIVISION

E. C. Bishop

6.1 INTRODUCTION

The program being performed at Westinghouse Advanced Reactors Division is entitled "Validation of High Temperature Design Methods and Criteria," (189a No. 04165). Two of the tasks in this program are "Basic Specimen Testing" and "Tubular Specimen Testing." The objective of these tasks is to design and test specimens of increasing complexity to determine the inelastic behavior and strain tolerances of Types 304 and 316 stainless steel under complex stress distributions. This report covers the work performed during the period from June 1, 1973 to August 31, 1973.

6.2 BASIC SPECIMEN TESTING - N. Ettenson, M. Manjoine (Westinghouse Research Laboratories)

A variety of specimen designs have been selected for this task, as shown in Table 6.1. Data obtained to date are presented in Table 6.2.

6.2.1 Uniaxially Loaded Specimen Models with Uniform Gage Section (304 SS, Heat 9T2796)

6.2.1.1 Type A

The gage section is long, uniform, and rectangular. The ends of the gage length have fillets, and the area at the heads is more than five times that of the gage section. The state of stress is essentially plane over much of the gage section.

The creep rupture data for this specimen will be directly comparable with the smooth bar data generated by the ORNL program and will serve as a base line for this size plate material.

6.2.1.2 Type B

This is a plate specimen with a width to thickness ratio of 10 and a uniform gage length approximately equal to the width. A high degree of plan strain is generated at the ends of the gage length by restricting the lateral motion and minimizing the restraint in the thickness direction.

Table 6.1 Specimen Types

Specimens from Base Material

A. Plane Stress Specimen
1/3 x 2/3 x 3 in. (8.5 x 17 x 76.2 mm) gage section

B. Plate Specimen
1/3 x 10/3 x 3 in. (8.5 x 85 x 76.2 mm) gage section

C. Plate Specimen with Central Hole of 1/3 in.(8.5 mm) Diameter
1/3 x 10/3 x 3 in. (8.5 x 85 x 76.2 mm) plate section

D. Round Circumferentially Notched Specimen
Major Diameter = 0.96 in. (24.4 mm), Minor Diameter = 0.64 in. (16.2 mm)
Root Radius = 0.018 in. (0.46 mm)
Two nearly identical notches in specimen.

G. Plane Strain Specimen
1/3 x 10/3 x 1 in. (8.5 x 85 x 26 mm) gage section
Ends constrained in transverse direction.

H. Biaxially Loaded Notched Plates
Wedge-opening-loaded Plates with 1/3 in. (8.5 mm) Diameter Notch.

Specimens with Welds

BTW - B-type plate specimen with transverse weld at mid-length of gage section

BAW - B-type plate specimen with axial weld at center of gage section

CTW - C-type specimen with hole through transverse weld

CAW - C-type specimen with hole through axial weld

DTW - D-type specimen with notch root in transverse weld

DZTW - D-type specimen with notch root at weld fusion line or heat affected zone (HAZ)

GTW - G-type specimen with transverse weld at mid-gage length

GAW - G-type specimen with axial weld at center of gage section

Table 6.2 Summary of Creep Data, Type 304 Stainless Steel at 1100°F

Test No. (Gage Section)	Loading Data: Stress (ksi)	Stress (MPa)	Plastic Strain (%)	Creep Data: Creep Rate (%/hr)	Increment: Strain (%)	Increment: Time (hr)	Accumulated: Strain (%)	Accumulated: Time (hr)	Permanent Strain (%)
A1	21.0	144.8	4.66	2.2×10^{-3}	1.10	303	1.10	303[a]	5.76
(1/3 x 2/3 x 3 in.)				2.2×10^{-3}	0.89	403	1.99	706[a]	6.65
(8.5 x 17 x 76.2 mm)							3.47	1250[b]	8.13
							3.65	1270[c]	8.31
								1826[d]	12.0[d]
A2	10.0	68.95	0.215	8.5×10^{-5}	0.228	2180	0.228	2180[a]	0.443
(1/3 x 2/3 x 3 in.)				6.2×10^{-5}	0.028	405	0.256	2585[e]	0.471
(8.5 x 17 x 76.2 mm)	11.0	75.84	0	8.6×10^{-5}	0.124	1349	0.380	3934[e]	0.595
	12.5	85.68	0	2.0×10^{-4}	0.213	1002	0.593	4936[e]	0.808
	15.0	103.4	0.014	2.5×10^{-4}	0.811	1848	1.404[a]	6784[e]	1.619
	21.0	144.8	0.646	4.5×10^{-3}	28.75	4266	30.15	11050[h]	31.01
B1	21.0	144.8	5.34	1.4×10^{-3}	1.76	666	1.76	666[a]	7.10
(1/3 x 10/3 x 3 in.)				8.8×10^{-4}	1.03	1005	2.79	1671[a]	
(8.5 x 85 x 76.2 mm)				1.7×10^{-3}				3000[c]	
					1.72	1587	4.51	3258[a]	9.85[g]
								3525[h]	
B2	10.0	68.95	0.273[i]	8.6×10^{-5}	0.31	1644	0.31	1644[a]	0.58
(1/3 x 10/3 x 3 in.)	j			9.0×10^{-5}	0.17	1462	0.45	3106[e]	0.72
(8.5 x 85 x 76.2 mm)	11.0	75.84	0	1.1×10^{-4}	0.16	1804	0.61	4910[e]	0.88
	12.5	85.68	0	2.0×10^{-4}	0.33	1364	0.94	6274[e]	1.21
	15.0	103.4	0.051	4.7×10^{-4}	1.0	1302[a]	1.93	7576[e]	1.98
	21.0	144.8	1.88	8.2×10^{-3}	16.33	1563	18.26	9139[h]	20.19
	23.3	160.5	8[n]		1.7[n]	100[c]			
C1							22.9[n]	138[d]	
(1/3 x 10/3 x 3 in.)									
(8.5 x 85 x 76.2 mm)									
CENTRAL HOLE									
1/3 in. (8.5 mm) Dia.									
C2	10.0[k]	68.95	0.14[n]		0.62[n]	2808[a]	0.62[n]	2808[e]	
(1/3 x 10/3 x 3 in.)	11.0[k]	75.84	0		0.4[n]	1290	1.02[n]	4098[e]	
(8.5 x 85 x 76.2 mm)	12.5	85.68	0		0.5[n]	1360[a]	1.5[n]	5398[e]	
CENTRAL HOLE	15.0	103.4	0.27[n]		0.82[n]	1148	2.39[n]	6546[e]	
1/3 in. (8.5 mm) Dia.	18.0	124.5	0.06[n]		3.31[n]	1630[a]	5.7[n]	8176	
						f			

[*] HT 9T2796, annealed 2000F(1094C)

[a] Interrupted for photographic measurement

[b] Transition at 0.2% OFFSET

[c] Transition at double minimum rate

[d] Rupture, R

[e] Stress raised (step-loaded test)

[f] Test in progress

[g] Crack initiated

[h] Test terminiated, Crack Tearing

[i] Strain gage average, bending noted

[j] Specimen rotated 180° to investigate bending

[k] Net Section Stress, Gross Section stress = 0.9 N.S.S.

[l] Data & fracture bending analyzed

[m] Average strain at central hole

[n] Average overall strain

[p] Test in preparation

[q] Specimen to be sectioned to determine damage at 78% of estimated rupture life

[r] Deflection of notch, inches (25.4 mm)

[t] True strain = ln(Ao/A)

Table 6.2 (Continued)

Test No. (Gage Section)	Loading Data: Stress (ksi)	Stress (MPa)	Plastic Strain (%)	Creep Data: Creep Rate (%/hr)	Increment: Strain (%)	Increment: Time (hr)	Accumulated: Strain (%)	Accumulated: Time (hr)	Permanent Strain (%)
C3	21.0[k]	144.8	4.4[n]		1.5[n]	325[c]			
(same as above)							4.1[n]	397[h]	8.5[n]
Notched Round									
D = 0.96 in (24.4 mm),									
d = 0.64 in (16.2 mm),									
R = 0.019 in (0.46 mm)									
D1-1	30.0	206.8	2.6[t]		0.3[t]	137	0.3[t]	137	2.9[t]
					0.2[t]	102	0.5[t]	239[g]	3.1[t]
D1-2	30.0		2.2[t]		0.26[t]	137	0.26[t]	137	2.46[t]
					0.22[t]	113	0.48[t]	250[c]	2.68[t]
							10.92[t]	305R[d]	13.12[t]
D2-1	25.0	172.4	0.009[r]				0.006[r]	1371	0.015[r]
								1371[g]	2.17[t]
D2-2	25.0		0.009[r]				0.006[r]	1240[c]	
								1371[d]	5.3[t]
D3	21.0	144.8	0.002[r]					4100[f]	
D4	10.0	68.95	0			406		406[e]	
	11.0	75.84	0			477		883[e]	
	12.5	85.68	0			434		1317[e]	
	15.0	103.4	0			404		1721[e]	
	21.0	144.8	0.001[r]			433		2154[e]	
	25.0	172.4	0.003[r]			1581		3735[a]	
D5	23.0	162.4	0			800[f]		800[f]	
G2	21.0	144.8	0.43	3.9×10^{-4}	1.34	1195[a]	1.34	1195	1.77
			0	1.2×10^{-4}	0.83	5520[a]	2.17	6715[e]	2.6
	25.0	172.4	0.01			f			
BAW1	25.0	172.4	0.25		4.35	477[a]	4.35	477[a]	
					5.04	476[a]	9.39	953[a]	9.64

*HT 9T2796, annealed 2000F(1094C)

[a]Interrupted for photographic measurement

[b]Transition at 0.2% OFFSET

[c]Transition at double minimum rate

[d]Rupture, R

[e]Stress raised (step-loaded test)

[f]Test in progress

[g]Crack initiated

[h]Test terminiated, Crack Tearing

[i]Strain gage average, bending noted

[j]Specimen rotated 180° to investigate bending

[k]Net Section Stress, Gross Section stress = 0.9 N.S.S.

[ℓ]Data & fracture bending analyzed

[m]Average strain at central hole

[n]Average overall strain

[p]Test in preparation

[q]Specimen to be sectioned to determine damage at 78% of estimated rupture life

[r]Deflection of notch,inches (25.4 mm)

[t]True strain = ln(Ao/A)

Therefore, the transverse stress will be greatest at the ends and will diminish toward the center of the gage length. This stress will increase with increasing plastic flow.

6.2.1.3 Type G

To achieve a high degree of plane strain over the gage section, the G specimen has a shorter gage length than for the Type B specimen. The ratio of the biaxial stress (transverse to axial) for the Type B specimen approached 0.5 with increasing plastic strain. The ratio of the Mises Effective Stress to the maximum principal stress approached 0.86. The flow and rupture characteristics of specimens A, B, and G will be compared and an evaluation made of the relative damage for the biaxial stress states.

6.2.1.4 Current Results

Tests A-1, A-2, B-1, and B-2 have been completed and the results are being evaluated. The test of G2 loaded to 21 ksi has been in progress for 6692 hours.

A damage evaluation given in Table 6.3 is based on a linear damage rule using the ORNL data as a base for rupture. The values of damage for these uniform gage section specimen vary by a factor of over 4 and a factor of 2 above and below the reference data. This damage rule does not adequately describe the damage mechanisms. Therefore, another rule is proposed; i.e.,

$$\text{Damage} = A\sum\left(\frac{t_i}{t_{r_i}}\right)_{\sigma 1,\ \tau} + B\sum\left(\frac{\varepsilon_i}{\varepsilon_{L_i}}\right)_{\dot{\varepsilon},T,T.F}.$$

The first term is based on the time at a given maximum principal stress and the second term relates the strain at a given strain rate to a strain limit at that strain rate. This strain limit depends on the strain rate, temperature, and triaxiallity factor, T.F., which is a function of the principle and effective stresses. Data from the uniform and the other types of specimen models are being analyzed to describe the strain limit, ε_L.

Table 6.3 Damage Calculations for Type 304 Stainless Steel[a]
Temperature 1100°F (593°C)

Specimen	Stress[b] (ksi)	Stress[b] (MPa)	Δt_i (h)	t_{r_i} (h)	$\frac{\Delta T_i}{t_{r_i}}$	Damage $\sum \frac{\Delta ti}{t_{r_i}}$
A1	21.0	144.8	1826	$3x10^3$	0.61	0.61
A2	10.0	68.95	2585	10^6	0.003	----
	11.0	75.84	1349	$6.5x10^5$	0.002	----
	12.5	85.68	1002	$3.3x10^5$	0.003	----
	15.0	103.4	1848	10^5	0.018	0.026
	21.0	144.8	4266	$3x10^3$	1.422	1.448
B1	21.0	144.8	3525	$3x10^3$	1.17	1.17
B2	10.0	68.95	3106	10^6	0.003	----
	11.0	75.84	1804	$6.5x10^5$	0.003	----
	12.5	85.68	1364	$3.3x10^5$	0.004	----
	15.0	103.4	1302	10^5	0.013	0.023
	21.0	144.8	1563	$3x10^3$	0.521	0.544
G2	21.0	144.8	6715	$3x10^3$	2.24	2.24
	25.0	172.4	(c)	----	----	(c)

(a) Rupture life, t_r, based on ORNL data for HT9T2796 annealed 2000°F (1094°C)

(b) Net section stress = P/Ao

(c) Test in progress

6.2.2 Specimens With Welds (304 SS, Heat 9T2796)

In a letter dated March 26, 1973, ORNL proposed a test matrix for uniaxial tensile, creep, and creep-rupture tests on weldments to aid in analysis of the basic plate specimens. It was understood that the uniaxial tests will be performed by ORNL.

ARD concurred with the test conditions and types of test specimens proposed. However, the number of uniaxial tests can be reduced considerably. The following test matrix was proposed and summarized in Tables 6.4 and 6.5.

Table 6.4 Nominally-Constant-Strain-Rate Tensile Tests For Weldment Characterization at 1100°F

Strain Rate (in./in./min.)	Specimens to be Tested[a]
5×10^{-2}	LWM
5×10^{-3}	LWM, LWM, LWM_I, LWM_{II}, LWM_{III}, TWM, LPM

Table 6.5 Creep Tests for Characterization of Plate Weldments at 1100°F

Test No.	Specimen Type[a]	Stress (psi)	Expected Test Duration (hours)	Priority Ranking
1-2	LWM, LWM_I, LWM_{II}, LWM_{III}	32	100	1
1-3	LWM	28	500	1
1-4	LWM	25	2000	1
1-5	LWM, LWM_{II}	20	2500	1
1-6	LWM	15	2500	1
2-2	TWM, TWM_{II}	32	100	2
2-4	TWM	25	2000	2
2-5	TWM	20	2500	2
2-6	TWM	15	2500	2
3-4	LPM	25		3
3-5	LPM	20		3

(a) LWM-longitudinal weld metal
TWM-transverse weld metal
LPM-longitudinal parent metal

I-centerline .12 below surface
II-centerline .25 below surface
III-centerline .37 below surface

It was recommended that the tensile tests be reduced from 13 to 8. Tests at strain rates of 2.5×10^{-1}/min. and 5×10^{-4}/min. can be eliminated because of negligible sensitivity to rate in this range. A single test was proposed as a checkpoint at the strain rate (5×10^{-2}/min) nominally used by Westinghouse in the loading of the basic specimens.

It was proposed that many of the TWM specimens be eliminated because of the complexity of the sample and difficulty in interpretation of the results. Although it was desirable to have properties in the transverse direction, it was not clear at this point how the data from the TWM tests would be utilized. Thus, it was recommended that the TWM tensile test be performed early in the test sequence, and if the results proved to be interpretable, additional TWM test specimens would be added to the test matrix. Accordingly, provision would be made for additional test specimens.

The creep tests recommended in Table 6.5 were reduced in number from 27 to 16. This reduction stems from 1) elimination of the 35 ksi tests because the results would be affected by plastic deformation during loading, 2) elimination of some of the TWM specimens, and 3) elimination of most of the LPM specimens as non-essential.

The above comments were submitted in fulfillment of the commitment made at the RRD-ORNL-ARD meeting at ARD on July 18-19, 1973.

6.3 TUBULAR SPECIMEN TESTING - K. C. Thomas, P. C. S. Wu

6.3.1 Uniaxial Creep Testing (304 SS, Heat 9T2796 ORNL Reference Heat)

A uniaxial creep test matrix for tubular specimens of Type 304 stainless steel was completed and the data were analyzed to compare with the Blackburn equation and the ORNL creep law. The results showed that the Blackburn constants and ORNL constants do not represent the experimental data. An additional test at 1100°F and a stress level of 7,700 psi was initiated to provide an additional datum point for analysis. This specimen, test No. 3C, has accumulated a total strain of 0.095 percent after 1682 hours with a creep strain of 0.049 percent and an initial loading strain of 0.046 percent. The percentage creep as a function of time for this test is shown in Figure 6.1.

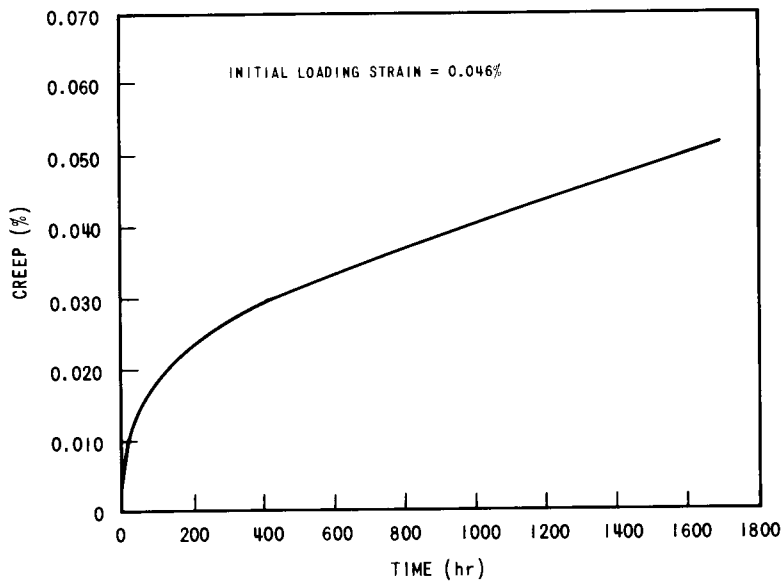

Figure 6.1 Axial Strain of Type 304 Stainless Steel Tube at 1100°F and 7,700 psi Axial Stress. Heat 9T2796 (ORNL Reference Heat)

6.3.2 Multiaxial Creep Testing (304 SS, Heat 9T2796 ORNL Reference Heat)

The "Argon Pressurizing Unit" for the multiaxial creep tests has been installed and pressure tested at 1.25 times the maximum working pressure.

Multiaxial creep tests were initiated early this quarter. The test conditions for the multiaxial creep test are shown in Table 6.6 and milestones during the present fiscal year are listed in Table 6.7. The test set-up and the arrangement of strain measuring devices are shown in Figure 6.2. The strains are indicated on the displacement meters shown in Figure 6.3. The test temperature is controlled by the equipment shown in the same figure.

Two multiaxial creep tests are being performed. Test No. 5 was to be run at 1100°F and an internal pressure of 1814 psi but during a check of the temperature after 45 hours, using a calibrated potentiometer, it was observed that the temperature was actually at 1115°F. Procedures have been taken to minimize such malfunctioning of the temperature recorder within the calibration period. The test will continue at 1115°F. Preliminary results obtained from this test are shown in Figure 6.4 and 6.5. The multiaxial creep test No. 4 was interrupted after the diametral strain measuring system malfunctioned. After making an adjustment, the system

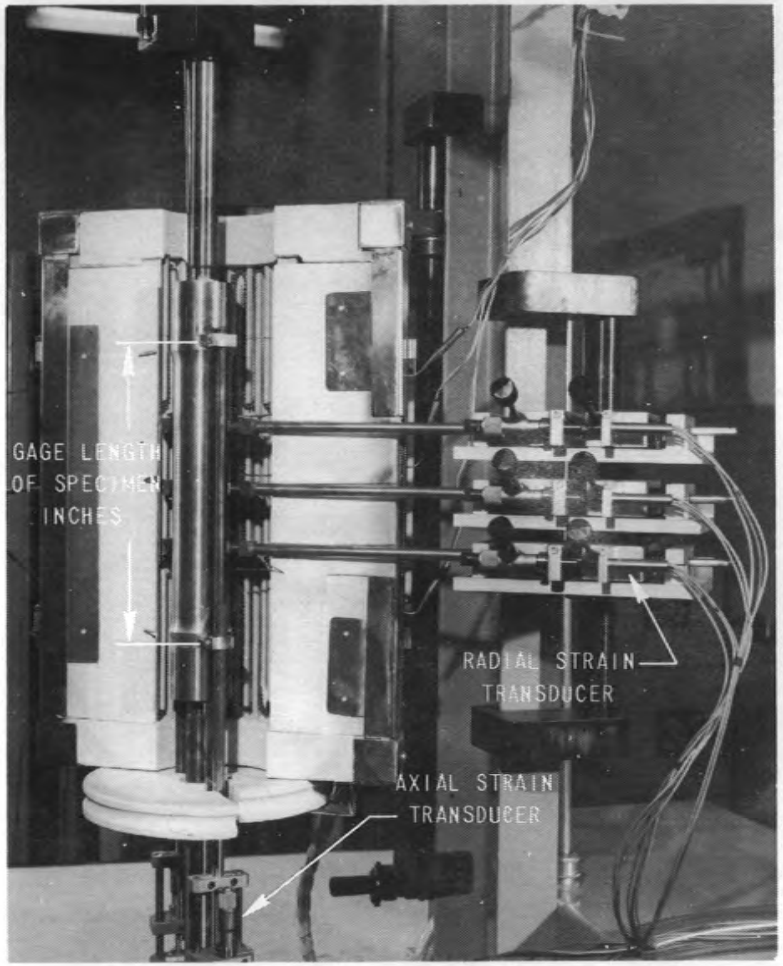

Figure 6.2 Sample Arrangement and the Capacitive Type (SLVC) Strain Measuring System

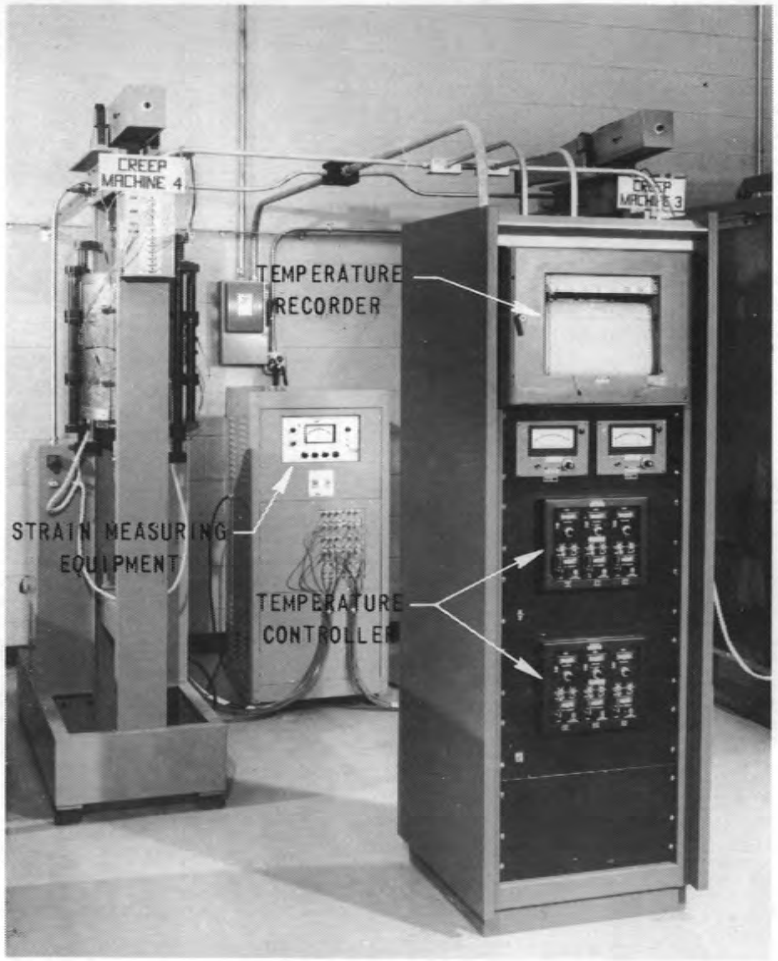

Figure 6.3 Test Assembly and the Temperature Control and Strain Measuring Systems

Table 6.6 Test Loads for Multiaxial Tubular Specimens of Type 304 Stainless Steel

Test No.	Effective Stress @ Inner Surf.	Press. (psi)	Axial (#)	Spec. Surface	Stress Ratio, σ_2/σ_1	Total Stresses (psi)			
						σ_1	σ_2	σ_3	σ_e
4	10,000	1209.5	323	Inside	2.0	5,158	10,316	-1209.5	10,000
				Mid	1.872	5,158	9,658	- 551.15	8,862
				Outside	1.766	5,158	9,107	0	7,910
5	15,000	1814.3	484	Inside	2.0	7,737.5	15,475	-1814.3	15,000
				Mid	1.872	7,737.5	15,487	- 827.3	13,294
				Outside	1.766	7,737.5	13,661	0	11,865
6	20,000	2419	646	Inside	2.0	10,316.5	20,633	-2419	20,000
				Mid	1.872	10,316.5	19,316	-1103	17,725
				Outside	1.766	10,316.5	18,214	0	15,820
7	10,000	1180	1211	Inside	1.5	6,710	10,065	-1180	10,000
				Mid	1.404	6,710	9,422	- 538	8,919
				Outside	1.324	6,710	8,885	0	8,022
8	15,000	1770	1816.5	Inside	1.5	10,065	15,097	-1770	15,000
				Mid	1.404	10,065	14,133	- 807	13,379
				Outside	1.324	10,065	13,327	0	12,033
9	20,000	2360	2422	Inside	1.5	13,420	20,130	-2360	20,000
				Mid	1.404	13,420	18,845	-1076	17,838
				Outside	1.324	13,420	17,769	0	16,043
10	10,000	1049.4	2670	Inside	1.0	8,951	8,951	-1049.4	10,000
				Mid	0.936	8,951	8,379	- 478.5	9,157
				Outside	0.883	8,951	7,901	0	8,475
11	15,000	1574.0	4005	Inside	1.0	13,425	13,425	-1574	15,000
				Mid	0.936	13,425	12,568	- 718	13,736
				Outside	0.883	13,425	11,851	0	12,713
12	20,000	2098.8	5341	Inside	1.0	17,902	17,902	-2098.8	20,000
				Mid	0.936	17,902	16,759	- 957	18,314
				Outside	0.883	17,902	15,803	0	16,950

Table 6.7 Tubular Testing Milestone for Fiscal Year 1974

	July	Aug.	Sept.	Oct.	Nov.	Dec.	Jan.	Feb.	March	April	May	June
Test Planning	▽1			▽2								
Design and fabricate test models	▽3			▽4	▽5	▽		▽7	▽8		▽9	
Design and fabricate test setup	▽10	▽11			▽12							
Test preparation	▽13 ▽14	▽15										
Testing	▽16			▽17	▽18	▽19		▽20	▽21 ▽22	▽23	▽24	25 ▽ 26 ▽
Analysis				▽27								▽28

MILESTONES:

1. Complete the revised test plan and confirm the load for the multiaxial tubular tests
2. Complete the revised test plan for the 3 step load tests
3. Complete fabrication of 9 304 SS models
4. Fabricate 2 additional 304 SS models
5. Complete 2 additional 304 SS test models
6. Initiate fabrication of models for the 3 step load tests
7. Complete 3 step load test models
8. Initiate fabrication of 316 SS test models
9. Complete 316 SS test models
10. Complete design of two multiaxial test setup
11. Initiate fabrication of 2 additional multiaxial test setup
12. Complete fabrication of 2 additional multiaxial test setup
13. Initiate preparation of first 2 models for testing
14. Complete preparation of first 2 models for testing
15. Complete preparation of models for testing
16. Initiate multiaxial test 1 and 2
17. Complete multiaxial test 1 and 2
18. Initiate multiaxial test 1 and 2
19. Initiate multiaxial test 5 and 6
20. Complete multiaxial test 3 and 4
21. Initiate multiaxial test 7 and 8
22. Complete multiaxial test 5 and 6
23. Initiate multiaxial test 9
24. Complete multiaxial test 7 and 8
25. Complete multiaxial test 9
26. Initiate 3 step load test
27. Initiate analysis on the multiaxial tests
28. Complete analysis on the multiaxial tests

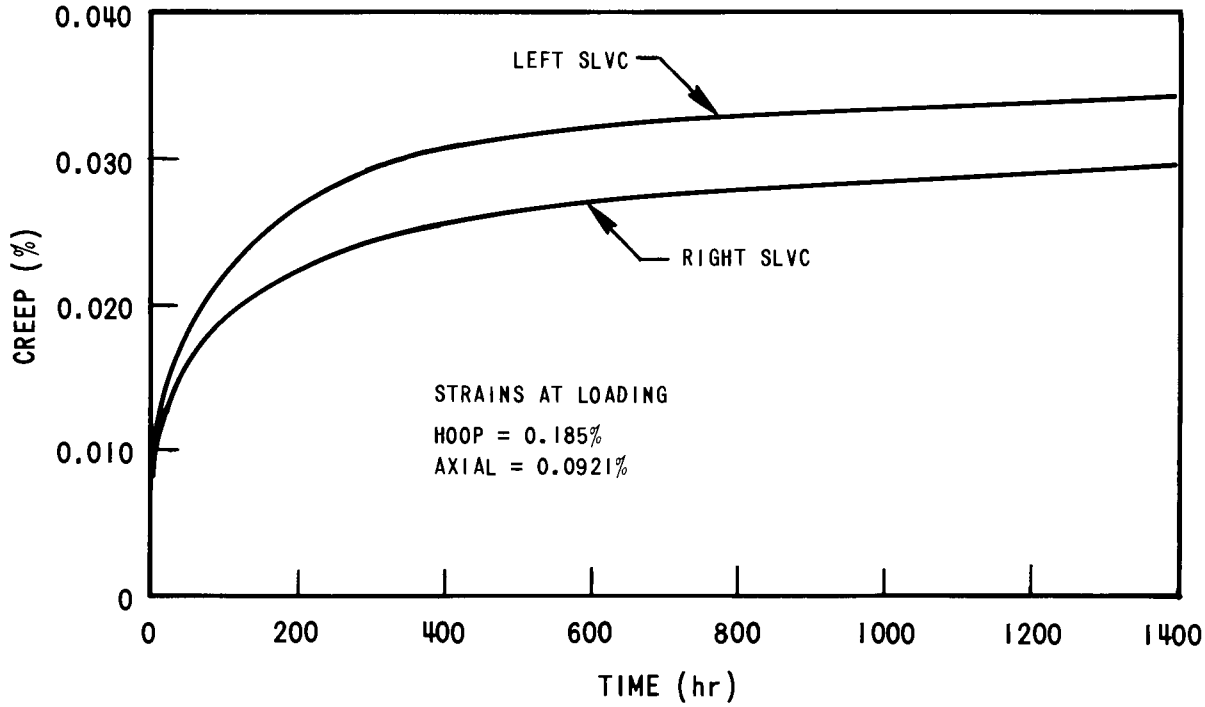

Figure 6.4 Axial Creep Strains Measured for Test No. 5 at 15,000 psi Effective Stress and 1150°F

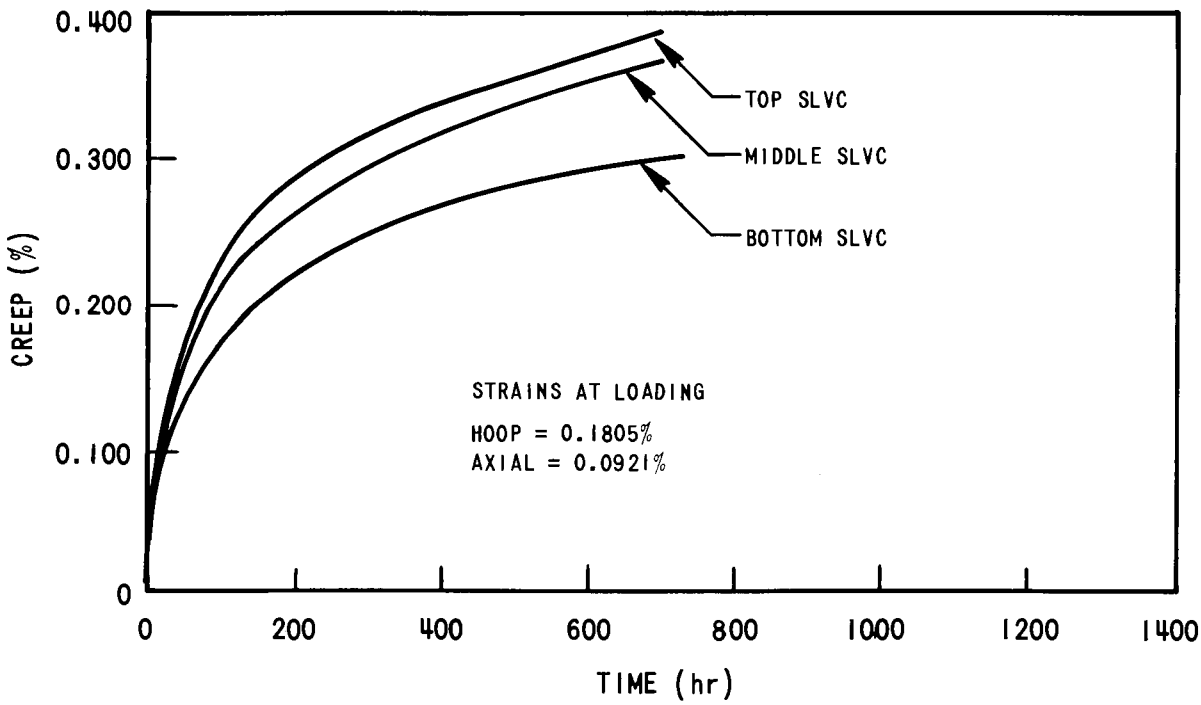

Figure 6.5 Diametral Creep Strains Measured for Test No. 5 at 15,000 psi Effective Stress and 1150°F

6049-5,6

has been operating successfully for the substitute test No. 4-A. The axial and diametral creep strains obtained in this test are shown in Figure 6.6 and 6.7. The reason for the discontinuity in Figure 6.7 is unknown at the present time. The dashed line represent the repositioning of the data obtained from the top transducer after 220 hours and is justified because the test is in the secondary creep range. Analysis of the test results will be performed during the next reporting period.

The third multiaxial creep test, Number 7, is being set up. This specimen will be tested at 1100°F and 1180 psi internal pressure. The strains will be measured by the LVDT displacement measuring devices. The test set up and the arrangement of the strain measuring systems are shown in Figure 6.8. Another multiaxial creep test, Number 10, with similar strain measuring equipment, will be initiated after the completion of the uniaxial creep test, Number 3-C, at 7,700 psi stress level.

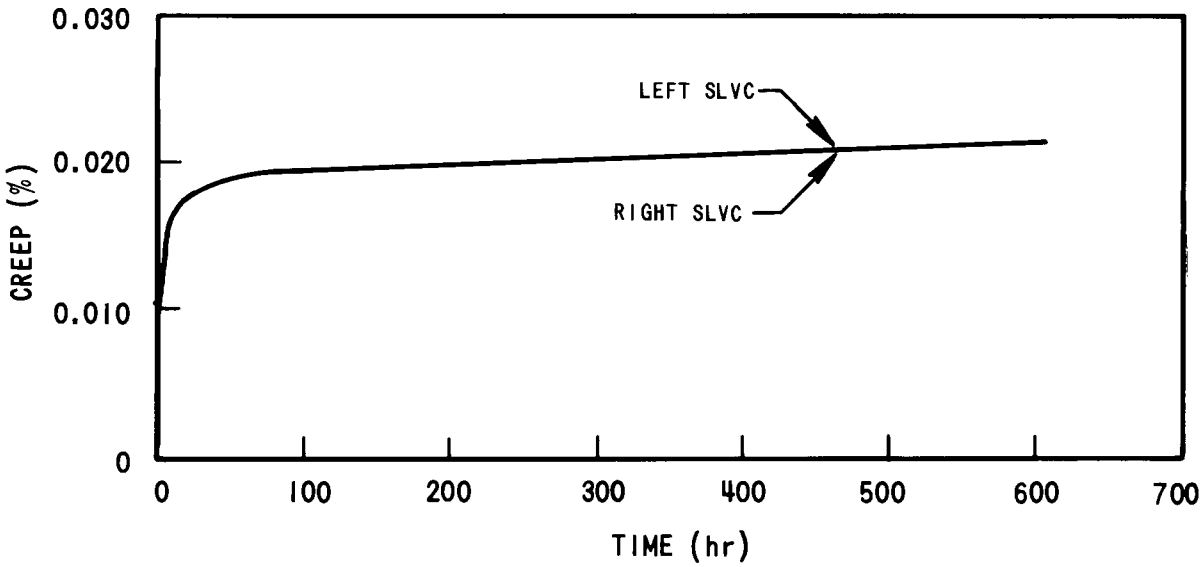

Figure 6.6 Axial Strain Measured for Test No. 4-A at 10,000 psi Effective Stress and 1100°F

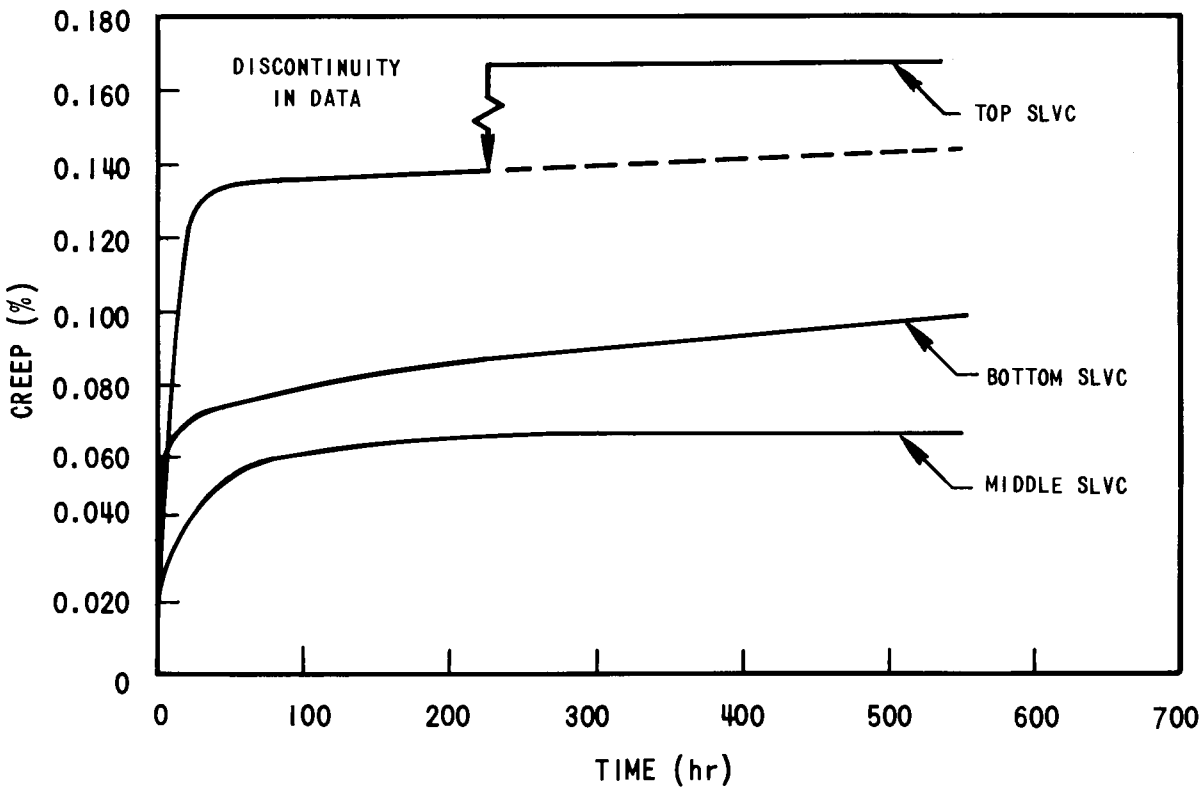

Figure 6.7 Diametral Creep Strains Measured for Test No. 4-A at 10,000 psi Effective Stress and 1100°F

6049-7,8

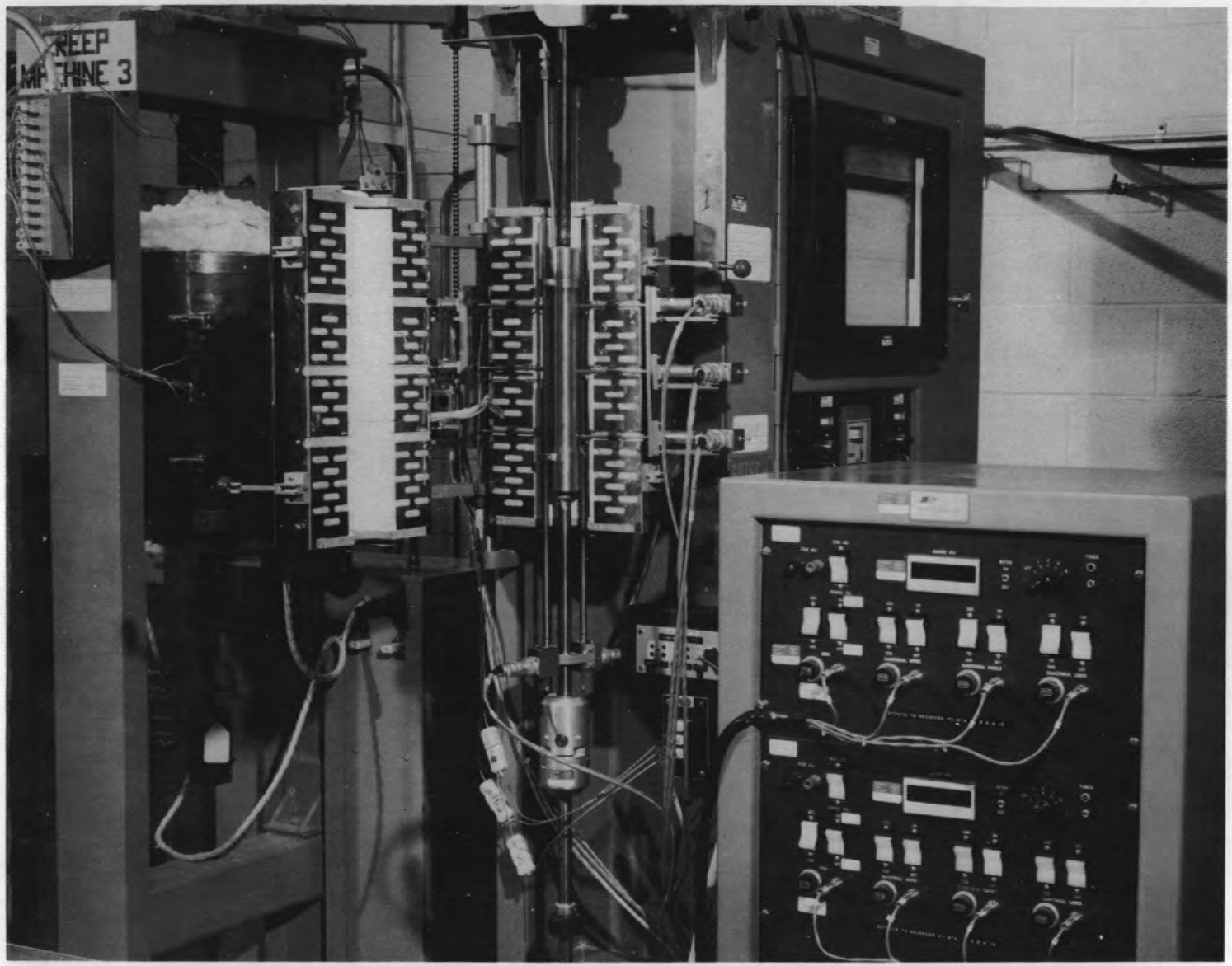

Figure 6.8 Sample Arrangement and the LVDT Strain Measuring System

INDEX

Test	Material	Page
Chemical Analysis Data		
	type 304 SS	37,40,49,52, 95,108,140 171
	type 304L SS	52
	type 316 SS	32,52,130
	type 316L SS	52
	type 308 SS S/A weld	49,52
	type 308 SS SMA weld	52,141
	type 316 SS S/A weld	52
	type 316 SS SMA weld	134
	NiCrMo plates, forgings, and weld deposits	63
Creep Test Data		
Base-Line Data		
	type 304 SS	81—89,104—107,113,123—125,168—174, 176—178,180—183
	type 316 SS SMA weld metal . .	133—139
	2 1/4 Cr-1 Mo steel	152—154
Correlations		
	type 304 SS	111—118
	2 1/4 Cr-1 Mo steel	160—169
Effect of Aging		
	type 308 SS SMA weld metal . .	145—152
Effect of Environment		
	type 316 SS	30—32
Effect of Test Temperature		
	type 316 SS	30—32
Fatigue Test Data		
Cyclic Fatigue Test Data		

Test	Material	Page
Correlations		
	type 304 SS	24–30
Effect of Heat Treatment		
	type 304 SS	16–18
	Inconel 718	7,8
Effect of Hold Time		
	type 304 SS	20–23,127, 128,174–176, 178,179
	Inconel 718	6–8
	type 304/308 SS welds	2–5
Effect of Irradiation		
	type 304/308 SS welds	3–5
Effect of Mean Strain		
	type 304 SS	21,22
Effect of Strain Range		
	type 304 SS	16–18,23
	type 316 SS	23,24
	type 304/308 SS welds	3
Effect of Strain Rate		
	type 304 SS	19,20
	Inconel 718	8,9
Effect of Stress Amplitude		
	type 304 SS	23,24
	type 316 SS	23,24
Effect of Test Temperature		
	type 304 SS	17,18,23
	Inconel 718	6–9
Crack Growth Rate Data		
Correlations		
	type 304 SS (J-integral)	46–51
	type 308 SS weld metal (J-integral)	46–51
Effect of Cold Work		
	type 304 SS	37–43

Test	Material	Page
Effect of Environment		
	type 304 SS	38,45
Effect of Stress Intensity Factor ΔK		
	type 304 SS	38–40
Effect of Test Temperature		
	type 304 SS	37–44
Impact Test Data		
Effect of Aging		
	type 304 SS	55–57,61
	type 316 SS	55,58,61
	type 308 SS weld metal	55–57,59,61
	type 316 SS weld metal	55,58,61
	NiCrMo welds with 2 1/4 Ni-Mn-Mo and 2 1/4 Cr-1 Mo-Ni filter metal	66,72,75
Effect of Cold Work		
	type 304 SS	47,50,51
Effect of Irradiation		
	type 304 SS	55,56,57
	type 316 SS	55,58
	type 308 SS SA weld metal	55,56
	type 316 SS weld metal	55,58
Effect of Test Temperature		
	NiCrMo forgings	68,75
	NiCrMo plate	66,67
	NiCrMo welds with 2 1/4 Ni-Mn-Mo, 2 1/4 Cr-1 Mo Ni, and 2 1/4 Cr-1 Mo filler	69,71–75
	type 304 SS	55–57,60
	type 304L SS	60
	type 316 SS	55,58,60
	type 316L SS	60
	type 308 SS weld metal	55–57
	type 316 SS weld metal	55,58
	Inconel 718	8,9

Test	Material	Page
	Inconel 718 GTAW weldments . .	10
Stress Relaxation Data		
	type 304 SS	125,126,178
Tensile Test Data		
Base-Line Data		
	type 304 SS	96–107,168–170
	type 316 SS	129–132
Correlations		
	2 1/4 Cr-1 Mo steel	158–161, 166–167
Effect of Aging		
	type 308 SS SMA weld metal . .	145–150
Effect of Cold Work		
	type 304 SS	40
Effect of Heat Treatment		
	type 304 SS	96–107
	type 316 SS	129,132
	2 1/4 Cr-1 Mo steel	152–154
Effect of Irradiation		
	type 304 SS	49
Effect of Strain Rate		
	type 304 SS	88–94
Effect of Test Temperature		
	type 304 SS	49,88–94, 107–112,117–122,175
	type 304 SS forging with type 308 SS overlay	154–158
	type 316 SS	129–132
	type 308 SS S/A weld	49,59
	type 308 SS SMA weld metal . .	142–145
	type 316 SS SMA weld metal . .	133–135

ORNL-4936
UC-79b, -h, -k
(Liquid Metal Fast
Breeder Reactors)

INTERNAL DISTRIBUTION

(3) Central Research Library
ORNL — Y-12 Technical Library
Document Reference Section
(10) Laboratory Records Department
Laboratory Records, ORNL RC
ORNL Patent Office
G. M. Adamson, Jr.
M. Bender
R. G. Berggren
C. R. Brinkman
D. A. Canonico
J. Corum
F. L. Culler
J. E. Cunningham
J. H. DeVan
R. G. Donnelly
G. Fee
M. H. Fontana
W. R. Gall
B. L. Greenstreet
W. O. Harms
(5) M. R. Hill
D. O. Hobson
F. J. Homan
P. R. Kasten
R. T. King
R. L. Klueh
A. L. Lotts
R. E. MacPherson
(20) W. R. Martin
C. L. Matthews
H. E. McCoy
H. C. McCurdy
W. T. McDuffee
C. J. McHargue
P. Patriarca
S. Peterson
H. Postma
C. E. Pugh
P. L. Rittenhouse
A. C. Schaffhauser
J. L. Scott
G. M. Slaughter
W. J. Stelzman
J. O. Stiegler
R. W. Swindeman
D. B. Trauger
W. E. Unger
T. N. Washburn
J. R. Weir, Jr.
G. D. Whitman
J. W. Woods
R. G. Wymer
T. Yahr

Subcontractors and Consultants

Atomic International, P.O. Box 309, Canoga Park, CA 91304

R. I. Jetter
A. Little
J. Shively

Babcock & Wilcox Company, P.O. Box 835, Alliance, OH 44601

W. E. Leyda
C. C. Schultz
D. B. Van Fossen

Battelle Memorial Institute, 505 King Avenue, Columbus, OH 43201

C. E. Jaske
E. C. Rodabaugh
G. H. Workman

Brown University, Providence, RI 02912

W. N. Findley

The Catholic University of America, Washington, DC 20017

A. J. Durelli

Combustion Engineering, Inc., 911 West Main Streeet, Chattanooga, TN 37401

T. Cullen
T. Ward

Cornell University, Department of Material Science and Engineering, Ithaca, NY 14850

G. V. Smith

E. P. Esztergar, 7993 Prospect Place, La Jolla, CA 92037

Foster Wheeler Corporation, Nuclear Department, 110 South Orange Avenue, Livingston, NJ 07039

W. R. Apblett, Jr.
R. Barratt

Franklin Institute Research Laboratories, The Benjamin Franklin Parkway, Philadelphia, PA 19103

Zenons Zudans

General Electric Company, 175 Curtner Ave., San Jose, CA 95125

Y. R. Rashid

Gulf General Atomic, P.O. Box 1608, San Diego, CA 92138

M. Jakub
D. I. Roberts

O'Donnell & Associates, Inc., 5100 Centre Avenue, Pittsburgh, PA 15232

W. J. O'Donnell

Pennsylvania State University, University Park, PA 16802

S. Y. Zamrik

Teledyne Materials Research Company, 303 Bear Hill Road, Waltham, MA 02154

W. E. Cooper
J. L. McLean

University of Alabama, College of Engineering, P.O. Box 1968, University, AL 35486

E. Carden

University of California, Lawrence Radiation Laboratory, Inorganic Materials Research Division, Berkeley, CA 94720

Leo Brewer

University of California, Revelle College, Department of Physics, P.O. Box 109, La Jolla, CA 92037

Walter Kohn

University of Cincinnati, Materials Science and Metallurgical Engineering Department, Cincinnati, OH 45221

J. Moteff

University of Illinois, Department of Physics, Urbana, IL 61801

W. S. Williams

EXTERNAL DISTRIBUTION

USAEC DIVISION OF REACTOR RESEARCH AND DEVELOPMENT, Washington, DC 20545

(2) Director

USAEC-RRD SENIOR SITE REPRESENTATIVE, Oak Ridge National Laboratory, Oak Ridge, TN 37830

USAEC OAK RIDGE OPERATIONS OFFICE, P.O. Box E, Oak Ridge, TN 37830

Research and Technical Support Division

USAEC TECHNICAL INFORMATION CENTER, Office of Information Services, P.O. Box 62, Oak Ridge, TN 37830

For distribution as shown in TID-4500 Distribution Category, UC-79b (Fuels and Materials Engineering Development); UC-79h (Structural Materials and Design Engineering); UC-79k (Components)